A CLINICOPATHOLOGICAL AND MOLECULAR GENETIC ANALYSIS OF LOW-GRADE GLIOMA IN ADULTS

Presented by

ANUSHREE SINGH MSc

A thesis submitted in partial fulfilment of the

requirements of the University of Wolverhampton

for the degree of Doctor of Philosophy

Brain Tumour Research Centre

Research Institute in Healthcare Sciences

Faculty of Science and Engineering

University of Wolverhampton

November 2014

DECLARATION

This work or any part thereof has not previously been presented in any form to the University or to any other body whether for the purposes of assessment, publication or for any other purpose (unless otherwise indicated). Save for any express acknowledgments, references and/or bibliographies cited in the work, I confirm that the intellectual content of the work is the result of my own efforts and of no other person.

The right of Anushree Singh to be identified as author of this work is asserted in accordance with ss.77 and 78 of the Copyright, Designs and Patents Act 1988. At this date copyright is owned by the author.

Signature: **Anushree**

Date: 30th November 2014

ABSTRACT

The aim of the study was to identify molecular markers that can determine progression of low grade glioma. This was done using various approaches such as *IDH1* and *IDH2* mutation analysis, *MGMT* methylation analysis, copy number analysis using array comparative genomic hybridisation and identification of differentially expressed miRNAs using miRNA microarray analysis.

IDH1 mutation was present at a frequency of 71% in low grade glioma and was identified as an independent marker for improved OS in a multivariate analysis, which confirms the previous findings in low grade glioma studies. *IDH1* mutation was associated with *MGMT* promoter methylation when partially methylated tumours were grouped with methylated tumours.

Grade II and grade III tumour comparison analysis revealed 14 novel significant miRNAs with differential expression. A miRNA signature was shown for histological subtypes, oligoastrocytoma and anaplastic oligoastrocytoma, following the miRNA expression analysis in grade II and grade III tumors based on histology. Oligoastrocytoma presented a more similar profile to oligodendroglioma, but anaplastic oligoastrocytoma was more similar to anaplastic astrocytoma. Five novel miRNAs were identified in grade III tumours, when comparing *IDH1* mutant and *IDH1* wild type tumours.

Analysis of paired samples of primary/recurrent tumours revealed that additional genomic changes may promote tumour progression. For each of the pair, the two samples were genomically different and in each case, the reccurent tumours had more copy number aberrations than the corresponding primary tumours.

Cell cultures derived from the tumour biopsies were not representative of the low grade glioma *in vivo*, which was evident from the differences identified in the miRNA expression and copy number changes in the paired samples. *IDH1* mutation present in tumour biopsies was not maintained in their respective cell cultures.

These findings give an insight into the molecular mechanisms involved in the tumourigenesis of low grade glioma and also tumour progression.

TABLE OF CONTENTS

LIST OF FIGURES

LIST OF TABLES

LIST OF ABBREVIATIONS

2-HG	2-hydroxyglutarate
α-KG	α-ketoglutarate
A	diffuse astrocytoma
AA	anaplastic astrocytoma
aCGH	array comparative genomic hybridisation
ALL	acute lymphoblastic leukemia
AML	acute myeloid leukemia
ANOVA	analysis of variance
AO	anaplastic oligodendroglioma
AOA	anaplastic oligoastrocytoma
ATCC	American Type Culture Collection
CCH	columnar cell hyperplasia
CGH	comparative genomic hybridisation
CHOP	cyclophosphamide, doxorubicin, vincristine, and prednisone
CNA	copy number aberration
CNS	central nervous system
CREB	cyclic adenosine monophosphate response element-binding protein
CTCL	cutaneous T-cell lymphomas
CX43	connexion 43
DAB	diaminobenzidene
DLBCL	diffuse large B-cell lymphoma
DMSO	dimethyl sulfoxide
EMA	epithelial membrane antigen
EMP3	epithelial membrane protein 3
EMT	epithelial-mesenchymal transition
EORTC	European Organization for Research and Treatment of Cancer
ESCC	esophageal squamous cell carcinoma

FFPE	formalin-fixed paraffin embedded
FGFR3	fibroblast growth factor receptor 3
FISH	fluorescent *in situ* hybridisation
FLAIR	Fluid-Attenuated Inversion Recover
GBM	glioblastoma multiforme
G-CIMP	glioma CpG island methylator phenotype
GFAP	glial fibrillary acidic protein
Glut1	glucose transporter 1
HBSS	Hanks' buffered salt solution
HCC	hepatocellular carcinoma
HIF-1α	hypoxia-inducible factor 1-alpha
IDH1	isocitrate dehydrogenase 1
IDH2	isocitrate dehydrogenase 2
IHC	immunohistochemistry
JHDM	Jumonji-C-domain-containing histone demethylases
LGG	low-grade glioma
LOH	loss of heterozygosity
MGMT	O^6-methylguanine-DNA-methyltransferase
miRNA	microRNA
MM	multiple myeloma
MMSE	Mini-Mental Status Examination
MRI	magnetic resonance imaging
MRS	magnetic resonance spectroscopy
MS PCR	methylation specific PCR
NADPH	nicotinamide adenine dinucleotide phosphate
NaSCN	sodium thiocyanate
NF1	neurofibromatosis type 1
NSCLC	non-small cell lung cancer
O	oligodendroglioma

OA	oligoastrocytoma
OS	overall survival
PBS	phosphate buffered saline
PCa	prostate cancer
PCA	principal component analysis
PCV	procarbazine, CCNU, vincristine
PDGFRA	platelet-derived growth factor receptor α
PDGFRB	PDGF receptor β
PDPN	podoplanin
PDT	photodynamic therapy
PET	positron emission tomography
PFS	progression free survival
PGK1	phosphoglycerate kinase 1
PMP22	peripheral myelin protein
PTEN	phosphatase and tensin homolog
PTL	peripheral T-cell lymphoma
PUMA	p53-upregulated modulator of apoptosis
QC	quality control
RBP1	retinol binding protein 1
RIN	RNA Integrity number
RISC	RNA-induced silencing complex
RT	radiotherapy
RT-qPCR	quantitative reverse transcription PCR
SRB	sulforhodamine
TACE	transarterial chemoembolization
TBS	tris buffered saline
TCA	trichloroacetic acid
TCGA	The Cancer Genome Atlas
TET	Ten-Eleven-Translocation

TMZ	temozolomide
VEGF	vascular endothelial growth factor
WHO	World Health Organisation

ACKNOWLEDGEMENTS

I would like to express my deepest gratitude to my supervisory team, Dr Katherine Karakoula, Professor John Darling and my director of studies, Dr Tracy Warr. This work would not have been possible without your continued support and guidance throughout. I am so pleased to have been given the opportunity to work with them.

I would like to convey my sincere thanks to Ms Kate Ashton and Professor Tim Dawson at Royal Preston Hospital for providing assistance with clinical pathology of the samples. Many thanks to Dr Carol Walker at The Walton Centre, Liverpool for assisting on sending tumour samples.

I would like to specially thank my colleagues at the Brain Tumour Research Centre, Dr Farzana Rowther, Prasanna Channathodiyil, Lawrence Eagles, Henrik Townsend and Hoda Kardooni and colleagues at the university, Dr Angel Armesilla and Rhiannon Baggott for their support and advice over the years.

Thank you to all the research technicians at the University for their support during the research and Dr Malcom Inman for assistance with microscopy. I would also like to thank Ms Raman Kaur for her continuous support with my research administrative work.

My heartfelt thanks to my dear friends, Shawna, Niki, Tania, Shaymaa, Manasi and Supriya for their endless support and advice throughout the years. I couldn't have done it without you all.

Lastly, I would like to thank my family for their love and encouragement. I would like to dedicate this thesis to my parents, AJ and Vandana, my sister and brother-in-law,

Tanu and Sid, my grandparents and to Sergio. Last but not the least, to my lovely dogs, Suzy and Rocky.

CHAPTER 1
INTRODUCTION

Glioma are the most common primary brain tumours, comprising 70% of all central nervous system (CNS) neoplasms and are classified according to the World Health Organisation (WHO) classification into grades I to IV based on their histopathological and clinical criteria (Louis *et al*., 2007). Grade I glioma, are usually curable with complete surgical resection and rarely progress to malignant phenotypes. Conversely, grade II and grade III glioma are invasive, often progress to higher-grade lesions and have a poor outcome. Grade IV tumours, glioblastoma multiforme (GBM), are the most malignant type of glioma and have a poor prognosis (Stupp *et al*., 2005; Wen *et al*., 2008).

1.1 INCIDENCE OF GLIOMA

The age-adjusted incidence of all glioma ranged from 0.03 to 5.33 per 100,000 persons, while that for grade II astrocytoma was 0.70 to 5.33, for oligoastrocytoma was 0.03 to 0.27, for oligodendroglioma was 0.10 to 0.40, for anaplastic astrocytoma was 0.13 to 0.44, for anaplastic oligodendroglioma was 0.06 to 0.11 and for GBM was 0.59 to 3.69 per 100,000 persons as shown in Table 1.1 (reviewed by Ostrom *et al*., 2014). Patients with grade II astrocytoma tumours were younger (typically 20-34 years) (Marko *et al*., 2013), than those with oligodendroglioma and oligoastrocytoma tumours who were mainly in the 35-44 age group and patients with anaplastic astrocytoma and GBM had peak incidence in the 75-84 age group (Ostrom *et al*., 2014).

Table 1.1 Incidence rates per 100,000 persons by histology and country (all ages) (Modified from Ostrom *et al*., 2014)

Histologic Type	Region (organization)	Years	Overall	
			Rate	95% CI
Anaplastic astrocytoma	Austria (ABTR)	2005	0.44	0.33–0.58
	Korea	2005	0.13	
	US (CBTRUS)	2006–2010	0.37	0.36–0.38
Glioblastoma	Australia	2000–2008	3.40	
	England	1999–2003	2.05	
	Korea	2005	0.59	
	US (CBTRUS)	2006–2010	3.19	3.16–3.21
	Greece	2005–2007	3.69	
Oligodendroglioma	Austria (ABTR)	2005	0.20	0.13–0.30
	England	1999–2003	0.21	
	Korea	2005	0.10	
	US (CBTRUS)	2006–2010	0.27	0.26–0.28
Anaplastic oligodendroglioma	England	1999–2003	0.09	
	Korea	2005	0.06	
	US (CBTRUS)	2006–2010	0.11	0.10–0.11
Oligoastrocytoma	Austria (ABTR)	2005	0.27	0.19–0.39
	England	1999–2003	0.10	
	Korea	2005	0.03	
	US (CBTRUS)	2006–2010	0.20	0.20–0.21
Astrocytic tumors	Austria (ABTR)	2005	5.33	4.93–5.75
	England	1999–2003	3.48	
	Europe (RARECARE)	1995–2002	4.80	
Oligodendroglial tumors	Austria (ABTR)	2005	0.70	0.55–0.86
	Europe (RARECARE)	1995–2002	0.40	

ABTR, Austrian Brain Tumour Registry; CBTRUS, Central Brain Tumour Registry of the United States; RARECARE, Surveillance of rare Cancer in Europe (EU).

1.2 GLIOMA HISTOLOGY

1.2.1 Astrocytoma

Diffuse astrocytoma (A) (WHO grade II) is a slow-growing, well differentiated tumour with a tendency to infiltrate surrounding brain tissues (Ohgaki *et al*., 2005; Louis *et al*., 2007). It consists of fibrillary and gemistocytic astroyctes on a loose matrix (Forst *et al*., 2014) and has a low proliferative activity (Schiff *et al*., 2007). Typically, overall survival (OS) of patients with astrocytoma is 5-10 years (Smith *et al*., 2008; Bauman *et al*., 2009). It often shows recurrence after surgical resection and progresses to malignant phenotypes such as anaplastic astrocytoma (AA) (WHO grade III) and subsequently, to GBM (WHO grade IV).

1.2.2 Oligoastrocytoma

Oligoastrocytoma (OA) (WHO grade II) is comprised of a mixture of cells of two different neoplastic cell types morphologically similar to tumour cells in oligodendroglioma and low-grade astrocytoma (Okamoto *et al*., 2004). Oligoastrocytoma is intermediate between low-grade astrocytoma and oligodendroglioma with regards to gene abnormalities and patient survival. Anaplastic oligoastrocytoma (AOA) (WHO grade III) is a malignant oligoastrocytoma (Okamoto *et al*., 2004; Louis *et al*., 2007).

1.2.3 Oligodendroglioma

Oligodendroglioma (O) (WHO grade II) is a slow-growing, well-differentiated, diffusely infiltrating tumour in adults, predominantly consisting of cells similar to oligodendroglia (Louis *et al*., 2007). It consists of uniform nuclei and perinuclear clearing, having a "fried-egg" appearance (Forst *et al*., 2014). It is characteristically located in the cerebral hemispheres (Louis *et al*., 2007; Rees *et al*., 2010). Patients with oligodendroglioma have OS of 10-15 years (Smith *et al*., 2008; Bauman *et al*., 2009). Anaplastic oligodendroglioma (AO) (WHO grade III) is a malignant oligodendroglioma with less favourable prognosis.

1.2.4 Glioblastoma multiforme (GBM)

GBM (WHO Grade IV) exhibits features of malignancy including vascular proliferation and necrosis. It develops from two different pathways and is classified as primary or secondary GBM (Ohgaki *et al*., 2007). Primary GBM develops *de novo* rapidly after a short clinical history in elderly patients and is distinguished by a distinct set of genetic aberrations when compared with the less frequent secondary GBM, which develops by progression from pre-existing low-grade glioma (LGG) (Figure 1.1). The median survival of GBM patients has been reported as 14.6 months and a 2-year survival rate of 26.5% (Stupp *et al*., 2005; Stupp *et al*., 2009).

Figure 1.1 Primary and secondary GBM

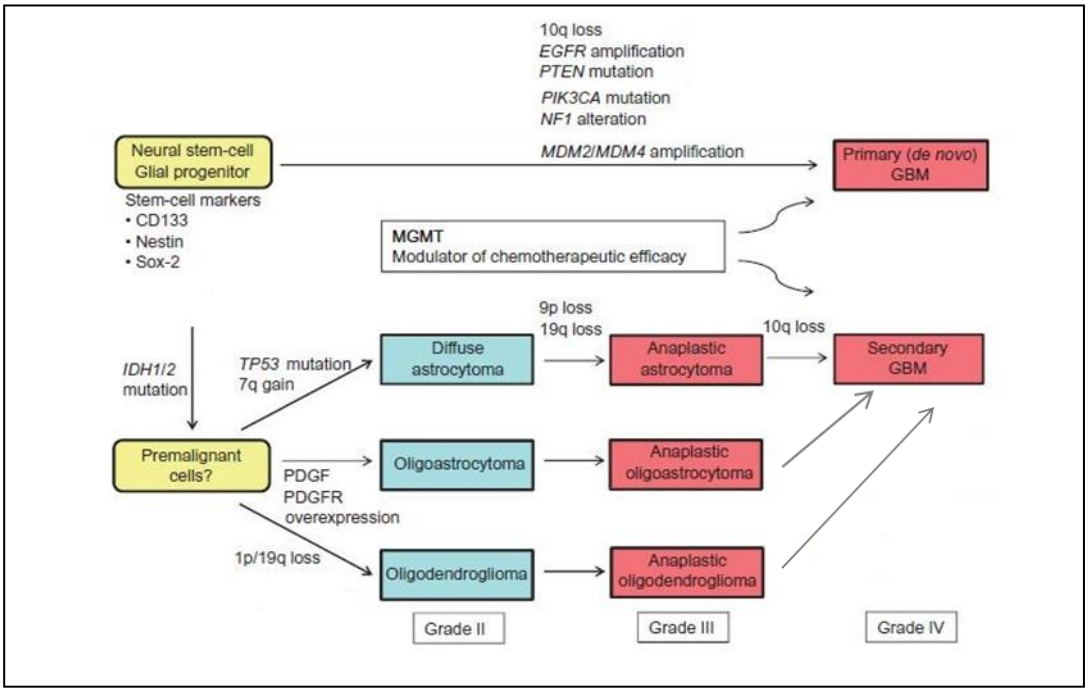

Pathways for the development of primary and secondary GBM showing genetic alterations in different histologic types of glioma (Modified from Masui *et al*., 2012).

1.3 CLINICAL SIGNS AND SYMPTOMS OF LGG

Clinical signs and symptoms vary depending on the mass invasion of the tumour into the surrounding tissues (Forst *et al*., 2014). Siezure is the most common presenting symptom in about 80% of the patients, others include cognitive or behavioural changes, focal neurological deficits and clinical symptoms of increased intracranial pressure such as headache and papilledema. Some of the patients may be asymptomatic with no evidence of abnormalities on neurological examination.

LGG are diagnosed by a combination of imaging, histopathological and molecular diagnostic analysis (Forst *et al*., 2014). On magnetic resonance imaging (MRI), LGG show low signal intensity on T1-weighted sequences and hyperintensity on T2-weighted and Fluid-Attenuated Inversion Recovery (FLAIR) sequences. Contrast enhancement is low and is more likely observed in oligodendroglioma tumours. Tumour grading cannot be determined by imaging alone and therefore, histopathological analysis of the tissue is the standard diagnostic and grading tool for these tumours.

1.4 PROGNOSTIC FACTORS FOR LGG

Clinical prognostic factors for LGG patients have been identified, including age, size of the lesion, histology subtype, tumour crossing the midline, performance status, mental status and localization of the tumour in an eloquent area (Pignatti *et al*., 2002; Shaw *et al*., 2002; Brown *et al*., 2004; Chang *et al*., 2008; Daniels *et al*., 2011).

In two European Organization for Research and Treatment of Cancer (EORTC) trials, EORTC-22844 used as a construction set (281 patients) and EORTC-22845 used for validation (253 patients) (Pignatti *et al*., 2002), prognostic factors including age (< 40 or

> 40 years), largest diameter of the tumour (< 6 vs ≥ 6 cm), tumour crossing midline, WHO perfomance status (0 vs > 0) and histology subtype (oligoastrocytoma/mixed vs astrocytoma) were analysed. Multivariate analysis revealed that age ≥ 40 years (p = 0.0077), largest diameter of the tumour ≥ 6cm (p = 0.0003), tumour crossing midline (p = 0.0005) and histology subtype, astrocytoma (p = 0.005) were significant unfavourable prognostic factors for survival in LGG. The results were confirmed in the validation set; age ≥ 40 years (p = 0.0005), largest diameter of the tumour ≥ 6cm (p = 0.0350), tumour crossing midline (p = 0.0051) and histology subtype, astrocytoma (p = 0.0006) (Daniels *et al*., 2011). Univariate analysis of the EORTC prognostic factors showed that astrocytoma histology (p = 0.004) and tumour ≥ 6cm (p = 0.0001) were significant predictors for poor OS and for progression free survival (PFS) (astrocytoma histology, p = 0.003 and tumour ≥ 6cm, p < 0.0001). Similarly, the NCCTG-RTOG-ECOG trial showed a significant association of longer OS with younger age, < 40 years (p = 0.0245), smaller tumour size < 5cm (p = 0.008), oligodendroglioma/mixed histology (p = 0.0001) and high baseline Mini-Mental Status Examination (MMSE) status score of ≥ 28 (p = 0.0030) (Shaw *et al*., 2002). Histological subtype and age combined were important predictors of OS. The 5-year survival rates for younger patients (< 40 years) with oligodendroglioma was 82% compared with 32% for older patients (≥ 40 years) with astrocytoma. Data collected from an intergroup trial was analysed to determine the prognostic significance of baseline MMSE score in 187 patients with LGG (Brown *et al*. 2004). The patients with an abnormal baseline MMSE score (< 26) had a worse 5-year survival rate of 31% compared with 76% for those with normal baseline MMSE score (> 26) (p < 0.001). An abnormal baseline MMSE score was a predictor of worse OS for both high-dose and low-dose treatment patients. Another study collected data for 281 patients with hemispheric LGG for assessment of predictors of OS (Chang *et al*.,

2008). Multivariate analysis revealed that eloquent location of the tumour ($p = 0.0018$), age > 50 years ($p = 0.0412$) and tumour diameter > 4cm ($p = 0.0014$) were associated with a shorter OS.

1.5 MANAGEMENT AND TREATMENT OF LGG

The optimal management of LGG is a challenge as many patients remain asymptomatic for a prolonged period of time and may deteriorate after treatment due to side effects (Olson *et al*., 2000; Reijneveld *et al*., 2001; Surma-aho *et al*., 2001; Douw *et al*., 2009). Currently, treatment options include watch-and-wait policy, surgery, radiotherapy (RT) and chemotherapy (van den Bent *et al*., 2012).

In case of watch-and-wait policy, neuroradiological follow-up is required for patients in need of histological diagnosis and treatment (van den Bent *et al*., 2012). Radioactive labeled PET (positron emission tomography) scanning may distinguish between LGG and histological high grade and MRI is used for non-enhancing tumours (Kunz *et al*., 2011). The only evidence for early versus delayed treatment is the randomized EORTC 22845 trial initiated in 1986 and long-term results have reported that early radiotherapy improved PFS with no change in OS (van den Bent *et al*., 2005). Patients from 24 centres across Europe were selected and randomly assigned early radiotherapy or delayed radiotherapy until the time of progression (control group) with 157 patients in both groups. The median PFS in the early radiotherapy group was 5.3 years and 3.4 years in the control group ($p < 0.0001$). OS was similar in the two groups; median survival in early radiotherapy group was 7.4 years and 7.2 years in the control group ($p = 0.872$). The study showed that outcome was not affected adversely with delayed radiotherapy. Radiotherapy treatment in LGG patients may lead to poor quality of life

and cognitive deficits (Taphoorn *et al*., 1994; Olson *et al*., 2000; Correa *et al*., 2008; Douw *et al*., 2009).

1.5.1 Surgery

Surgery on a patient with a suspected LGG provided four worthwhile benefits: (1) histological analysis of the lesion, (2) improvement in the neurological condition, (3) reducing the risk of tumour growth and (4) prevention of malignant transformation (van den Bent *et al*., 2012). Previous studies have shown that surgery may improve neurological condition and control the seizures (Duffau *et al*., 2002; Gunnarsson *et al*., 2002; Chang, *et al*., 2008). Surgeons use preoperative functional MRI and tractography, as well as intraoperative neurophysiological monitoring to allow safe maximum resection of tumours involving eloquent areas (Forst *et al*., 2014). Intraoperative MRI and MRS (magnetic resonance spectroscopy) may be used to determine the extent of tumour resection during surgery and identify residual tumour (Pamir *et al*., 2009; Pamir *et al*., 2013). Patients with tumours that cannot be safely resected may undergo stereotactic biopsy using preoperative or intraoperative MRI imaging for histopathological diagnosis. For biopsy resection, surgeons target the potential high grade part of the lesion using contrast enhancement with reported accuracy rates of 51-83% (Pouratian *et al*., 2007).

1.5.2 Radiotherapy

The importance of radiotherapy (RT) in LGG was demonstrated in the EORTC 22845 trial, where an increase in time to progression with early RT in comparison to observation (with RT at the time of progression) was demonstrated (van den Bent *et al*., 2005). The NCCTG-RTOG-ECOG trial observed a response to RT in one-third of the patients and small retrospective surveys suggested improvement in neurological

condition or improved seizure control after radiation (Shaw *et al*., 2002; Soffietti *et al*., 2005). The randomized trial was conducted from 1986-1994 for adult supratentorial low-grade glioma with 203 eligible patients randomized for radiotherapy; 101 to low-dose RT (50.4 Gy/28 fractions) and 102 to high-dose RT (64.8 Gy/36 fractions). Histology subtype was astrocytoma for 32% and oligodendroglioma for 68% of patients. Survival at 2 and 5 years (94% and 72%) was better with low-dose RT than that with high-dose RT (85% and 64%) (log rank p = 0.48), however, this was not significant. Similar results were obtained from the EORTC 22844 trial, where the importance of RT and dose-response relationship was evaluated (Karim *et al*., 1996). A total of 379 patients with cerebral LGG were randomized to receive radiotherapy postoperatively (or post biopsy) with 45 Gy in 5 weeks or 59.4 Gy in 6.6 weeks. After a median follow-up of 74 months, there was no significant difference in OS (58% in low-dose and 59% in high-dose group) or PFS (47% in low-dose and 50% in high-dose group) and there was no evidence of dose-response relationship for RT in LGG.

1.5.3 Chemotherapy

Recent studies regarding the role of chemotherapy in LGG have described using temozolomide (TMZ) and older studies have described using PCV (procarbazine, CCNU, vincristine).

The RTOG 9802 trial compared LGG patients treated with radiation alone versus radiation followed by 6 weeks of PCV chemotherapy (Shaw *et al*., 2012). A total of 251 patients were enrolled from 1998-2002 and a statistical significance was observed in PFS but not OS in the RT+PCV group. OS and PFS were similar in the first two years of treatment and longer follow-up demonstrated that 2-year survivors in RT+PCV group

had a significant probability of OS for additional 3 years and 5 years compared to non-chemotherapy patients.

In a phase II trial involving 46 patients with LGG, the response of patients to TMZ was examined and measured as an end point in this study. A total of 61% achieved response (24% achieved complete response and 37% achieved partial response) (Quinn *et al*., 2003). The median PFS was 22 months with a 6-month PFS of 98% and a 12-month PFS of 76%. Another phase II trial with TMZ based chemotherapy in high-risk LGG was the RTOG 0424 trial, where 3-year survival of high-risk LGG patients treated with TMZ alone was compared with those enrolled in EORTC 22844 and 22845 (Fisher *et al*., 2013). In this study, patients received radiation and daily TMZ for 6 weeks followed by TMZ for an additional 12 months postradiation. Patients in the RTOG 0424 trial had a 3-year OS of 73.1%, which was longer than those in comparison from the EORTC trials. This study has a limitation due to the comparison with patients from EORTC trials conducted 20 years earlier (Forst *et al*., 2014).

An observational study with 149 LGG patients was performed to determine the influence of 1p/19q co-deletion on the response and outcome of LGG treated with TMZ (Kaloshi *et al*., 2007). A total of 53% patients achieved an objective response to TMZ (15% with partial response and 38% with minor response), 37% were stable and 10% had progression. The median PFS was 28 months (95% CI: 23.4 to 32.6). Loss of heterozygosity (LOH) of 1p/19q was present in 42% of the patients and was significantly associated with longer objective response to TMZ ($p = 0.017$) and longer PFS ($p = 0.000041$) and OS ($p = 0.04$).

1.6 GENETIC ALTERATIONS IN LGG

1.6.1 Copy number aberrations in LGG

Karyotyping has been performed for only 22 untreated patients with grade II oligodendroglioma. Majority of these tumours had near-diploid karyotypes with a few numerical and/or structural chromosomal rearrangements (Mitelman *et al*., 2011). G-banding using grade II oligoastrocytoma revealed only four tumours with loss of Y chromosome as the only aberration (Jenkins *et al*., 1989).

The most common aberration in grade II diffuse astrocytomas is trisomy/polysomy of chromosome 7 (Reifenberger *et al*., 2004). Gain of chromosome 7 or 7q was detected in more than 50% of the cases using comparative genomic hybridization (Schrock *et al*., 1996) or interphase fluorescent *in situ* hybridization (FISH) (Wessels *et al*., 2002). Aberrations at a smaller frequency include losses of 22q, 13q, 10p, 6 and the sex chromosomes (Kleihues *et al*., 2000). Comparative genomic hybridisation (CGH) experiments revealed the most predominant gains on the whole chromosome 7 or 7q and 8q in grade II astrocytoma and losses mainly on chromosome arm 1p, 10p and 19q (Schröck *et al*., 1996; Ichimura *et al*., 1998; Nishizaki *et al*., 1998; Shapiro, 2002; Hirose *et al*., 2003; Arslantas *et al*., 2007; Holland *et al*., 2010). The molecular changes in glioma are classified as early changes (chromosome 1p/19q loss and *TP53* mutation) which are detected in LGG and are thought to be early events in tumour progression (Kujas *et al*., 2005). The late alterations are associated with anaplastic glioma; LOH 9p, p16 homozygous deletions, LOH 10q, LOH 19q without 1p loss and *EGFR* amplification. In a study of 131 LGGs, the most common aberrations were chromosome 1p loss, p53 mutation (combined 89%) and chromosome 9p loss (44%) (Kujas *et al*., 2005). Hirose *et al*., reported gain on chromosome 7q, 5p and losses on 19q and 1q as

the most common aberrations in grade II astrocytomas (Hirose *et al*., 2003). Gain of platelet-derived growth factor receptor α (*PDGFRA)* was investigated in a study of LGG consisting of 166 low-grade diffuse astrocytomas, 61 oligoastrocytomas and 115 oligodendroglioma and it was correlated with *IDH1* mutation (Motomura *et al*., 2013). *PDGFRA* gain was significantly more frequent in diffuse astrocytomas (16.3%) than in oligoastrocytomas (6.6%) and oligodendroglioma (2.6%) ($p < 0.0001$). Majority of diffuse astrocytomas (93%) had *PDGFRA* gain and/or *IDH1/IDH2* mutations.

The most common aberration in oligodendroglioma is a combined loss on 1p and 19q, present in about 50% of these tumours (Reifenberger *et al*., 1994; Louis *et al*., 2007; Rees *et al*., 2010). Loss of 1p/19q is mutually exclusive of LOH on 17p and *TP53* mutation (Maintz *et al*., 1997; von Deimling *et al*., 2000; Mueller *et al*., 2002; Ueki *et al*., 2002). Co-deletions of 1p/19q are present in 30-50% of oligoastrocytomas (Reifenberger *et al*., 1994; Kraus *et al*., 1995; Maintz *et al*., 1997; Okamoto *et al*., 2004) and *TP53* mutations are present in 30% of them (Reifenberger *et al*., 1994; Maintz *et al*., 1997; Mueller *et al*., 2002; Okamoto *et al*., 2004). Oligoastrocytomas with 1p/19q codeletions have similar histological features as that of oligodendroglioma, while those with *TP53* mutations are more similar to astrocytomas histologically (Maintz *et al*., 1997). Other aberrations include deletions at chromosome 4, 6, 11p, 14, 22q, that are less frequent (Reifenberger *et al*., 2003; Jeuken *et al*., 2004) and losses of chromosome 9 and 10, that are more frequent (Louis *et al*., 2007).

1.6.2 *TP53* abnormalities in LGG

TP53 is located at 17p13.1 and p53 protein is involved in regulation of the cell cycle, the response of cells to DNA damage, cell differentiation and apoptosis (Marko *et al*.,

2013). Activation of *TP53* occurs as a result of DNA damage and further induces transcription of the *p21* gene (Ohgaki *et al*., 2009). Wild type *TP53* induces *MDM2*, which binds to both mutant and wild type *TP53*, thus inhibiting activation of transcription by wild type *TP53*. *MDM4* also regulates *TP53* activity and $p14^{ARF}$ negatively regulates *TP53*. Therefore, *TP53* activity may be influenced by *MDM2*, *MDM4* and $p14^{ARF}$.

TP53 mutations are present in about 60% of diffuse astroyctomas (Ichimura *et al*., 2000; Kleihues *et al*., 2000) and they are often accompanied by LOH on 17p, resulting in complete absence of wild type *TP53* (Reifenberger *et al*., 2004). In a study of 360 LGG, *TP53* mutations were present in 53% diffuse astrocytoma, 39% oligoastrocytoma and 8% oligodendroglioma (Kim *et al*., 2010). The most common mutation was G:C to A:T at CpG sites in 42% followed by G:C to A:T at non-CpG sites in 16% and A:T to G:C in 14% of the cases.

1.6.3 Altered epression of platelet derived growth factor receptor in low grade glioma

Diffuse astrocytomas frequently exhibit increased levels of the *PDGFRA* and the corresponding ligand PDGFα, stimulating growth of the tumour cells (Hermanson *et al*., 1992; Guha *et al*., 1995). Overexpression of *PDGFRA* was primarily found in tumours with LOH on 17p (Hermanson *et al*., 1996). The PDGF pathway was investigated by studying the kinase activity of PDGF receptor β (*PDGFRB*) in 130 cases of LGG (Debien *et al*., 2011). The authors showed that LGG patients with co-presence of high PDGFRB activity, low level of DNA methylation and low level of apoptotic activity had poor prognosis. This indicates that the PDGF pathway plays a crucial role in apoptotic evasion in LGG.

1.7 ENDOGENOUS ROLE OF *IDH1* AND *IDH2*

The *IDH1* (isocitrate dehydrogenase 1) gene is located at 2q33.3 and the enzyme has been mostly detected in cytosol and peroxisomes (Narahara *et al*., 1985; Geisbrecht *et al*., 1999). It catalyses the oxidative carboxylation of isocitrate to α-ketoglutarate (α-KG) leading to the production of nicotinamide adenine dinucleotide phosphate (NADPH) in the Kreb's cycle (Geisbrecht *et al*., 1999; Devlin, 2006; Reitman *et al*., 2010) (Figure 1.2). Heterozygous mutations in *IDH1* hinder wild type *IDH1* by formation of catalytically inactive heterodimers (Zhao *et al*., 2009). The isoform *IDH2* gene is located at 15q26.1 and expressed in the mitochondria (Grzeschik, 1976). *IDH2* may be the main catalyst for the oxidation of isocitrate to α-ketoglutarate in the Kreb's cycle (Hartong *et al*., 2008). $NADP^+$ functions as the electron acceptor for IDH1 and IDH2 proteins and both require a divalent metal ion, Mn^{2+} for enzymatic activity (Colman, 1972; Villafranca *et al*., 1972; Northrop *et al*., 1974; Carlier *et al*., 1978; Kelly *et al*., 1981a; Kelly *et al*., 1981b; Bailey *et al*., 1987).

Figure 1.2 Function of IDH1 and IDH2

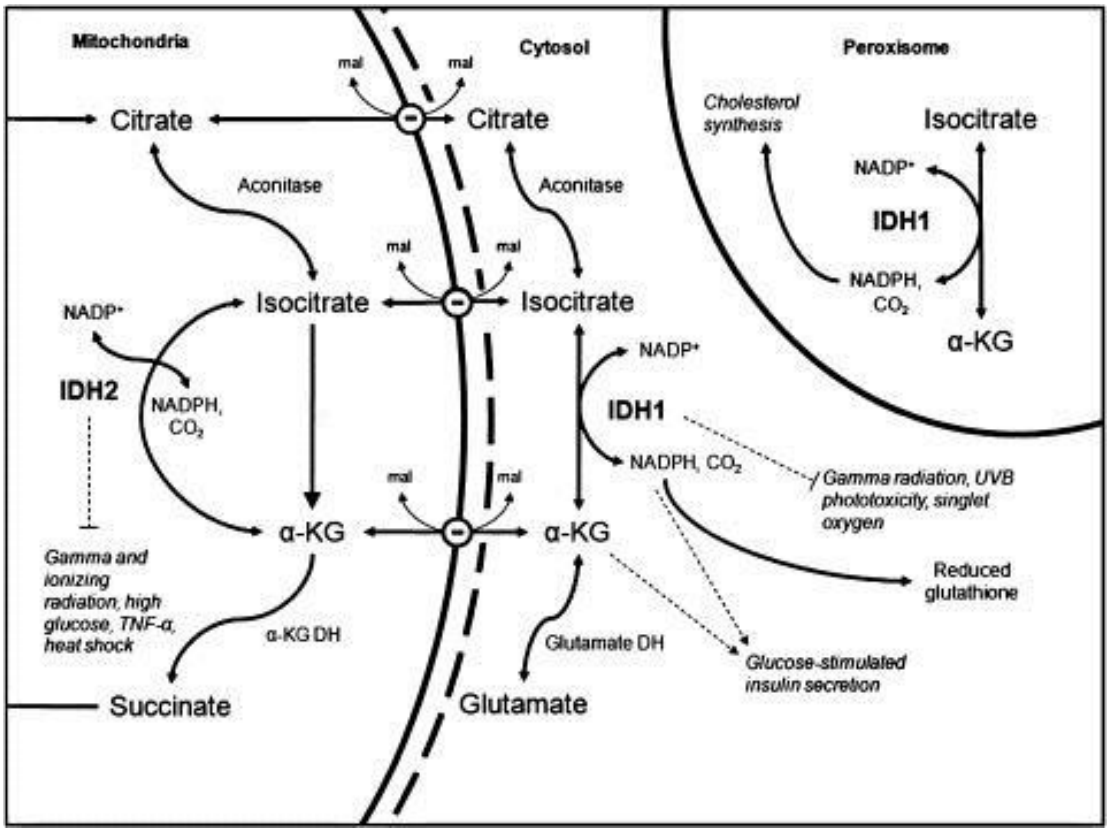

Part of Krebs cycle showing the role of IDH1 and IDH2 in the reversible conversion of isocitrate to α-ketoglutarate and $NADP^+$ to NADPH (Modified from Reitman *et al*., 2010).

1.8 FREQUENCY AND TYPE OF *IDH* MUTATIONS IN GLIOMA

Mutations in *IDH1* gene were first identified in 2008 as a result of large scale sequencing analysis of 22 GBM tumours (Parsons *et al*., 2008). All mutations were restricted to the conserved residue R132 located in the substrate-binding site of *IDH1*. Multiple studies confirmed these findings and also revealed that *IDH1* mutations are most frequent (>80%) in LGG; diffuse astrocytoma, oligodendroglioma and oligoastrocytoma (Balss *et al*., 2008; Nobusawa *et al*., 2009; Watanabe *et al*., 2009; Yan *et al*., 2009). *IDH2* mutations are mutually exclusive with *IDH1* mutations (Hartmann *et al*., 2009; Sonoda *et al*., 2009; Yan *et al*., 2009). They are rare in occurence in grade II, grade III tumours and secondary GBM, affecting residue R172 only (Balss *et al*., 2008; Nobusawa *et al*., 2009; Yan *et al*., 2009). In addition, *IDH2* mutations were reportedly more common in oligodendroglial tumours as compared to astrocytomas (Hartmann *et al*., 2009). Mutations of *IDH1* and *IDH2* are somatic, missense, heterozygous and affect only codon 132 in *IDH1* and codon 172 in *IDH2* (Kloosterhof *et al*., 2011). The most common mutation of *IDH1* was R132H (92.7%) followed by R132C (4.1%), R132S (1.5%), R132G (1.4%) and R132L (0.2%) amongst all 716 tumours comprising astrocytoma, anaplastic astrocytoma, oligodendroglioma, anaplastic oligodendroglioma, oligoastrocytoma and anaplastic oligoastrocytoma (Hartmann *et al*., 2009). In case of *IDH2*, R172K (60%) was the most common followed by R172M (19%) and R172W (16%) in 31 tumours comprising the glioma mentioned above. The discrepancy in studies related to the low frequencies of IDH1-R132S, R132G and R132L may be due to variations in number of samples and different histological types analysed. *IDH1* mutations were present in majority of low-grade astrocytoma, oligodendroglioma and oligoastrocytoma suggesting that these mutations are early events in tumour formation.

In addition, *IDH1* and *IDH2* mutations have also been reported in acute myeloid leukemia (AML), acute lymphoblastic leukemia (ALL), myeloid proliferative neoplasms, chondromas and chondrosarkomas, prostate cancer, colon cancer and paraganglioma (Figueroa *et al*., 2010; Amary *et al*., 2011; Megova *et al*., 2014).

1.9 FUNCTIONAL CONSEQUENCES OF *IDH1* MUTATION

1.9.1 HIF-1 pathway

IDH1 mutation results in loss of function of *IDH1* gene with reduced production of α-KG from isocitrate leading to accumulation of hypoxia-inducible factor 1-alpha (HIF-1α), suggesting that activation of HIF-1α pathway may be involved in oncogenesis (Zhao *et al*., 2009). HIF-1 is a transcription factor that detects low cellular oxygen levels and regulates expression of genes involved in glucose metabolism, angiogenesis and other signalling pathways that are important for tumour growth. HIF-1α protein levels in U87-MG cells were found to be high in response to *IDH1* knockdown by shRNA and reduced HIF-1α protein levels were observed in HeLa and U87-MG cells due to overexpression of wild type *IDH1*. Overexpression of *IDH1*-R132H mutant resulted in increased HIF-1α protein levels in U87-MG and HEK293T cells. These findings suggest that *IDH1* regulates HIF-1α levels via α-KG. Furthermore, reduction in IDH1 activity led to reduction in α-KG levels and stabilization of HIF-1α. The study also determined upregulation of HIF-1α target genes, *Glut1* (glucose transporter 1), *VEGF* (vascular endothelial growth factor) and *PGK1* (phosphoglycerate kinase 1) by inhibition of IDH1 enzyme activity. Quantitative RT-PCR was used to determine the expression levels of the target genes and the results revealed that knockdown of IDH1

induced the expression of HIF-1α target genes. Furthermore, *IDH1*-R132H mutant strongly induced the expression of the target genes and not *IDH1* wild type.

1.9.2 2-Hydroxyglutarate

Mutation of *IDH1* results in gain of function with conversion of α-KG to 2-hydroxyglutarate (2-HG) (Dang *et al*., 2009), an oncometabolite that induces DNA hypermethylation, causing genome-wide epigenetic changes (Xu *et al*., 2011). α-KG is an important cofactor for enzymes such as TET (Ten-Eleven-Translocation) family and JHDMs (Jumonji-C-domain-containing histone demethylases) (Chowdhury *et al*., 2011; Xu *et al*., 2011). CpG islands are genomic regions with higher frequency of CG dinucleotides (CpG sites) including transcription start site and transcription factor binding sites and are involved in regulation of gene transcription. TET1 and TET2 convert methylcytosine to hydroxymethylcytosine, a limiting step in the demethylation of CpG islands in the genome (Pastor *et al*., 2013) and JHDMs are involved in demethylation of lysine on histone, H3 (van Lith *et al*., 2014). *IDH1* mutant tumours have high levels of glutamate uptake with conversion to α-KG in the cytosol, providing high levels of substrate for 2-HG production (Dang *et al*., 2009). Malignant tumours with *IDH1* mutations were found to have 100-fold higher levels of 2-HG compared to tumours with *IDH1* wild type. The increase in 2-HG levels in R132H *IDH1* mutated tumours was statistically significant ($p < 0.0001$). Increased 2-HG levels result in increased ROS (reactive oxygen species) levels, with an increased risk of cancer (Kolker *et al*., 2002; Latini *et al*., 2003). 2-HG may also be toxic to cells by inhibiting glutamate and/or α-KG utilizing enzymes, which include α-KG dependent prolyl hydroxylases that regulate HIF-1α levels (Dang *et al*., 2009).

1.9.3 G-CIMP

Glioma CpG island methylator phenotype (G-CIMP) was found to be associated with *IDH1* mutations with majority (78%) of G-CIMP positive tumours presenting *IDH1* mutation (Noushmehr *et al*., 2010). G-CIMP that identified promoter hypermethylation of a specific set of genes was described in a TCGA study with GBM tumours. DNA methylation levels of 7 hypermethylated loci (*ANKRD43, HFE, MAL, LGALS3, FAS-1, FAS-2,* and *RHO-F*) and one hypomethylated locus (*DOCK5*) were determined in the cohort to validate the G-CIMP. A tumour was considered G-CIMP positive if at least 6 of the genes were methylated including DOCK5 hypomethylation. Grade II tumours had approximately 10-fold higher frequency of G-CIMP positive tumours compared to GBM tumours and grade III tumours had an intermediate proportion. Based on the histology types, oligodendroglioma with G-CIMP positivity (93%) were approximately twice as compared to astrocytomas (45%). G-CIMP positive status was significantly associated with improved survival in LGG ($p < 0.01$) and was found to be maintained at recurrence. Turcan *et al*., (2012) demonstrated that IDH1-R132H mutation in primary human astrocytes induced histone modifications and extensive DNA hypermethylation, leading to remodelling of the methylome and establishing G-CIMP. Expression of *IDH1* mutant in human astrocytes led to production of 2-HG. Methylomes of astrocytes with wild type or mutant *IDH1* was analysed over 50 successive passages. Increased hypermethylation of large number of genes was observed along with hypomethylation of few genes with expression of mutant *IDH1*. Methylome data included hypermethylated genes that had *de nevo* methylation as well as genes with originally low levels of methylation that acquired high levels of methylation.

1.9.4 PI3K-Akt signalling pathway

IDH1 mutant has been shown to inhibit PI3K/Akt signalling pathway in a study of 354 glioma patients comprising 72 grade II tumours (33 astrocytomas, 26 oligodendroglioma, and 13 oligoastrocytomas), 32 grade III tumours (12 astrocytomas, 8 oligodendroglioma, and 12 oligoastrocytomas) and 250 grade IV tumours (249 GBM and 1 gliosarcoma) (Birner *et al*., 2014). Activation of PI3K/Akt signalling pathway is associated with aggressive behaviour in glioma (Koul, 2008) and the activation is mainly caused by loss of the PI3K inhibitor *PTEN* (phosphatase and tensin homolog) or a gain-of-function mutation of *PI3KCA* (Cheng *et al*., 2009). *PDPN* (podoplanin) and *RBP1* (retinol binding protein 1) are two of the top downregulated genes of PI3K pathway in glioma associated with a high frequency of *IDH1* mutations (Noushmehr *et al*., 2010). *IDH1* mutant was inversely associated with the presence of pAkt ($p < 0.001$, chi square test) and *PDPN* expression ($p < 0.001$, chi square test) (Birner *et al*., 2014). The expression of mutant *IDH1* inhibited PI3K signalling in LN-319 glioma cells transfected with mutant *IDH1*, however, it was unable to downregulate *PDPN* expression in glioma cells.

1.10 PROGNOSTIC VALUE OF GENETIC ALTERATIONS

1.10.1 1p/19q

Complete loss of chromosomes 1p and 19q is most commonly present in oligodendroglioma. In a study of grade II and grade III tumours, analysis of 1p/19q co-deletion was carried out in 83 tumours, of which 43 were analysed by FISH, 18 by LOH and 22 by both methods (Sabha *et al*., 2014). Co-deletion of 1p/19q was identified in 25% (10/40) astrocytoma, 50% (4/8) oligoastrocytoma, 89% (8/9) oligodendroglioma,

20% (3/15) anaplastic astrocytoma, 50% (2/4) anaplastic oligoastrocytoma and 100% (7/7) anaplastic oligodendroglioma tumours. Co-deletion of 1p/19q was also significantly associated with longer OS in the entire cohort (p = 0.01). Alentorn *et al*., (2014) investigated the clinical significance of 1p/19q co-deletion in LGG. Co-deletion of 1p/19q was present in 8.7% (2/23) astrocytoma, 10% (5/50) oligoastrocytoma and 47.2% (25/53) oligodendroglioma tumours. The authors showed that co-deletion of 1p/19q was associated with better prognosis in terms of PFS (p = 0.024) and OS (p = 0.0002) and with oligodendroglial phenotype (p < 0.0001). A study involving LGG, anaplastic tumours and GBM reported complete loss of 1p/19q in 35% LGG (11% A, 12% OA and 82% O), in 51% anaplastic tumours (14% AA, 13% AOA and 77% AO) and 3% of GBM tumours (Boots-Sprenger *et al*., 2013). Patients with LGG and anaplastic tumours having complete 1p/19q co-deletion were significantly associated with longer OS, while no significance with OS was found in GBM patients having co-deletion of 1p/19q.

1.10.2 MGMT

The *MGMT* (O^6-methylguanine-DNA-methyltransferase) gene is located at 10q26 and produces a DNA repair protein that removes alkyl groups from O^6 position of guanine (Gerson, 2004). Hypermethylation of 5'CpG island leads to inactivation of *MGMT*, which is frequently observed in secondary GBM (>70%) and less often in primary GBM (~40%) (Weller *et al*., 2010). *MGMT* promoter methylation is heterogeneous in malignant glioma; it is not known which CpG sites need to be methylated to inactivate the gene. The most commonly used method to detect the methylation is methylation specific PCR (MS PCR) followed by direct sequencing. *MGMT* is an important molecular marker that predicts the response of malignant glioma to alkylating agents

such as nitrosoureas (Esteller *et al*., 2000), TMZ (Hegi *et al*., 2005) or a combination of both (Herrlinger *et al*., 2006). *MGMT* promoter methylation causes decreased expression and increased sensitivity to TMZ (Horbinski, 2013). In patients with GBM, *MGMT* promoter methylation predicted longer survival irrespective of the initial treatment (Wick *et al*., 2009; van den Bent *et al*., 2010). With regard to LGG treated with TMZ, patients with *MGMT* promoter methylation reportedly had better outcome in a phase II study (Kesari *et al*., 2009).

1.11 CLINICAL CORRELATION OF *IDH1* MUTATION

A meta-analysis was performed involving 12 studies with a range of cohort sizes from 49 to 407 patients, of which one study included grade II tumours, four studies included grade III tumours, four studies included grade IV tumours, one study included grade II-IV tumours and two studies included tumours of all grades (Zou *et al*., 2013). The authors showed that *IDH* mutations were independent prognostic markers for longer OS ($p < 0.001$) and PFS ($p < 0.001$). In a study involving 41 oligodendroglioma, 47 anaplastic oligodendroglioma and 46 GBM, the prognostic significance of *IDH1* mutation was analysed (Myung *et al*., 2012). The median survival was 68.4, 54.2 and 19.7 months for oligodendroglioma, anaplastic oligodendroglioma and primary GBM tumours respectively. OS was higher in both oligodendroglioma and anaplastic oligodendroglioma with *IDH1* mutation compared to those without *IDH1* mutation ($p = 0.03$ and $p = 0.013$). No significant difference was seen in OS in patients with GBM. A positive correlation between *IDH1* mutation and long-term survival was observed in grade II and III astrocytoma and oligodendroglioma and OS was similar for primary GBM with wild-type *IDH1* and those with *IDH1* mutation (Mellai *et al*., 2011). Mutations of *IDH* genes were associated with improved outcome in patients with GBM

and median OS of 31 months was reported, which was significantly higher than the 15 month survival for patients with no mutation ($p = 0.002$) (Yan *et al*., 2009). The median OS for patients with anaplastic astrocytomas carrying *IDH1* or *IDH2* mutation was 65 months as compared to 20 months for patients without mutations ($p < 0.001$; log-rank test). Longer survival was associated with *IDH1* mutation in all tumours including astrocytoma, anaplastic astrocytoma, oligodendroglioma, anaplastic oligodendroglioma, oligoastrocytoma, anaplastic oligoastrocytoma and GBM ($p < 0.001$; log-rank test) (Ichimura *et al*., 2009). In LGG, *IDH* mutations were associated with a better 5-year survival rate (93% vs 51%, $p = 0.000001$) and lack of *IDH* mutations was an independent, unfavourable prognostic marker ($p = 0.006$) (Metellus *et al*., 2010). There was no significant difference in survival rates for *IDH1* mutant primary and secondary GBM (Yan *et al*., 2009). Primary GBM with *IDH1* mutation had a mean survival period of 30 months, which was significantly longer than 11.3 months for wild-type *IDH1* patients ($p < 0.0001$). Secondary GBM patients with *IDH1* mutation had a mean survival time of 23.8 months ($p = 0.4971$).

1.12 MOLECULAR CHANGES ASSOCIATED WITH *IDH1* MUTATION

Glioma with *IDH1* mutation exhibit a different set of genetic alterations than those without *IDH1* mutation (Yan *et al*., 2009). *IDH1* mutations are mainly associated with *TP53* mutation and co-deletions of 1p/19q in diffuse astrocytoma, oligoastrocytoma and oligodendroglioma, all of which undergo malignant progression (Ichimura *et al*., 2009; Watanabe *et al*., 2009; Toedt *et al*., 2011). 1p and 19q losses, separately or combined were significantly more associated with oligodendroglioma than astrocytoma or oligoastrocytoma ($p < 0.0001$) (Barbashina *et al*., 2005), while *TP53* mutations were

frequent in astrocytoma and rare in oligodendroglioma (Mueller *et al*., 2002). Mutations of *IDH1* are inversely associated with *EGFR* amplification (p = 0.005) (Nobusawa *et al*., 2009).

1.12.1 EMP3

EMP3 (epithelial membrane protein 3), located at 19q13.3 is a myelin-related gene that belongs to *PMP22* (peripheral myelin protein) family of small membrane glycoproteins (Taylor *et al*., 1995; Ben-Porath *et al*., 1996; Taylor *et al*., 1996). It may be involved in cell proliferation, cell-cell interactions and apoptosis based on the functions of *PMP22*. *EMP3* is mainly expressed in blood leukocytes, ovary, intestine and various embryonic tissues (Ben-Porath *et al*., 1996; Taylor *et al*., 1996). Hypermethylation in the promoter region of *EMP3* was determined using MS PCR and higher frequency of *EMP3* hypermethylation was found in oligoastrocytoma (70%) and oligodendroglioma (63%) than astrocytoma (18%) (P < 0.0001) (Mellai *et al*., 2013). The frequency of methylation was 75% in grade II oligoastrocytoma, 62.5% in grade III oligoastrocytoma, 78.6% in grade II oligodendroglioma, 41.9% in grade III oligodendroglioma, 22.2% in grade I pilocytic astrocytoma, 33.3% in grade II astrocytoma and 37.5% in grade III astrocytoma. Methylation was significantly higher in secondary GBM (100%) than primary GBM (8.1%) (p < 0.0001). According to grades, hypermethylation was significantly more frequent in grade II tumours (71.4%) than grade III tumours (44.7%) (p = 0.0001). *EMP3* hypermethylation was significantly associated with *IDH* mutations in astrocytoma (p = 0.0088), oligodendroglioma (p = 0.0006), oligoastrocytoma (p = 0.0095) and GBM (p = 0.0012). The correlation of *EMP3* hypermethylation with survival was evaluated in 64 oligodendroglial tumours

(38 grade II and 26 grade III) and Kaplan-Meier analysis revealed significantly longer OS in grade II ($p = 0.001$) and grade III tumours ($p = 0.034$).

1.13 MICRORNA (miRNA)

The recent discovery of microRNAs (miRNAs) and their pivotal role in regulation of genes leading to cancer development and progression has been widely examined in a number of studies. miRNA was first discovered in *Caenorhabditis elegans* in the early 1990s, where a small RNA encoded by *lin-4* was found to deregulate the expression of the protein-coding gene *lin-14* (Lee *et al*., 1993; Wightman *et al*., 1993). The small RNA of *lin-4* was subsequently revealed to be a miRNA.

miRNAs are non-coding 20-22 nucleotide RNA molecules that regulate gene expression (Ambros *et al*., 2004; Lee *et al*., 2009). Over 1500 human miRNAs are currently known which contributes to regulation of about 30% of total mRNA (Kozomara *et al*., 2011). miRNAs regulate gene expression via sequence complementarity between the sequence of the miRNA and that of the mRNA leading to altered transcription and/or translation. Such alterations affect biological processes including differentiation, proliferation and apoptosis, which are hallmarks of cancer. miRNAs may downregulate the expression of tumour-promoting genes and act as a tumour suppressor or may inhibit the expression of tumour suppressing genes and act as oncogenic factors (Malzkorn *et al*., 2010).

Mature miRNAs are generated using a multistep process, where pri-miRNA is transcribed and exported out of the nucleus with terminal processing forming a 21-23 nucleotide mature miRNA (Karsy *et al*., 2012). The miRNA is taken up by the RNA-induced silencing complex (RISC). Complete complementarity of the miRNA to mRNA leads to degradation of the mRNA via the RISC complex, while partial complementarity

may result in repression of translation or degradation of mRNA (Figure 1.3). Based on these molecular interactions, each miRNA is known to target multiple genes, subsequently altering a signalling pathway (Li *et al*., 2013).

Figure 1.3 Formation of mature miRNAs

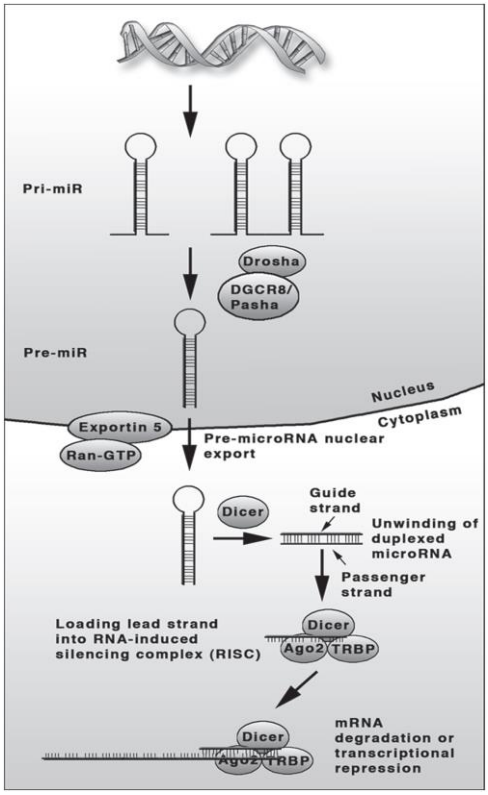

Mature miRNAs are formed from pre-miRNA via a multistep process using RISC (Adapted from Garzon *et al*., 2009).

1.13.1 miRNA in glioma

Important pathways in GBM have been shown to be targeted by miRNAs including tyrosine kinase signalling, cell cycle progression, gliomagenesis via stem-cell regulation and malignant progression (Masui *et al*., 2012). The role of specific miRNAs including miR-17-92, mir-21, miR-23a, miR-30e*, miR-34a and miR-128 in glioma development have been described below in a few studies.

The miR-17-92 cluster consists of two regulatory loops (Li *et al*., 2013). In loop 1, miR-17-92 suppressed proliferation and cell cycle progression by repressing E2F1 and c-myc. In loop 2, *CDKN1A* was targeted, activating CCND1/CDK4 complex and cell proliferation (Esquela-Kerscher *et al*., 2006; Sylvestre *et al*., 2007; Woods *et al*., 2007; Monzo *et al*., 2008; Pickering *et al*., 2009; Osada *et al*., 2011; Knoll *et al*., 2013). During gliomagenesis, miR-17-92 cluster was overexpressed, promoting the proliferative effects of loop 2 and c-myc upregulation inhibited anti-proliferative function of miR-17-92 in loop 1. Therefore, miR-17-92 enhanced the progression of glioma with the regulation of the two loops (Ernst *et al*., 2010).

miR-21 which is upregulated in glioma may contribute to *TGF-β*, p53 and EGFR-PI3K-Akt signalling pathways (Zavadil *et al*., 2007; Gabriely *et al*., 2008; Papagiannakopoulos *et al*., 2008). miR-221/222 cluster targets p27, p57, *PTEN*, *TIMP3*, p53-upregulated modulator of apoptosis (*PUMA*) and connexion 43 (*CX43*), which are associated with biological processes such as cell cycle progression and cell survival/apoptosis (Fornari *et al*., 2008; Garofalo *et al*., 2009; Zhang *et al*., 2010; Hao *et al*., 2012).

Studies have characterised miRNAs as regulatory molecules in the cellular signalling networks (Li *et al*., 2013). For example, mir-23a expression in GBM was found to be activated by cyclic adenosine monophosphate response element-binding protein (CREB), targeting and suppressing *PTEN* expression, leading to activation of the PI3K-Akt signalling pathway (Tan *et al*., 2012).

In glioma, miRNAs were reported to disrupt the negative feedback loops, resulting in activation of oncogenic signalling molecules (Li *et al*., 2013). For example, miR-30e* was found to be upregulated in glioma, targeting IκBα mRNA and suppressing its expression, therefore, negating the inhibitory effect of IκBα on NF-κB. mir-486 also induced overactivation of NF-κB signalling by suppressing the expression of A20, *CYLD* and Cezanne proteins (Song *et al*., 2013).

miR-34a expression was investigated by analysing the expression of its target genes, which includes mainly oncogenes such as *c-Met*, *Notch-1*, *Notch-2*, *CDK6* and *PDGFRA* (Li *et al*., 2009). Transfection of miR-34a in U87 cells and glioma stem cells reduced protein levels of Notch-1, Notch-2 and CDK6. In GBM tissue, miR-34a expression was found to be lower than in normal brain and miR-34a was also found to inhibit malignancy by regulating c-Met and Notch expression. The authors suggest that miR-34a might be a potential therapeutic agent for glioma.

1.13.2 Role of miRNA in malignant progression

A study investigated the role of 157 miRNAs in malignant progression in a cohort of 4 primary grade II tumours (3A, 1OA) that progressed to GBM (Malzkorn *et al*., 2010). Twelve miRNAs (miR-9, miR-15a, miR-16, miR-17, miR-19a, miR-20, miR-21, miR-25, miR-28, miR-130b, miR-140 and miR-210) showed upregulation associated with progression and 2 miRNAs (miR-184 and miR-328) showed dowregulation associated with progression in a majority of tumours examined. miR-10b was found to be associated with glioma malignancy as the expression levels of miR-10b in GBM are much higher than in other tumour grades (Sasayama *et al*., 2009). Other miRNAs implicated in malignancy of glioma include miR-296, miR-15b, miR-146b, miR-125b,

miR-153, miR-196a, miR-195, miR-455-3p, miR-10a, let-7 and miR-182 (Zhang et al., 2012).

1.14 CELL CULTURE MODEL

To study the functional and metabolic characteristics of the glioma, a cell culture model that represents the glioma *in vivo* is required. Short-term cell cultures derived from the original glioma or its archival source have been used to investigate their *IDH* mutation status, cell phenotype and growth rates. It has been reported by several studies that *in vitro IDH1* mutation in standard cell culture conditions cannot be maintained (Piaskowski *et al*., 2011). The reason for the elimination of the mutation is not clearly understood. Direct sequencing analysis of the frozen tumour cells and their corresponding cell cultures was performed and *IDH1* mutation was present in only the frozen tumour samples and not in cells derived from the tumours with *IDH1* mutations even after first passage. Furthermore, none of the 15 commercially available cell lines presented *IDH1* mutation.

Luchman *et al*., (2012) have established a brain tumour stem cell line (BT142) with an endogenous *IDH1* R132H mutation from an *IDH1* mutant anaplastic oligoastrocytoma tumour biopsy. The neurosphere method was used to establish the cell line and an orthotopic xenograft model was also developed. Endogenous 2-HG production was seen in both cell culture medium and the xenograft serum.

1.15 AIMS AND OBJECTIVES

Currently, there are no molecular markers that can determine the time and rate of malignant progression in LGG. This study focuses on understanding the genetic and epigenetic mechanisms involved in LGG that will allow identification of molecular markers for progression of LGG to more malignant tumours. The aims of this study include:

- To determine the *IDH1* and *IDH2* mutation status, *MGMT* methylation status in a panel of tumour samples and correlation with clinical parameters such as grade, age and histology. Mutations in *IDH1* and *IDH2* have been strongly associated with low grade glioma and are prognostic factors for a better outcome. *MGMT* methylation has been linked with the presence of *IDH1* mutation and is a predictive marker for response to alkylating agents such as TMZ.

- To identify and compare miRNA expression profiles of primary tumours based on grade, histology and *IDH* mutation status. Grade III tumours were included to determine if the grade III tumours were *de novo* or if they were grade II tumours misdiagnosed at the time of diagnosis.

- To identify differentially expressed miRNAs associated with different grades of LGG as well as deregulated pathways and associated genes that may play a role in LGG progression. Paired samples of primary and recurrent tumours were analysed to determine significant miRNAs that may promote genes involved in tumour progression. Copy number analysis was performed for these paired samples to determine any additional changes that may influence tumour progression.

- To ascertain if short-term cell culture is a good representative model to study LGG *in vitro*. To achieve this, the growth characteristics of short-term cell cultures, the mutation and methylation status of *IDH1*/*IDH2* and *MGMT* respectively was determined. The genomic and expression profiles of biopsy tissues and their derived short-term cell cultures were identified by copy number and miRNA expression analysis.

CHAPTER 2

MATERIALS AND METHODS

2.1 TUMOUR SAMPLES

This study was conducted under ethical approval granted by the Life Sciences Ethics Committee, University of Wolverhampton, LSEC/22/0909. Consented tumour biopsy samples were taken from the Brain Tumour North West and Walton Research Tissue Banks, UK (Ethics Committee approval reference number 09/H0304/8). Additional historical samples collected from the National Hospital of Neurology and Neurosurgery, London, UK previous to 1996 before implementation of HTA (Human Tissue Authority) were also used in this study. All samples were anonymised at source.

All samples were classified according to WHO classification (2007) (Louis *et al*., 2007) and they comprised of 36 A (WHO grade II), 7 OA (WHO grade II), 12 O (WHO grade II), 11 AA (WHO grade III), 16 AOA (WHO grade III), 10 AO (WHO grade III) and 3 GBM (WHO grade IV).

Analysis for primary/recurrent and biopsy/cell culture pairs was carried out using 12 and 17 paired samples respectively, although, not all pairs were available for each experiment.

2.2 TISSUE CULTURE

All cell culture protocols were performed in a sterile class II laminar flow cabinet (Telstar, UK) after sterilisation with 70% ethanol and 1% Trigene solution. Growth medium used for all cultures contained HEPES buffered Ham's F10 nutrient mix (Life Technologies Ltd, UK) with 10% foetal calf serum (FCS) (Life Technologies Ltd, UK).

2.2.1 Primary cultures:

Immediately after surgical resection, the tumour biopsy was placed in growth medium without 10% FCS, which contained 100U/ml penicillin (Sigma-Aldrich Company Ltd, UK), 100 µg/ml streptomycin (Sigma-Aldrich Company Ltd, UK) and 50 µg/ml kanamycin (Sigma-Aldrich Company Ltd, UK). The biopsy was stored at 4ºC for collection until transfer to the laboratory.

Approximately 10 mg of tissue was diced into fine pieces using crossed scalpels and transferred to a 25 ml universal tube containing the growth medium with the same concentration of antibiotics used in the collection media. The fragments were allowed to settle down and the supernatant was discarded after centrifugation at 11700 rpm for 5 minutes, this process was repeated twice. The tissue fragments were re-suspended in growth medium with 1ml collagenase (2000 U/ml) (Sigma-Aldrich Company Ltd, UK) and incubated at 37ºC for 4 hours. The sample was pipetted several times to promote disaggregation, centrifuged at 333 rpm for 5 minutes and the supernatant discarded. The cell solution was re-suspended in fresh growth medium containing antibiotics and transferred to a 25 cm^2 cell culture flask with overnight incubation at 37ºC. The medium was changed after 24 hours and cells were maintained at 37ºC.

2.2.2 Maintaining cells in culture:

The medium was changed twice weekly or when the medium turned yellow. The old medium was aspirated and replaced with fresh growth medium.

2.2.3 Passaging cells:

At confluence, cells were passaged as mentioned below and the passage number of the cell culture was increased by 1 each time. Each flask was split in a ratio of 1:3. The old media was aspirated and cells were rinsed with 3 ml Hanks' buffered salt solution (HBSS) (Sigma-Aldrich Company Ltd, UK). The cells were treated with 3ml trypsin (Life Technologies Ltd, UK) and incubated at 37ºC for 10-15 minutes to detach cells from the surface of the flask. The cell solution was transferred to a universal tube after addition of 7 ml media to inactivate trypsin and centrifuged at 1300 rpm for 5 minutes. The supernatant was carefully aspirated without disturbing the pellet, re-suspended in 10 ml of growth medium and transferred to a cell culture flask. The flask was incubated at 37ºC and the growth of the cells was monitored periodically. Antibiotics were used in the medium until cells reached passage 1 (p1).

Passaging of cells into flasks:
1 x 25cm^2 flask to 3 x 25cm^2 flasks or 1 x 75cm^2 flask
1 x 75cm^2 flask to 3 x 75cm^2 flasks or 1 x 175cm^2 flask
1 x 175cm^2 flask to 3 x 175cm^2 flasks

2.2.4 Reviving cells from storage in liquid nitrogen:

Cell suspension along with 10 ml growth medium was transferred to a universal, centrifuged at 1300 rpm for 5 minutes and the supernatant was removed. The pellet was re-suspended in 10 ml media and transferred to a flask. The flask was incubated at 37ºC and media was changed after 24 hours.

2.2.5 Preparation of cells for storage in liquid nitrogen:

The cells were trypsinised and re-suspended in fresh 10 ml media, as described above. Cells were counted using the Coulter Counter (Beckman Coulter Inc., USA) with 0.4 ml of cell solution and 19.6 ml of isoton solution (Beckman Coulter Inc., USA). The remaining cell solution was centrifuged at 1300 rpm for 5 minutes to form a pellet. The supernatant was removed and cells were re-suspended in a solution with 90% FCS and 10% dimethyl sulfoxide (DMSO) (Sigma-Aldrich Company Ltd, UK) to a final concentration of $1x10^6$ cells/ml. A volume of 1ml cell solution was transferred to each cryovial and stored in liquid nitrogen.

2.3 CALCULATION OF DOUBLING TIME

A growth curve was generated for the cell cultures used in the study to determine the growth characteristics of each cell culture with calculation of doubling times. For each culture, 5000 cells per well were seeded in triplicates into 96-well plates. After 24 hours incubation, the cells were fixed with 10% trichloroacetic acid (TCA) followed by staining with sulforhodamine (SRB) solution (0.4% SRB dye and 1% Acetic acid) before reading the absorbance each day. The experiment was performed in triplicate for each cell culture for a maximum period of 11 days using a GloMax®-Multi+ Microplate Multimode Reader with Instinct® (Promega, UK) at 560nm. The growth curve is shown with three phases; *lag phase*, *log phase* and *stationary phase*. The *lag phase* represents the time it takes for the cells to attach, the *log phase* represents the time when the cells grow exponentially and the *stationary phase* is when the cell culture becomes confluent and the growth rate is slow. The population doubling time was calculated in Excel using two marked points on the log phase to determine the doubling time.

2.4 ASSESSMENT OF TUMOUR CELL GROWTH ON FEEDER LAYERS

An assay with 3T3 cells as a feeder layer was performed to investigate the tumourigenicity of short-term cell cultures derived from tumour biopsy. Approximately $1x10^6$ 3T3 cells (NIH 3T3 mouse fibroblast cells; European Collection of Cell Cultures (ECACC)) were grown until confluent in a 25 cm^2 flask and treated with 2 µg/mL mitomycin C (Sigma-Aldrich Company Ltd., UK) at 37°C for 2 hours to arrest the cell cycle. After incubation, the cells were washed three times with serum free media and maintained at 37°C in growth medium. Next day, the medium was changed and the cells were incubated at 37°C for 24 hours. LGG cells with a seeding density of 2.5-10 x 10^4 cells were seeded onto the 3T3 feeder layer and incubated at 37°C. The cells were grown for a period of time until colonies were observed.

2.5 IMMUNOSTAINING

Approximately $1x10^5$ cells were grown in each well of 8-well chamber slide (Thermo Scientific, UK) in 0.5 ml growth medium until 50-60% confluent. Media was removed and cells were washed with 1X Tris buffered saline (TBS) three times before fixing with pre-chilled 1:1 methanol:acetone. Cells were then rehydrated with TBS and washed three times. Cells were incubated for 30 minutes at room temperature with 100 µl primary mouse monoclonal antibody against glial fibrillary acidic protein (GFAP at dilution 1:50) (Dako, UK), IDH1-R132H (1:200; Dianova, Germany), nestin (1:200; Millipore, UK), Ki-67 (1:50; Dako, UK), p53 (1:25; Dako, UK), CD34 (1:100; Leica Biosystems, UK), epithelial membrane antigen (EMA) (1:50; Leica Biosystems, UK) and MGMT (Abcam, UK). A negative control without any primary antibody was included. After incubation, the antibody solution was discarded and cells were rinsed

twice with TBS. 100 µl of biotinylated secondary antibody (Vectastain Universal Elite ABC Kit, Vector Laboratories, UK) was added to each chamber and incubated for 30 minutes at room temperature. Cells were rinsed twice with TBS and 100 µl of tertiary antibody, streptABComplex/HRP solution, (Vectastain Elite ABC Reagent, Vector Laboratories, UK) was added to each chamber and incubated for 30 minutes at room temperature. The cells were washed twice with TBS and 100 µl diaminobenzidene (DAB) solution (Dako, Agilent Technologies, UK) and incubated for 5 minutes before washing with distilled water. Cells were counterstained with haematoxylin for 5 seconds followed by rinsing with warm tap water several times and dehydration of cells through a graded alcohol series. The chamber was removed after the last rinse and the slide was rinsed in xylene before mounting with a large coverslip using styrolite. Scoring was done following a certain criteria for each of the molecular markers. Scoring for MGMT expression was done using quick Allred score method based on the proportion of positively stained nuclei and intensity of staining (NHSBSP January 2005). Tonsil was used as a positive control as recommended by the manufacturer of the antibody against MGMT. Scores for proportion were assigned as follows: 0, no staining; 1, <1% nuclei staining; 2, 1-10% nuclei staining; 3, 11-33% nuclei staining; 4, 34-66% nuclei staining and 5, 67-100% nuclei staining. Scores for intensity were as follows: 0, no staining; 1, weak staining; 2, moderate staining and 3, strong staining.

2.6 ISOLATION OF DNA

DNA was extracted from frozen tissue, cultured cells and formalin-fixed paraffin embedded (FFPE) sections using QIAamp DNA Mini and Blood kit (Qiagen Ltd, UK) according to Agilent array comparative genomic hybridisation (aCGH) protocol (v4.0).

2.6.1 Frozen tissues:

Approximately 25 mg of tissue was diced into smaller pieces, placed in a 1.5 ml centrifuge tube containing 180 µl buffer ATL. The solution was homogenised using a syringe with a gauge size of 0.6 mm x 30 mm (BD Microlance, USA). The tissue was incubated with 20 µl proteinase K (20mg/ml) at 56ºC for 30 minutes or until the tissue was completely lysed. The sample was centrifuged briefly before adding 200 µl buffer AL followed by vortexing and incubation at 70ºC for 10 minutes. The solution was transferred to the QIAamp Mini spin column after addition of 200 µl 100% ethanol and centrifuged at 8000 rpm for 1 minute. After centrifugation, the column was washed with buffer AW1 and 80% ethanol. The QIAamp Mini spin column was placed in a new 1.5 ml centrifuge tube and 20 µl nuclease-free water was added to the column. The sample was centrifuged at 8000 rpm for 1 minute to elute the DNA and was stored at -20ºC until further use.

2.6.2 Cultured cells:

A cell pellet with 2-5 x 10^6 cells was washed with 200 µl phosphate buffered saline (PBS) (Sigma-Aldrich Company Ltd, USA) and incubated with 20 µl of proteinase K at 56ºC for 10 minutes to promote the lysis of cells. It was briefly centrifuged, 200 µl of 100% ethanol was added and the tube vortexed. Thereafter, the same steps were followed as for the frozen tissues and DNA was stored at -20ºC.

2.6.3 FFPE tissues:

Paraffin cores measuring 2.0 mm were extracted using the Harris Uni-Core (Ted Pella, Inc., USA) from H&E sections that had been confirmed as tumour by a neuropathologist (Professor Tim Dawson, Royal Preston Hospital, UK). The core was washed with 480 µl PBS and 20 µl of 10% Tween 20 was added. The sample was

incubated at 90ºC for 10 minutes followed by immediate centrifugation at 13,000 rpm for 15 minutes and placed on ice for 2 minutes. The wax disc was removed using forceps and the supernatant was removed. To the pellet, 1 ml 100% ethanol was added, vortexed and centrifuged at 13,000 rpm for 5 minutes. Ethanol was removed without disturbing the pellet and residual ethanol was left to evaporate with the lid open at room temperature. The pellet was mixed with 400 µl of 1M sodium thiocyanate (NaSCN) solution (Sigma-Aldrich Company Ltd, UK) and incubated overnight at 37ºC. The sample was centrifuged for 20 minutes at 13000 rpm and the supernatant was removed followed by washing with 400 µl PBS. The sample was treated with 360 µl buffer ATL and 40 µl proteinase K and incubated overnight at 56ºC. The sample was centrifuged before addition of 40 µl proteinase K and incubation at 56ºC for 6-8 hours. Another 40 µl proteinase K was added to the sample and incubated at 56ºC overnight. Finally, 400 µl buffer AL was added to the mix and incubated at 56ºC for 10 minutes. The sample was centrifuged at 8000 rpm for 30 seconds and 440 µl of 100% ethanol was added. The sample mix was added to the DNeasy Mini spin column, centrifuged for 1 minute at 8000 rpm and the column was placed in a fresh 2 ml collection tube. Buffer AW1 and 80% ethanol was used to wash the column and the same steps were performed to elute the DNA as for the frozen tissues.

The quality of the DNA extracted from the paraffin tissue was determined by electrophoresis through a 2% agarose gel at 100 V for 1 hour and compared with a 1 Kb ladder (Thermo Scientific, UK). Good quality FFPE DNA was visualised as a smear using a UV transilluminator (Syngene, UK) and photographed using GeneSnap (Syngene, UK).

2.7 ISOLATION OF miRNA

Total RNA containing microRNA was extracted using the mirVana miRNA isolation kit (Life Technologies Ltd, UK) according to the manufacturer's instructions. For cultured cells, 3-6 x 10^6 cells were lysed using 300-600 µl Lysis/Binding solution depending on the size of the pellet. The solution was vortexed briefly to lyse the cells completely. For frozen tissue, 10 volumes of Lysis/Binding buffer were added to approximately 25 mg of tissue on ice. The solution was homogenized using a syringe with a needle gauge size of 0.6 mm x 30 mm (BD Microlance, USA) and 1/10 volume of miRNA homogenate additive was added to the mixture followed by 10 minutes incubation on ice. A volume of Acid-Phenol:Chloroform (Sigma-Aldrich Company Ltd, UK) equal to the lysate volume was added and vortexed. The sample was centrifuged at 13000 rpm speed at 4ºC to separate the aqueous and organic phases. The aqueous (upper) phase was transferred into a fresh 1.5 ml centrifuge tube and 1.25 volumes of 100% ethanol was added and passed through the column followed by centrifugation at 13000 rpm for 15 seconds. The column was washed with 700 µl miRNA Wash Solution 1 and twice with 500 µl Wash Solution 2/3. Total RNA was eluted in 20 µl nuclease-free water by centrifuging at 13000 rpm speed for 20-30 seconds and stored at -80ºC.

2.8 ASSESSMENT OF DNA AND RNA

The quantity and quality of DNA and RNA was assessed using a NanoDrop 2000 spectrophotometer (Thermo Scientific, UK). Samples with an A260/280 ratio of 1.8-2.0 and A260/230 of more than 2.0 were considered good quality DNA. Good quality RNA with an A260/280 ratio of 2.0 and A260/230 of 2.0-2.2 was used for miRNA expression analysis.

For miRNA quality assessment, Agilent 2100 Bioanalyzer (Agilent Technologies Ltd, UK) was used and the sample was screened for the presence of two ribosomal peaks representing 18S and 28S along with a peak for smaller RNAs. The Bioanalyzer assigned an RIN number (RNA Integrity number) ranging from 1 to 10; 1 being the most degraded and 10 being the most intact. Samples with a high RIN number > 9 and with a peak representing the smaller RNAs were used for miRNA array analysis.

2.9 PCR AMPLIFICATION FOR *IDH1* AND *IDH2*

IDH1 and *IDH2* primer sets (Sigma-Aldrich Company Ltd, UK) used for PCR amplification were adopted from a study by Sonoda et al. (2009). A negative control containing all PCR components except template DNA was included in each experiment. Exons 4 of *IDH1* and *IDH2* genes containing codons 132 and 172 respectively were amplified using the primer sequences, *IDH1* forward – ATAGGTCGTCATGCT, *IDH1* reverse – AGCATGACGACCTA and *IDH2* forward – CAAGCTGAAGAAGATGTGGAA, *IDH2* reverse – CAGAGACAAGAGGATGGCTA.

PCR amplification was performed using 100ng DNA in a final volume of 20 µl containing 10 mM dNTP mix, 10 mM of forward and reverse primers and 2 U HotStarTaq DNA polymerase (Qiagen Ltd, UK) supplemented with 25 mM $MgCl_2$. Following a 15 minute denaturation step at 95°C, 40 cycles of 30 seconds at 95°C, 30 seconds at 56ºC and 40 seconds at 72ºC with a final 10 minute extension at 72ºC was used. Amplification products were visualised under UV light after separation through a 2% agarose gel containing 1X TAE and 10 mg/ml ethidium bromide solution at 100 V for 1 hour using a 100 bp ladder (Thermo Scientific, UK).

2.10 PREPARATION OF PCR PRODUCTS FOR SEQUENCING

The amplification products were purified using GenElute PCR Clean-Up Kit (Sigma-Aldrich Company Ltd, UK) according to the manufacturer's instructions. A GenElute Miniprep Binding column was prepared with 0.5 ml of column preparation solution and centrifuged at 13000 rpm for 1 minute. The eluate was discarded and 5 volumes of binding solution were added to 1 volume of PCR product. The solution was transferred into the binding column and centrifuged at 13000 rpm for 1 minute. The column was washed with 0.5 ml of wash solution and centrifuged at maximum speed (> 14000 rpm) for 3 minutes to remove leftover ethanol. The miniprep column was transferred to a fresh 2 ml collection tube and 15 µl elution solution was added to elute purified DNA.

2.11 DIRECT SEQUENCING

The Sanger sequencing method (Sanger *et al*., 1977) was used to determine the sequence of nucleotides within a sample. PCR purified products (1 ng/µl per 100bp) were analysed by Source BioScience LifeSciences (Cambridge, UK). The sequencing was performed using the BigDye® Terminator v3.1 cycle sequencing kit (Life Technologies Ltd, UK) with 3.2 pmol of each primer on an ABI 3730xl DNA analyser (Applied Biosystems Ltd, UK). Analysis was performed using the Sequence Scanner software v1.0 (Life Technologies Ltd, UK).

2.12 BISULFITE MODIFICATION OF DNA

DNA was bisulfite-modified using EZ DNA Methylation-Gold Kit (Zymo Research, UK) with 200–500 ng of DNA as starting material. The sample was mixed with CT

conversion reagent and incubated at 95°C for 12 minutes and 64°C for 2.5 hours. The DNA mix was added to a column placed in a collection tube with 600 µl M-binding buffer. The sample was mixed well with inversion a few times and centrifuged at 13000 rpm for 30 seconds. Flow-through was discarded; 100 µl of wash buffer was added to the column and centrifuged at 13000 rpm for 30 seconds. Desulphonation buffer was added to the column, incubated at room temperature for 15-20 minutes and centrifuged at full speed (> 14000 rpm) for 30 seconds. The sample was washed twice with wash buffer followed by addition of elution buffer to elute the DNA. DNA was stored at -20°C until further use.

2.13 METHYLATION SPECIFIC PCR (MS PCR)

Amplification of *MGMT* gene was carried out using two sets of primers for unmethylated and methylated modified DNA, previously described by Esteller *et al*., (1999). PCR amplification was performed in a final volume of 20 µl containing 10x buffer (Qiagen Ltd., UK), 200 µM dNTP mix (Sigma-Aldrich Company Ltd., UK), 10 pmol of forward and reverse primers (Sigma-Aldrich Company Ltd., UK), 5U HotStarTaq DNA polymerase (Qiagen Ltd., UK) and 200 – 500 ng bisulfite-modified DNA. A positive control (IN699) and a negative control (with no DNA) were included in each experiment. Following an initial incubation at 95°C for 15 minutes, 35 cycles at 94°C for 30 seconds, 59°C for 30 seconds and 72°C for 30 seconds were performed with a final extension at 72°C for 5 minutes.

Amplification products were separated using a 3% agarose gel at 100 V for 1 hour and a 50bp ladder (Thermo Scientific, UK). PCR products were visualised under UV light.

2.14 STATISTICAL ANALYSIS

Statistical analysis was performed using GraphPad Prism v6 (USA) and SPSS statistics v20 (IBM, USA). Non-parametric tests such as log-rank (Mantel Cox) test, Fisher's exact test and Mann Whitney test were used to determine significance between various molecular characteristics and correlation with PFS and OS as described in Chapter 3. Non-parametric tests were appropriate for this study as they are more robust and take fewer assumptions. Cox proportional hazard model for multivariate analysis was used to determine strong and independent factors for a better outcome. A p-value < 0.05 was considered as statistically significant.

2.15 ARRAY COMPARATIVE GENOMIC HYBRIDIZATION (aCGH)

Array CGH was carried out on a 244K array (Agilent Technologies Ltd, UK) using Agilent Oligonucleotide Array-Based CGH for Genomic DNA Analysis v4.0.

2.15.1 Heat fragmentation

The optimal size range of DNA for aCGH is 1000-3000bp (Agilent specialist recommendation) and high molecular weight samples as well as reference samples underwent heat fragmentation for 0, 5 and 10 minutes to achieve this size range. Following fragmentation, the size range of each sample was assessed using a 0.8% agarose gel and HighRanger 1 kb DNA ladder (Geneflow Ltd, UK) as shown in Appendix II.

2.15.2 Labelling

A concentration of 1500 ng DNA in a final volume of 16.5 µl made up with nuclease-free water was heat-fragmented at 95°C for an appropriate time determined as above and kept on ice for 3 minutes. A master mix (3.5 µl) with 10x labelling solution (2 µl) and ULS-Cy3 or ULS-Cy5 dyes (1.5 µl for both; Agilent Technologies Ltd, UK) was prepared; tumour samples were labelled with Cy3 and sex-matched with reference samples (male/female human genomic DNA; Promega, UK) labelled with Cy5. The sample mixture containing the DNA and labelling mix was incubated at 85°C for 30 minutes, 4°C for 3 minutes and centrifuged briefly after incubation. Agilent KREApure columns were used for removal of non-reacted ULS-Cy by preparing the columns and rinsing them with nuclease-free water. ULS-labelled DNA was added to the column and centrifuged at maximum speed to collect the purified labelled DNA which was quantified to determine the degree of labelling calculated as below:

$$\text{Degree of labelling} = \frac{340 \times \text{pmol per µl dye}}{\text{ng per µl DNA} \times 1000} \times 100\%$$

The optimal range for Cy5 degree of labelling was 0.75-2.5% and for Cy3 was 1.75-3.5% with a Cy3 minus Cy5 range of 1-2%.

Labelled gDNA sample was mixed with the reference sample to a total volume of 37 µl. If required, DNASpeed Vac DNA 110 (Savant Instruments Inc., USA) was used to concentrate the samples to a volume of 37 µl in order to give a final volume of 390 µl following the addition of the hybridisation mix described below.

2.15.3 Hybridisation

Blocking agent (100x) (Agilent Technologies Ltd, UK) was prepared with nuclease-free distilled water, vortexed and incubated at room temperature for 60 minutes to

reconstitute before storage at -20°C. Hybridisation master mix was made with nuclease-free water (37.8 µl), 1.0 mg/ml Cot-1 DNA (50 µl; Invitrogen, UK), 100x Agilent Blocking agent (5.2 µl) and 2x HI-RIPM hybridisation buffer (260 µl; Agilent Technologies Ltd, UK) and added to each labelled gDNA sample. Sample mix was incubated at 95ºC for 3 minutes and 37ºC for 30 minutes before Agilent-CGH Block (130 µl; Agilent Technologies Ltd, UK) was added and mixed well to stop the labelling reaction.

A clean gasket slide was loaded onto the Agilent SureHyb chamber (according to manufacturer's instructions) and hybridisation sample mix was slowly dispensed in a drag and dispense manner. A microarray slide was placed onto the gasket slide and the SureHyb chamber was then covered onto the slides with tightening of the clamps firmly. The assembled chamber was vertically rotated to assess the mobility of the bubbles and to uniformly spread the liquid on the slides. The assembly was tapped hard to move the stationary bubbles. The assembled chamber was incubated at 65ºC rotating at 20 rpm for 40 hours in a hybridisation oven (Agilent Technologies Ltd, UK).

2.15.4 Microarray washes

After the incubation, the microarray slide was washed with wash buffer 1 at room temperature for 5 minutes, wash buffer 2 at 37°C for 1 minute, acetonitrile at room temperature for 10 seconds and stabilisation and drying solution at room temperature for 30 seconds. The slides were placed in a slide holder and stored in dark until ready to be scanned to avoid oxidising of the Cy5 dye.

2.15.5 Array scanning and Analysis

The Agilent Microarray scanner (model G2565B) was used to scan each microarray slide with the AgilentHD_CGH protocol (CGH_107_Sep09) with the following default

QC settings: scan region of 61 x 21.6 mm, scan resolution of 5 µm, 16 bit TIFF image and laser scanning at 100% for both red and green signals.

The TIFF image was used for data extraction using the Feature Extraction program (Agilent Technologies Ltd) generating a QC report and .txt file containing all the probes and aberrations. The .txt file was analysed using CytoGenomics (v2.7; Agilent Technologies Ltd, UK) and Partek Genomics Suite (version 6.6; Partek Inc., USA) softwares.

The Feature Extraction program summarises the statistics for the metrics on each QC report and shows if the thresholds were exceeded. The metrics include grid, derivative of log ratio SD, for both red and green signals, background noise, signal to noise and signal intensity. Arrays with QC metrics within the excellent and good ratio thresholds were used for further analysis.

2.16 miRNA ARRAY

The quality of the RNA samples was assessed using Agilent 2100 bioanalyser (Agilent Technologies Ltd, UK) and QC (quality control) reports were generated for each sample showing the RNA integrity represented by RIN as discussed previously in this chapter. Both QC and microarray analysis were performed at Cambridge Genomics Services (Cambridge, UK). Microarray analysis was performed using 3D Gene Human miRNA oligo chips (Toray, Japan) containing 1719 human miRNAs selected from the miRBase database, release 19. Spike controls were included in the array for QC. High quality RNA sample containing miRNA was assessed using a bioanalyser and 250 ng of sample was used for the microarray.

2.16.1 Labelling

The extracted RNA was labelled with Hy5 using the miRCURY LNA Array miR labeling kit (Exiqon, Vedbaek, Denmark). Total RNA with a concentration of 250 ng in 5 µl volume was made up with nuclease-free water and placed in a 1.5 ml centrifuge tube. A labelling reaction mix containing the total RNA, 0.5 µl CIP buffer, 0.5 µl Calf intestine phosphatase and 1 µl miRNA spike control to a total volume of 4 µl made up with nuclease-free water was incubated at 37°C for 30 minutes, 95°C for 5 minutes and left on ice for 2 minutes. Three µl labelling buffer, 1.5 µl fluorescent label (Hy5), 2 µl DMSO and 2 µl labelling enzyme were then added to a total volume of 12.5 µl. The reaction was incubated at 16°C for 1 hour followed by 15 minutes at 65°C and was stored at 4°C until hybridisation.

2.16.2 Preparation of hybridisation solution

To the labelled miRNA, 0.6 µl hybridisation buffer A and 52.5 µl miRNA hybridisation buffer V2 was added and degasified (ULVAC, Inc.: MDA-015) for 18 minutes. The degasified solution was incubated at 65°C for 3 minutes before centrifuging at 16000 rpm for 1 minute. The hybridisation solution was incubated at 32°C for 5 minutes before proceeding to the next step.

2.16.3 Hybridisation

The reaction chamber on the 3D-Gene miRNA chip was loaded with 50 µl of the hybridisation solution and sealed with a cover. The hybridisation chamber was mounted on the shaker and 30 µl nuclease free water was added into both sides of the chamber to maintain humidity. The chamber was placed horizontally with the cover plate on top and screwed to seal the chamber. The hybridisation was carried out at 32°C for 16 hours rotating at 250 rpm in a hybridisation oven.

2.16.4 Washing

The 3 wash solutions were warmed up at 30°C before removing the hybridisation chamber from the oven. The slide was washed in first wash solution for 5 minutes, second wash solution for 10 minutes and third wash solution for 5 minutes with constant shaking. The miRNA chip was stored in the dark until ready to be scanned.

2.16.5 Scanning and analysis

The fluorescent signals were scanned by a 3D-Gene scanner (Toray) with default settings and the raw data files were analysed using Partek Genomics Suite (version 6.6; Partek Inc., USA) software.

CHAPTER 3

ANALYSIS OF *IDH* MUTATION AND *MGMT* METHYLATION IN PRIMARY LOWER GRADE DIFFUSE GLIOMA

3.1 INTRODUCTION

IDH1 mutation is most frequent in LGG (~80%) and is an important prognostic marker for better outcome (Thon *et al*., 2012). The isoform *IDH2* is less frequently mutated and occurs mutually exclusively to *IDH1* mutation. The most frequent mutation of *IDH1* involves substitution of arginine residue at position 132 to histidine (R132H) and the *IDH2* mutation involves the equivalent position 172 where arginine is substituted to lysine (R172K) as the most common mutation. *MGMT* promoter methylation is the only predictive marker for response to alkylating agents such as TMZ used in chemotherapy (Takahashi *et al*., 2013). In tumours with hypermethylation of *MGMT*, expression of *MGMT* is reduced and cytotoxicity of alkylating agents is enhanced. Both *IDH1* mutation and *MGMT* methylation are associated with better outcome in glioma.

The aim of this chapter was to investigate relationships between *IDH1* and *IDH2* mutation and/or *MGMT* methylation status and clinicopathological parameters including grade, age, histology and outcome in primary tumours. The hypothesis was that tumours with *IDH1* mutation are *MGMT* methylated and tumours with *IDH1* wild type are unmethylated. The comparative assessment of two methods for analysis of *MGMT* methylation, MS PCR and immunohistochemistry (IHC) is also described in this chapter. Moreover, association of *IDH1* mutation, *MGMT* status, age and grade with PFS and OS was determined.

3.2 SAMPLE COHORT

The sample cohort comprised 66 primary tumours, 38 of which were grade II tumours (25 A, 6 OA, 7 O) and 28 were grade III tumours (8 AA, 13 AOA, 7 AO). Patients were treated with a range of different therapies including radiotherapy and chemotherapy using PCV and TMZ. Treatment information was available for 15 cases as detailed in Appendix III.

3.3 *IDH* MUTATION ANALYSIS

The *IDH* mutation status of 66 tumour samples was determined by direct sequencing and the frequency and spectrum of the mutations is summarised in Table 3.1. *IDH1* mutation was detected in 60% A (15/25), 83% OA (5/6), 100% O (7/7), 25% AA (2/8), 38% AOA (5/13) and 57% AO (4/7). All mutations were heterozygous and the overwhelming majority (97%, 37/38) were R132H (CGT to CAT) with R132S (CGT to AGT) present in only 1 AO tumour (BTNW67). *IDH2* mutation analysis was completed for 41 cases due to constraints on availability of tumour DNA. An R172K (AGG to AAG) mutation was detected in BTNW15 (AO) which was *IDH1* wild type. Numerous studies have demonstrated that *IDH2* mutations are mutually exclusive with *IDH1* mutations (Hartmann *et al*., 2009; Sonoda *et al*., 2009; Yan *et al*., 2009). Of the 25 tumours for which *IDH2* mutation analysis was not completed, 22 had *IDH1* mutation, and hence, it is extremely unlikely that concurrent *IDH2* mutations were present. Examples of the chromatograms for the mutations identified in this study are given in Figure 3.1.

Table 3.1 *IDH* mutation status in primary grade II and grade III glioma

Tumour	Age[a]	Sex[b]	Grade	Histology[c]	*IDH1* status[d]	*IDH2* status[e]	PFS[f]	OS[g]
BTNW17	69	F	II	A	WT	WT	4.5	4.5 (D)
BTNW20	26	M	II	A	R132H	WT	83	94 (A)
BTNW61	32	M	II	A	R132H	WT	-	88.5 (A)
BTNW124	29	M	II	A	WT	WT	-	65.5 (D)
BTNW160	35	M	II	A	R132H	NA	67	78 (A)
BTNW203	42	F	II	A	R132H	WT	52.5	75 (A)
BTNW210	53	F	II	A	R132H	NA	-	74.5 (A)
BTNW212	50	M	II	A	R132H	NA	-	45.5 (D)
BTNW365	42	F	II	A	R132H	WT	28.5	37.5 (D)
BTNW367	56	M	II	A	WT	WT	1	62 (A)
BTNW381	54	M	II	A	WT	WT	-	25.5 (D)
BTNW680	59	M	II	A	WT	WT	-	13 (D)
BTNW736	63	F	II	A	WT	WT	-	8 (D)
BTNW761	25	M	II	A	R132H	NA	-	40.5 (A)
BTNW818	60	F	II	A	WT	WT	24.5	29 (D)
BTNW823	61	F	II	A	R132H	NA	-	36.5 (A)
BTNW830	21	M	II	A	WT	NA	-	36 (A)
BTNW868	39	F	II	A	R132H	NA	22.5	33.5 (A)
BTNW870	17	M	II	A	WT	WT	1	33 (A)
BTNW931	30	M	II	A	R132H	NA	-	28.5 (A)
BTNW1005	43	F	II	A	R132H	NA	-	13.5 (A)
BTNW1028	40	M	II	A	R132H	NA	-	13.5 (A)
Liv002	34	F	II	A	R132H	WT	-	25 (A)
Liv003	30	F	II	A	R132H	WT	-	22 (A)
Liv007	40	M	II	A	WT	WT	-	8 (D)
BTNW13	40	F	II	OA	R132H	NA	44.5	74 (D)
BTNW503	51	M	II	OA	R132H	NA	42.5	53.5 (A)
BTNW613	37	M	II	OA	R132H	NA	37	49.5 (A)
BTNW726	45	M	II	OA	R132H	NA	17	43.5 (A)
BTNW929	43	F	II	OA	WT	WT	-	29 (A)
Liv015	36	M	II	OA	R132H	WT	-	13 (A)
BTNW188	43	F	II	O	R132H	NA	-	76 (A)
BTNW326	56	F	II	O	R132H	NA	33.5	37.5 (D)
BTNW531	29	M	II	O	R132H	NA	-	52 (A)
BTNW882	82	M	II	O	R132H	NA	-	32 (A)
Liv020	75	M	II	O	R132H	WT	-	24.5 (A)
Liv024	30	M	II	O	R132H	WT	-	12 (A)
Liv026	58	M	II	O	R132H	WT	-	13.5 (A)
BTNW19	42	F	III	AA	R132H	NA	-	70 (D)
BTNW38	48	M	III	AA	WT	WT	-	4.5 (D)
BTNW126	66	M	III	AA	WT	WT	5	6 (D)
BTNW173	50	M	III	AA	R132H	WT	-	5.5 (D)
BTNW211	72	M	III	AA	WT	WT	-	2 (D)
BTNW421	59	M	III	AA	WT	WT	-	7.5 (D)
BTNW458	71	F	III	AA	WT	WT	-	17 (D)
BTNW925	78	M	III	AA	WT	NA	-	1.5 (D)
BTNW9	62	F	III	AOA	WT	WT	-	17.5 (D)
BTNW14	43	M	III	AOA	R132H	WT	64.5	95.5 (A)
BTNW120	27	M	III	AOA	R132H	NA	95.5	138 (D)
BTNW174	42	F	III	AOA	WT	WT	36	45.5 (D)
BTNW183	66	F	III	AOA	WT	WT	-	0.5 (D)
BTNW325	46	M	III	AOA	WT	NA	230.5	263 (D)
BTNW495	71	F	III	AOA	WT	WT	-	8.5 (D)
BTNW527	59	F	III	AOA	WT	WT	-	2.5 (D)
BTNW614	49	M	III	AOA	R132H	NA	14.5	21.5 (D)
BTNW686	56	M	III	AOA	WT	WT	-	16 (D)
BTNW703	46	M	III	AOA	R132H	NA	-	45.5 (A)
BTNW825	62	F	III	AOA	WT	WT	-	36 (A)
BTNW864	39	M	III	AOA	R132H	NA	-	34 (A)
BTNW15	56	M	III	AO	WT	R172K	13.5	14.5 (D)
BTNW67	62	F	III	AO	R132S	WT	-	2 (D)
BTNW179	35	F	III	AO	R132H	WT	-	14.5 (D)
BTNW460	29	M	III	AO	R132H	WT	-	22 (D)
BTNW738	66	M	III	AO	WT	WT	-	12 (D)
BTNW757	72	M	III	AO	WT	WT	-	6 (D)
BTNW804	44	M	III	AO	R132H	WT	-	11 (D)

[a] Age at diagnosis in years; [b] M, male; F, female; [c] A, astrocytoma; OA, oligoastrocytoma; O, oligodendroglioma; AA, anaplastic astrocytoma; AOA, anaplastic oligoastrocytoma; AO – anaplastic oligodendroglioma; [d] R132H, *IDH1* mutant; WT, wild type; [e] R172K, *IDH2* mutant; WT, wild type; [f] PFS in months; [g] OS in months; A, alive; D, dead; NA, not available.

Figure 3.1 Sequencing chromatogram depicting *IDH1* and *IDH2* mutations

***IDH1* mutation**

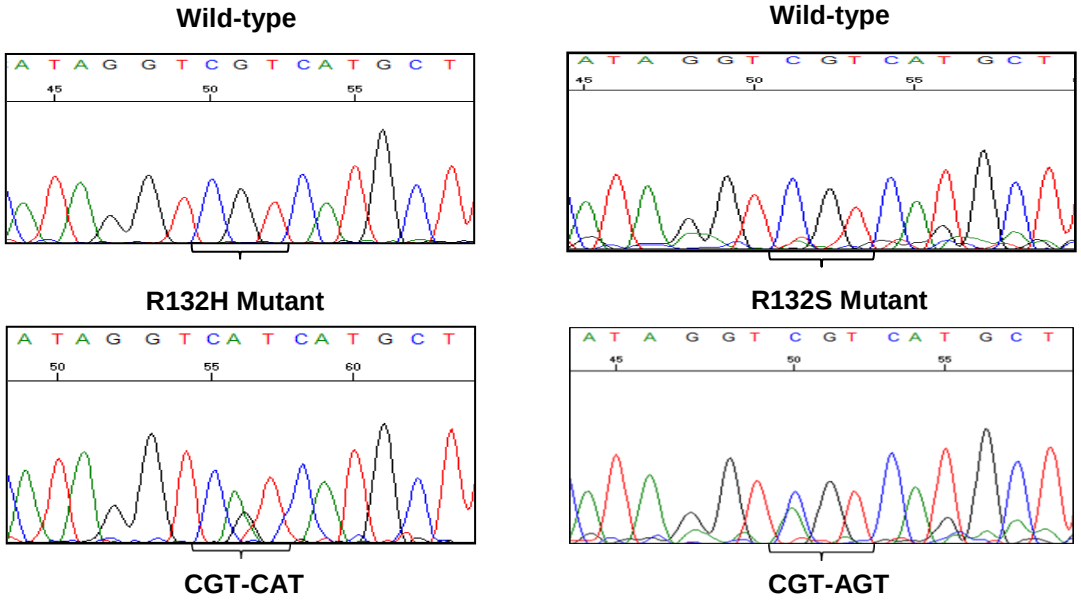

***IDH2* mutation**

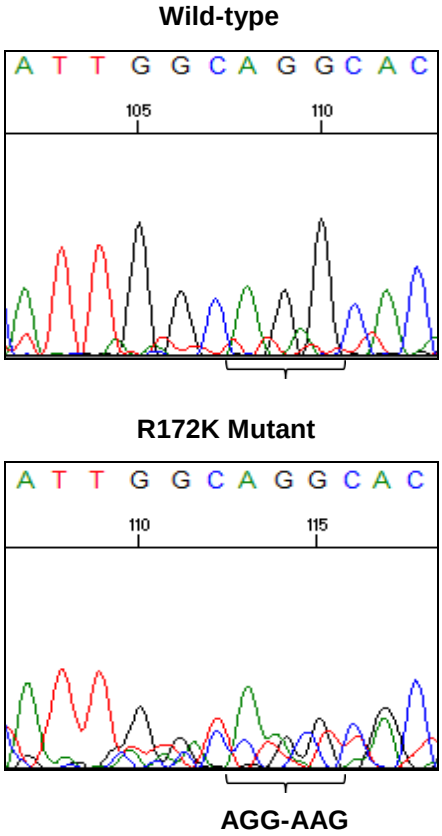

Representative examples for IDH1-R132H, IDH1-R132S and IDH2-R172K mutation as determined by direct sequencing.

3.3.1 Relationship between IDH1 status and grade

The frequency of *IDH1* mutation was significantly higher in grade II tumours, 27/38 (71%) compared with grade III tumours, 11/28 (39%) ($p < 0.0001$; Fisher's exact test).

3.3.2 Relationship between IDH1 status and histology

IDH1 status was analysed in each of the histological groups comprising A, OA, O, AA, AOA and AO tumours and the results are summarised in Table 3.2. *IDH1* mutations were most frequently present in grade II tumours with an oligodendroglial component (O 100%, 7/7; OA 83%, 5/6 too few cases in comparative groups to complete statistical analysis) compared to pure astrocytic tumours (A 60%, 15/25, $p = 0.178$; Fisher's exact test). Similarly, in the grade III tumours, a higher proportion of AO (57%, 4/7, $p = 0.011$; Fisher's exact test) and AOA (38%, 5/8, $p = 0.008$; Fisher's exact test) carried *IDH1* mutations compared to AA (27%, 2/6, $p = 0.054$; Fisher's exact test).

3.3.3 Relationship between IDH1 status and age

Patients with *IDH1* mutations were younger than those with wild type *IDH1* ($p = 0.0002$; Mann Whitney test) and the data is represented in Figure 3.2. The median age for patients with tumours carrying *IDH1* mutation was 42 years and that of patients with *IDH1* wild type tumours was 59 years. When broken down by histology as illustrated in Figure 3.3 and Table 3.3, patients with *IDH1* wild type tumours tended to be older than those with *IDH1* mutant tumours in all histological groups although this only reached statistical significance for AOA ($p = 0.0081$).

Figure 3.2 Relationship between age and *IDH1* status

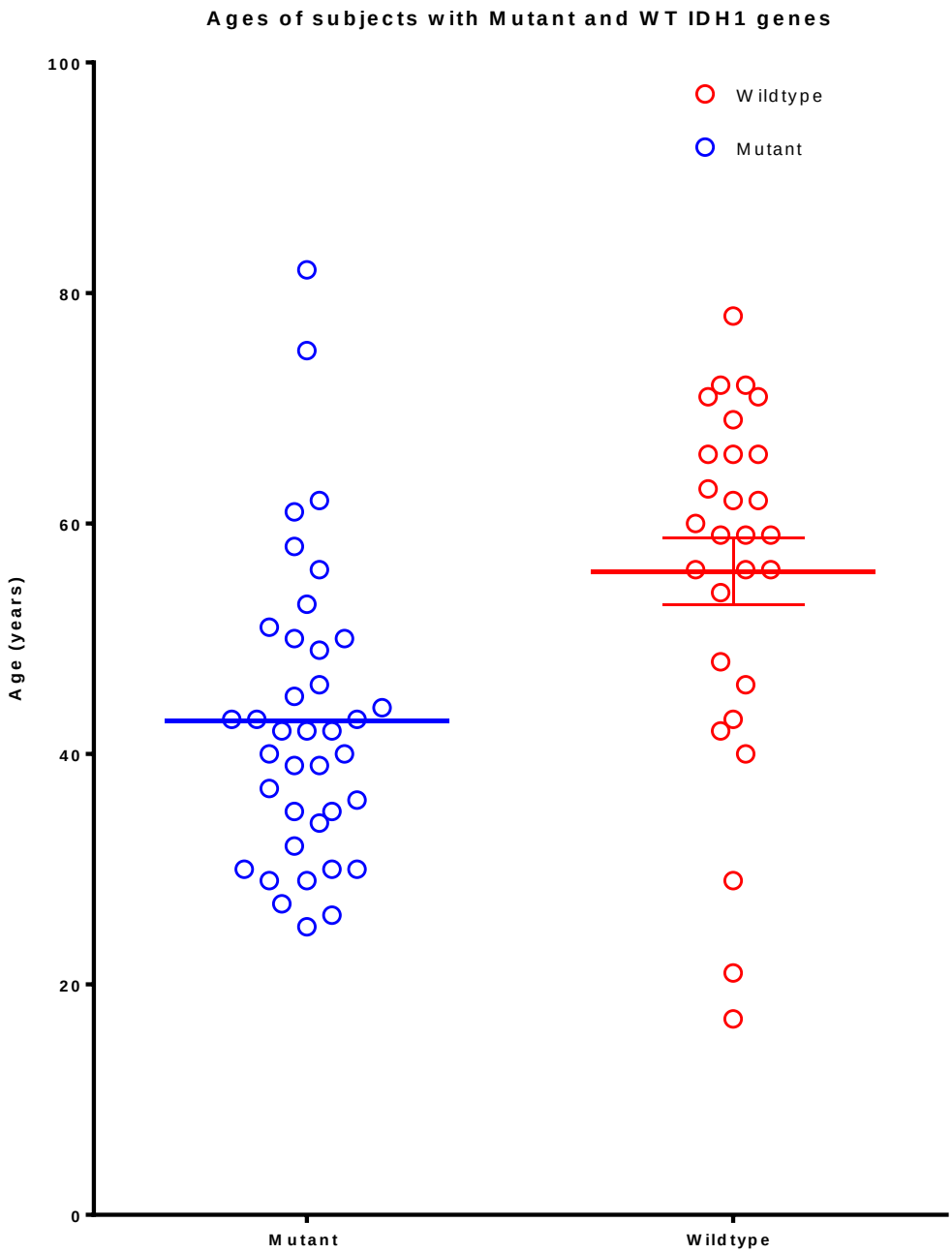

Patients with *IDH1* wildtype (n = 28) and *IDH1* mutant (n = 38) tumours were used for the relationship analysis. The bar represents the median age for the patients with mutant and wildtype tumours. The median for patients with wildtype tumours was 59 years and that for patients with mutant tumours was 42 years. Patients with *IDH1* mutations were significantly younger than those with wild type *IDH1* (p = 0.0002).

Table 3.2 Relationship between *IDH1* status and histology

Histology	*IDH1* Mutant		*IDH1* Wild type		p value
	Number of cases	%	Number of cases	%	
A	15	60	10	40	0.178
OA	5	83	1	17	N/A
O	7	100	0	0	N/A
AA	2	25	6	75	0.054
AO	3	57	3	43	0.011
AOA	5	38	8	62	0.008

Table 3.3 Summary of tumour histology, grade and age in *IDH1* mutant and wild type tumours

Histology	*IDH1* mutant		*IDH1* wild type		p value
	Mean age	Median age	Mean age	Median age	
A	38.8	39	46.8	55	0.178
OA	41.8	40	43*	43*	N/A
O	53.29	56	No data	No data	N/A
AA	46	46	65.67	68.5	0.054
AO	36	35	64.67	66	0.064
AOA	40.8	43	58	60.5	0.008

* single case only

Figure 3.3 Relationship between tumour histology, grade, age and *IDH1* mutation status

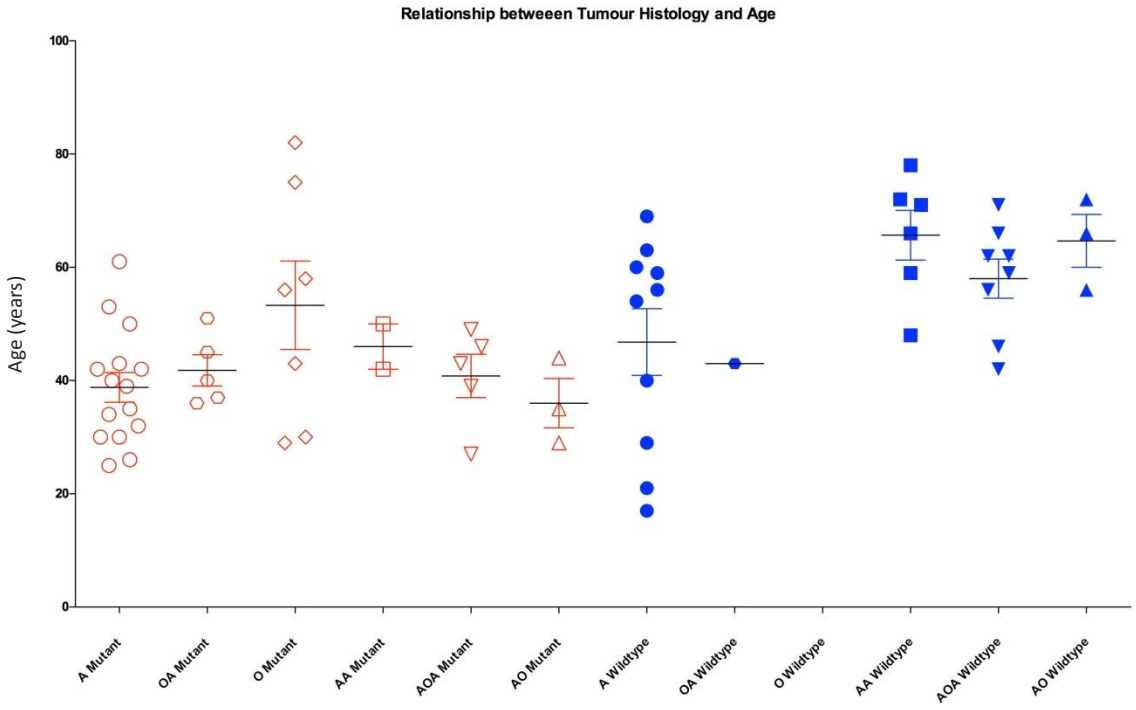

Tumour samples in red are *IDH1* mutant tumours and samples in blue are *IDH1* wild type. Significant difference in age was observed in only AOA group, *IDH1* mutant vs *IDH1* wild type.

3.3.4 Relationship between age, tumour grade and histology

Patients with grade III tumours were significantly older than those with grade II tumours ($p = 0.008$). Patients with grade II tumours had an age range of 17-82 years with a median of 42 years and those with grade III tumours had an age range of 27-78 years with a median of 56 years. Patients with AA were older than patients with either A ($p = 0.0026$) or OA ($p = 0.007$) with a trend towards AOA patients being older than A patients.

3.3.5 Comparison of IHC and sequencing to identify IDH1 status

IHC for mutated IDH1 protein had previously been performed in 27 samples with sufficient tissue available. Results for mutation analysis were consistent with both direct sequencing and IHC for all the 27 tumours analysed by the two methods. Of the 27 cases, 15 were positive and 12 were negative for the IDH1 mutant protein and all the samples analysed had the *IDH1* R132H mutation. Tumour samples were analysed by the neuropathologist (Professor Tim Dawson, Royal Preston Hospital, UK) after carrying out IHC using IDH1-R132H antibody (Dianova, UK).

3.4 RELATIONSHIP BETWEEN CLINICAL PARAMETERS AND OUTCOME

Kaplan Meier curves were generated to illustrate the correlations of molecular markers with OS and are shown in Figure 3.4. OS was defined as the time from diagnosis until death or last follow up of the patient. PFS was defined as the time between diagnosis and confirmation of recurrence by histological analysis. A patient with an AOA tumour

was the longest survivor in the cohort with OS of 263 months. Interestingly, the tumour was *IDH1* wild type. The upper limit for OS was taken as 150 months for the analysis.

3.4.1 Relationship between tumour grade and outcome

Patients with grade II tumours survived longer than those with grade III tumours ($p < 0.0001$; log rank Mantel-Cox test) shown in Figure 3.4A. The median survival for patients with grade II tumours was 34.7 months and that for patients with grade III tumours was 14.5 months.

3.4.2 Relationship between age and outcome

Age was a significant factor for OS. Younger patients (< 50 yrs) lived longer than older patients (> 50 yrs) ($p = 0.0002$; log rank Mantel-Cox test) as shown in Figure 3.4B, and this relationship was observed in patients with both grade II ($p = 0.0460$; log rank Mantel-Cox test) and grade III ($p = 0.0017$; log rank Mantel-Cox test) tumours (Figure 3.4C and D). The median survival for patients aged < 50 years was 74 months and that for patients aged > 50 years was only 16 months. In patients with grade II tumours, the median survival for younger patients (< 50 yrs) was 39 months against 30.5 months in older patients (> 50 yrs). In patients with grade III tumours, the median survival for younger patients (< 50 yrs) was 45.5 months compared to only 7.5 months in older patients (> 50 yrs).

3.4.3 Relationship between tumour histologies and outcome

Histology did not seem to be related to outcome in patients with grade II tumours, ($p = 0.4856$; log rank Mantel-Cox test), but in patients with grade III tumours, patients with AOA lived longer than those patients with AO or AA ($p = 0.0091$; log rank Mantel-Cox test). These results are presented in Figure 3.4E and F. Patients with A, OA and O tumours had a median survival of 33.5 months, 46.5 months and 32 months respectively. The median survival for patients with AA, AOA and AO tumours was 5.75 months, 33.5 months and 12 months respectively.

3.4.4 Relationship between IDH1 status and outcome

Patients with *IDH1* mutant tumours lived longer than patients with wild type *IDH1* ($p < 0.0001$; log rank Mantel-Cox test). Patients carrying *IDH1* mutation had a median survival of 37 months, which was longer than the 13.75 months for patients with wild type tumours (Figure 3.4G). Patients carrying *IDH1* mutation had a favourable outcome in grade II tumours ($p = 0.0001$; log rank Mantel-Cox test) but the mutation did not seem to influence the outcome in grade III tumours ($p = 0.0923$; log rank Mantel-Cox test) (Figure 3.4H and I). In grade II tumours, the median survival of patients with *IDH1* mutant tumours was 45.5 months and that for patients with *IDH1* wild type tumours was 29 months. In grade III tumours, the median survival of patients with *IDH1* mutant tumours was 22 months and that for patients with *IDH1* wild type tumours was only 9 months (Figure 3.4J).

Figure 3.4 Kaplan Meier survival curves depicting correlation of OS with *IDH1* mutation, age and grade

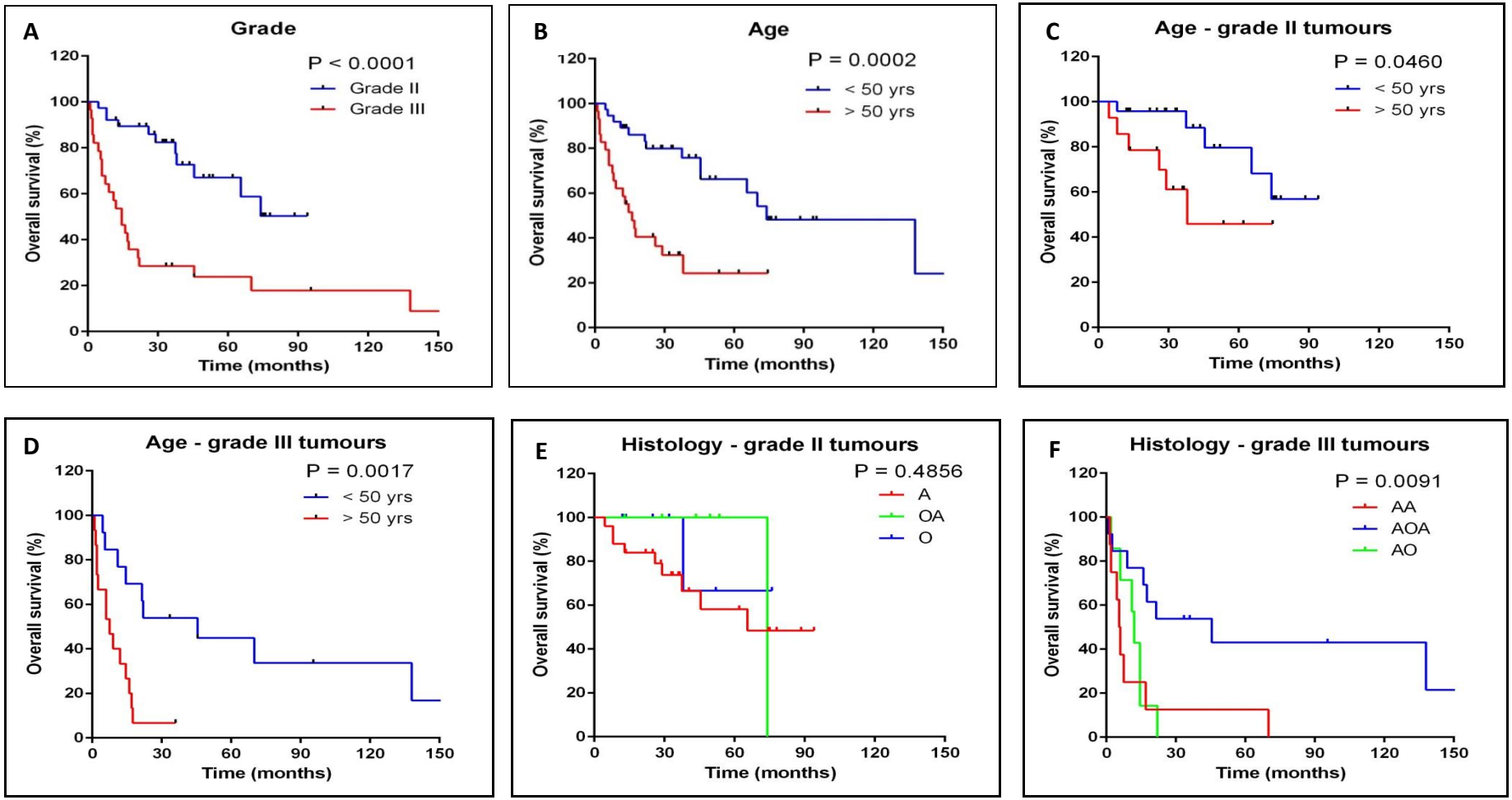

Figure 3.4 Kaplan Meier survival curves depicting correlation of OS with *IDH1* mutation, age and grade (cont'd)

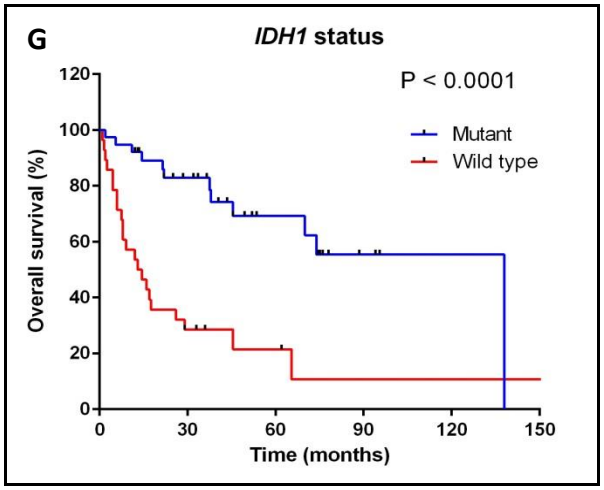

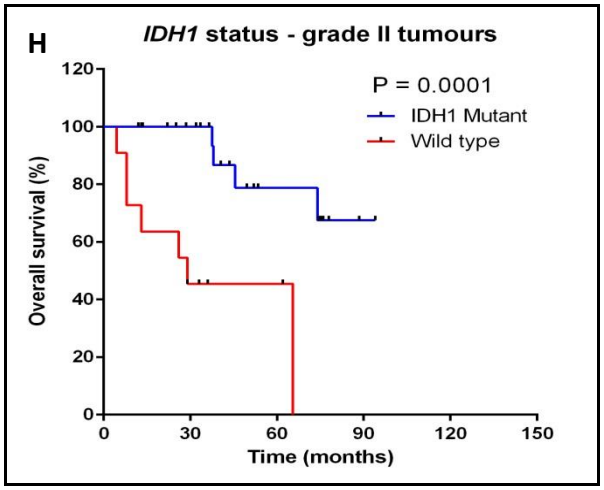

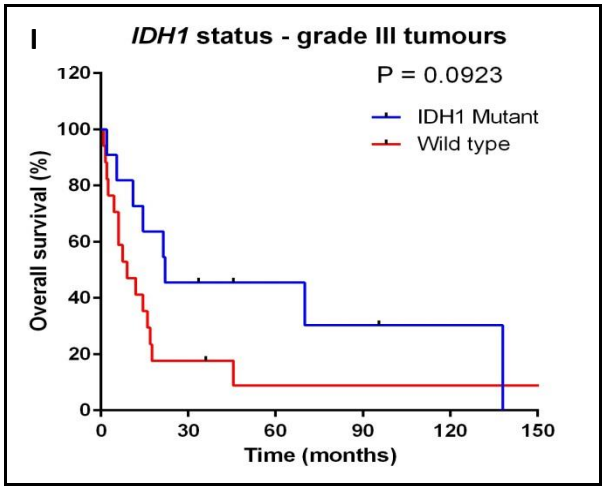

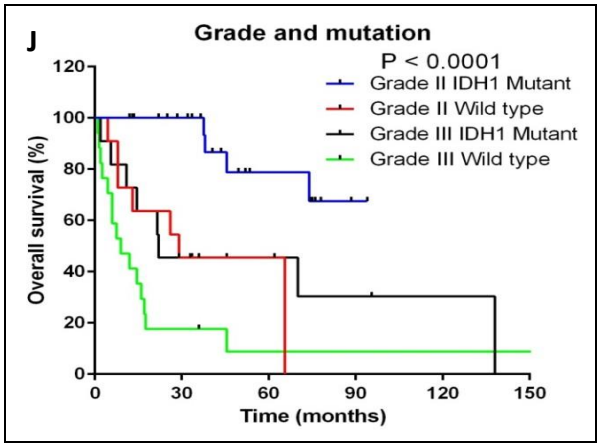

3.5 ANALYSIS OF *MGMT* PROMOTER METHYLATION BY MS PCR AND IHC

MGMT promoter methylation was determined by MS PCR in 57 tumours comprising 32 grade II tumours (21 A, 5 OA, 6 O) and 25 grade III tumours (8 AA, 12 AOA, 5 AO). Of these, 14% (8/57) were methylated, 19% (11/57) were partially methylated and 67% (38/57) were unmethylated as detailed in Table 3.4. An example of MS PCR data is shown in Figure 3.5.

IHC was carried out in 51 primary tumours and MS PCR data was available for 47/51 of these samples (Table 3.4). Areas of high cellularity without any haemorrhage were selected to score the proportion of stained nuclei indicative of MGMT protein expression and 100 cells were examined in three fields to get an average score. The quick (Allred) scoring system was used to determine the proportion and intensity of the staining. Examples of IHC results are shown in Figure 3.6. Two tumours (BTNW 761 and BTNW537) had completely negative staining and a score of zero. A further 14 tumours had a combined Allred score of 1-4 (low expression), whilst the majority of samples (35) had a higher combined Allred score of 5-8 (high expression). If the proportion of stained cells only was considered, 11 tumours had a low expression score between 1-2 and 38 cases had a high expression score between 3-5.

Table 3.4 MGMT methylation status by IHC and MS PCR in primary grade II and grade III glioma

Tumour	Age[a]	Grade	Histology[b]	*MGMT* methylation status (MS PCR)[c]	IHC proportion	IHC intensity	IHC Combined score	PFS[d]	OS[e]
BTNW17	69	II	A	U	NA	NA	NA	4.5	4.5 (D)
BTNW20	26	II	A	U	1	3	4	83	94 (A)
BTNW61	32	II	A	U	5	3	8	-	88.5 (A)
BTNW124	29	II	A	U	NA	NA	NA	-	65.5 (D)
BTNW160	35	II	A	PM	3	1	4	67	78 (A)
BTNW203	42	II	A	U	4	2	6	52.5	75 (A)
BTNW210	53	II	A	U	1	2	3	-	74.5 (A)
BTNW212	50	II	A	M	3	2	5	-	45.5 (D)
BTNW365	42	II	A	NA	3	2	5	28.5	37.5 (D)
BTNW367	56	II	A	PM	5	3	8	1	62 (A)
BTNW381	54	II	A	U	2	2	4	-	25.5 (D)
BTNW680	59	II	A	U	5	2	7	-	13 (D)
BTNW736	63	II	A	U	1	2	3	-	8 (D)
BTNW761	25	II	A	U	0	0	0	-	40.5 (A)
BTNW818	60	II	A	U	5	3	8	24.5	26 (D)
BTNW823	61	II	A	U	3	3	6	-	36.5 (A)
BTNW830	21	II	A	U	4	2	6	-	36 (A)
BTNW868	39	II	A	U	4	3	7	22.5	33.5 (A)
BTNW870	17	II	A	U	4	2	6	1	33 (A)
BTNW931	30	II	A	NA	4	2	6	-	28.5 (A)
LIV002	34	II	A	U	NA	NA	NA	-	25 (A)
LIV003	30	II	A	PM	NA	NA	NA	-	22 (A)
LIV007	40	II	A	U	NA	NA	NA	-	8 (D)
BTNW13	40	II	OA	U	4	2	6	44.5	74 (D)
BTNW503	51	II	OA	U	3	1	4	42.5	53.5 (A)
BTNW613	37	II	OA	PM	5	3	8	37	49.5 (A)
BTNW726	45	II	OA	U	5	3	8	17	43.5 (A)
BTNW929	43	II	OA	NA	3	2	5	-	29 (A)
LIV015	36	II	OA	U	NA	NA	NA	-	18 (A)
BTNW188	43	II	O	M	4	2	6	-	76 (A)
BTNW326	56	II	O	M	4	3	7	33.5	37.5 (D)
BTNW531	29	II	O	M	3	2	5	-	52 (A)
BTNW882	82	II	O	U	4	2	6	-	32 (A)
LIV020	75	II	O	PM	NA	NA	NA	-	24.5 (A)
LIV024	30	II	O	PM	NA	NA	NA	-	12 (A)
BTNW19	42	III	AA	U	NA	NA	NA	-	70 (D)
BTNW38	48	III	AA	PM	3	2	5	-	4.5 (D)
BTNW126	66	III	AA	U	4	2	6	5	6 (D)
BTNW173	50	III	AA	U	1	1	2	-	5.5 (D)
BTNW211	72	III	AA	U	4	2	6	-	2 (D)
BTNW421	59	III	AA	U	5	3	8	-	7.5 (D)
BTNW458	71	III	AA	M	3	2	5	-	17 (D)
BTNW925	78	III	AA	U	1	1	2	-	1.5 (D)
BTNW9	62	III	AOA	U	1	2	3	-	17.5 (D)
BTNW14	43	III	AOA	M	1	2	3	64.5	95.5 (A)
BTNW120	27	III	AOA	PM	1	2	3	95.5	138 (D)
BTNW174	42	III	AOA	M	3	1	4	36	45.5 (D)
BTNW183	66	III	AOA	PM	4	2	6	-	0.5 (D)
BTNW325	46	III	AOA	NA	3	2	5	230.5	263 (D)
BTNW495	71	III	AOA	U	3	2	5	-	8.5 (D)
BTNW527	59	III	AOA	U	0	0	0	-	2.5 (D)
BTNW614	49	III	AOA	U	5	3	8	14.5	21.5 (D)
BTNW686	56	III	AOA	U	NA	NA	NA	-	16 (D)
BTNW703	46	III	AOA	U	4	3	7	-	45.5 (A)
BTNW825	62	III	AOA	U	1	1	2	-	36 (A)
BTNW864	39	III	AOA	U	3	3	6	-	33.5 (A)
BTNW15	56	III	AO	M	3	2	5	13.5	14.5 (D)
BTNW460	29	III	AO	U	3	3	6	-	22 (D)
BTNW738	66	III	AO	U	2	2	4	-	12 (D)
BTNW757	72	III	AO	U	4	2	6	-	6 (D)
BTNW804	44	III	AO	PM	4	2	6	-	11 (D)

[a] Age at initial diagnosis in years; [b] A, astrocytoma; OA, oligoastrocytoma; O, oligodendroglioma; AA, anaplastic astrocytoma; AOA, anaplastic astrocytoma; AO, anaplastic oligodendroglioma; [c] M, methylated; PM, partially methylated; U, unmethylated; [d] PFS in months; [e] OS in months; A, alive; D, dead; NA, not available.

Figure 3.5 *MGMT* methylation analysis by MS PCR

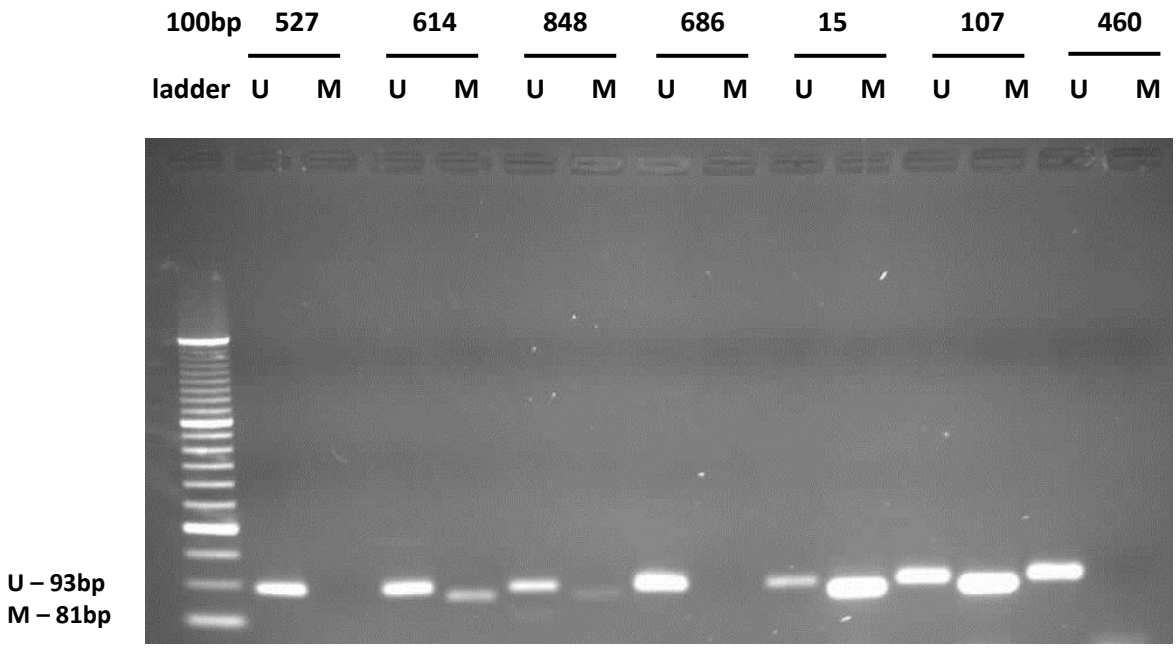

Amplification products were separated by electrophoresis through 2% agarose. 1 sample was methylated (BTNW15), 3 samples were partially methylated (BTNW614, BTNW848 and BTNW107) and 3 samples were unmethylated (BTNW527, BTNW686 and BTNW460). M, methylated; U, unmethylated.

Figure 3.6 IHC staining for MGMT in tissues

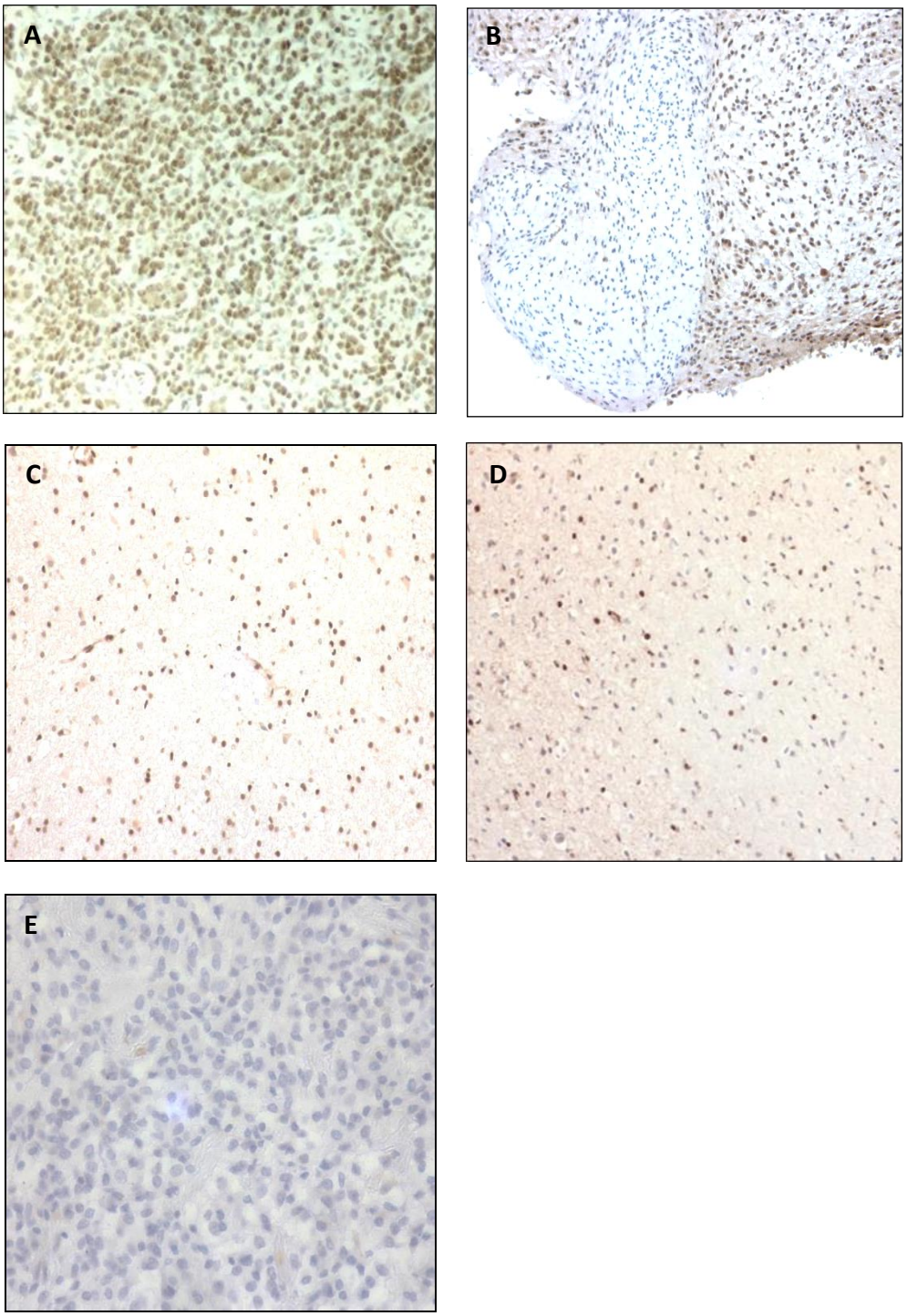

Representative example, slides were stained positively with streptavidin/HRP-biotin staining and counterstained with haematoxylin. A: Tonsil used as a positive control for MGMT, 40x magnification; B: BTNW61 (A) showing clonal populations with areas of negative staining next to areas of positively stained cells, 20x magnification; C: BTNW367 (A) with 100% MGMT positive staining, 40x magnification; D: BTNW326 (O) with an egg-fried appearance representing an oligodendroglioma with positive staining for MGMT, 40x magnification and E: BTNW527 (AOA) showing negative staining for MGMT, 40x magnification.

3.6 COMPARISON OF MS PCR AND IHC METHODOLOGIES TO IDENTIFY *MGMT* METHYLATION

In tumour samples with low IHC scores, MS PCR analysis would be expected to demonstrate *MGMT* methylation and conversely, cases with high Allred scores would be expected to have unmethylated *MGMT* promoter. Seven tumours had the highest combined score of 8 by IHC, 6 of which were unmethylated and 1 was partially methylated. However, two tumours (BTNW 761 and BTNW537) showed negative staining for MGMT by IHC, but had unmethylated *MGMT* detected by MS PCR.

Both proportion and combined score of IHC staining was used for correlation between the two methods. For this analysis, low MGMT expression (Allred score 0-2 or 0-4) and high MGMT expression (Allred score 3-5 or 5-8) were compared with *MGMT* methylation status determined by MS-PCR as detailed in Table 3.5. There was no significant correlation between level of MGMT protein expression and gene promoter methylation regardless of whether partially methylated tumours were combined with unmethylated or methylated samples. Figure 3.7 shows a comparison of the MGMT staining patterns (determined using the Allred scoring system) in 47 tumours in which the methylation status of the *MGMT* promoter had been established using MS PCR.

Table 3.5 Comparison of MGMT methylation status determined by MS PCR and IHC

***MGMT* methylation status MS PCR**	**MGMT IHC overall score 0-4**	**MGMT IHC overall score 5-8**	**p value**
Unmethylated, n=32	13	19	
Partially methylated, n=7	3	4	
Methylated, n=8	2	6	
Unmethylated vs Partially methylated/Methylated			0.753
Unmethylated/Partially methylated vs Methylated			0.692
	MGMT IHC proportion score 0-2	**MGMT IHC proportion score 3-5**	
Unmethylated, n=32	11	21	
Partially methylated, n= 7	1	6	
Methylated, n=8	1	7	
Unmethylated vs Partially methylated/Methylated			0.175
Unmethylated/Partially methylated vs Methylated			0.146

Statistical analysis was performed using GraphPad Prism and p-values were determined using the Wilcoxon signed-rank test for each of the analyses.

Figure 3.7 Comparison of MGMT IHC staining patterns and *MGMT* promoter methylation status

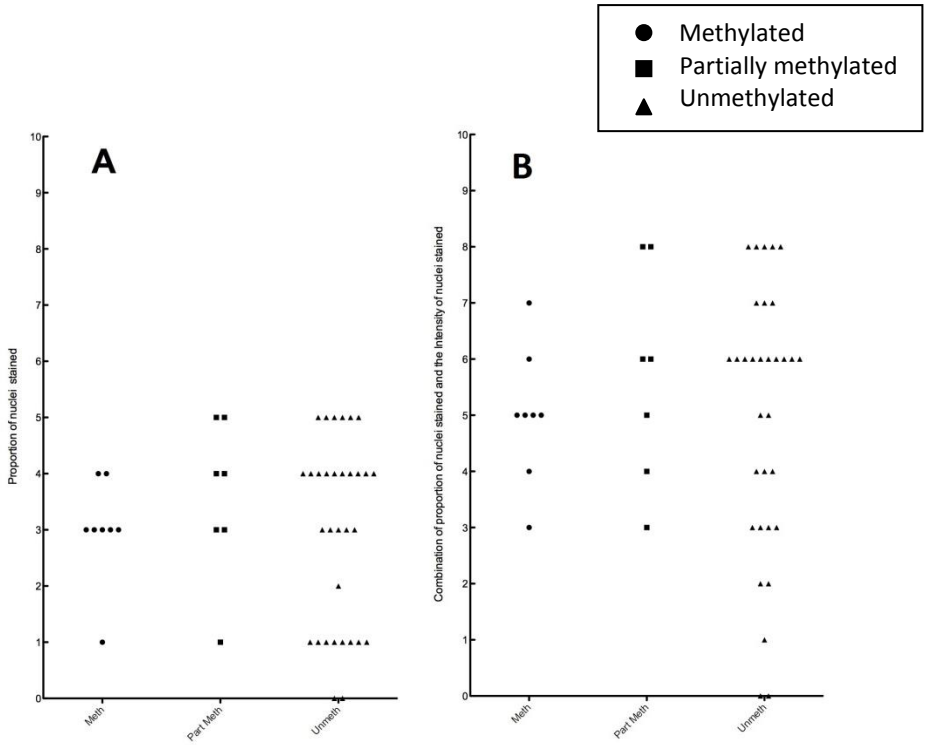

A: Proportion of nuclei stained; B: Combined Allred score with proportion and intensity scores. Meth, methylated; Part Meth, partially methylated; Unmeth, unmethylated.

3.6.1 Relationship between MGMT status and tumour grade

By MS PCR, in grade II tumours, 12% (4/32) were methylated, 19% (6/32) were partially methylated and 69% (22/32) were unmethylated. In grade III tumours, 16% (4/25) were methylated, 20% (5/25) were partially methylated and 64% (16/25) were unmethylated. There was no significant association of *MGMT* methylation with tumour grade combining either unmethylated with partially methylated cases ($p = 1.0$) or partially methylated with methylated tumours ($p = 0.781$). Similarly, there was no significant association of level of MGMT expression (low compared to high) with tumour grade using either proportion or combined Allred scoring systems ($p = 0.336$ and $p = 0.547$, respectively).

3.6.2 Relationship between MGMT status and age

There was no association between *MGMT* promoter methylation and age combining either unmethylated with partially methylated cases ($p = 0.715$) or partially methylated with methylated tumours ($p = 0.101$). In younger patients (< 50 yrs), *MGMT* methylation and partial methylation was observed in 16% (5/31) and 29% (9/31) of tumours respectively. *MGMT* was unmethylated in 55% (17/31) of cases. In older patients (> 50 yrs), methylation was detected in 11% (3/26) of tumours, partial methylation in 11% (3/26) of tumours and 77% (20/26) of cases were unmethylated. Similarly, there was no association between level of MGMT protein expression (low compared to high) with patient age using either proportion or combined Allred scoring systems ($p = 0.207$ and $p = 0.791$, respectively).

3.6.3 Relationship between MGMT status and tumour histology

Promoter methylation was detected by MS PCR in 5% (1/21) A, 50% (3/6) O, 12% (1/8) AA, 17% (2/12) AOA and 20% (1/5) AO, partial methylation was present in 14% (3/21) A, 20% (1/5) OA, 33% (2/6) O, 12% (1/8) AA, 8% (1/12) AOA and 20% (1/5) AO and unmethylation was present in 81% (17/21) A, 80% (4/5) OA, 17% (1/6) O, 75% (6/8) AA, 58% (7/12) AOA and 60% (3/5) AO. Low MGMT protein expression was present in 33% (6/12) A, 0% (0/4) O, 0% (0/5) OA, 29% (2/7) AA, 42% (5/12) AOA and 20% (1/4) AO determined by both proportion and combined Allred scoring systems. Statistical analysis could not be performed due to small number of samples in each group. However, when the number of tumours with methylation and partial methylation are combined, there appears to be a higher frequency of *MGMT* promoter methylation in O (83% of samples) compared to A (19%) and OA (20%). This trend is also present to a lesser extent in the grade III tumours with 40% AO tumours having partial or complete *MGMT* methylation compared to 25% AA and 25% AOA.

3.7 RELATIONSHIP BETWEEN *IDH1* MUTATION AND *MGMT* METHYLATION

The association between *IDH1* mutation and *MGMT* promoter methylation was determined in 57 tumours, for which both *IDH1* mutation and *MGMT* promoter methylation status had been established. In *IDH1* mutated tumours, the *MGMT* promoter was methylated in 16% (5/31) of cases with partial methylation being present a further in 23% (7/31) of cases and no methylation detected in 61% (19/31) of the tumours as presented in Table 3.6. In the group of *IDH1* wild type tumours, *MGMT* methylation and partial methylation were both detected in 11.5% (3/26) of cases and

77% (20/26) tumours were unmethylated at the *MGMT* promoter. The single case in the present series with an *IDH2* mutation also had *MGMT* promoter methylation. The association of *MGMT* methylation status and *IDH1* mutation status was analysed in two groupings, firstly counting those tumours with methylated *MGMT* promoter and those with partially methylated *MGMT* promoter. In this case, *IDH1* mutation correlated with *MGMT* status ($p = 0.014$, chi square test, $p = 0.0214$, Fisher's exact test). However, if *MGMT* methylation status was analysed by grouping the partially methylated tumours with the unmethylated cases, there was no correlation with *IDH1* mutation ($p = 0.34$, chi square test; $p = 0.41$, Fisher's exact test).

Table 3.6 Relationship between *IDH1* and *MGMT* status

***IDH1* status**	***MGMT* Methylation status**		
	Methylated (% of tumours)	**Partially methylated (% of tumours)**	**Unmethylated (% of tumours)**
Mutant, n = 31	16	22	61
Wild type, n = 26	11.5	11.5	77

***IDH1* status**	**Methylated and partially methylated (% of tumours)**	**Unmethylated (% of tumours)**
Mutant, n = 31	39	61
Wild type, n = 26	23	77

***IDH1* Status**	**Methylated (% of tumours)**	**Partially methylated and unmethylated (% of tumours)**
Mutant, n = 31	16	84
Wild type, n = 26	11.5	88.5

3.8 RELATIONSHIP BETWEEN *MGMT* METHYLATION AND OUTCOME

MGMT promoter methylation was correlated with OS, where methylated/partially methylated were combined against unmethylated and unmethylated/partially methylated were combined against methylated; the results are summarised in Table 3.7 and neither combination were statistically significant in all cases or when samples were segregated by grade. Kaplan meier curves for *MGMT* methylation status by MS PCR are shown in Figure 3.8. Correlation of MGMT protein expression with OS was also performed using proportion and combined Allred scores as described. No significant association with level of MGMT expression (low versus high) with OS was observed (Table 3.7).

In a multivariate analysis using the Cox proportional hazard model with *IDH1* mutation status, grade, age and *MGMT* status as variables, *IDH1* mutation ($p = 0.001$) and grade ($p = 0.002$) were strong and independent predictors for a better outcome.

PFS data included 21 patients and a significant association was found with age ($p = 0.0038$) and grade plus *IDH1* mutation ($p = 0.0249$) (Figure 3.9). PFS was not significant for *IDH1* mutation, grade and *MGMT* methylation.

Table 3.7 Correlation of OS with *MGMT* methylation by IHC and MS PCR

Overall Survival	Groups	IHC Score	p value
MGMT IHC - Proportion			
All (Grade II, Grade III)	Low	0-2	0.26
	High	3-5	
Grade II	Low	0-2	0.43
	High	3-5	
Grade III	Low	0-2	0.12
	High	3-5	
MGMT IHC - Combined			
All (Grade II, Grade III)	Low	0-4	0.88
	High	5-8	
Grade II	Low	0-4	0.69
	High	5-8	
Grade III	Low	0-4	0.74
	High	5-8	
MGMT – MS PCR			
All (Grade II, Grade III)	Methylated/Partial		0.30
	Unmethylated		
Grade II	Methylated/Partial		0.36
	Unmethylated		
Grade III	Methylated/Partial		0.52
	Unmethylated		
All (Grade II, Grade III)	Methylated		0.79
	Partial/Unmethylated		
Grade II	Methylated		0.75
	Partial/Unmethylated		
Grade III	Methylated		0.35
	Partial/Unmethylated		

Figure 3.8 Kaplan Meier survival curves showing correlation of OS with *MGMT* methylation status

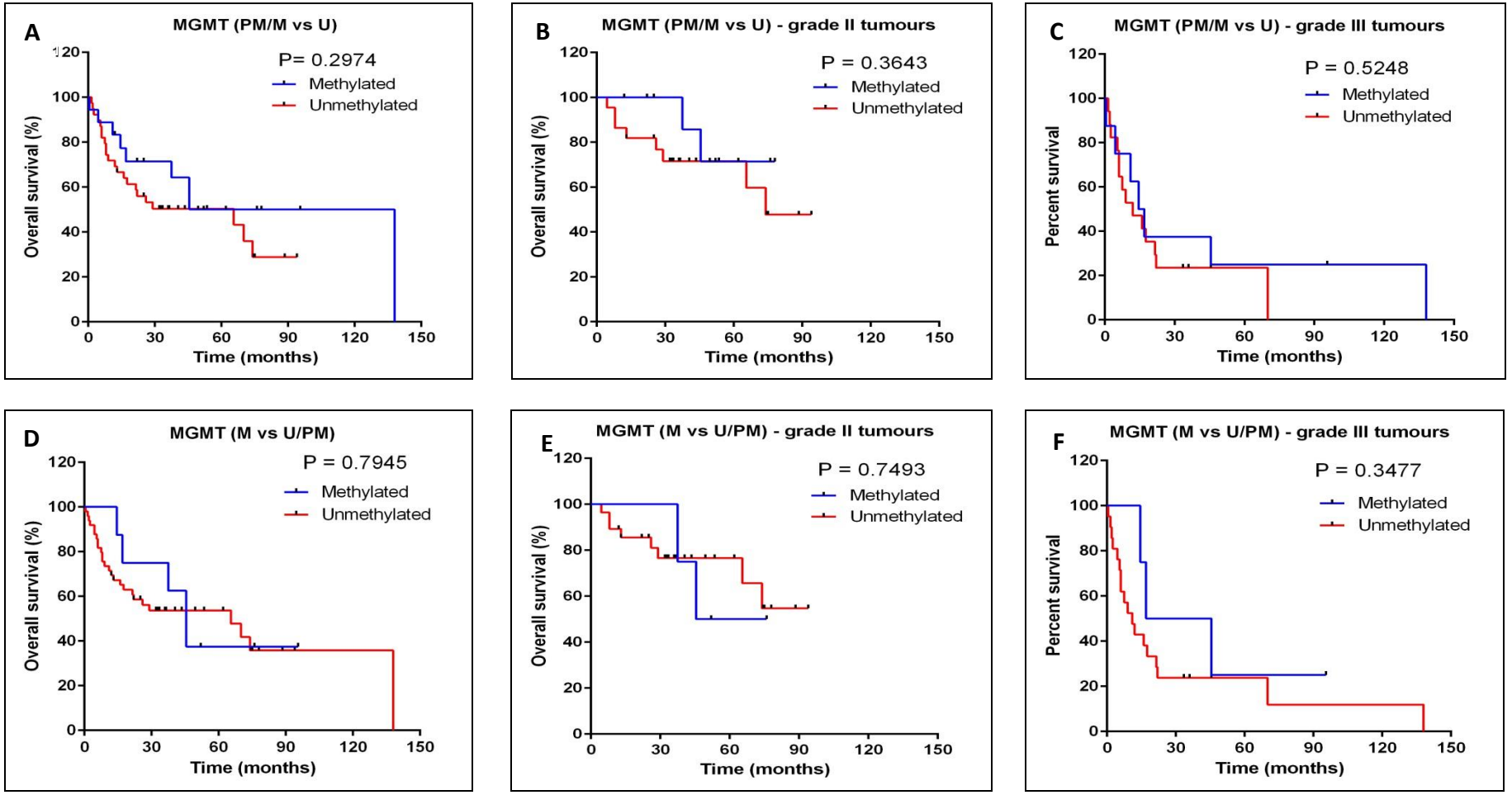

M, methylated; PM, partially methylated; U, unmethylated

Figure 3.9 Correlation of PFS with age and tumour grade plus *IDH1* mutation shown using Kaplan Meier curves

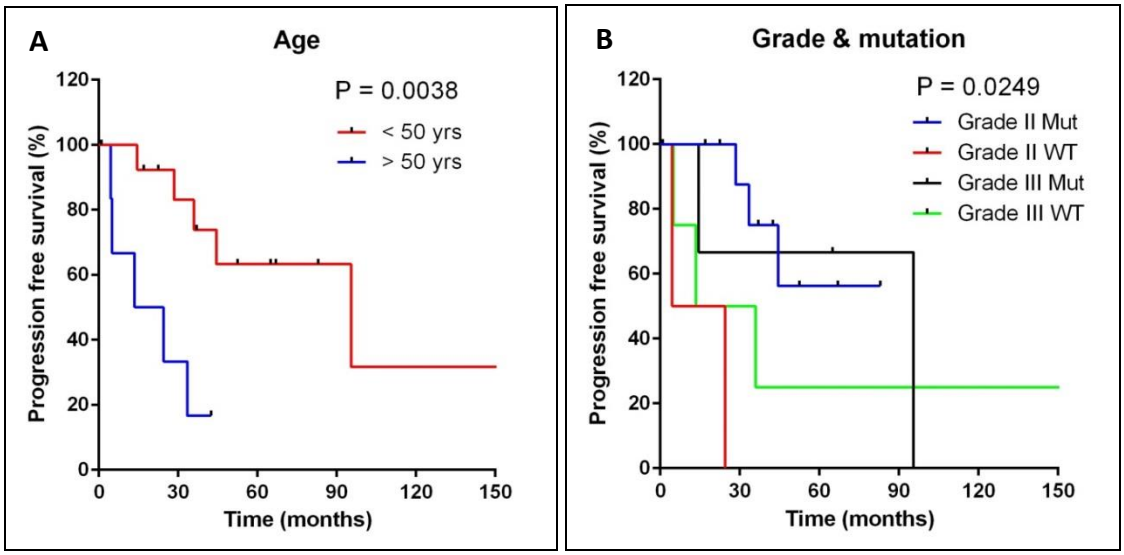

3.9 DISCUSSION

In this study, the mutation status of *IDH1* and *IDH2* and *MGMT* methylation status in glioma was determined in different grades and histological groups of primary tumours. OS and PFS was correlated with clinical criteria and analysis for relationships between the clinical parameters was performed.

3.9.1 Incidence of *IDH1* mutation

Although *IDH1* mutations were found in both grade II and grade III tumours and in all histological subtypes, they were more frequent in grade II tumours than grade III tumours and the mutation was associated with histological findings with the highest frequency in O followed by OA and A. Similarly, in grade III tumours, *IDH1* mutation was more frequent in AO than AOA and AA. These results are consistent with previous studies reporting > 80% *IDH1* mutations in LGG tumours. Watanabe *et al*., (2009) showed that *IDH1* mutation was present in 88% (60/68) A, 94% (16/17) OA and 79% (31/39) O. Yan *et al*., (2009) reported that *IDH1* mutation was most frequent in grade II tumours, present in 83% (25/30) A, 100% (3/3) OA and 80% (41/51) O. Gupta *et al*., (2013) showed *IDH1* mutation at a frequency of 75% (18/24) in A, 60% (3/5) in OA and 100% (14/14) in O. All mutations were R132H, except for one which was R132S in the current study. This is in accordance with previous studies showing *IDH1* R132H as the most common mutation (Hartmann *et al*., 2009; Nobusawa *et al*., 2009; Sanson *et al*., 2009; Myung *et al*., 2012).

3.9.2 Incidence of *IDH2* mutation

IDH2 mutation is known to be less frequent in glioma and in this study it was present in only one AO tumour with wild type *IDH1*. Wang *et al*., (2014) determined *IDH2* mutation status in 980 tumours (61A, 134OA, 243O, 33AA, 141AOA, 220AO and 312GBM) and *IDH2* mutation was present in 3.1% (30/980) of the cases, with O and AO being the most common tumours to exhibit the mutation. No tumour had both *IDH1* and *IDH2* mutation. Lu *et al*., (2013) also showed that *IDH2* mutation was present at a low frequency (4.9%, 2/41) in a study of O and AO tumours. Another study involving 287 glioma patients, reported that *IDH2* mutation was present in only one case, an oligodendroglioma with *IDH1* wild type (Mellai *et al*., 2011). Similarly, in AML cases, the frequency of *IDH2* mutation was low at about 7% shown in multiple studies (Paschka *et al*., 2010; Patel *et al*., 2011; Chotirat *et al*., 2012; Berenstein *et al*., 2014).

3.9.3 Relationship of *IDH1* mutation to *MGMT* methylation

IDH1 mutation is a prognostic factor while *MGMT* is a predictive marker for response to TMZ. As described previously, *IDH1* mutations result in global hypermethylation establishing G-CIMP, which is correlated with *MGMT* promoter methylation (Molenaar *et al*., 2014). *IDH* mutations promote gene promoter methylation by accumulation of the oncometabolite 2-HG, which is converted from α-KG. 2-HG contributes to impaired demethylation of genomic DNA, subsequently leading to remodelling of the methylome and transcriptome, including methylation of *MGMT*. It would be expected that tumours carrying *IDH* mutation are more likely to have *MGMT* promoter methylation. However, this was not the case in the present study where only a small proportion (15%, 5/33) of tumours with *IDH1* mutation had complete *MGMT* methylation and the majority (57%,

19/31) of the tumours had no methylation of *MGMT*, while the remaining cases (21%, 7/33) showed partial methylation. The proportion of methylated tumours was much less (36%, 12/33) than expected even after combining the partially methylated and methylated tumours. In a study of 210 LGG, the correlation between *IDH* mutation and *MGMT* methylation was established (Leu *et al*., 2013). The authors reported that 84% of the *IDH* mutated tumours also had methylation of *MGMT* and *IDH* mutation was positively associated with *MGMT* methylation ($p < 0.001$). Similarly, Mulholland *et al*., (2012) reported that tumours with *IDH* mutations had a high frequency (98%, 127/129) of *MGMT* methylation irrespective of tumour grade and histology, in a sample cohort including A, OA, O, AA, AOA, AO and GBM tumours.

A possible explanation for having a low frequency of *MGMT* methylated tumours is a small cohort size in the present study and also methods of MGMT detection such as IHC and MS PCR are less sensitive compared to pyrosequencing.

3.9.4 *IDH* and outcome

The clinical correlation was performed using OS instead of PFS as the data for OS was available for all cases included in this study and PFS was known for only a few patients. Different parameters may be used to establish time to progression and/or recurrence such as date of radiological MRI scans and date of biopsy or further resection plus histological diagnosis.

Mutations in *IDH1* and *IDH2* do not exert the same effects including activation of HIF-1 pathway, inducing G-CIMP and inhibition of PI3K-Akt signalling pathway, all of which are consequences of *IDH1* mutation. The effects of *IDH2* mutation in glioma are still unknown and need to be examined. Although *IDH1* and *IDH2* are isoforms, the

mutations in each of the genes might cause different effects. In terms of survival, patients with tumours carrying either *IDH1* or *IDH2* mutation have a better survival rate, as mentioned previously in Chapter 1. The explanation for a better outcome may be related to the biological effects of *IDH* mutation. Bralten *et al*., (2011) showed that overexpression of *IDH1*-R132H mutation in a transfected glioma cell line *in vitro* led to a decrease in proliferation rate, decreased Akt phosphorylation, alteration in morphology and more contact-dependent cell migration. The decrease in proliferation is due to D-2HG produced by *IDH1* mutation. The transition of R132 with any of the amino acids observed in glioma (His, Ser, Gly, Cys, Val and Leu) may have a reduced affinity to isocitrate and dominantly inhibit activity of IDH1 wildtype through the formation of catalytically inactive heterodimers. This may lead to the cells being more susceptible to oxidative stress by chemotherapy and radiotherapy (Zou *et al*., 2013).

It has been reported in a previous study that patients with grade II tumours having *IDH1* mutation had a median OS of 12.6 years compared to 5.5 years for those with tumours having *IDH1* wild type (Sanson *et al*., 2009). Other studies have shown that *IDH* mutations were an independent prognostic indicator for longer PFS and OS in patients with grade III tumours (Hartmann *et al*., 2010; Juratli *et al*., 2012; Shibahara *et al*., 2012). In LGG, *IDH* mutations were associated with a better outcome ($p = 0.000001$) and *IDH* wild type was an independent unfavourable prognostic factor ($p = 0.006$) (Metellus *et al*., 2010). In a study by Song-Tao *et al.* (2012), *IDH* mutations with *MGMT* methylation and 1p/19q co-deletion were associated with longer PFS. Wang *et al*., (2014) confirmed that in each of the grades, grade II, grade III and grade IV, patients with *IDH* mutated tumours had significantly longer OS and PFS than those with *IDH* wild type tumours. The authors also reported that *IDH* mutation was an independent predictor of a better outcome ($p < 0.0001$). Gorovets *et al*., (2012) showed

that tumours with *IDH* mutation were present significantly in younger patients with longer OS compared to those with *IDH* wild type tumours ($p < 0.0001$). In the present study, *IDH1* mutation was significantly associated with a longer OS in grade II tumours but not in grade III tumours ($p = 0.0001$, $p = 0.0923$ respectively; log rank Mantel-Cox test).

3.9.5 *MGMT* and outcome

MGMT, the DNA repair enzyme removes alkyl groups from the O^6 position of guanine, which is the site of chemotherapy induced alkylations. Promoter hypermethylation of *MGMT* is associated with reduced DNA repair enzyme activity and increased sensitivity to alkylating agents including nitrosourea and TMZ. *MGMT* methylation status has been linked with improved outcome in patients treated with TMZ. A meta-analysis study involving 16 studies investigated the prognostic significance of *MGMT* promoter methylation and it was shown that *MGMT* methylation was associated with longer OS in elderly patients treated with TMZ (12 studies, 635 patients, $p < 0.0001$) (Yin *et al*., 2014). However, in the absence of treatment with TMZ, no significant difference for OS was found in patients with or without *MGMT* methylation (4 studies, 368 patients, $p < 0.0001$) (Piccirilli *et al*., 2006; Malmstrom *et al*., 2012; Reifenberger *et al*., 2012; Wick *et al*., 2012). Leu *et al*., (2013) examined 210 LGG and showed that *MGMT* methylation had a significant and positive impact on OS ($p = 0.053$). In a study of 267 malignant glioma including anaplastic astrocytoma, anaplastic oligoastrocytoma, anaplastic oligodendroglioma and GBM tumours, patients with tumours having *MGMT* methylation had longer survival than those without the methylation ($p < 0.001$) (Takahashi *et al*., 2013). In the present study, there was no correlation between *MGMT*

methylation status and OS which may be due to the relatively small cohort and patients receiving different treatment regimen including radiotherapy and chemotherapy using TMZ and PCV. Of the 15 patients for whom treatment information was available, 5 patients underwent chemotherapy with TMZ. Furthermore, *MGMT* methylation data was not completed for all the cases due to availability of tissue.

Some of the tumours were partially methylated for *MGMT*, which represents one allele as methylated and the other as unmethylated for *MGMT* or alternatively, there could be mixed population of cells, some with *MGMT* methylation and some without. A good example of this is BTNW61 showing clonal populations (Figure 3.6). The biological sequela of partial methylation has not been investigated and therefore, in this study, partially methylated tumours were grouped with both methylated and unmethylated tumours to determine the correlation of *MGMT* methylation status with OS. However, no significant association was found between *MGMT* methylation status and OS in either of the groups. There is a lack of standard criteria to identify tumours with partial methylation. In a study by Kitange *et al*. (2009), *MGMT* methylation was correlated with response to TMZ using 13 GBM xenograft lines. MS PCR was used to identify the *MGMT* promoter methylation status and the sample was considered to be methylated when the gel showed a single band for methylated DNA or for both methylated and unmethylated DNA. Conversely, the sample was unmethylated only when a single band for unmethylated DNA was observed. A method to determine the percentage of methylation would be more accurate to determine the *MGMT* methylation status compared to MS PCR, where tumours could be partially methylated.

The clinical outcome results in the present study are not in accordance with these previous studies. The discrepancy in the results could be due to different techniques used for *MGMT* methylation analysis, one of which was a quantitative primer extension

based assay to determine the percentage of methylated DNA in the tumours. Secondly, the cohort size in the two previous studies were relatively much larger compared to the sample size in this study.

3.9.6 Age, grade, histology and outcome

Clinical features such as tumour grade, age and histology were correlated with outcome in this study. Multivariate cox proportional hazard model showed that patient age > 50 years was associated with a shorter OS ($p = 0.041$) in a study of 281 LGG patients (Chang *et al*., 2008). Astrocytoma histology was a significant predictor of a worse OS ($p = 0.004$) shown in a study involving a dataset of 203 LGG patients treated in a North American Intergroup trial (86-72-51) (Daniels *et al*., 2011). Kim *et al*., (2010) showed that the median survival of patients with oligodendroglioma (60.2 months) was significantly longer than those with astrocytoma tumour (52.5 months; $p = 0.0019$) in a study of 443 LGG. The results in this study are in accordance with the previous studies; younger patients (< 50 yrs), patients with tumours having an oligodendroglial component and patients with grade II tumours, all of these parameters showed a positive correlation with a better outcome.

3.9.7 MS PCR and IHC correlation

The Allred scoring system, recommended by neuropathologist Professor Tim Dawson, was used to determine the MGMT protein expression by IHC. It is based on the assessment of the proportion and intensity of staining for a protein. There was a lack of correlation for *MGMT* methylation between the two methods, MS PCR and IHC, in this

study. Samples with low MGMT expression were expected to be methylated and those with high MGMT expression to be unmethylated but only a small proportion of the tumours showed a correlation between MGMT expression and promoter methylation status. The number of nuclei stained for MGMT would depend on the number of cells expressing the protein. The intensity of staining may be attributable to the technique or the definite reactivity of the cell expressing the protein or the number of protein molecules in each cell which would determine the percentage of MGMT expression. A standardised method for scoring needs to be implemented to compare results across different studies. For IHC scoring, only the proportion of stained nuclei should be considered and not the intensity of staining as it may lead to discrepancy in results due to observer variability. Comparatively, MS PCR is a more reliable method to identify *MGMT* methylation status in a tumour where primers used for MS PCR can be designed in such a way that all the CpG sites are covered in order to obtain accurate results. A comparative study of 5 methods to analyse MGMT methylation was performed using 100 GBM patients and the authors confirmed the prognostic value of *MGMT* promoter methylation determined by MS PCR (Quillien *et al*., 2012). Several studies have shown significant association of MGMT expression by IHC (Jaeckle *et al*., 1998; Nakasu *et al*., 2004; Brell *et al*., 2005; Pollack *et al*., 2006; Capper *et al*., 2008) and *MGMT* promoter methylation status (Hegi *et al*., 2004; Paz *et al*., 2004; Hegi *et al*., 2005; Idbaih *et al*., 2007) with patient outcome in glioma. However, no significant association was observed in this study. The small number of samples analysed by both the methods may explain the inconsistency in the results.

In conclusion, this study shows that *IDH1* mutation, grade II and patient age < 50 years are all favourable prognostic markers for longer OS. In relation to age, patients with

grade III tumours were older than those with grade II tumours. Histology was not associated with outcome in grade II tumours, while grade III tumour patients with AOA had longer OS than those with AO or AA. Also, patients with grade II tumours carrying *IDH1* mutant had a longer OS, however, in grade III tumours, *IDH1* mutation was not associated with outcome. In case of MS PCR, partially methylated tumours could be categorised separately as these tumours did not behave like either methylated or unmethylated tumours. *IDH1* mutation only correlated with *MGMT* promoter status, when tumours with *MGMT* methylated promoter and those with partially methylated promoter were combined. However, *MGMT* promoter status was not significantly associated with outcome in the entire cohort.

CHAPTER 4

miRNA EXPRESSION PROFILING OF PRIMARY TUMOURS

4.1 INTRODUCTION

MicroRNAs (miRNAs) are small non-coding RNAs involved in regulation of biological processes such as cell proliferation, apoptosis, differentiation and metabolism (Brennecke *et al*., 2003; Xu *et al*., 2003; Sempere *et al*., 2004; Cheng *et al*., 2005). As mentioned previously in Chapter 1, a number of studies have been conducted to understand the role of miRNAs in GBM but little is known about their role in the development and progression of LGG. miRNAs have been shown to play a critical role in development and progression of cancers (Li *et al*., 2013). Deregulation of miR-9 for example, has been shown to play an important role in esophageal squamous cell carcinoma (ESCC) metastasis by inducing epithelial-mesenchymal transition (EMT) in ESCC, a key event in tumor metastasis (Song *et al*., 2014). Loss of miR-34a has also been found to accelerate medulloblastoma formation in animal models (Thor *et al*., 2014).

IDH mutations are also an important characteristic feature of LGG and the primary function of *IDH1* mutation is to establish the G-CIMP, which alters the methylome and hence, transcriptome, as described in previous Chapters. As tumours with *IDH* mutations are genomically and transcriptomally distinct from those without the mutations, it is possible that miRNA expression profiles of *IDH* mutant tumours and *IDH* wild type tumours are different. The aims of this chapter were to identify differentially expressed miRNAs associated with different grades of LGG as well as deregulated pathways affected by those miRNAs that may play a role in LGG

progression. The potential relationships between miRNA expression and tumour grade and histology were also investigated.

4.2 Tumour samples

The samples for miRNA analysis consisted of biopsy tissues from primary grade II and grade III tumours for which *IDH1* and *IDH2* mutation status has been determined. The cohort of 32 samples is detailed in Table 4.1 and comprised 20 grade II tumours (15 A, 2 OA, 3 O) and 12 grade III tumours (2 AA, 4 AOA, 6 AO).

4.3 Data analysis

miRNA expression analysis was performed using Partek Genomics Suite (version 6.6; Partek Inc., USA). Raw data was normalised with log 2 median and one-way analysis of variance (ANOVA) test was used to identify miRNAs that had $\geq$ 2-fold change in expression. Various analyses were performed using a number of sample cohorts with different criteria, grade II (n = 20) vs grade III tumours (n = 12); *IDH* mutant (n = 13) vs *IDH* wild type (n = 7) in grade II tumours; *IDH* mutant (n = 5) vs *IDH* wild type (n = 7) in grade III tumours; A (n = 15) vs OA (n = 2) in grade II tumours; OA (n = 2) vs O (n = 3) in grade II tumours; A (n = 15) vs O (n = 3) in grade II tumours; AA (n = 2) vs AOA (n = 4) in grade III tumours; AOA (n = 4) vs AO (n = 6) in grade III tumours and AA (n = 2) vs AO (n = 6) in grade III tumours. Supervised hierarchical clustering and principal components analysis (PCA) was used to determine differential miRNA expression amongst different group of samples. Significant miRNAs (p value < 0.05) with differential expression were reported in the study.

Table 4.1 Primary tumours used for miRNA analysis

Sample	Age at diagnosis[a]	Sex[b]	Grade	Histology[c]	*IDH1* mutation[d]	*IDH2* mutation[e]
BTNW20	26	M	II	A	R132H	WT
BTNW61	32	M	II	A	R132H	WT
BTNW203	42	F	II	A	R132H	WT
BTNW365	42	F	II	A	R132H	WT
BTNW680	59	M	II	A	WT	WT
BTNW818	60	F	II	A	WT	WT
BTNW830	21	M	II	A	WT	ND
BTNW868	39	F	II	A	R132H	ND
BTNW1005	43	F	II	A	R132H	ND
BTNW1028	40	M	II	A	R132H	ND
IN2190	45	M	II	A	WT	WT
IN2800	32	M	II	A	WT	WT
Liv007	40	M	II	A	WT	ND
Liv015	36	M	II	A	R132H	ND
Liv020	75	M	II	A	R132H	ND
BTNW13	40	F	II	OA	R132H	ND
UWLV7	38	M	II	OA	R132H	WT
IN99/81	NA	F	II	O	R132H	WT
IN2723	55	F	II	O	WT	WT
UWLV3	43	M	II	O	R132H	WT
BTNW126	66	M	III	AA	WT	WT
BTNW458	71	F	III	AA	WT	WT
BTNW9	62	F	III	AOA	WT	WT
BTNW527	59	F	III	AOA	WT	WT
BTNW614	49	M	III	AOA	R132H	ND
BTNW686	56	M	III	AOA	WT	WT
BTNW15	56	M	III	AO	WT	R172K
BTNW179	35	F	III	AO	R132H	WT
BTNW460	29	M	III	AO	R132H	WT
BTNW738	66	M	III	AO	WT	WT
BTNW757	72	M	III	AO	WT	WT
BTNW804	44	M	III	AO	R132H	WT

[a] age at diagnosis in years; [b] M, male; F, female; [c] A, astrocytoma; AA, anaplastic astrocytoma; OA, oligoastrocytoma; AOA, anaplastic oligoastrocytoma; O, oligodendroglioma; AO, anaplastic oligodendroglioma; [d] R132H, *IDH1* mutant; WT, wild type, [e] R172K, *IDH2* mutant; ND, not done; NA, not available.

4.4 miRNA target prediction

Predicted targets for the differentially expressed miRNAs were determined using TargetScan 6 (Lewis *et al*., 2005) (www.targetscan.org), miRDB (Wang *et al*., 2008; Wang, 2008) (http://mirdb.org/miRDB/) and miRanda database (John *et al*., 2004) (www.microrna.org). TargetScan determines the presence of conserved 8mer (an exact match to positions 2-8 of the mature miRNA) and 7mer (an exact match to positions 2-7 of the mature miRNA) sites that matches the seed region of each miRNA (Lewis *et al*., 2005). miRanda database predicts targets based on complementarity between mature miRNA and mRNA (John *et al*., 2004). miRNA target mining was performed with miRDB using the default settings that include targets with scores > 60 and miRNAs with < 800 targets. The top 10 targets chosen arbitrarily for each of the miRNA were mentioned in this study.

4.5 Pathway analysis

Pathway analysis for the differentially expressed miRNAs was performed using DIANA-miRPath v2.0 (Vlachos *et al*., 2012) and KEGG pathway analysis v58.1 (Kanehisa *et al*., 2012).

4.6 miRNA EXPRESSION ANALYSIS OF PRIMARY TUMOURS

Unsupervised clustering analysis was used to cluster samples with similar miRNA expression profiles irrespective of any molecular characteristics. Initially, unsupervised hierarchical clustering analysis of all 32 primary tumours comprising 18 tumours with *IDH* mutation and 14 *IDH* wild types was performed using 1719 miRNAs and is represented as a dendrogram with similar expression profiles clustered together (Figure 4.1). Two samples, BTNW13 (OA) and IN99/81 (O) (both *IDH* mutant) clustered independently to any other tumour. The remaining 30 samples formed two large clusters that separated predominantly according to grade. Cluster 1 comprised mainly grade II tumours (12/14, 86%) with the two grade III cases (BTNW614 and BTNW126). The majority of tumours in cluster 2 were grade III (10/16, 62.5%). There was a relatively even distribution between tumours with mutant and wild type *IDH* between the two main clusters. In cluster 1, 9/14 (64%) of tumours were *IDH* mutant and 5/14(36%) were *IDH* wild type. In cluster 2, 9/16 (56%) of tumours were *IDH* mutant and 7/16 (44%) were *IDH* wild type. *IDH* mutant tumours were marginally overrepresented in the predominantly grade II cluster 1 which probably reflects the predominance of *IDH* mutations in grade II versus grade III tumours. In cluster 1, 10/14 (71%) of tumours have a pure astrocytoma histology and 4/14 (29%) of cases have an oligodendroglial component. In contrast, only 7/16 (44%) of tumours in cluster 2 were purely astrocytic compared to 9/16 (56%) of cases with whole or partial oligodendroglial histology.

4.7 COMPARISON OF miRNA EXPRESSION PROFILES OF GRADE II AND GRADE III TUMOURS

Supervised hierarchical clustering was used to determine differentially expressed miRNAs when comparing two groups of samples based on certain characteristic such as grade, *IDH1* mutation status and histology. Forty two miRNAs were significantly differentially expressed between primary grade II and grade III tumours as illustrated in the hierarchical clustering dendrogram in Figure 4.2. Two grade II tumours, IN99/81 (O) and IN2800 (A) clustered together, independently of the remaining cases which separated into two large clusters. Cluster 1 comprised mainly grade II tumours (8/10, 80%) whereas cluster 2 contained equal numbers of grade II and grade III cases. Tumours with astrocytic and oligodendroglial components are equally distributed between the two large clusters.

Of the 42 differentially expressed miRNAs, 21 miRNAs were differentially expressed between grade II and grade III tumours in $\geq$ 70% of cases. The 21 miRNAs were used to identify targets and pathways. These miRNAs were all upregulated in 70% of grade II tumours and downregulated in 83% of grade III tumours as detailed in Table 4.2.

Figure 4.1 Unsupervised hierarchical clustering for 32 primary tumours

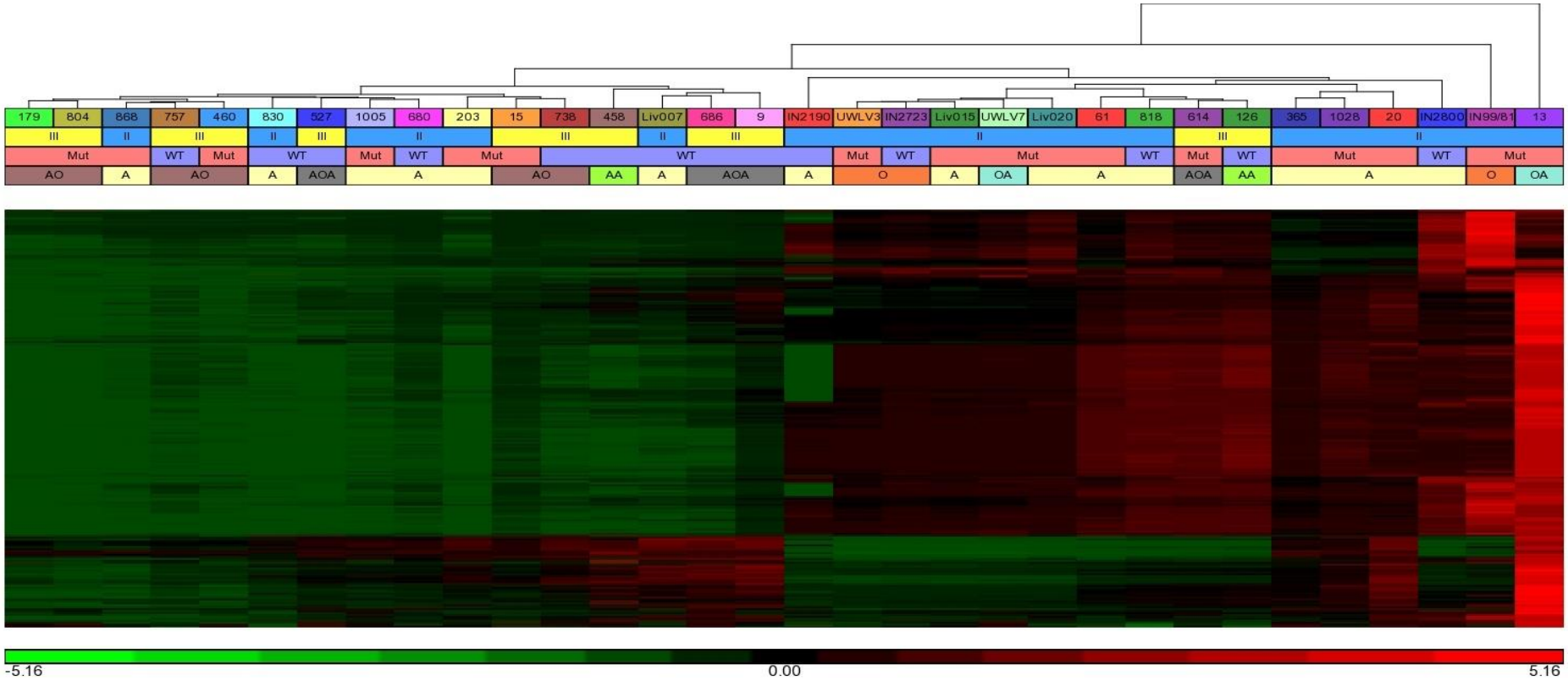

miRNA expression of 1719 miRNAs in 32 primary tumours using Partek Genomics Suite. Red colour represents high levels of miRNA expression and green colour represents low levels of miRNA expression in the tumour. II – Grade II, III – Grade III, Mut – *IDH1*/*IDH2* mutant, WT – *IDH1*/*IDH2* wild type, A – astrocytoma, OA – oligoastrocytoma, O – oligodendroglioma, AA – anaplastic astrocytoma, AOA – anaplastic oligoastrocytoma, AO – anaplastic oligodendroglioma.

Figure 4.2 Supervised hierarchical clustering for 32 primary tumours (grade II vs grade III)

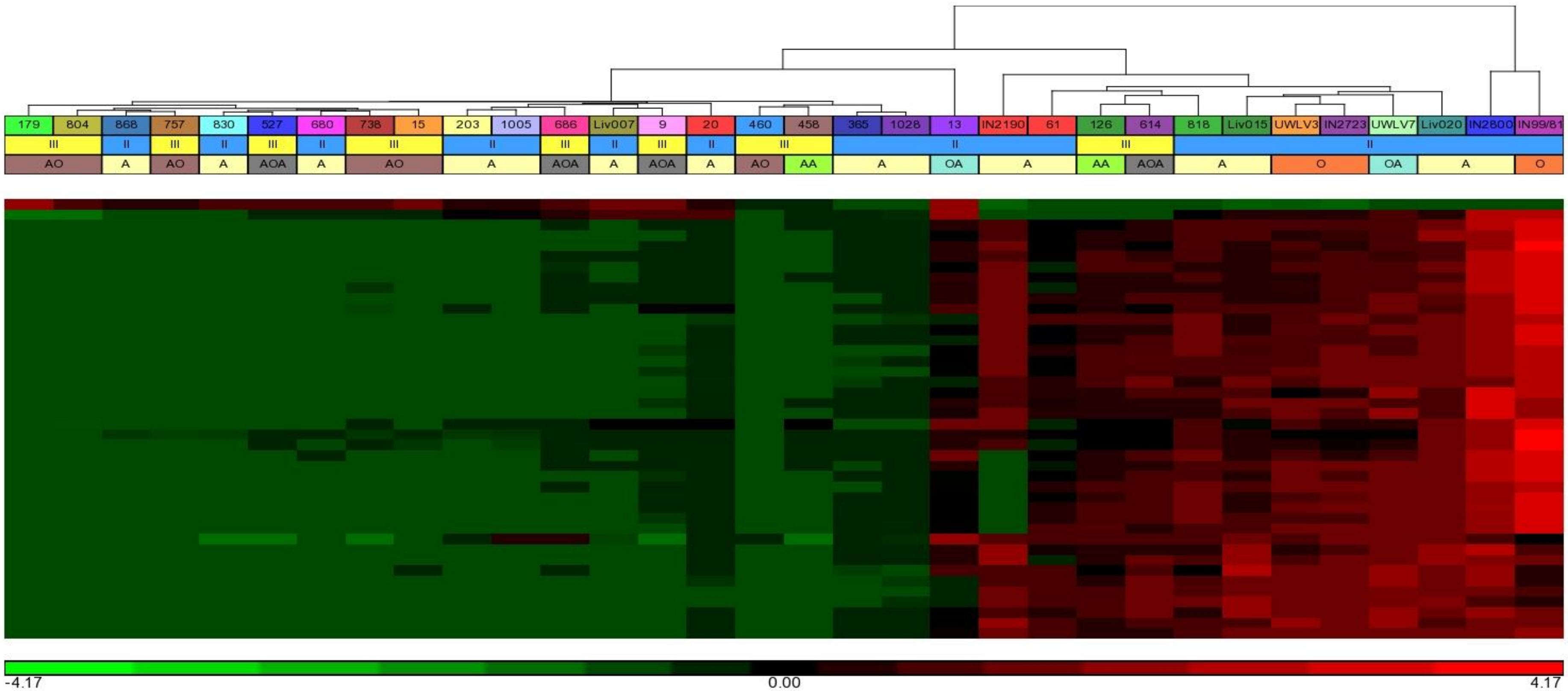

All 42 significant miRNAs with differential expression of ≥ 2 fold change identified using Partek Genomic Suite by ANOVA and with a significance of $p < 0.05$. Red colour represents high levels of miRNA expression and green colour represents low levels of miRNA expression in the tumour. II – Grade II, III – Grade III, A – astrocytoma, OA – oligoastrocytoma, O – oligodendroglioma, AA – anaplastic astrocytoma, AOA – anaplastic oligoastrocytoma, AO – anaplastic oligodendroglioma.

Table 4.2 Differentially expressed miRNAs between grade II and grade III tumours (≥ 2 fold change) with percentage of differential expression in each grade.

miRNA	p-value	Fold change (II vs III)	Upregulation (% of tumours)		Downregulation (% of tumours)		Target	Pathway
			Grade II	Grade III	Grade II	Grade III		
miR-466	0.03	4	70	17	30	83	*PHOSPHO2-KLHL23, PLCXD1, KLHL23, GPR137C, DCLK1, DCUN1D4, TNRC6B, VAMP4, RIMKLB, LEMD3*	PI3K-Akt signalling pathway, TGF-beta signalling pathway, T cell receptor signalling pathway, Chronic myeloid leukemia, Non-small cell lung cancer
miR-3658	0.02	4	70	17	30	83	*AEBP2, DCUN1D5, LPP, MCTS1, GNB4, LRP6, TMED5, UBE2K, SMAD5, UHMK1*	TGF-beta signalling pathway, GABAergic synapse, Wnt signalling pathway, Prostate cancer, Chronic myeloid leukemia
miR-3142	0.03	4	70	17	30	83	*WDFY3, EVC, SEH1L, SPOPL, CASK, PCYT1B, ITGB1BP1, OGFR, THAP4, GABRA1*	Renal cell carcinoma, Nicotinate and nicotinamide metabolism, mTOR signalling pathway
miR-449c	0.03	4	70	17	30	83	*NUP50, STMN2, CDK19, ODZ1, CREB1, PAPOLA, MAPK1IP1L, ACTL6A, TMEM48, STK38L*	Hepatitis B, Phosphatidylinositol signalling system, ErbB signalling pathway, Salmonella infection, Inositol phosphate metabolism
miR-2113	0.01	3.8	70	17	30	83	*PIK3C2A, COL4A3BP, CRH, ELL2, NCBP1, CNTLN, MAP4K3, CASK, SNTB2, CCDC6*	Notch signalling pathway, Pathways in cancer, Renal cell carcinoma, Long-term potentiation, Adherens junction
miR-4529-5p	0.02	3.6	70	17	30	83	*CBLL1, SS18L1, CSDE1, PKP3, MEX3C, PIP4K2C, LRP1, KIRREL2, GRIN2B, DNAJC14*	Leukocyte transendothelial migration, Bacterial invasion of epithelial cells, Salmonella infection, N-Glycan biosynthesis, Wnt signalling pathway
miR-4471	0.04	3	70	17	30	83	*CDS2, POU2F1, GSTO2, IRS1, SLAMF8, DNAJB4, ANKIB1, EPB41L5, LIN52, B3GNT2*	Metabolism of xenobiotics by cytochrome P450, Biosynthesis of unsaturated fatty acids, Regulation of actin cytoskeleton, Neuroactive ligand-receptor interaction, Melanogenesis

Table 4.2 Differentially expressed miRNAs between grade II and grade III tumours (≥ 2 fold change) with percentage of differential expression in each grade (cont'd).

miRNA	p-value	Fold change (II vs III)	Upregulation (% of tumours)		Downregulation (% of tumours)		Target	Pathway
			Grade II	Grade III	Grade II	Grade III		
miR-181a*	0.04	3.5	70	17	30	83	*ALDH18A1, ATP13A4, ALDH6A1, NIPA2, RIBC1, CFL2, RHOBTB1, H1F0, AP1S3, ARL4A*	Ubiquitin mediated proteolysis, Endocytosis, Ether lipid metabolism, Nucleotide excision repair, Synaptic vesicle cycle
miR-181a-2*	0.01	3	70	17	30	83	*ANTXR2, PRSS12, MGAT4A, ARNTL2, PARP16, SRPK2, NR1D2, ANKRD44, FEZ1, PAG1*	Same as above for miR-181a*
miR-3616-5p	0.03	2.7	70	17	30	83	*SERBP1, DDX3X, CHL1, KDM5B, JMJD1C, PRSS35, WDR72, KCNMA1, SOSTDC1, TSPAN7*	Valine, leucine and isoleucine biosynthesis, Pantothenate and CoA biosynthesis, Terpenoid backbone biosynthesis, mRNA surveillance pathway, Calcium signalling pathway
miR-4733-3p	0.03	2.7	70	17	30	83	*CHMP1, DGAT1, LARP1, RIMS3, FKBP15, DDX18, CCL8, MIS12, PPP6R2, ABHD4*	ABC transporters, Pathogenic Escherichia coli infection, Gap junction, ECM-receptor interaction, Cyanoamino acid metabolism
miR-4741	0.01	2	70	17	30	83	*NCS1, SDR16C5, MMAB, IL17RA, PRPF38A, TDRKH, CHRFAM7A, ACOX3,DPYSL5, FOXP2*	Axon guidance, Lysine degradation, Aminoacyl-tRNA biosynthesis, Endocytosis, Hedgehog signalling pathway
miR-4268	0.02	2	70	17	30	83	*BBS5, SNX1, MSMO1, IL6ST, GOSR1, HOXB6, RIMS4, ADCY1, RAD54B, SRCIN1*	Cell cycle, Prostate cancer, Pancreatic cancer, Pathways in cancer, Chronic myeloid leukemia
miR-323b-5p	0.03	2	70	17	30	83	*TAF5, STK38, PIK3R3, BTAF1, JAK1, LMAN1, SERF2, GLRA2, TBC1D23, ALPK3*	Cell cycle, Pathways in cancer, Prostate cancer, Pancreatic cancer, Chronic myeloid leukemia

Table 4.2 Differentially expressed miRNAs between grade II and grade III tumours (≥ 2 fold change) with percentage of differential expression in each grade (cont'd).

miRNA	p-value	Fold change (II vs III)	Upregulation (% of tumours)		Downregulation (% of tumours)		Target	Pathway
			Grade II	Grade III	Grade II	Grade III		
miR-3650	0.02	2	70	17	30	83	*RTN41P1, CDK14, ABO, SH3BP2, DCLRE1C, ELN, STEAP2, EIF2C3, BNC2, HDX*	Pathways in cancer, Prostate cancer, Pancreatic cancer, Adherens junction, MAPK signalling pathway
miR-4252	0.03	2	70	17	30	83	*FNDC3A, CDK6, AK2, HFM1, CDK17, AKIRIN2, RELN, DAAM1, TGFBR1, DSTYK*	Pathways in cancer, Adipocytokine signalling pathway, Thyroid cancer, Small cell lung cancer, Non-small cell lung cancer
miR-4500	0.01	2	70	17	30	83	*IGF2BP1, HMGA2, DDI2, COIL,GATM, USP38, IGDCC3, MRS2, MAP4K3, CCNJ*	ECM-receptor interaction, PI3K-Akt signalling pathway, Glycosaminoglycan biosynthesis – chondroitin sulphate, Amoebiasis, p53 signalling pathway
miR-4302	0.02	2	70	17	30	83	*ITGB1BP1, GAB3, FGD6, SMG7, AGAP1, ROCK1, CDS2, DYRK1A, TM2D2, FABP2*	Pathways in cancer, Acute myeloid leukemia, Chronic myeloid leukemia, B cell receptor signalling pathway, ErbB signalling pathway
miR-141	0.01	2	70	17	30	83	*TMEM170B, TNRC6B, ATP8A1, DEK, CHD9, IBA57, KIDINS220, STRN, DR1, ABL2*	Pathways in cancer, Cell cycle, p53 signalling pathway, Chronic myeloid leukemia, Prostate cancer
miR-3689a-5p	0.01	2	70	17	30	83	*GPR123, ITM2B, RBM41, TNRC6B, EXOC5, TRPS1, CDH9, HCN1, MED13, GDAP1*	Drug metabolism – cytochrome P450, Endocrine and other factor-regulated calcium reabsorption, Synaptic vesicle cycle, Retinol metabolism, Vassopresin-regulated water reabsorption
miR-320d	0.03	2	70	17	30	83	*CREB5, TGOLN2, LPPR1, ARPP19, ABHD13, PBX3, TRIAP1, TMEM108, TMEM47, ARFIP1*	Prostate cancer, Endometrial cancer, mTOR signalling pathway, Circadian rhythm, Biotin metabolism

Gene targets and pathways that were common between the miRNAs are highlighted in different coloured text. *miR, originates from the same precursor as the mature miRNA and the predominant product is given the main name and miR* is from the opposite arm of the precursor.

4.8 miRNA EXPRESSION PROFILING OF GRADE II TUMOURS

The expression profiles of 20 grade II tumours comprising 15 A, 2 OA and 3 O were compared. There were 13 cases with *IDH1* R132H mutation and 7 with wild type *IDH1*. Unsupervised hierarchical clustering was performed using 1719 miRNAs and the resulting dendrogram is shown in Figure 4.3. As in Figure 4.1, BTNW13 and IN99/81 clustered independently to the remaining cases. Tumours did not separate independently according to histology or *IDH* mutation status.

Supervised hierarchical clustering identified a single significant miRNA (let-7c) that was differentially expressed based on *IDH* mutation status. Let-7c was upregulated in 61% *IDH* mutant cases compared to 28% in tumours with *IDH* wild type. It was downregulated in 38% *IDH* mutant compared to 71% in *IDH* wild type tumours. The top 10 targets for let-7c are *HMGA2, GATM, PRTG, MAP4K3, COIL, USP38, CCNJ, ADRB2, IGDCC3* and *GDF6*. According to KEGG pathway analysis, it is involved in ECM-receptor interaction, glycosaminoglycan biosynthesis – chondroitin sulphate, PI3K-Akt signalling pathway, amoebiasis and protein digestion and absorption.

Figure 4.3 Unsupervised hierarchical clustering for 20 grade II tumours

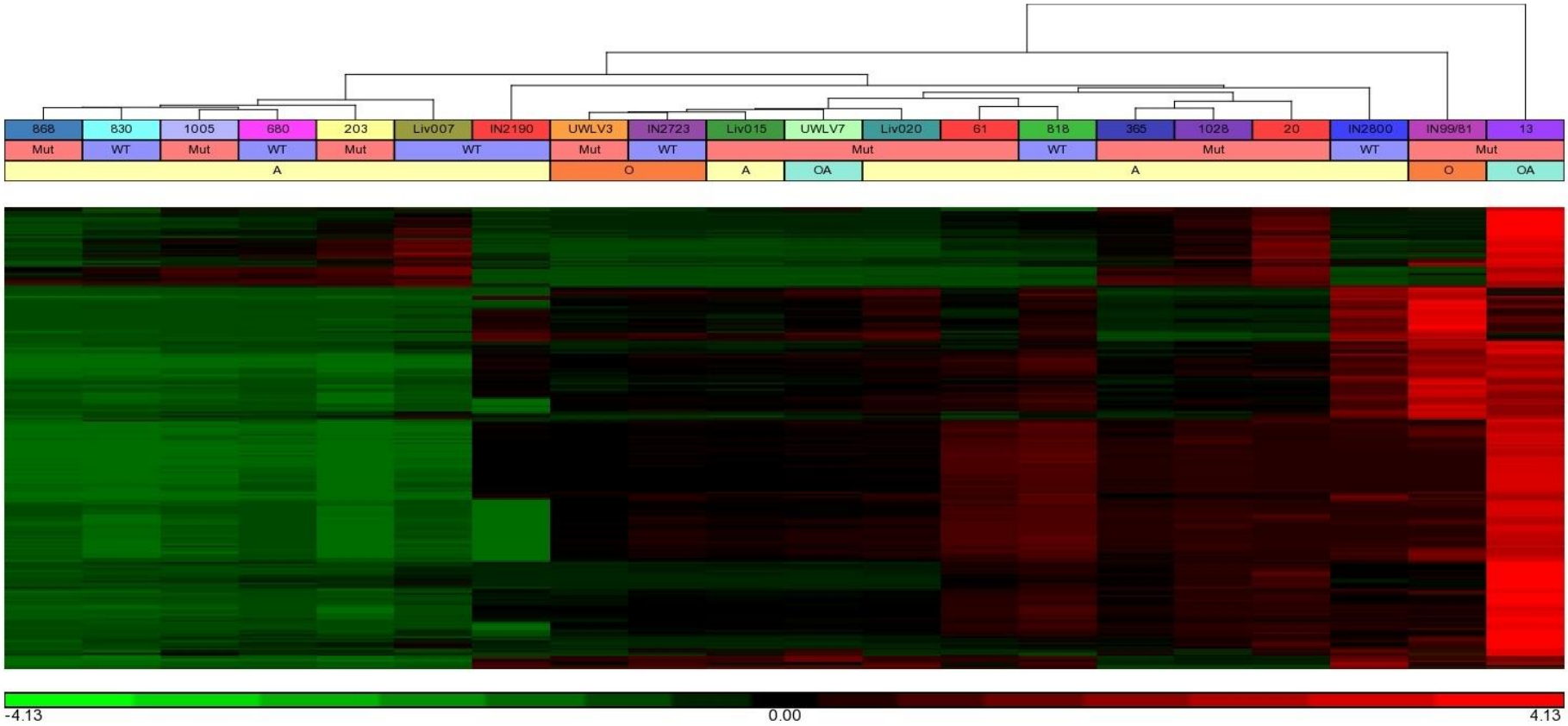

Expression of 1719 miRNAs in 20 grade II tumours identified using Partek Genomic Suite by ANOVA and with a significance of $p < 0.05$. Red colour represents high levels of miRNA expression and green colour represents low levels of miRNA expression in the tumour. Mut – *IDH1*/*IDH2* mutant, WT – *IDH1*/*IDH2* wild type, A – astrocytoma, OA – oligoastrocytoma, O – oligodendroglioma.

4.9 miRNA EXPRESSION PROFILING OF GRADE II TUMOURS BASED ON HISTOLOGY

miRNA expression was determined in three histological groupings; A vs OA (n = 17), OA vs O (n = 5) and A vs O (n = 18). Hierarchical clustering was performed for each group and significant differentially expressed miRNAs were identified (Figure 4.4). In A vs OA, only 2 OA and 15 A tumours were present. BTNW13 (OA) was different in miRNA expression from rest of the tumours as determined by supervised hierarchical clustering. The remaining tumours were divided into two large clusters and UWLV7 (OA) had different expression profile from the rest of the tumours in one of the clusters. In OA vs O, hierarchical clustering resulted in tumours forming 2 independent clusters according to histology. In A vs O, only 3 O and 15 A tumours were present. IN99/81 (O) and IN2800 (A) clustered together and had different profiles from the remaining tumours with the rest of the cases dividing into 2 large clusters. UWLV3 and IN2723 (both O) clustered together with similar expression profiles. Common differentially expressed miRNAs between the three histological groups are detailed in Figure 4.5.

The four common differentially expressed miRNAs between A vs OA and OA vs O were miR-21, miR-23a, miR-30c and miR-99a, while common miRNAs differentially expressed between A vs OA and A vs O were miR-885-3p, miR-936, miR-4736 and miR-4728-5p (Table 4.3).

Figure 4.4 Supervised hierarchical clustering for 20 grade II tumours based on histology

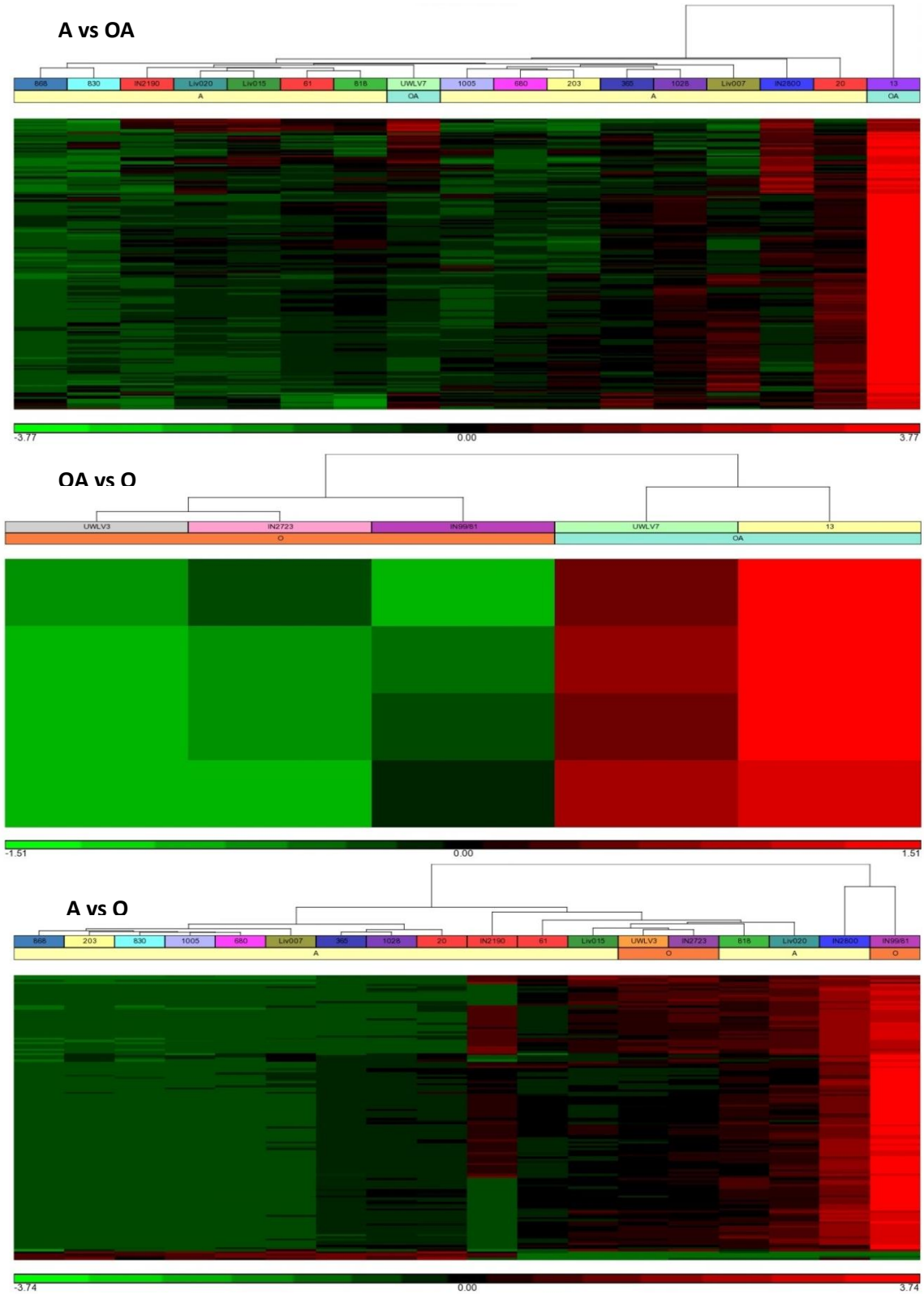

Expression of differentially expressed miRNAs with ≥ 2 fold change in expression change identified using Partek Genomic Suite by ANOVA and with a significance of $p < 0.05$. Red colour represents high levels of miRNA expression and green colour represents low levels of miRNA expression in the tumour. A – astrocytoma, OA – oligoastrocytoma, O – oligodendroglioma.

Figure 4.5 Venn diagram showing common and unique miRNAs among the three groups.

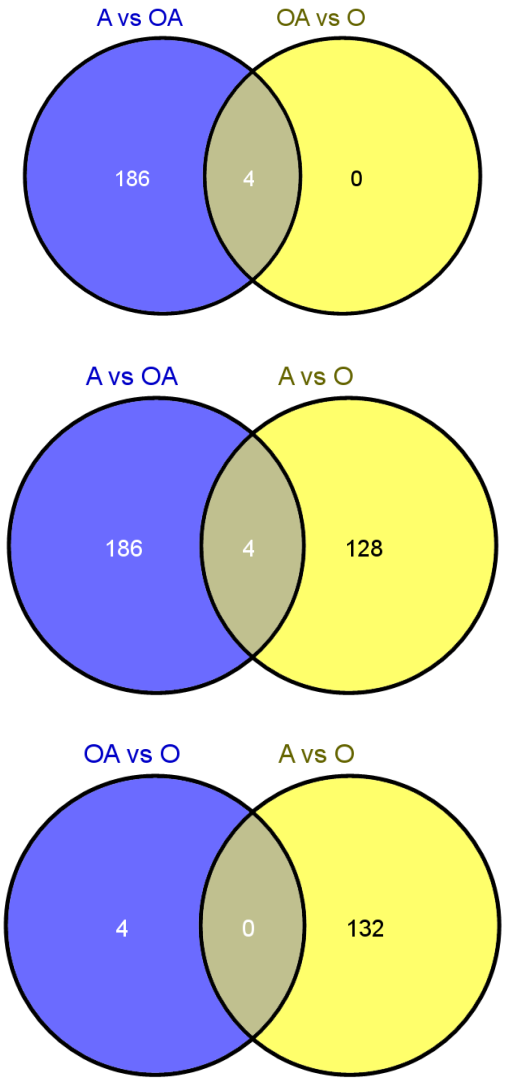

Using Partek Genomics Suite, A vs OA and OA vs O was compared and four common miRNAs were identified with ≥ 2 fold change in expression and significance of $p < 0.05$ by ANOVA; when comparing A vs OA and A vs O, four common miRNAs were also identified with ≥ 2 fold change in expression and significance of $p < 0.05$ by ANOVA but these were different from that identified between A vs OA and OA vs O; Comparison of OA vs O and A vs O identified no common miRNAs with ≥ 2 fold change in expression and significance of $p < 0.05$ by ANOVA. A, astrocytoma; OA, oligoastrocytoma; O, oligodendroglioma.

Table 4.3 Common miRNAs in the three groups, A vs OA, OA vs O and A vs O with percentage of differential expression in different histology types of grade II tumours.

miRNA	Upregulation (% of tumours)[a]			Downregulation (% of tumours)			Target	Pathway
	A	OA	O	A	OA	O		
Common between A vs OA and OA vs O								
miR-21	47	100	33	53	0	67	*YOD1, KRIT1, WTH3DI, GPR64, PLEKHA1, SKP2, FBXO11, MALT1, PELI1, PBRM1*	Cytokine-cytokine receptor interaction, TGF-beta signalling pathway, MAPK signalling pathway, Melanoma
miR-23a	40	100	67	60	0	33	*GIPC3, PTPRT, PCDHB16, PPA2, DSC3, XXYLT1, PIK3C2A, USH2A, ASTN1, CORT*	Transcriptional misregulation in cancer, Osteoclast differentiation, Pathogenic Escherichia coli infection, Glycolysis/Gluconeogenesis, RNA degradation
miR-30c	40	100	67	60	0	33	*TNRC6A, CELSR3, MIER3, EED, LHX8, PPARGC1B, PHTF2, SCN2A, ANKRA2, RTKN2*	Neuroactive ligand-receptor interaction, Phosphatidylinositol signalling system, Dilated cardiomyopathy, Axon guidance, Focal adhesion
miR-99a	40	100	67	60	0	33	*KBTBD8, TARDBP, TMPRSS13, SMARCA5, AP1AR, ZADH2, THAP2, MTOR, NOX4, VNN1*	Pathways in cancer, Colorectal cancer, ErbB signalling pathway, Chronic myeloid leukemia, Prostate cancer
Common between A vs OA and A vs O								
miR-885-3p	33	100	100	67	0	0	*NAA11, LIN9, WWC3, CARM1, TCL1A, PKNOX1, CLIP4, PPP3CB, NDST1, PDE7B*	Glycosaminoglycan biosynthesis – heparan sulphate/heparin, Glioma, Pathogenic Escherichia coli infection, Adherens junction, Melanoma
miR-936	33	100	100	67	0	0	*ANKRD17, FLRT3, GABRA1, SLC35D1, ATP1B1, LRRC4C, GPR137C, FGF2, PHACTR2, DTNA*	Glycosaminoglycan biosynthesis – chondroitin sulphate, GABAergic synapse, ErbB signalling pathway, Gastric acid secretion, Morphine addiction
miR-4736	33	100	100	67	0	0	*ORAI2, SSR1, TBC1D13, MAVS, ABCD3, SYT2, KCNMA1, H2AFV, MAP1B, ERC1*	ErbB signalling pathway, GnRH signalling pathway, Vitamin B6 metabolism, Calcium signalling pathway, SNARE interactions in vesicular transport
miR-4728-5p	33	100	33	67	0	67	*FOXP4, NOS1, GNAT1, ORAI2, SMARCD1, FAIM2, AR, DUSP8, LRP1, RALB*	Vasopressin-regulated water reabsorption, Axon guidance, Cell adhesion molecules (CAMs), Prostate cancer, Pathogenic Escherichia coli infection

[a] A, astrocytoma; OA, oligoastrocytoma; O, oligodendroglioma. Common pathways between miRNAs are highlighted in different coloured text.

4.10 miRNA EXPRESSION PROFILING OF GRADE III TUMOURS

Expression analysis of 12 grade III tumours was performed comprising 2 AA, 4 AOA and 6 AO. Five tumours were *IDH* mutant and 7 were *IDH* wild type. Unsupervised hierarchical clustering was performed using 1719 miRNAs and BTNW614 (AOA) and BTNW126 (AA) had different profiles from the remaining tumours as shown in Figure 4.6. All AO tumours form a large cluster with a single case of AOA (BTNW527).

Supervised hierarchical clustering based on *IDH* mutation status identified 8 miRNAs ($\geq$ 2-fold change) with differential expression. The dendrogram in Figure 4.7 shows that the tumours were divided into 2 clusters. The smaller group of 5 cases were all *IDH* wild type tumours with a mixture of histologies (1AA, 3AOA and 1AO). The larger cluster comprised a majority of *IDH* mutant (5/7, 71%) samples and 6/7 (86%) AO. Seven of the miRNAs were upregulated in 71% *IDH* wild type tumours and downregulated in 80% *IDH* mutated tumours, while miR-21 was upregulated in 86% wild type tumours and downregulated in 100% *IDH* mutated tumours as detailed in Table 4.4.

Figure 4.6 Unsupervised hierarchical clustering for 12 grade III tumours

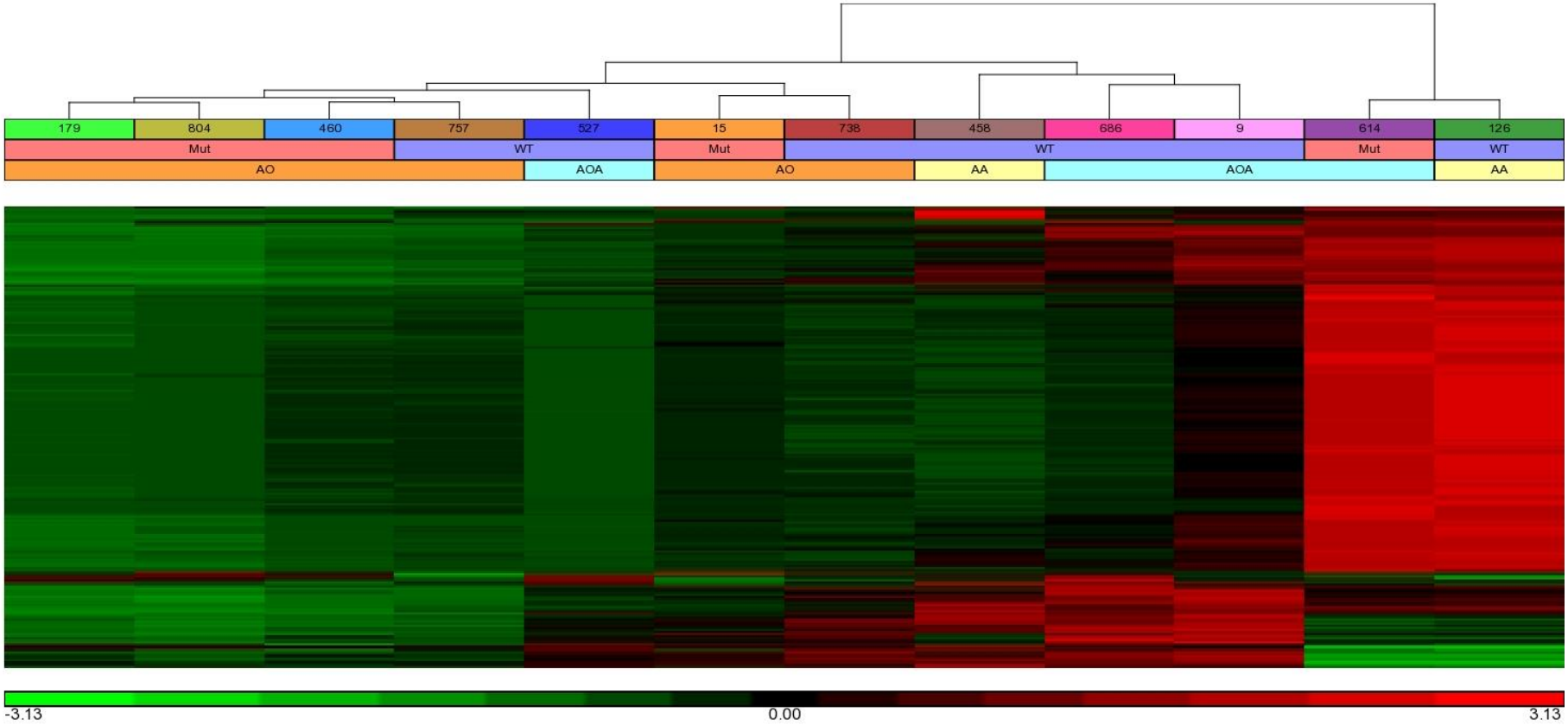

Expression of 1719 miRNAs in 12 grade III tumours identified using Partek Genomic Suite. Red colour represents high levels of miRNA expression and green colour represents low levels of miRNA expression in the tumour. Mut – *IDH1*/*IDH2* mutant, WT – *IDH1*/*IDH2* wild type, AA – anaplastic astrocytoma, AOA – anaplastic oligoastrocytoma, AO – anaplastic oligodendroglioma.

Figure 4.7 Supervised hierarchical clustering for 12 grade III tumours based on *IDH* mutation status

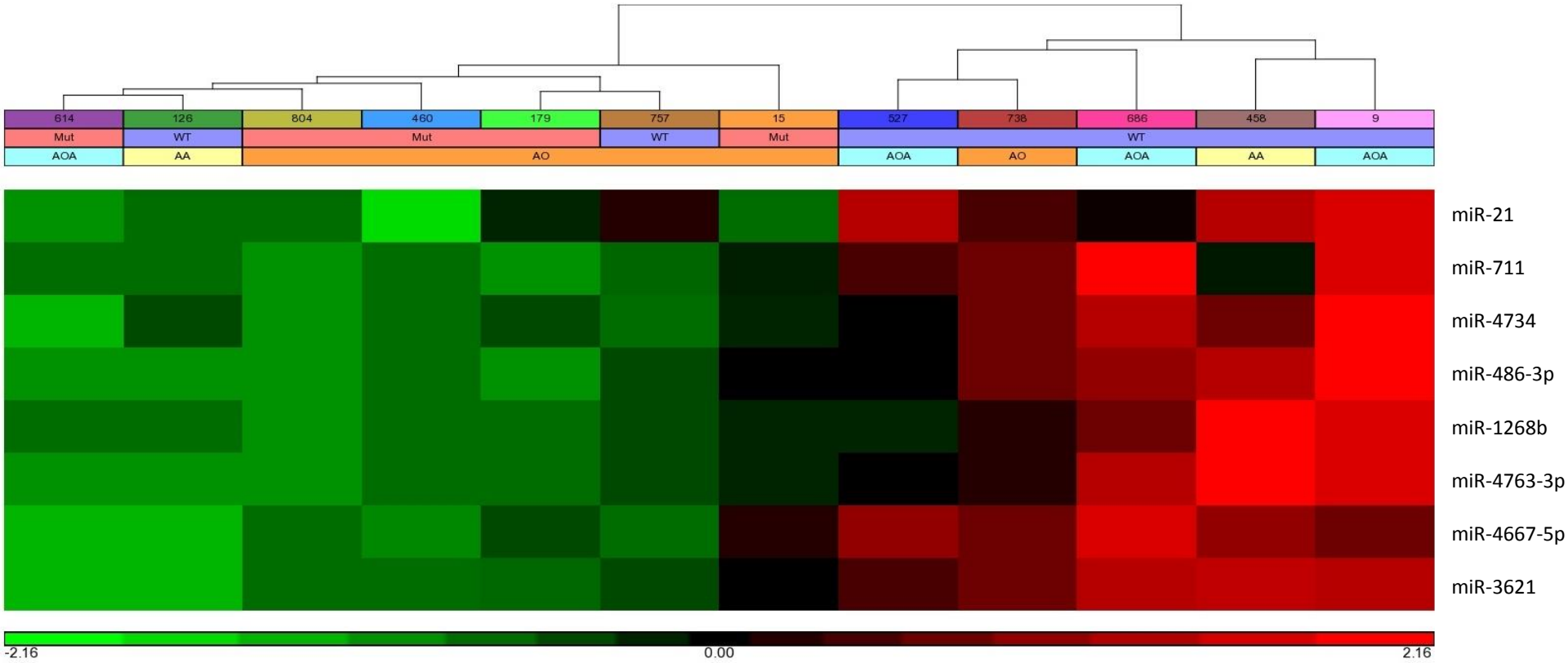

Expression of 8 differentially expressed miRNAs with ≥ 2 fold change in expression identified using Partek Genomic Suite by ANOVA and with a significance of $p < 0.05$. Red colour represents high levels of miRNA expression and green colour represents low levels of miRNA expression in the tumour. Mut – *IDH1*/*IDH2* mutant, WT – *IDH1*/*IDH2* wild type, AA – anaplastic astrocytoma, AOA – anaplastic oligoastrocytoma, AO – anaplastic oligodendroglioma.

Table 4.4 Differentially expressed miRNAs (≥ 2 fold change) in grade III tumours based on *IDH* mutation.

miRNA	P value	Fold change[a] (Mut vs WT)	Upregulation (% of tumours)		Downregulation (% of tumours)		Target	Pathway
			Mut	WT	Mut	WT		
miR-1268b	0.04	-2	20	71	80	28	*ADAMTS4, KCNA3, TMEM229A, PGR, HIF3A, EGR4, COG2, TOLLIP, RBM19*	Ubiquinone and other terepenoid-quinone biosynthesis, Phenylalanine metabolism, Calcium signalling pathway, ABC transporters, Type II diabetes mellitus
miR-711	0.04	-2	20	71	80	28	*MAFG, RGS5, FGD2, KRTAP20-3, ACTR10, CNKSR2, MAD2L1BP, MUC15, CD44, IL18BP*	Pathways in cancer, Colorectal cancer, Wnt signalling pathway, Chronic myeloid leukemia, Toll-like receptor signalling pathway
miR-4667-5p	0.04	-2	20	71	80	28	*AAK1, KCNC1, VSTM4, ADCY6, STAM2, DAGLA, ATF6B, KSR2, RASSF4, ITGA10*	PI3K-Akt signalling pathway, Steroid hormone biosynthesis, Regulation of actin cytoskeleton, Fatty acid elongation, Pancreatic cancer
miR-4763-3p	0.04	-2	20	71	80	28	*ORAI2, THEM5, PGPEP1, CD276, MAFG, CHPF, LHPP, TMEM120B, CD3EAP, ASB6*	Glycosaminoglycan biosynthesis – chondroitin sulphate, Adherens junction, Synaptic vesicle cycle, Calcium signalling pathway, Glycosaminoglycan biosynthesis – heparan sulphate/heparin
miR-4734	0.02	-2.8	20	71	80	28	*USP36, ANKRD52, ANKRD13A, SSTR2, INSIG1, COL6A6, CUL1, LYL1*	NIcotinate and nicotinamide metabolism, Morphine addiction, Oocyte meiosis, N-glycan biosynthesis, Circadian rythm
miR-486-3p	0.03	-2.9	20	71	80	28	*RAB11FIP4, PLCB1, PRX, FLOT2, NSD1, DAB2IP, SF3A1, TMEM132E, ORAI2, H6PD*	Synaptic vesicle cycle, Lysine degradation, RNA polymerase, ErbB signalling pathway, Shigellosis
miR-3621	0.04	-2.9	20	71	80	28	*CARD9, CDC16, USP19, H3F3B, ECE1*	Pathways in cancer, TGF-beta signalling pathway, Melanogenesis, Renal cell carcinoma, Long-term potentiation
miR-21	0.01	-3.6	0	86	100	14	*YOD1, KRIT1, WTH3DI, GPR64, PLEKHA1, SKP2, FBXO11, MALT1, PELI1, PBRM1*	Cytokine-cytokine receptor interaction, TGF-beta signalling pathway, MAPK signalling pathway, Melanoma

[a] Mut, *IDH* mutant; WT, *IDH* wild type. Pathways common between miRNAs are highlighted in different coloured text.

4.11 miRNA EXPRESSION PROFILING OF GRADE III TUMOURS BASED ON HISTOLOGY

Similar to the analysis for grade II tumours, comparisons of miRNA expression were performed in three histological groupings; AA compared with AOA (n = 6), AOA compared with AO (n = 10) and AA compared with AO (n = 8). Significant differentially expressed miRNAs were identified in the three groups and hierarchical clustering is shown in Figure 4.8. No differentially expressed miRNAs were found when comparing AA with AOA. When comparing AOA with AO, there were 2 clusters with one comprising 3 AOA and the other cluster comprising of all AO tumours and 1 AOA (BTNW527). AA and AO were separated independently according to histology. Three miRNAs (miR-3135b, miR-4706 and miR-4748) were differentially expressed between the AOA and AO and also between AA and AO as detailed in Figure 4.9. All 3 miRNAs were upregulated in all AA, 75% of AOA and 17% of AO while they were downregulated in 25% of AOA and 83% of AO (Table 4.5).

Figure 4.8 Supervised hierarchical clustering for 10 grade III tumours based on histology

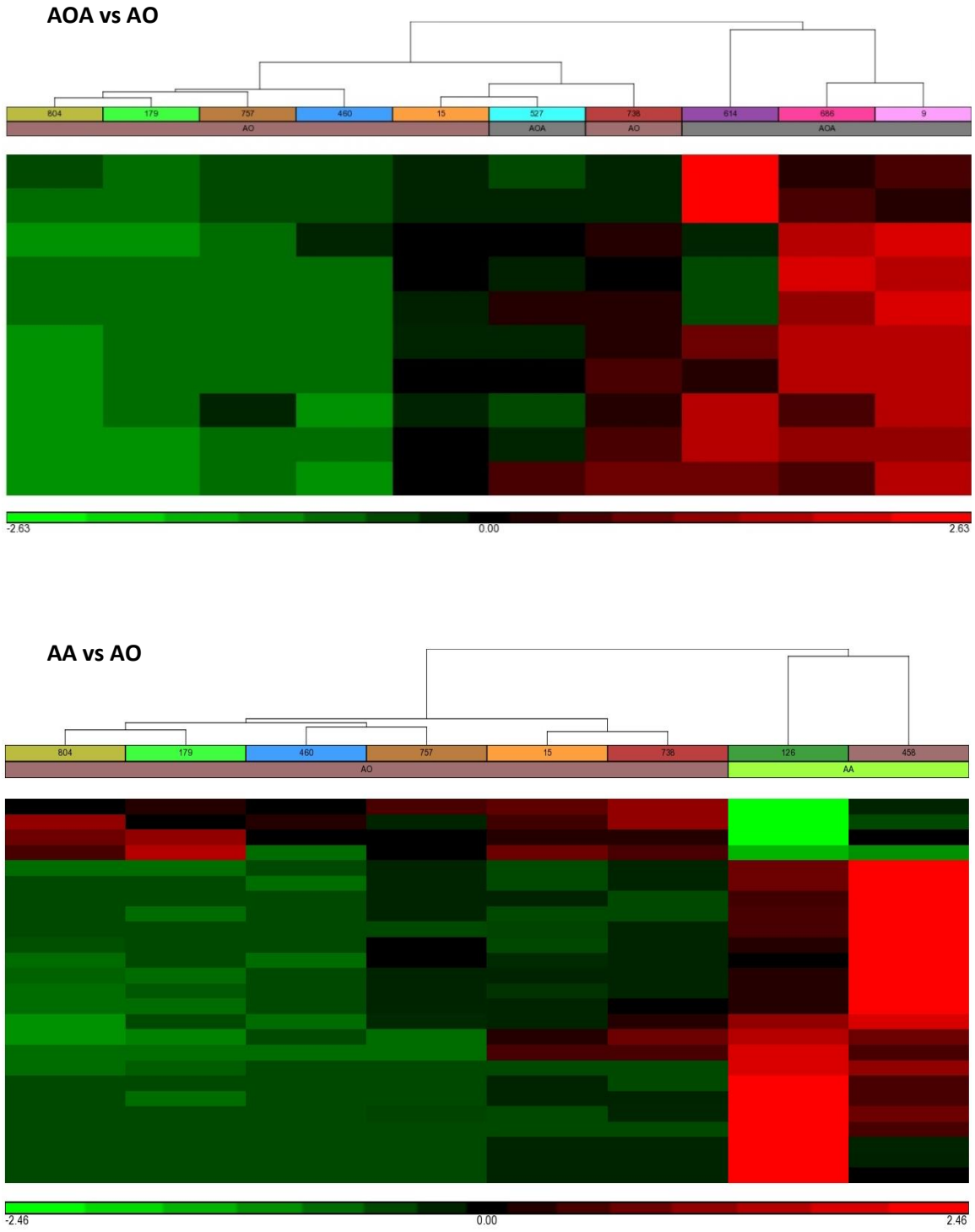

Expression of differentially expressed miRNAs with ≥ 2 fold change in expression identified using Partek Genomic Suite by ANOVA and with a significance of $p < 0.05$. Red colour represents high levels of miRNA expression and green colour represents low levels of miRNA expression in the tumour. AA – anaplastic astrocytoma, AOA – anaplastic oligoastrocytoma, AO – anaplastic oligodendroglioma.

Figure 4.9 Venn diagram showing common and unique miRNAs in the two groups (AA vs AO and AOA vs AO)

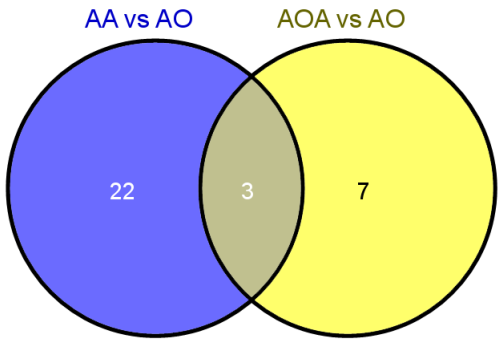

Using Partek Genomics Suite, AA vs AO and AOA vs AO was compared and three common miRNAs were identified with ≥ 2 fold change in expression and significance of $p < 0.05$ by ANOVA. AA, anaplastic astrocytoma; AO, anaplastic oligodendroglioma; AOA, anaplastic oligoastrocytoma.

Table 4.5 Common miRNAs between AA vs AO and AOA vs AO with percentage of differential expression in the three histologies of grade III tumours.

miRNA	Upregulation (% of tumours)[a]			Downregulation (% of tumours)			Target	Pathway
	AA	AOA	AO	AA	AOA	AO		
miR-3135b	100	75	17	0	25	83	*KLHL31, NOS1, TRPM7, RORC, AKNA, EPHA10, RBBP5, COG2, VIPR2, PACS1*	Mucin type O-Glycan biosynthesis, Valine, leucine and isoleucine biosynthesis, Other glycan degradation, Osteoclast differentiation, Vasopressin-regulated water reabsorption
miR-4706	100	75	17	0	25	83	*FOXE1, GPRC5B, ANKRD52, TUBB4A, SAP18, PTAR1, FOXRED2, ANKRD13A, ELAC2, LRRC15*	Tryptophan metabolism, Cocaine addiction, Amphetamine addiction, Tyrosine metabolism, Phenylalanine metabolism
miR-4748	100	75	17	0	25	83	*TSFM, PPP2R5A, KALRN, CTSL2, GABRG2, TMEM106B, SNF8, ABCD4, GM2A, FERMT1*	Colorectal cancer, Endometrial cancer, Epstein-Barr virus infection, B cell receptor signalling pathway

[a] AA, anaplastic astrocytoma; AOA, anaplastic oligoastrocytoma; AO, anaplastic oligodendroglioma.

4.12 COMPARISON OF miRNA EXPRESSION PROFILES OF *IDH* MUTANT AND *IDH* WILD TYPE TUMOURS

Supervised hierarchical clustering analysis was performed for primary tumours of both grade II (n = 17) and grade III tumours (n = 15) based on *IDH* mutation status but no significantly differentially expressed miRNAs were identified. This study suggests that tumour grade and histology were the most influential factors on the expression profiles of tumours.

4.13 RELATIONSHIP BETWEEN miRNA EXPRESSION AND OUTCOME

In order to determine if there was a relationship between differentially expressed miRNAs and patient survival, the miRNA profile was compared in patients who survived less than or more than 2 years and also in patients who survived less than or more than 3 years from initial diagnosis. There was no significant association between miRNA expression and OS.

4.14 DIFFERENTIAL EXPRESSION OF miRNAS IN LGG USING THE CANCER GENOME ATLAS (TCGA) DATA

In order to validate the expression pattern of miRNAs identified and to determine the significance of miRNA expression profiling in the present study cohorts, large publically available cohorts of LGG (N=530) with available miRNA-seq data from TCGA were used**.**

4.14.1 Data analysis

miRNA-seq data for the 530 LGG was downloaded from the TCGA data portal and analysed using Subio platform V.1.18 (Subio Inc., Japan). The data reads_per_million_miRNA_mapped was used as the Ch1 raw signal for analysis. Alongside the miRNA expression data, metadata for the patients containing information on histological types (A, OA and O), histological grades (G2 and G3), *IDH1* mutation status (*IDH1* mutation - Yes and No) and survival (below or above 3 years) was also included. miRNA data series for the LGG TCGA cohorts with all the information was created. Undetected miRNA within the data series were assigned a value of '0'. The raw data was firstly normalized by setting low signal cut off to '0.1', followed by $\log_2$ transformation and finally data centering using median values, to obtain processed signal for further analysis. Processed signal stands for $\log_2$ ratio against the averages of expression patterns per miRNA. The processed signal was analysed for differential expression based on specific patients' data e.g. based on *IDH1* mutation status. The differential expression analysis was based on $\geq$ 2 fold change and $p < 0.05$ (Mann-Whitney U test). Supervised hierarchical clustering using Pearson correlation coefficient was performed to determine the relationship of significant differentially expressed miRNAs.

4.14.2 Differential expression of miRNA in tumours based on histology

The TCGA cohort consisted of 165 A, 177 OA and 111 O tumours. A total of 453 patients were used for the analysis as the remaining patients lacked information regarding the histology of the tumours.

As illustrated in Figure 4.10, the differentially expressed miRNAs between A and OA tumours consisted of miR-96, miR-10b and miR-196b and those between A and O patients consisted of miR-124-1, miR-124-2, miR-7-3, miR-888, miR-196a-1, miR-592, miR-2114, miR-21, miR-203, miR-204, miR-891a, miR-891b, miR-10b, miR-3923, miR-1-2, miR-124-3, miR-1224, miR-137, miR-892b, miR-3622a, miR-96, miR-1262, miR-892b, miR-3065, miR-196b and miR-455. Differentially expressed miRNA between OA and O consisted of let-7d, let-7e and miR-3923.

On comparison of the OA and O data from the TCGA cohort and the present study, two common miRNAs (let-7d and let-7e) were identified in the two cohorts as shown in Figure 4.11.

Figure 4.10 Differentially expressed miRNAs in grade II tumours based on histology

(A)

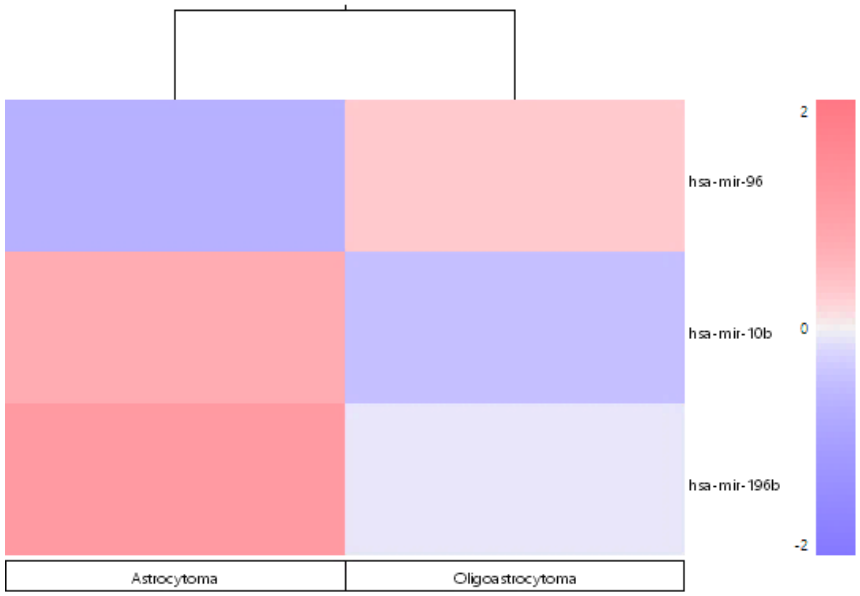

(B)

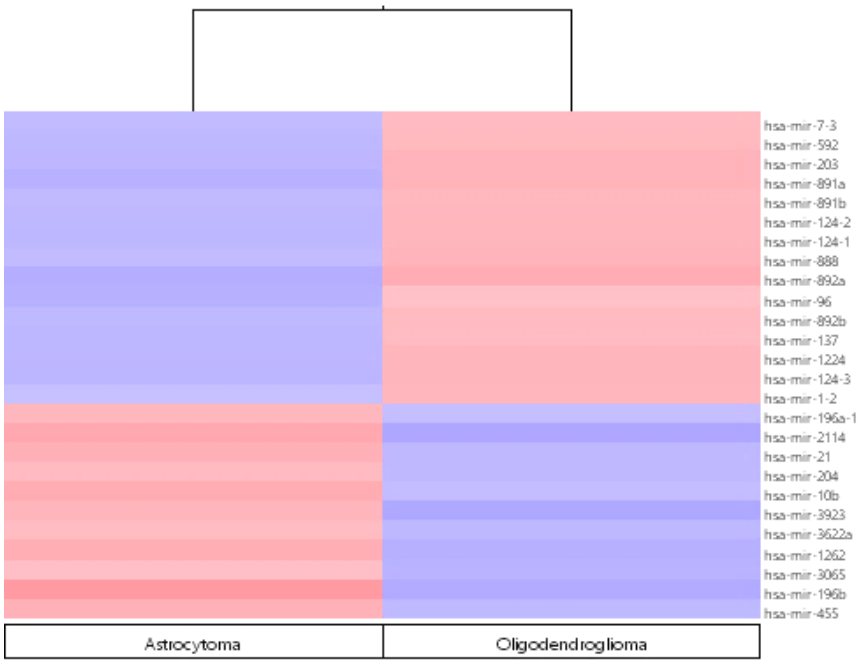

A: Supervised hierarchical clustering showing 3 differentially expressed miRNAs between astrocytoma and oligoastrocytoma tumours. B: Supervised hierarchical clustering showing 26 differentially expressed miRNAs between astrocytoma and oligodendroglioma tumours. The dendrogram colour saturation is proportional to the magnitude of the difference from the mean, ranging from red (over-expressed) to blue (under-expressed).

Figure 4.11 Comparison of TCGA data with the present study

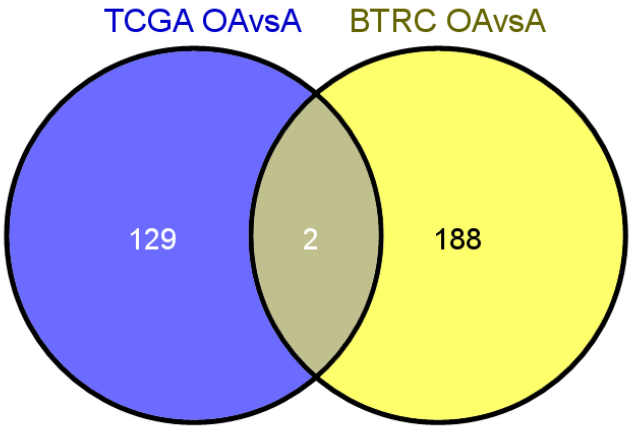

On comparison of the two data sets, TCGA, The Cancer Genome Atlas; BTRC, Brain Tumour Research Centre, two common miRNAs with ≥ 2 fold change in expression were identified by ANOVA with a significance of $p < 0.05$.

4.14.3 Differential expression of miRNA in tumours based on grade

The TCGA cohort consisted of 217 grade II and 236 grade III tumours. A total of 453 patients were used for the analysis as the remaining patients lacked information regarding the grades of the tumours.

As shown in Figure 4.12, the differentially expressed miRNAs between grade II and grade III patients consisted of miR-196a, miR-10b and miR-196b.

4.14.4 Differential expression of miRNA in tumours based on *IDH1* status

The TCGA cohort consisted of 77 *IDH1* mutant and 29 *IDH1* wild type tumours. A total of 106 patients were used for the analysis as the remaining patients lacked information regarding the *IDH1* mutation status of the tumours.

As shown in Figure 4.13, 46 differentially expressed miRNAs between *IDH1* mutant and *IDH1* wild type tumours were identified. These included mir-574, mir-615, mir-599, mir-887, mir-135a-2, mir-34a, mir-196a-2, mir-196a-1, mir-2115, mir-148a, mir-2114, mir-767, mir-34c, mir-21, mir-224, mir-221, mir-204, mir-222, mir-146b, mir-200a, mir-429, mir-200b, mir-3923, mir-187, mir-10a, mir-2277, mir-182, mir-16-2, mir-1295, mir-942, mir-31, mir-155, mir-15b, mir-1266, mir-675, mir-892a, mir-651, mir-1468, mir-1248, mir-452, mir-196b, mir-135b, mir-455, mir-493, mir-671 and mir-23a.

Figure 4.12 Differentially expressed miRNAs between grade II and grade III tumours

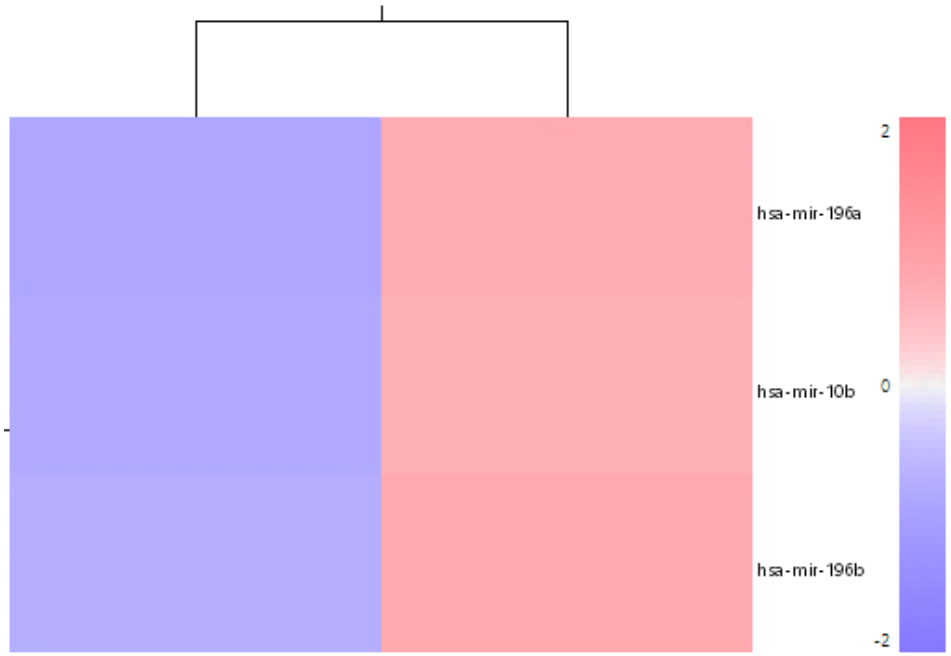

Grade II **Grade III**

Supervised hierarchical clustering showing 3 differentially expressed miRNAs between grade II and grade III tumours. The dendrogram colour saturation is proportional to the magnitude of the difference from the mean, ranging from red (over-expressed) to blue (under-expressed).

Figure 4.13 miRNA differential expression in *IDH1* mutant and *IDH1* wild type tumours

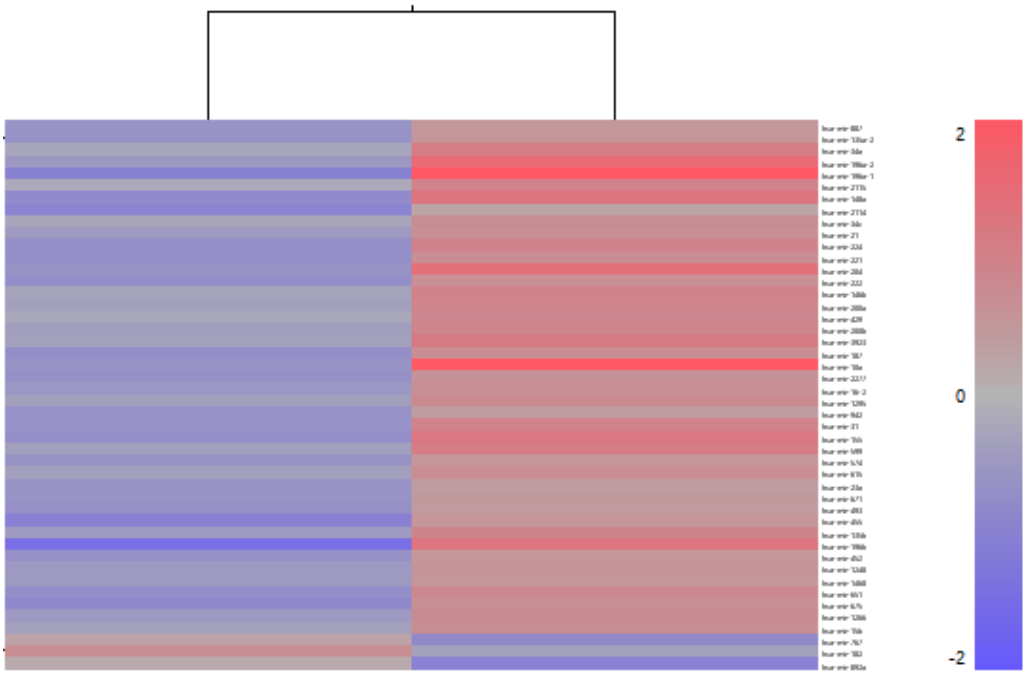

Supervised hierarchical clustering showing 46 differentially expressed miRNAs between *IDH1* mutant and *IDH1* wild type tumours. The dendrogram colour saturation is proportional to the magnitude of the difference from the mean, ranging from red (over-expressed) to blue (under-expressed).

4.14.5 Differential expression of miRNA in tumours based on *IDH1* status and grade

In addition, analysis based on *IDH1* mutation status and tumour grades was also performed. As illustrated in Figure 4.14, no miRNA was significantly differentially expressed between *IDH1* mutants of grade II and III. Similarly, no miRNA was differentially expressed between *IDH1* wild types of grade II and III. However, 25 differentially expressed miRNAs were identified between *IDH1* mutants and *IDH1* wild types in grade II and grade III tumours.

The differentially expressed miRNAs were mir-574, mir-599, mir-887, mir-34a, mir-196a-2, mir-196a-1, mir-224, mir-221, mir-222, mir-204, mir-200a, mir-200b, mir-10a, mir-187, mir-2277, mir-16-2, mir-942, mir-155, mir-31, mir-675, mir-651, mir-1248, mir-196b, mir-455 and mir-493.

Figure 4.14 miRNA differential expression based on *IDH1* mutation status and grade

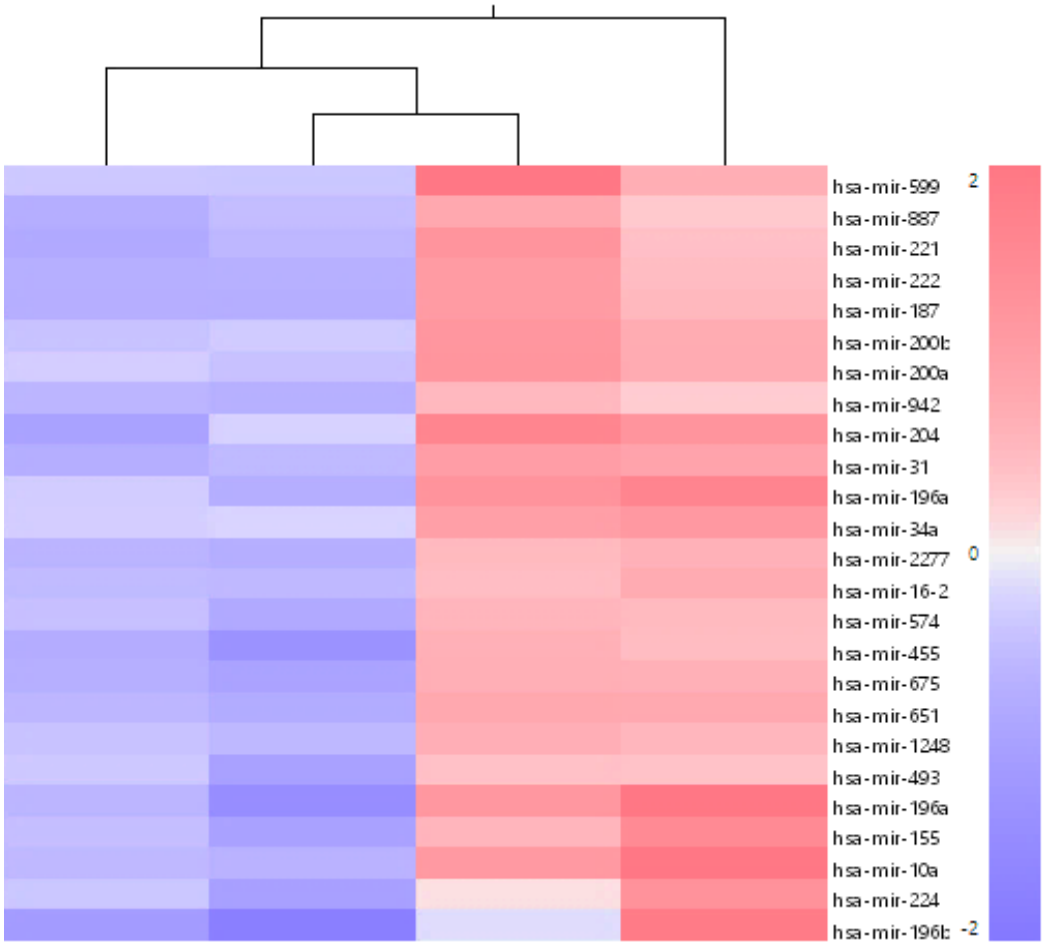

Supervised hierarchical clustering showing 25 differentially expressed miRNA between *IDH1* mutants and *IDH1* wild types of grade II and grade III tumours. The dendrogram colour saturation is proportional to the magnitude of the difference from the mean, ranging from red (over-expressed) to blue (under-expressed).

4.14.6 Differential expression of miRNA in patients based on outcome

Survival information for patients within the TCGA cohort was available in only 74 patients which were classified according to survival rate of >3 and <3 years within this group. The differentially expressed miRNAs between the two groups of patients included mir-135a-2, mir-34a, mir-196a-2, mir-196a-1, mir-148a, mir-34b, mir-34c, mir-21, mir-221, mir-204, mir-1179, mir-200a, mir-429, mir-200b, mir-1275, mir-187, mir-10a, mir-1298, mir-1296, mir-216a, mir-211, mir-504, mir-31, mir-155, mir-217, mir-1247, mir-651, mir-196b and mir-135b and are presented in Figure 4.15.

Figure 4.15 miRNA differential expression of patients based on outcome

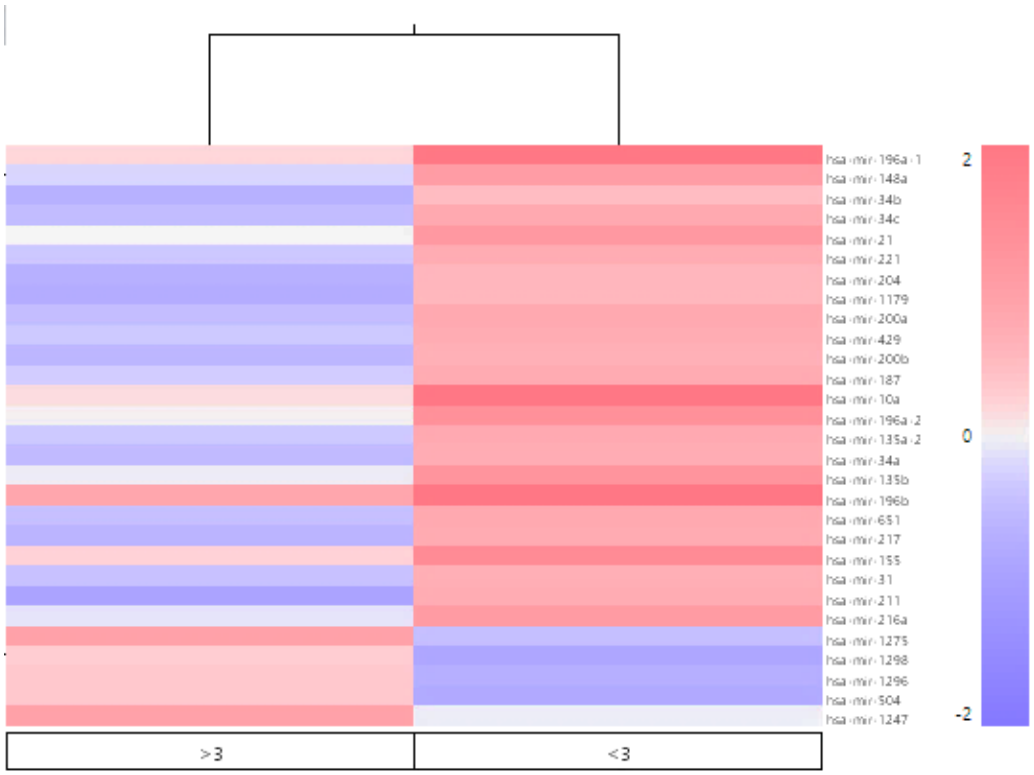

Supervised hierarchical clustering showing 29 differentially expressed miRNAs between patients with survival rate of >3 years and <3 years. The dendrogram colour saturation is proportional to the magnitude of the difference from the mean, ranging from red (over-expressed) to blue (under-expressed).

4.15 DISCUSSION

This chapter focused on understanding the significance of miRNAs in the development and progression of LGG. Unsupervised hierarchical clustering of all the primary tumours showed a major influence of tumour grade and histology (within each grade) on the expression profiles whereas *IDH* mutation did not have an effect on the profiles.

Unsupervised clustering of all 32 primary tumours resulted in independent clustering of two samples, BTNW13 (OA) and IN99/81 (O), both of which were *IDH1* mutant. These two samples were no different to the remaining samples and they were included as part of the analysis and excluding them would mean altering the actual data.

4.15.1 Comparison of miRNA expression profiles of grade II and grade III tumours

Supervised hierarchical clustering identified independent clustering of two samples, IN99/81 (O) and IN2800 (A) in this analysis. Seven of the miRNAs identified in this analysis, mir-3658, mir-449c, miR-4741, miR-4252, miR-4500, miR-141 and miR-120d have been studied in other types of cancer.

In the present study, miR-3658 was upregulated in 70% of grade II tumours and downregulated in 83% of grade III tumours. In a study of multiple myeloma (MM) patients, dysregulation of miR-3658 was confirmed in MM patients compared to healthy donors by quantitative reverse transcription PCR (RT-qPCR) (Hao *et al*., 2014). In the present study, miR-449c had more than 4-fold differential expression. Previously, it has been reported to be downregulated in non-small cell lung cancer (NSCLC) tissues

and NSCLC cell lines, while overexpression of the miR-449c inhibited cell proliferation and promoted apoptosis in NSCLC cells compared with normal tissues (Miao *et al*., 2013). Moreover, *MYC* was directly targeted by miR-449c supressing MYC protein expression and downregulation of MYC expression was also observed in nude mice promoting carcinogenesis *in vivo*. miR-4741 had a 2.5 fold differential expression in the present study. In a study of hepatocellular carcinoma (HCC), the authors investigated the role of plasma circulating miRNAs in predicting the prognosis of HCC patients receiving the transarterial chemoembolisation (TACE) treatment (Liu *et al*., 2014). miR-4741 was validated and reported as a candidate biomarker for predicting the prognosis of TACE. miR-4252 had a differential expression of > 2 fold in the current study. Recently, it has been reported in association with gastric cancer, where it was found to be upregulated in patients with positive lymphatic metastasis of the primary gastric tumour (Yang *et al*., 2014). miR-4500 had > 2 fold differential expression in the present study. miR-4500 has been studied in NSCLC and downregulation of the miRNA was reported in NSCLC cell lines and tissues (Zhang *et al*., 2014). The miRNA expression was correlated with survival and high expression of miR-4500 was correlated with better survival rate, indicating a prognostic value of miR-4500 expression in NSCLC patients. miR-141 showed >2 fold differential expression. miRBase identified miR-141 as part of the miR-8 family consisting of miR-200a, miR-200b, miR-200c and miR-429. Higher expression of miR-141 was associated with shorter survival in patients with NSCLC adenocarcinoma (Tejero *et al*., 2014). miR-320d had a 2-fold differential expression in this study. A recent study examined the role of miRNAs in the pathogenesis of diffuse large B-cell lymphoma (DLBCL) and reported that low expression of miR-320d is associated with poor prognosis in DLBCL patients treated with cyclophosphamide, doxorubicin, vincristine, and prednisone

(CHOP) regimen (Wu *et al*., 2014). The novel miRNAs identified in the present study are miR-466, miR-3142, miR-2113, miR-4529-5p, miR-4471, miR-181a*, miR-181a-2*, miR-3616-5p, miR-4733-3p, miR-4268, miR-323b-5p, miR-3650, miR-4302 and miR-3689a-5p, which have not been studied previously in any type of cancer including glioma.

PI3K/mTOR pathway identified as a pathway associated with miRNAs according to KEGG pathway analysis, has been studied previously in grade II tumours (McBride *et al*., 2010). The relationship between OS and methylation status and expression of *PTEN*, a negative regulator of PI3K pathway and phosphorylation of proteins in the PI3K/mTOR pathway such as S6 and PRAS40 was investigated. *PTEN* methylated patients were associated with poor OS ($p = 0.128$) and expression of phosphor-PRAS40 was associated with decreased survival ($p = 0.077$). Expression of phosphor-S6 and OS showed an inverse relationship ($p = 0.029$). The regulation of PI3K-mTOR pathway and OS suggests that mTOR inhibitors could be used in the treatment of grade II tumours.

A study by Barbano *et al*., (2014) compared miRNA expression profiles of 8 grade II and 24 grade III+IV glioma and identified 22 differentially expressed miRNAs in the two groups. On validation, 13 of the 22 miRNAs had significant differential expression between grade II and grade III+IV tumours. Of the 13 miRNAs, miR-451 was the only miRNA that was significant in the results from the grade II and grade III comparison reported in the present study. It was differentially expressed in < 70% of the samples; upregulated in 40% grade II and 67% grade III tumours and downregulated in 60% grade II and 33% grade III tumours. This is in agreement with the data from Barbano *et*

al., (2014) where downregulation of miR-451 in grade II tumours and upregulation in grade III tumours was found.

4.15.2 miRNA expression in grade II tumours

BTNW13 and IN99/81 clustered independently to the remaining tumours as shown in Figure 4.1. In the present study, let-7c was the only miRNA identified when comparing expression profiles of *IDH* mutant and *IDH* wild type grade II tumours and it was downregulated in 71% tumours with *IDH* wild type. Let-7c is a member of the let-7 family and reportedly acts as a regulator of cell proliferation pathways (Johnson *et al*., 2007). It has been recently studied in breast cancer and prostate cancer. Björner *et al*., (2014) identified miRNA signatures that could represent alterations leading to breast cancer progression. Let-7c was downregulated in the epithelial compartment and increased proliferation in columnar cell hyperplasia (CCH), earliest stage linked to cancer progression. Ren *et al*., (2014) examined miRNA expression levels in prostate cancer (PCa) epithelium and stroma. Downregulation of let-7c was significantly associated with metastasis ($p = 0.01$) and androgen-dependent PCa ($p = 0.003$) and in PCa stromal cells, downregulation of let-7c was significantly associated with extraprostatic extension ($p = 0.02$).

4.15.3 miRNA expression in grade II tumours based on histology

As shown in Figure 4.5, identification of four common miRNAs between A vs OA and OA vs O clearly indicates that they represent differentially expressed miRNAs present in OA tumours. All four miRNAs upregulated in OA include miR-21, miR-23a, miR-30c and miR-99a, which have been previously studied in cancers including glioma.

According to Barbano *et al*. (2014), miR-21 showed a significant differential expression in grade II tumours compared to tumours of higher grades III and IV. miR-21 showed highest expression in astrocytic tumours characterised by worst prognosis. In a previous study of 152 glioma, expression of miR-21 was observed to be higher in grade III-IV (high-grade) tumours compared to grade I-II (low-grade) tumours ($p < 0.001$) (Wu *et al*., 2013). Patients with low miR-21 expression had significantly longer survival compared to those with high miR-21 expression ($p < 0.001$) and multivariate analysis showed that high miR-21 expression was a significant and independent indicator for poor prognosis in glioma patients ($p < 0.001$). In colorectal cancer blood and tissue samples, miR-23a expression was upregulated and significant reduction of cell viability and promotion of apoptosis was observed following transfection with miR-23a inhibitor (Yong *et al*., 2014). miR-30c was recently studied in breast cancer using TCGA dataset (Dobson *et al*., 2014). miR-30c was upregulated or had high copy number in about 4% of breast cancer patients. These patients had significantly worse OS compared to those with normal miR-30c, suggesting an important role of miR-30c in breast cancer progression. The role of miR-99a expression was studied in GBM cells and xenograft models in a previous study (Chakrabarti *et al*., 2013). The authors showed that photofrin based photodynamic therapy (PDT) and overexpression of miR-99a could inhibit fibroblast growth factor receptor 3 (FGFR3) and PI3K-Akt signalling pathways to promote p53-mediated apoptosis in p53 wild type GBM cells *in vitro* and *in vivo*.

Koshkin *et al*., (2014) investigated 20 significant miRNAs with differential expression in different grades identified from a previous study (de Biase *et al*., 2012) to determine correlation between the miRNA expression and tumour grades. Expression of two miRNAs, miR-21 and miR-23a was upregulated in higher grade tumours. Both the miRNAs were identified as differentially expressed in grade II tumours in this study.

miR-21 was most frequently upregulated and downregulated in OA (100%) and O (67%) respectively, whereas miR-23a showed most frequent upregulation in OA (100%) and most frequent downregulation in A (60%). The expression of miR-21 and miR-23a does not correlate with tumour grade and miRNA expression was significant in grade II tumours only.

The findings from the current study suggest that oligoastrocytoma tumours are more similar to oligodendroglioma as there were only four significant differentially expressed miRNAs identified between the two histological groups.

4.15.4 miRNA expression in grade III tumours

The miRNA expression of grade III tumours revealed independent clustering of two samples, BTNW614 (AOA) and BTNW126 (AA), both of which had different expression profiles from the remaining samples in the cohort. Of the eight miRNAs identified as differentially expressed in grade III tumours, only three (miR-21, miR-711 and miR-486-3p) have been previously reported in cancer studies.

miRNA-711 was studied in cutaneous T-cell lymphomas (CTCL) and the authors showed that it was one of the most induced miRNAs that distinguished CTCL from benign skin diseases with > 90% accuracy in a cohort of 148 patients (Ralfkiaer *et al*., 2011). It also distinguished malignant and benign lesions in peripheral T-cell lymphoma (PTL) and skin inflammation and in xenograft models of psoriasis and CTCL in an independent cohort of 50 patients. miR-486-3p was reported in a study of neurofibromatosis type 1 (NF1) examining the role of miRNAs in tumourigenesis of NF1 (Masliah-Planchon *et al*., 2013). miR-486-3p was the most significantly

upregulated miRNA in plexiform neurofibromas, which targets the tumour suppressor gene *PTEN*. miR-486-3p was studied in hepatocellular carcinoma to identify postoperative prognostic predictors (Huang *et al*., 2012). The prognostic value of miR-486-3p was examined and high expression of miR-486-3p was significantly associated with longer PFS ($p < 0.020$) and longer OS ($p < 0.041$). Multivariate analysis showed that miR-486-3p expression level was an independent predictor of PFS ($p = 0.004$). In the current study, 5 of the miRNAs, miR-4734, miR-1268b, miR-4763-3p, miR-4667-5p and miR-3621 were identified in glioma for the first time.

4.15.5 miRNA expression in grade III tumours based on histology

None of the three differentially expressed miRNAs (miR-3135b, miR-4706 and miR-4748) that were common between AA vs AO and AOA vs AO have been investigated in any cancer studies previously. Hierarchical clustering for histology comparison analysis indicates that anaplastic oligoastrocytoma tumours have more similar profiles to anaplastic astrocytoma tumours, as there were no differentially expressed miRNAs between the two histology types.

4.15.6 Comparison with the TCGA data

TCGA miRNA-seq data for LGG cohorts became only recently available after the commencement of the present study. Therefore, it was important to determine the status of the different clinical scenarios such as identification of differentially expressed miRNAs between different histological groups, tumour grades, *IDH* mutation status, progression and survival in a larger cohort of patients such as that of TCGA.

Differentially expressed miRNAs for OA vs A in the TCGA cohort had two common miRNAs (let-7d and let-7e) for the respective comparison in the present study cohort. Mitra *et al*., (2011) studied the regulation of miRNAs in breast cancer progression. The authors showed epigenetic repression of let-7e expression by the histone demethylase Jumonji/ARID1 B (JARID1B). JARID1B promotes cell proliferation by G1 to S transition. No other miRNAs were common between the data from the TCGA analysis and that from the present study. This is mainly due to a large difference in the size of the cohorts with 453 cases in the TCGA cohort and 32 cases in the present study.

Comparison of grade II and grade III tumours in the present study identified 42 differentially expressed miRNAs, while the TCGA analysis with more number of samples in the cohort had only 3 differentially expressed miRNAs between grade II and grade III tumours. These 3 miRNAs were different from the 42 differentially expressed miRNAs identified.

miRNA expression analysis for tumours with *IDH1* mutation and tumours with *IDH1* wild type showed no significant differentially expressed miRNAs in the current study. In the TCGA data analysis, 46 miRNAs were differentially expressed in *IDH1* mutant vs *IDH1* wild type tumour samples.

Differential expression of miRNA in patients based on outcome identified 29 differentially expressed miRNAs in the TCGA data between patients with survival rate of >3 years and <3 years, but no significant differentially expressed miRNAs were identified in the present study.

In conclusion, the present study shows that tumour grade has a greater impact on the miRNA expression profiles compared to the other parameters such as *IDH* status and histology. Forty-two significant differentially expressed miRNAs were identified between grade II and grade III tumours that had different expression levels in grade II and grade III tumours. Histological group analysis showed that OA was more similar in profile to O and AOA was more similar to AA suggesting a miRNA signature in the histological groups. The results from this study were compared to analysis of TCGA data and only two common miRNAs were identified in the two datasets, let-7d and let-7e from OA vs A analysis.

CHAPTER 5

GENETIC ANALYSIS OF PRIMARY/RECURRENT PAIRS

5.1 INTRODUCTION

LGG almost invariably recur and progress to a higher histological grade (grade III and IV) with worse prognosis (Westphal *et al*., 2011). It is not possible to predict when and if this progression will take place on an individual basis (Sanai *et al*., 2011) and little is known about the genetic differences between the primary and recurrent tumour and if that might give information relating to choice of treatment (Riehmer *et al*., 2014).

The aim of this chapter was to identify molecular markers between primary and recurrent tumours that could drive the malignant progression of LGG tumours. To achieve this, the mutation status of *IDH1/IDH2* and the *MGMT* promoter methylation status and MGMT expression was determined in a small cohort of patients, in which samples were available at the time of diagnosis and subsequently at the time of recurrence. In addition, the genomic and miRNA expression profiles of those primary/recurrent pairs were established using array CGH and miRNA array analysis respectively.

5.2 *IDH* MUTATION ANALYSIS

The cohort consisted of paired samples from 10 patients comprising 5 grade II (4A and 1O) and 5 grade III tumours (1AA, 3AOA and 1AO) at first diagnosis (Table 5.1). Of the 5 grade II cases, 2 tumours recurred at the same grade and 2 underwent malignant transformation and recurred as grade III tumours. In Patient 2, a grade II A progressed

to a grade III tumour with further malignant transformation to GBM and an additional recurrence. In the 5 grade III tumours, 4 recurred as same histological grade and in one of these patients, there was a subsequent recurrence at the same grade (Patient 8). One grade III case progressed to GBM.

Mutation analysis for *IDH1* was carried out by direct sequencing for all primary tumours and their recurrences. In addition, *IDH2* was sequenced for all samples with sufficient DNA as summarised in Table 5.1. The *IDH1* R132H mutation was present in 4 of 10 primary tumours with the *IDH2* R172K mutation present in an additional case. All these *IDH* mutations were maintained in subsequent recurrences, including those which had undergone malignant transformation. *IDH* wild-type genotypes were similarly preserved during tumour recurrence and progression.

Table 5.1 Primary and recurrent pairs used for *IDH* analysis

Patient Number	Tumour	Age[a]	Sex[b]	Grade	Histology[c]	*IDH1* status[d]	*IDH2* status[e]	Time to recurrence[f]	Overall survival[g]
1	BTNW20	26	M	II	A	R132H	WT	83	94 (A)
	BTNW1378			II	A	R132H	NA		
2	BTNW365	42	F	II	A	R132H	WT	28.5	37.5 (D)
	BTNW861			III	AA	R132H	NA		
	BTNW946			IV	GBM	R132H	NA		
	BTNW974			IV	GBM	R132H	NA		
3	BTNW367	56	M	II	A	WT	WT	0.5	62 (A)
	BTNW380			II	A	WT	WT		
4	BTNW870	17	M	II	A	WT	WT	1	33 (A)
	BTNW885			III	AA	WT	WT		
5	BTNW326	56	F	II	O	R132H	NA	33.5	37.5 (D)
	BTNW883			III	O	R132H	NA		
6	BTNW126	66	M	III	AA	WT	WT	5	6 (D)
	BTNW196			III	AA	WT	WT		
7	BTNW174	42	F	III	AOA	WT	WT	36	45.5 (D)
	BTNW749			III	AOA	WT	NA		
8	BTNW325	46	M	III	AOA	WT	NA	230.5	263 (D)
	BTNW515			III	AOA	WT	WT		
	BTNW778			III	AOA	WT	NA		
9	BTNW614	49	M	III	AOA	R132H	NA	14.5	21.5 (D)
	BTNW848			IV	GBM	R132H	NA		
10	BTNW15	56	M	III	AO	WT	R172K	13.5	14.5 (D)
	BTNW107			III	AO	WT	R172K		

[a] Age at diagnosis in years; [b] M, male; F, female; [c] A, astrocytoma; O, oligodendroglioma; AA, anaplastic astrocytoma; AOA, anaplastic oligoastrocytoma; AO – anaplastic oligodendroglioma; [d] R132H, *IDH1* mutant; WT, wild type; [e] R172K, *IDH2* mutant; WT, wild type; [f] Time to recurrence in months; [g] OS in months; A, alive; D, dead; NA, not available.

5.3 ANALYSIS OF MGMT PROMOTER METHYLATION BY MS PCR AND IHC

Due to constraints of DNA availability, it was only possible to determine *MGMT* methylation status by MS PCR in primary and recurrent tumours for 4 patients as detailed in Table 5.2. In Patient 6, the *MGMT* promoter was unmethlyated in the primary tumour and the recurrence and in Patient 10, methylation of *MGMT* was present in both primary and recurrent tumours. Conversely, in Patient 3, *MGMT* methylation was lost in the recurrent tumour and in Patient 9, *MGMT* was partially methylated in the recurrent tumour even though the promoter was unmethylated in the primary biopsy.

The level of MGMT expression was determined by IHC in primary and recurrent tumours for 6 patients and the Allred scoring system was used as described in Chapter 2 (Table 5.2). Examples of IHC results are shown in Figure 5.1. Patient 2 and Patient 3 maintained high levels of MGMT expression in primary tumours and the subsequent recurrences, using both the proportion and combined Allred scoring systems. The second recurrence (BTNW946) in Patient 2 had zero expression; however, given that high expression of MGMT was observed in previous (BTNW861) and subsequent (BTNW974) recurrences, this may be due to experimental failure. In these 2 patients, all tumours for which data was available had either no methylation or partial methylation of the *MGMT* gene promoter. In Patient 6, the level of MGMT expression was lower in the recurrent tumour sample using both the proportion and combined Allred scoring system although the same unmethylated *MGMT* gene promoter status was established by MS PCR in both primary and recurrent tumours. A reduction in MGMT expression at recurrence was also observed in Patient 7. However, the Allred scores of zero in recurrent tumour BTNW749 may also indicate technical failure. In Patient 8, high levels

of MGMT expression were noted in the primary tumour and first recurrence by both proportion and combined Allred scores. However, MGMT expression was reduced considerably in the second recurrence. Unfortunately, no MGMT promoter methylation data was available for this patient. In Patient 9, high levels of expression in the primary sample measured by Allred proportion and combined scores of 5 and 8, respectively, were reduced in the recurrent tumour to Allred proportion and combined scores of 3 and 5, respectively, and this was accompanied by a change in MGMT promoter status from unmethylated to partially methylated.

Table 5.2 MGMT methylation status of tumours by IHC and MS PCR

Patient Number	Tumour	Grade	Histology[a]	IHC			MS PCR[b]
				Proportion	Intensity	Combined score	
2	BTNW365	II	A	3	2	5	NA
	BTNW861	III	A	3	2	5	NA
	BTNW946	IV	GBM	0	0	0	PM
	BTNW974	IV	GBM	4	2	6	PM
3	BTNW367	II	A	5	3	8	PM
	BTNW380	II	A	5	2	7	U
6	BTNW126	III	AA	4	2	6	U
	BTNW196	III	AA	2	1	3	U
7	BTNW174	III	AOA	3	1	4	M
	BTNW749	III	AOA	0	0	0	NA
8	BTNW325	III	AOA	3	2	5	NA
	BTNW515	III	AOA	4	2	6	NA
	BTNW778	III	AOA	1	1	2	NA
9	BTNW614	III	AOA	5	3	8	U
	BTNW848	IV	GBM	3	2	5	PM
10	BTNW15	III	AO	NA	NA	NA	M
	BTNW107	III	AO	NA	NA	NA	M

[a] A, astrocytoma; AA, anaplastic astrocytoma; AOA, anaplastic astrocytoma; AO, anaplastic oligodendroglioma; GBM, glioblastoma multiforme; [b] M, methylated; PM, partially methylated; U, unmethylated; NA, not available.

Figure 5.1 IHC staining for MGMT expression in Patient 3

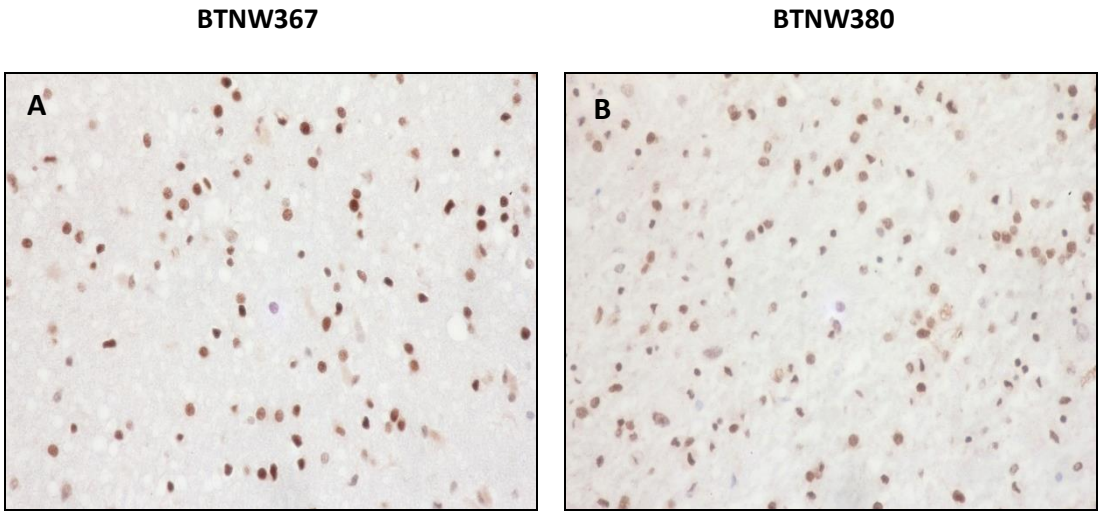

Slides were stained positively with streptavidin/HRP-biotin staining and counterstained with haematoxylin. Pictures taken at 40x magnification A: BTNW367, Tumour at diagnosis; B: BTNW380, Tumour at recurrence.

5.4 COMPARISON OF COPY NUMBER CHANGES IN PATIENTS WITH PAIRED SAMPLES AT DIAGNOSIS AND RECURRENCE

Copy number analysis for primary/recurrent pairs from 3 patients (Table 5.3) was performed using Agilent's 244K array as described previously in Chapter 2, section 2.15. Genomic segmentation (Partek) was used to identify regions of gain and loss on the chromosomes for each sample. Copy number aberrations (CNAs) were identified in all samples.

Table 5.3 Primary/recurrent pairs used for aCGH analysis

Patient number	Tumour samples	Histology at diagnosis[a]	Histology at recurrence[a]	*IDH1* status[b]	*IDH2* status[c]	Time to recurrence[d]
1	BTNW20/BTNW1378	A	A	R132H	WT	83
9	BTNW614/BTNW848	AOA	GBM	R132H	WT	14.5
10	BTNW15/BTNW107	AO	AO	WT	R172K	13.5

[a] A, astrocytoma; AOA, anaplastic oligoastrocytoma; AO, anaplastic oligodendroglioma; GBM, glioblastoma multiforme; [b] R132H, *IDH1* mutant; WT, wild type; [c] R172K, *IDH2* mutant; WT, wild type; [d] Time to recurrence in months.

5.4.1 Patient 1 (Samples BTNW20 and BTNW1378)

At diagnosis in sample BTNW20, there were 124 CNAs identified with 115 regions of gain and 9 regions of loss. In the recurrent tumour, the number of CNAs had increased to 206 with 196 gains and 10 losses (Figure 5.2). The majority (65%; 80/124) of CNAs were maintained in the recurrent tumour. CNAs are detailed in supplementary data.

The genomic profiles of the two tumour samples were divergent. CNAs that were no longer present in the recurrent tumour included gains on chromosomes 11p-q, 19p and losses on 15q and Xp. Similarly, CNAs that were detected in the recurrent tumour included gains on chromosomes 2q, 7q, 10p and 15q and losses at 1p, 4q, 14q and 18q. Chromosome 20 had no CNAs in BTNW20 but had a gain at 20q in the recurrent tumour. Chromosome 22 had no aberrations in both the tumour samples.

Figure 5.2 Genome summary with CNAs for Patient 1

BTNW20

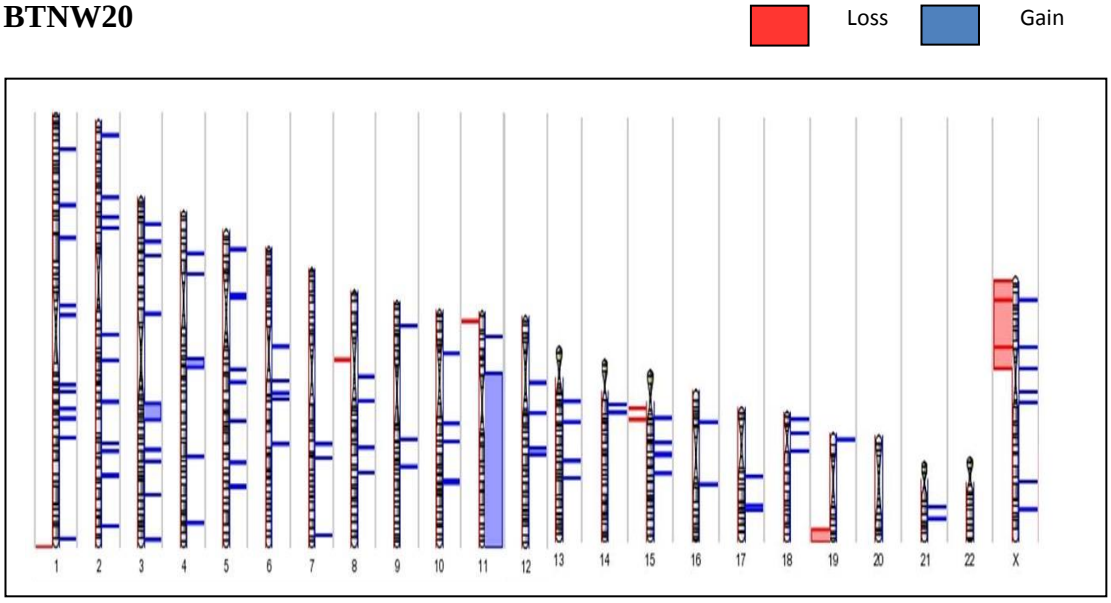

BTNW1378

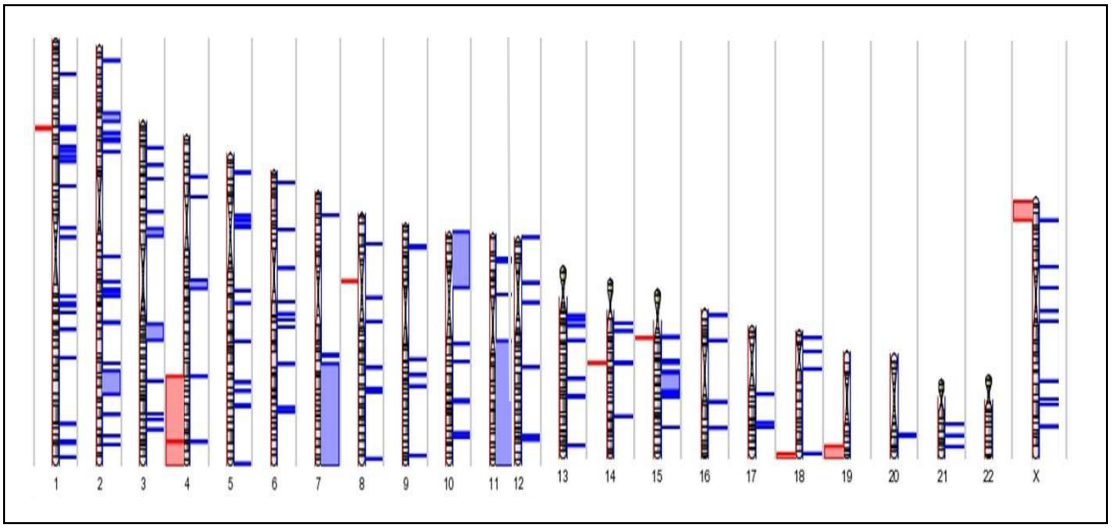

5.4.2 Patient 9 (Samples BTNW614 and BTNW848)

At diagnosis in sample BTNW614, there were 118 CNAs present with 95 regions of gain and 23 regions of loss. At recurrence in sample BTNW848, the number of CNAs had increased to 152, of which 136 were gains and 16 were losses (Figure 5.3). The number of CNAs maintained in the recurrent tumour was smaller than in Patient 1 (49%; 58/118). CNAs are detailed in supplementary data.

Some of the copy number changes in tumour at diagnosis were not present in the recurrent tumour which included gains on chromosomes 1p, 1q, 10p and 11q and losses on 2q, 3q, 4p, 6q, 12p, 12q, 18p, 22q and Xp. Gain of whole chromosome 7 was observed in BTNW614 whilst gains at 7p and 7q were detected in the recurrent tumour. New CNA changes that were present at recurrence included gains on chromosomes 16 and 20q and losses on 10, 11p and 18q. Gain of whole chromosome 8 was maintained in both the samples.

Figure 5.3 Genome summary with CNAs for Patient 9

BTNW614

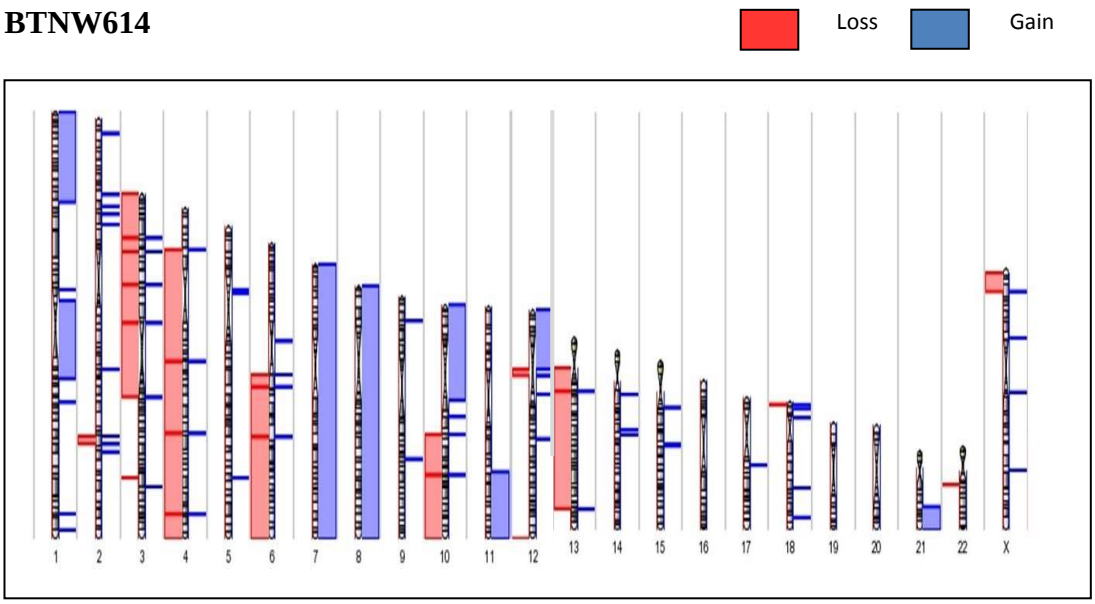

BTNW848

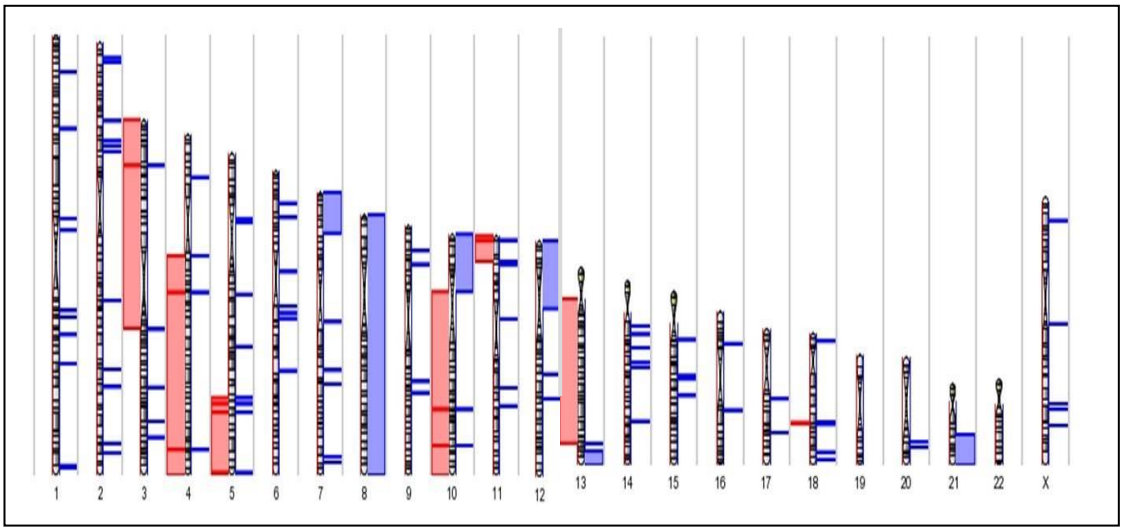

5.4.3 Patient 10 (Samples BTNW15 and BTNW107)

At diagnosis in sample BTNW15, there were 119 CNAs identified, of which 90 were regions of gain and 29 were regions of loss. At recurrence, the number of CNAs increased to 139 CNAs with 127 gains and 12 losses (Figure 5.4). In Patient 12, only 28% (34/119) of CNAs were maintained in the recurrent tumour. CNAs are detailed in supplementary data.

CNAs present in BTNW15 that were not maintained in the recurrent tumour were gains on chromosomes 2q, 7p and 11q and losses on 1p, 2p, 2q, 4p, 4q, 5p, 7q, 10q, 13q, 15q, 18q and 20q. CNAs present only at recurrence were gains on chromosomes 14q, whole chromosome 17, 20q and 21q and losses on 2q, 6p-q, 9p, 15p, 19 and Xp. On the contrary, loss on chromosome 22q was present in BTNW15 while chromosome 22 was normal in the recurrent tumour.

Figure 5.4 Genome summary with CNAs for Patient 10

BTNW15

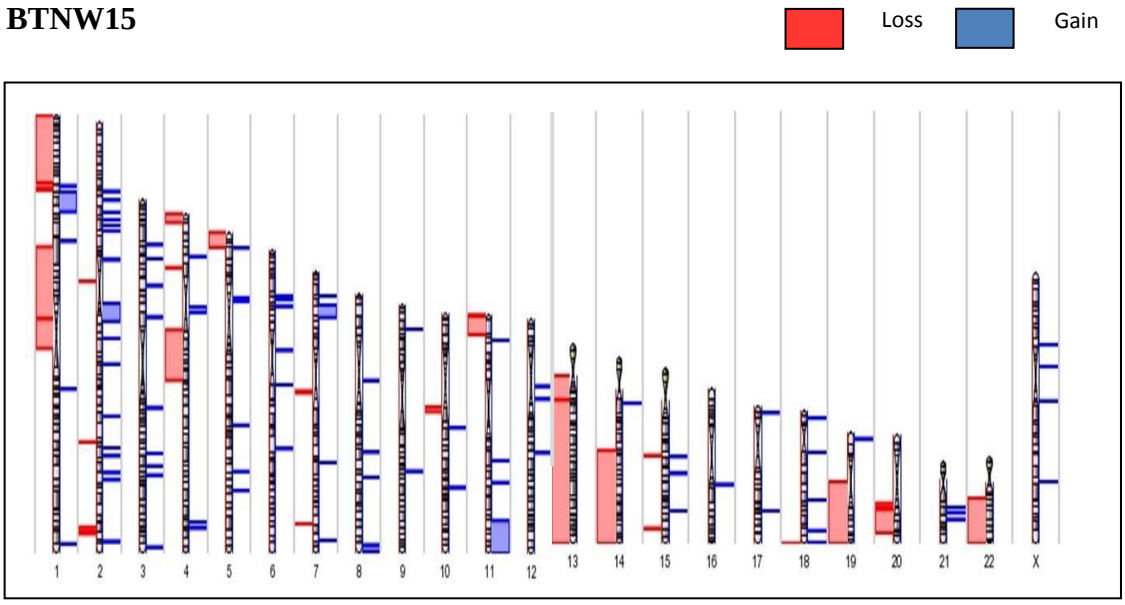

BTNW107

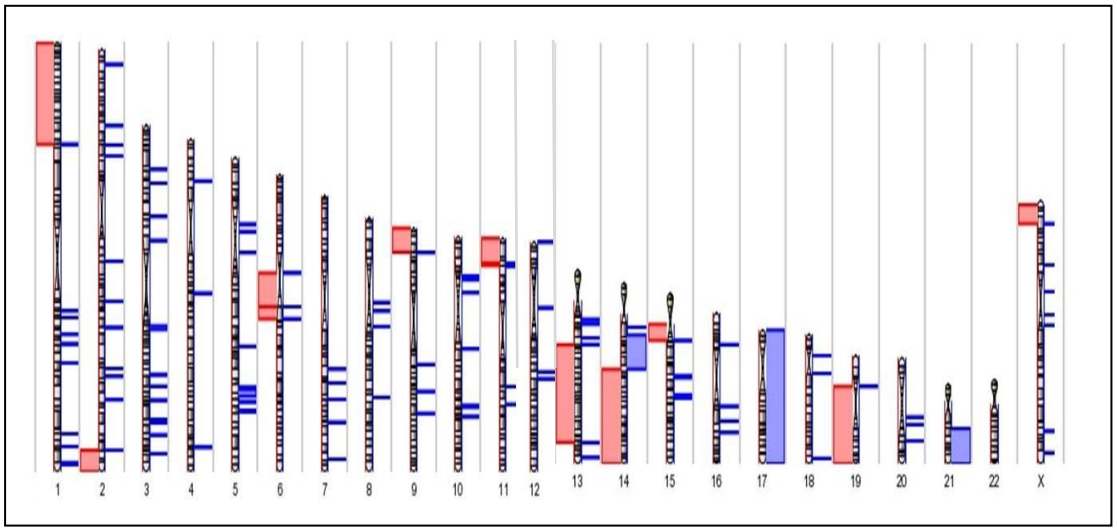

5.5 COMPARISON OF miRNA EXPRESSION IN 5 PATIENTS WITH PAIRED SAMPLES AT DIAGNOSIS AND RECURRENCE

Paired samples from 5 patients were available for miRNA analysis as described in Table 5.7. miRNA array analysis was carried out as described previously in Chapter 2, section 2.16. Data analysis was carried out using Partek Genomics Suite (version 6.6; Partek Inc., USA). Raw data was normalised with $\log_2$ median before ANOVA test was used to identify differentially expressed miRNAs with ≥ 2-fold change in expression. The number of differentially expressed miRNAs from pairwise comparisons with ≥ 2-fold change in expression are listed in Table 5.7. Two of the tumours that maintained the same grade at recurrence (BTNW20 and BTNW126) had the highest number of differentially expressed miRNAs, whilst tumour BTNW614 (AOA) that progressed to GBM had the least number of differentially expressed miRNAs.

Unsupervised hierarchical clustering of the 5 paired samples was performed using 1719 miRNAs and is represented by a dendrogram with the miRNA expression profiles of all pairs in Figure 5.5. Only the primary/recurrent pair from Patient 10 clustered together with similar expression profiles. PCA showed that primary and recurrent tumours from Patient 10 had the most similar profiles while tumour samples from Patient 6 had the most different profiles (Figure 5.6).

Table 5.7 Summary of primary/recurrent pairs showing differentially expressed miRNAs with different histology types and malignant progression and differentially expressed miRNAs (≥ 2-fold change) between primary and recurrent tumours.

Patient number	Tumour samples	Histology at diagnosis[a]	Histology at diagnosis[a]	*IDH1* status[b]	*IDH2* status[c]	Differentially expressed miRNAs (P vs R) (≥ 2-fold change)[d]
1	BTNW20/BTNW1378	A	A	R132H	WT	243
2	BTNW365/BTNW974	A	GBM	R132H	WT	78
6	BTNW126/BTNW196	AA	AA	WT	WT	209
9	BTNW614/BTNW848	AOA	GBM	R132H	NA	4
10	BTNW15/BTNW107	AO	AO	WT	R172K	42

[a] A, astrocytoma; AA, anaplastic astrocytoma; AOA, anaplastic oligoastrocytoma; AO, anaplastic oligodendroglioma; GBM, glioblastoma multiforme; [b] R132H, *IDH1* mutant; WT, wild type; [c] R172K, *IDH2* mutant; WT, wild type; [d] P, primary tumour; R, recurrent tumour; NA, not available.

Figure 5.5 Unsupervised hierarchical clustering for primary/recurrent pairs

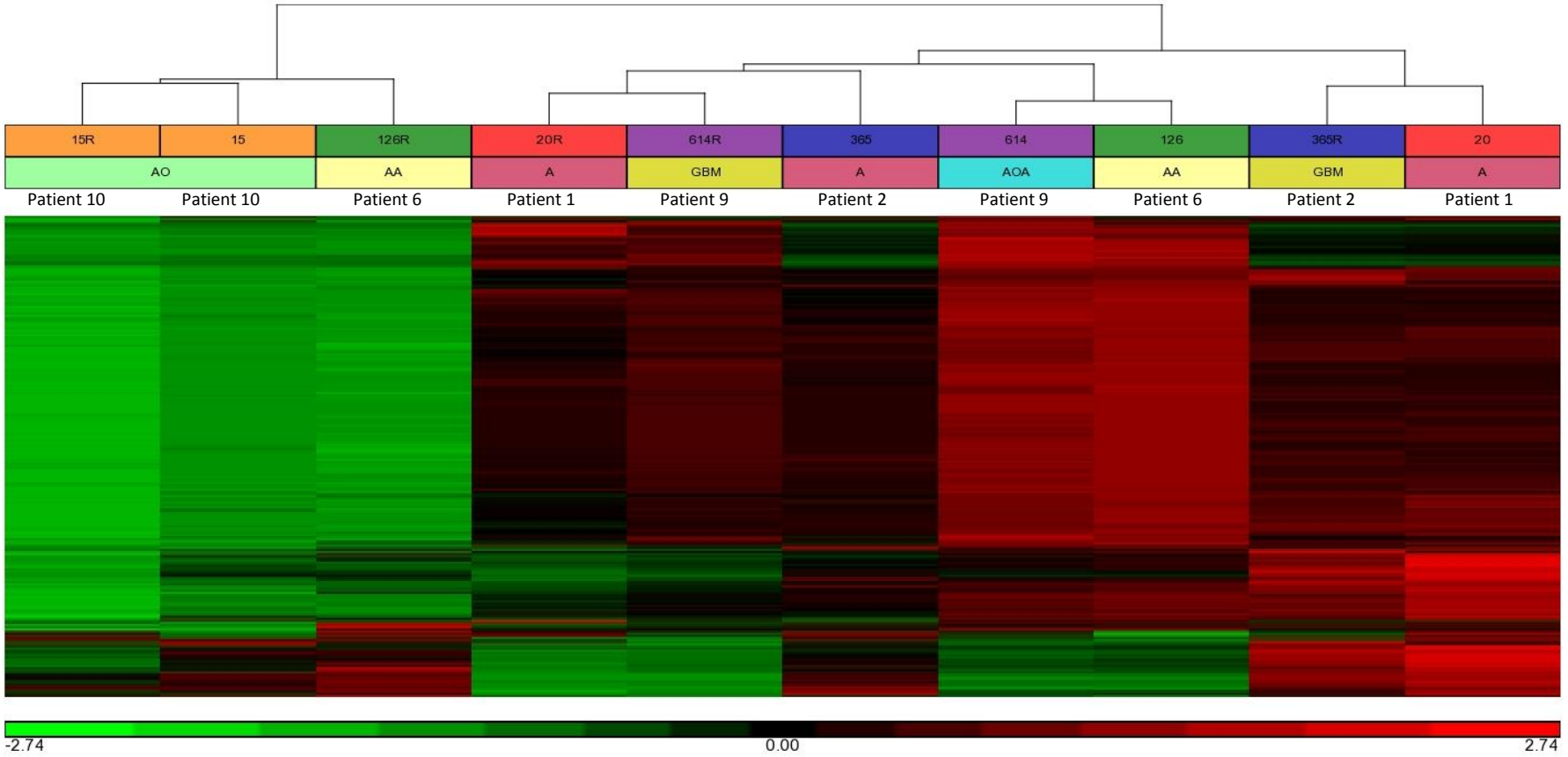

Expression of 1719 miRNAs in 5 paired samples. Red colour represents high levels of miRNA expression and green colour represents low levels of miRNA expression in the tumour. Abbreviations: R – recurrent tumour, A – astrocytoma, AA – anaplastic astrocytoma, AOA – anaplastic oligoastrocytoma, AO – anaplastic oligodendroglioma, GBM – glioblastoma multiforme.

Figure 5.6 PCA of primary/recurrent pairs

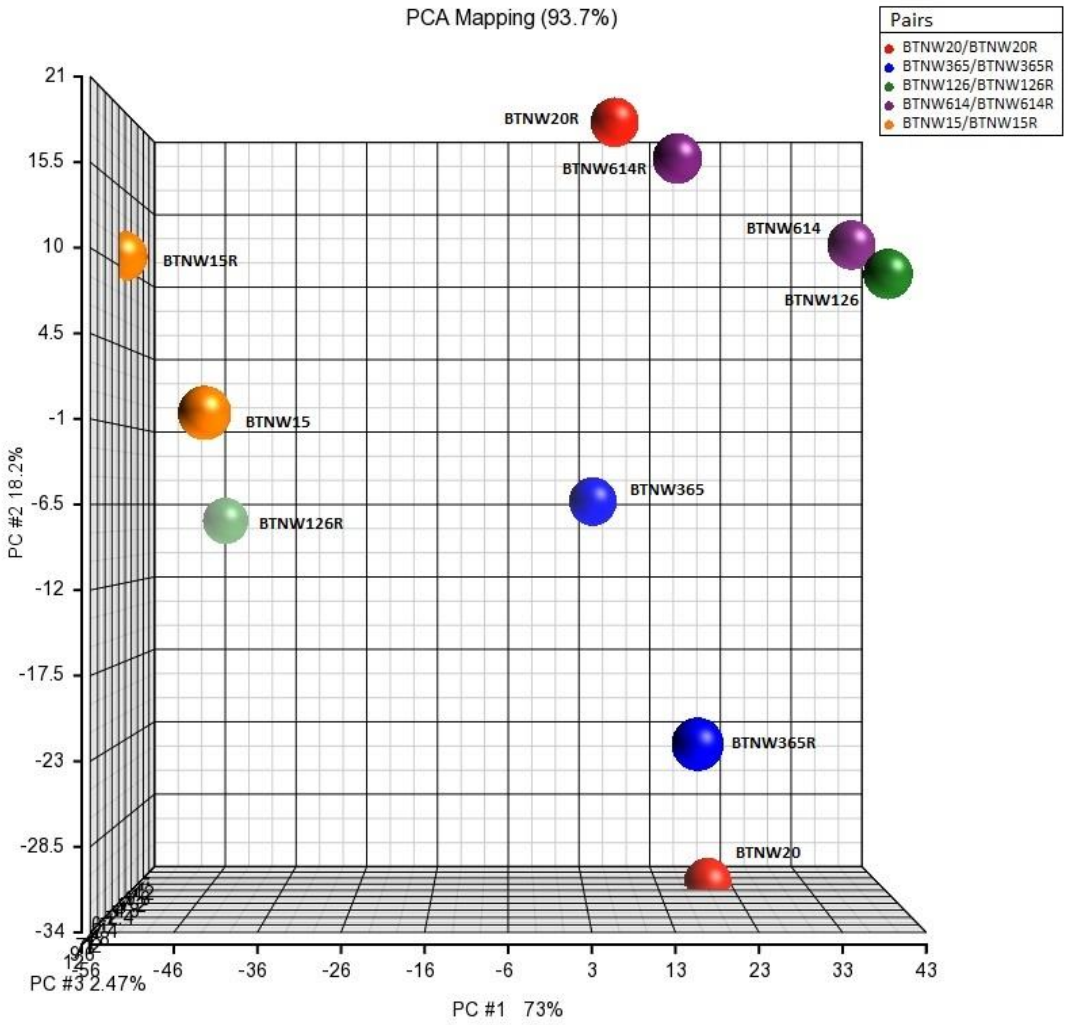

The results are depicted 3-dimensionally with PC1 (73%), PC2 (18.2%) and PC3 (2.47%) as the X, Y and Z axes, respectively. Primary and recurrent pairs for the same tumour are shown by the same colour. R – recurrent tumour

5.5.1 Patient 1 (Samples BTNW20 and BTNW1378)

There were 243 miRNAs that were differentially expressed with ≥ 2-fold change in expression, of which 189 were upregulated and 54 were downregulated in the primary tumour as compared to the tumour at recurrence. The 10 most differentially expressed miRNAs are listed in Table 5.8 with their targets and pathways.

5.5.2 Patient 2 (Samples BTNW365 and BTNW974)

In tumour samples from Patient 2, there were 78 differentially expressed miRNAs with ≥ 2-fold change in expression; 21 were upregulated and 57 were downregulated in the primary tumour as compared with its recurrence. The 10 most differentially expressed miRNAs were analysed for target prediction and pathway analysis as detailed in Table 5.9.

5.5.3 Patient 6 (Samples BTNW126 and BTNW196)

In this patient, 209 differentially expressed miRNAs with ≥ 2-fold change in expression were identified between tumour samples with 91 upregulated miRNAs and 118 downregulated miRNAs in the primary tumour compared with its recurrent tumour. The 10 most differentially expressed miRNAs are listed in Table 5.10 with the targets and pathways.

5.5.4 Patient 9 (Samples BTNW614 and BTNW848)

For these tumour samples, four differentially expressed miRNAs (≥ 2-fold change) were identified, all of which were upregulated in the primary tumour compared with its recurrence. These are presented with the targets and pathways in Table 5.11.

5.5.5 Patient 10 (BTNW15 and BTNW107)

A total of 42 differentially expressed miRNAs (≥ 2-fold change) were identified; 33 were upregulated and 9 were downregulated in the primary tumour compared with its recurrence. The 10 most differentially expressed miRNAs are listed in Table 5.12 with the targets and pathways.

Table 5.8 The 10 most differentially expressed miRNAs identified in Patient 1 with the predicted targets and pathways.

miRNA	Fold change (P vs R)[a]	Target	Pathway
miR-4454	448.889	*WDR72, ENAH, FAM125B, ENPP6, DLG5, GK, EIF4E3*	ErbB signalling pathway
miR-4787-5p	99.2121	*NFIX, TMEM2, SURF4, FGF18, PLK4, RBM41, DNAJB5, SPTSSA, FAM64A, HIPK2*	Propanoate metabolism, Glioma, Melanoma, Prostate cancer, PI3K-Akt signalling pathway
miR-4284	88.6408	*GNG13, VPS53, MAVS, ORAI2, SPN, TMEM120B, CYP20A1, CDK17, OPA3, RAB3B*	Morphine addiction, Retrograde endocannabinoid signalling, Serotonergic synapse, Circadian entrainment, Ether lipid metabolism
miR-3665	85.8987	*BOK, FUT6, NDFIP1, PTPRT, SUV39H1, SFMBT1, FAM155A, LEPROT, NCEH1, EVC*	Glycosphingolipid biosynthesis - lacto and neolacto series, Lysine degradation, Vasopressin-regulated water reabsorption, ABC transporters, Bile secretion
miR-4723-5p	78.4327	*MECP2, PLXNA4, PPP1R9B, SNX29, PACS1, NAT16, SLC28A1, CREB1, MUC3A, FOXE1*	Glycosaminoglycan biosynthesis - chondroitin sulphate, Tight junction, Circadian rhythm, Synaptic vesicle cycle, Cell adhesion molecules (CAMs)
miR-4471	-22.9926	*CDS2, POU2F1, GSTO2, IRS1, SLAMF8, DNAJB4, ANKIB1, EPB41L5, LIN52, B3GNT2*	Metabolism of xenobiotics by cytochrome P450, Biosynthesis of unsaturated fatty acids, Regulation of actin cytoskeleton, Neuroactive ligand-receptor interaction, Melanogenesis
miR-3142	-65.4807	*WDFY3, EVC, SEH1L, CASK, SPOPL, PCYT1B, ITGB1BP1, OGFR, THAP4, GABRA1*	Renal cell carcinoma, Nicotinate and nicotinamide metabolism, mTOR signalling pathway
miR-466	-70.607	*PLCXD1, KLHL23, GPR137C, DCLK1, DCUN1D4, TNRC6B, VAMP4, RIMKLB, LEMD3, INO80D*	PI3K-Akt signalling pathway, TGF-beta signalling pathway, T cell receptor signalling pathway, Chronic myeloid leukemia, Non-small cell lung cancer
miR-449c	-83.865	*NUP50, STMN2, CDK19, ODZ1, CREB1, PAPOLA, MAPK1IP1L, ACTL6A, TMEM48, STK38L*	Hepatitis B, Phosphatidylinositol signalling system, ErbB signalling pathway, Salmonella infection, Inositol phosphate metabolism
miR-4521	-549.28	*FOXM1, PABPC5, GABARAPL2, BTLA, SLC4A8, FBXW2, SRGAP1, MAPK1, HIPK2, IPMK*	Fc epsilon RI signalling pathway, Neurotrophin signalling pathway, Acute myeloid leukemia, VEGF signalling pathway, MAPK signalling pathway

[a] P, primary tumour; R, recurrent tumour. Common targets and pathways between miRNAs are highlighted in different coloured text.

Table 5.9 The 10 most differentially expressed miRNAs identified in Patient 2 with the predicted targets and pathways.

miRNA	Fold change (P vs R)[a]	Target	Pathway
miR-9	5.70413	*POU2F1, ONECUT2, PRTG, LYVE1, SH3TC2, MDGA2, TNC, SLC35B3, PRDM6, STARD13*	Cell adhesion molecules (CAMs), Axon guidance, Cytokine-cytokine receptor interaction, Pathways in cancer, Tight junction
miR-187*	4.33032	*CD276, SRSF8, MAN1B1, AQP4, DYRK2, EML2, RPP25*	Neuroactive ligand-receptor interaction, Type I diabetes mellitus, Cell adhesion molecules (CAMs)
miR-9*	4.10055	*YOD1, ONECUT2, CD109, BNIP3L, KITLG, ITGB1, SPOPL, ACTL6A, GABRA1, BICD2*	Biotin metabolism, mRNA surveillance pathway, TGF-beta signalling pathway, Glycosaminoglycan biosynthesis - chondroitin sulphate, Circadian rhythm
miR-125b	4.09974	*ISL2, NMI, KCTD20*	Calcium signalling pathway, Hypertrophic cardiomyopathy (HCM), Dilated cardiomyopathy, Arrhythmogenic right ventricular cardiomyopathy (ARVC), Cell adhesion molecules (CAMs)
miR-4324	2.8696	*FAM169B, LIN28A, PAPD5, ABCC5, CEP164, SYT2, IBA57, RPS6KL1, PPP1R12B, PCTP*	Glycosphingolipid biosynthesis - lacto and neolacto series, Regulation of autophagy, Notch signalling pathway, Pyrimidine metabolism, Lysine degradation
miR-4756-5p	-4.1132	*RPH3A, PRRT2, KSR2, SKI, WDTC1, SMARCD1, AIF1L, CDC42EP4, NFAM1, TMEM104*	ABC transporters, Notch signalling pathway, Cell adhesion molecules (CAMs), Leukocyte transendothelial migration, Pathways in cancer
miR-451	-4.15441	*PSMB8, TBC1D9B, MEX3C, CXCL16, MBP, CMTM6, CDKN2B, WDFY2, KCNK15, TSC1*	mTOR signalling pathway, Proteasome, Protein export, Glyoxylate and dicarboxylate metabolism, Propanoate metabolism
miR-4516	-5.14872	*SHOX, ENTPD7, AHCYL2, NTRK2, SLC7A6, UHRF1BP1, FAM105B, OTX1, TMCC2, MSN*	Glycosaminoglycan biosynthesis - chondroitin sulphate, Long-term potentiation, Wnt signalling pathway, Prostate cancer, Glycosaminoglycan biosynthesis - heparan sulfate / heparin
miR-4732-5p	-5.41818	*DBT, TMEM237, NHLH1, BCLAF1, WASL, RBPJ, PARM1, SFMBT1, ALKBH5, OXGR1*	Fatty acid metabolism, Basal transcription factors, PPAR signalling pathway, Notch signalling pathway, Proteasome
miR-1246	-5.79696	*GSG1L, MSR1, BRWD1, RTKN2, SMG7, SLC16A7, MUT, GLRB, BEND4, TMEM123*	Neurotrophin signalling pathway, N-Glycan biosynthesis, Inositol phosphate metabolism, Protein processing in endoplasmic reticulum, ErbB signalling pathway

[a] P, primary tumour; R, recurrent tumour. Common targets and pathways between miRNAs are highlighted in different coloured text.

Table 5.10 The 10 most differentially expressed miRNAs identified in Patient 6 with the predicted targets and pathways.

miRNA	Fold change (P vs R)[a]	Target	Pathway
miR-4521	551.415	*FOXM1, PABPC5, GABARAPL2, BTLA, SLC4A8, FBXW2, SRGAP1, MAPK1, HIPK2, IPMK*	Fc epsilon RI signalling pathway, Neurotrophin signalling pathway, Acute myeloid leukemia, VEGF signalling pathway, MAPK signalling pathway
miR-466	28.3463	*PLCXD1, KLHL23, GPR137C, DCLK1, DCUN1D4, TNRC6B, VAMP4, RIMKLB, LEMD3, INO80D*	PI3K-Akt signalling pathway, TGF-beta signalling pathway, T cell receptor signalling pathway, Chronic myeloid leukemia, Non-small cell lung cancer
miR-3142	23.1375	*WDFY3, EVC, SEH1L, CASK, SPOPL, PCYT1B, ITGB1BP1, OGFR, THAP4, GABRA1*	Renal cell carcinoma, Nicotinate and nicotinamide metabolism, mTOR signalling pathway
miR-4526	19.1503	*MIER1, FNBP1L, RIN2, FAM104B, CSF2RB, ATF3, RORA, RAP1A, MGAT4A, ATXN7*	Neurotrophin signalling pathway, Caffeine metabolism, Propanoate metabolism, Glioma, ErbB signalling pathway
miR-4661-5p	16.92	*FRS2, LCORL, DNALI1, HDGFRP3, DEPDC1B, JAG1, NFIB, WEE1, CCNB1, PRKAA1*	Synaptic vesicle cycle, Cell cycle, SNARE interactions in vesicular transport, Spliceosome, mRNA surveillance pathway
miR-1260b	-39.2843	*EIF2C1, CTAGE1, ABL2, NUB1, CDC25A, UGGT1, GPKOW, TARDBP, UNC13C, GPR316226*	Glycosaminoglycan biosynthesis - heparan sulfate / heparin, Complement and coagulation cascades, Citrate cycle, Rheumatoid arthritis
miR-1280	-56.2369	*JAG2, SEC14L2, UBTF, RALGAPB, PDE8A, NPY2R, PXMP4, NRXN2*	Pathways in cancer
miR-4286	-56.5281	*CLN8, PTBP2, KREMEN1, PLXNA2, FBXW2, PPP4R1, PTPRF, CCDC129, FOXO4, SREK1*	Glycosphingolipid biosynthesis - ganglio series, Mucin type O-Glycan biosynthesis, Amoebiasis, N-Glycan biosynthesis, Vasopressin-regulated water reabsorption
miR-3960	-63.1386	*EN1, CERS1, FAM127A, WWP2, RFX1*	Calcium signalling pathway, Neuroactive ligand-receptor interaction
miR-4454	-413.514	*ENAH, WDR72, FAM125B, DLG5, ENPP6, EIF4E3, GK*	ErbB signalling pathway

[a] P, primary tumour; R, recurrent tumour. Common targets and pathways between miRNAs are highlighted in different coloured text.

Table 5.11 Differentially expressed miRNAs identified in Patient 9 with the predicted targets and pathways.

miRNA	Fold change (P vs R)[a]	Target	Pathway
miR-4529-5p	3.37359	*CBLL1, SS18L1, CSDE1, PKP3, MEX3C, PIP4K2C, LRP1, KIRREL2, GRIN2B, DNAJC14*	Leukocyte transendothelial migration, Bacterial invasion of epithelial cells, Salmonella infection, N-Glycan biosynthesis, Wnt signalling pathway
miR-663b	2.92884	*SLC4A8, STAT5B, ATCAY, NCAM2, IL17D, GNAQ, NICN1, BSPRY, SCAI, STK40*	Other glycan degradation, Sphingolipid metabolism, Endocytosis, ECM-receptor interaction, Systemic lupus erythematosus
miR-4803	2.45766	*LPPR5, MKX, XIAP, ARMC8, ZEB1, CEP170, TAF2, SACS, LPHN3, NRCAM*	TGF-beta signalling pathway, MAPK signalling pathway, Nicotinate and nicotinamide metabolism, Wnt signalling pathway, PI3K-Akt signalling pathway
miR-4757-3p	2.22097	*SAR1B, IKBIP, RAB7L1, PCDHA12, PCDHA6, PCDHA2, PCDHA11, PCDHA7, PCDHA5, PCDHA10*	Cell adhesion molecules (CAMs), Apoptosis, Ubiquitin mediated proteolysis

[a] P, primary tumour; R, recurrent tumour. Common pathways between miRNAs are highlighted in different coloured text.

Table 5.12 The 10 most differentially expressed miRNAs identified in Patient 10 with the predicted targets and pathways.

miRNA	Fold change (P vs R)[a]	Target	Pathway
miR-451	6.08149	*PSMB8, TBC1D9B, MEX3C, CXCL16, MBP, CMTM6, CDKN2B, WDFY2, KCNK15, TSC1*	mTOR signalling pathway, Proteasome, Protein export, Glyoxylate and dicarboxylate metabolism, Propanoate metabolism
miR-1246	4.70218	*GSG1L, MSR1, BRWD1, RTKN2, SMG7, SLC16A7, MUT, GLRB, BEND4, TMEM123*	Neurotrophin signalling pathway, N-Glycan biosynthesis, Inositol phosphate metabolism, Protein processing in endoplasmic reticulum, ErbB signalling pathway
miR-4732-5p	4.25007	*DBT, TMEM237, NHLH1, BCLAF1, WASL, RBPJ, PARM1, SFMBT1, ALKBH5, OXGR1*	Fatty acid metabolism, Basal transcription factors, PPAR signalling pathway, Notch signalling pathway, Proteasome
miR-4530	3.9028	*VPS53, FUT3, SMARCD2, JRK, DDX6, NDOR1, FOXK1, MRPS25, DAGLA, MAVS*	N-Glycan biosynthesis, Glycosphingolipid biosynthesis - lacto and neolacto series, Fatty acid biosynthesis, Amino sugar and nucleotide sugar metabolism, Glycosaminoglycan degradation
miR-124	3.33354	*TXNRD1, SNX2, RSU1, FLRT3, DSCR6, COPS2, TMEM56, STRBP, UHRF1, ATPBD4*	Hypertrophic cardiomyopathy (HCM), Neurotrophin signalling pathway, Dilated cardiomyopathy, Arrhythmogenic right ventricular cardiomyopathy (ARVC), Axon guidance
miR-338-3p	-2.46375	*VPS53, DGKB, PREX2, SLC2A10, B4GALT7, NRP1, HMOX2, VAPB, TATDN3, CACNG8*	Glycolysis / Gluconeogenesis, Hypertrophic cardiomyopathy (HCM), ErbB signalling pathway, Dilated cardiomyopathy, Cardiac muscle contraction
let-7c	-2.71537	*LIN28B, IGF2BP1, HMGA2, FIGURENL2, LRIG3, DDI2, GATM, MAP4K3, PRTG, USP38*	Axon guidance, MAPK signalling pathway, Hypertrophic cardiomyopathy (HCM), T cell receptor signalling pathway, Dilated cardiomyopathy
miR-21	-2.96269	*YOD1, KRIT1, WTH3DI, GPR64, PLEKHA1, SKP2, FBXO11, MALT1, PELI1, PBRM1*	Cytokine-cytokine receptor interaction, TGF-beta signalling pathway, MAPK signalling pathway, Melanoma
miR-29b	-3.04418	*USP28, NEUROD1, ZDHHC5, LIN9, TNPO3, CLEC2B, WDR26, SNX30, SLC30A7, PROS1*	ECM-receptor interaction, Small cell lung cancer, Focal adhesion, Axon guidance, Pathways in cancer
miR-29a	-3.12436	*TET3, COL3A1, SESTD1, NFIA, PI15, HBP1, ATAD2B, PXDN, TET2, IGF1*	ECM-receptor interaction, Protein digestion and absorption, Amoebiasis, Focal adhesion, PI3K-Akt signalling pathway

[a] P, primary tumour; R, recurrent tumour. Common targets and pathways between miRNAs are highlighted in different coloured text.

Both Patients 1 and 6, who maintained the same grading at recurrence, had the largest fold changes in miRNA expression of > 500-fold change in the primary tumour compared to its recurrence. Paired samples from Patients 1 and 6 had four common differentially expressed miRNAs; miR-3142, miR-4454, mir-4521 and miR-466. All but miR-4454 were downregulated in the primary tumour in Patient 1, while all but miR-4454 were upregulated in the primary tumour in Patient 6. The difference in expression of miR-4454, with downregulation in 1 tumour and upregulation in the other may be due to primary tumours being of different tumour grades.

Differences in miRNA expression between tumour sample pairs from Patients 1, 6 and 10, with the same histological grading at recurrence were compared to identify common miRNAs, but none were found. The reason for this could be that two of the primary tumours were astrocytic and one was oligodendroglial in origin.

5.6 DISCUSSION

In the current study, *IDH1* and *IDH2* mutation status and *MGMT* methylation status was determined in paired samples at diagnosis and recurrence. Genomic profiles and miRNA expression analysis was also investigated in three and five patients respectively with paired samples at diagnosis and recurrence.

5.6.1 *IDH* mutation and *MGMT* methylation

IDH1 and *IDH2* mutation status of all tumours at diagnosis was maintained in their recurrent tumours. Of the four patients for *MGMT* methylation, the methylation status was maintained in tumour samples from two patients but showed variation in two cases. A recent study of 23 LGG primary tumours and their recurrences also reported that *IDH1* status was matched between the primary and the paired recurrent tumour (Johnson *et al*., 2014). Another study with 53 primary and recurrent paired tumours including 29 LGG, 16 anaplastic tumours and 8 GBM reported that *IDH1* and *IDH2* status in the recurrent tumours was consistent with their respective primary tumours (Yao *et al*., 2013). In a study of 21 primary and progressive paired O tumours, the authors showed that the *IDH1* status remained unchanged in all the tumours after progression, while the frequency of *MGMT* promoter methylation increased from 38.1% in primary tumours to 52.4% in the recurrent tumours (Kuo *et al*., 2013).

5.6.2 Copy number analysis

CNAs were identified in a cohort of three patients with paired tumour samples at diagnosis and recurrence. For all the patients, the paired samples were genomically different and the recurrent tumours had more CNAs than the corresponding primary tumours. Interestingly, for Patient 1, paired tumour samples which are grade II at

diagnosis and recurrence had a larger difference in the number of aberrations with 124 in the primary tumour and 206 aberrations in the recurrent tumour. For Patients 9 and 10, the difference in the number of aberrations between the tumour samples at diagnosis and at recurrence was relatively small with additional 34 and 20 aberrations respectively in the recurrent tumours. These findings suggest that paired tumour samples have clonal cell populations, some of which remain stable and unaffected by time or any treatment such as radiotherapy and chemotherapy. Recurrent tumours consist of tumour cells that proliferate with additional genomic changes to those present in the tumour at diagnosis. These new changes may have been developed during progression or present in a subclonal population of the primary tumour and selected for during therapy. The additional regions of genomic aberrations may contain genes linked to resistance against treatment, thereby, promoting tumour recurrence.

In a study by Kuo *et a*l. (2013), genetic profiles of 21 pairs of primary and progressive O tumours were investigated using aCGH. In the primary tumour, losses were identified on 1p36, 19q13 and 9p22 in 57.1% (12/21), 81% (17/21) and 52.3% (11/21) respectively of all the cases. In the recurrent tumour, additional losses on 1p, 9p, 10q, 17p, 19q and 22q were identified in 14.3% (3/21), 4.8% (1/21), 14.3% (3/21), 9.5% (2/21), 4.8% (1/21) and 14.3% (3/21) respectively of all the cases. In the present study, losses on 1p36 and 19q13 were observed in 33% (1/3) and 67% (2/3) respectively in the primary tumours, while in the recurrent tumours, additional losses on 1p, 9p, 10q and 19q were present in 67% (2/3), 33% (1/3), 33% (1/3) and 67% (2/3) respectively of all the cases.

In a recent study of 27 paired primary and recurrent GBM tumours, the genomic profiles of the paired samples were compared by aCGH (Riehmer *et al*., 2014). About

33% (9/27) of recurrent pairs had all chromosomal aberrations of the primary tumour plus some additional changes. In 41% (11/27) of the pairs, the genomic profiles of the paired primary and recurrent tumours were disparate with recurrent tumours having additional aberrations but had lost aberrations present in the primary tumour. The authors showed that 75% of recurrent GBM tumours develop additional genomic changes compared to their primary tumours and that this may be promoted by loss on 9p21.3 in primary tumours.

5.6.3 miRNA expression analysis

miRNA expression analysis was completed with paired tumour samples at diagnosis and recurrence from five patients. Patient 1 and Patient 6, with primary tumours of astrocytic origin had the most number of differentially expressed miRNAs between the paired samples with 243 and 209 miRNAs respectively.

miR-4521, a common differentially expressed miRNA identified in Patients 1 and 6 has been reported previously in a breast cancer study. Camps *et al*., (2014) investigated the regulation of miRNA expression by hypoxia in breast cancer cell line, MCF-7. Under hypoxic conditions, HIF family of transcription factors induce a transcriptional response affecting several biological processes such as glycolysis, angiogenesis and apoptosis. The expression of miR-4521 was downregulated after 16h, 32h and 48h of hypoxia in MCF-7 cells. The downregulation of miR-4521 observed by next generation sequencing was validated by qPCR and was in accordance.

No common differentially expressed miRNAs were found between the comparative analyses of the 5 patients. A possible explanation for this could be that the sample

cohort is small and comprised a mix of histologies and grades. As mentioned previously in Chapter 1, A, OA and O exhibit different genetic changes and therefore, the miRNA expression profiles may also be varied in the three histological groups in both grade II and grade III tumours. The results from this study demonstrate that miRNA expression profiles showed variation in histological groups in both the grades.

Ilhan-Mutlu *et al*., (2013) compared the miRNA expression levels between primary and recurrent GBM tumours. Seven miRNAs selected that had relevance with GBM from previous studies were miR-10b, miR-21, miR-181b, miR-181c, miR-195, miR-221 and miR-222. The miRNA expression levels were determined by qPCR and for all the miRNAs, no significant difference was observed between the paired primary and recurrent tumours. In contrast, the present study showed variation in miRNA expression levels in the paired tumour samples from the same patients. This could be a sequential effect altering the miRNA expression levels during progression or acquiring new aberrations that may induce changes in the expression profiles at recurrence.

In summary, the present study is one of only a few that have compared primary and recurrent tumours from the same patient and the findings of this study are important due to the lack of studies analysing primary/recurrent paired samples. Comparison of tumours at diagnosis and recurrence revealed that additional changes arise in the genomic and miRNA expression profiles of the recurrent tumours that may contribute to the malignant progression of the tumours.

CHAPTER 6

CHARACTERISATION OF LGG SHORT-TERM CELL CULTURES

6.1 INTRODUCTION

There are numerous established cell lines representing GBM available for research, but no cell lines representing LGG are listed in the American Type Culture Collection (ATCC) and ECACC databases. Short-term culture remains the only *in vitro* model at present.

The aim of the chapter was to assess the reliability of using LGG cell cultures grown as monolayers as representative *in vitro* models for LGG. Previous investigations had demonstrated that *IDH* mutations are not maintained in cell culture (Piaskowski *et al*., 2011). A number of paired frozen biopsy samples and their derivative short-term cell cultures were available for analysis in the present study. All samples were analysed for *IDH1* and *IDH2* mutation status and *MGMT* promoter methylation status was determined in 12 sample sets. Genomic copy number analysis and miRNA expression profiling were completed for subsets of eight and five paired samples respectively, depending on tissue availability. The expression of a panel of cellular markers was determined by IHC and comparative proliferation rates and tumourigenic potential was assessed in a small number of cases.

6.2 TUMOUR SAMPLES

The sample cohort of 17 lower grade diffuse glioma comprised 15 grade II tumours (9 A, 1 OA, 5 O) and 2 grade III tumours (2 AO). Patients with grade II tumours had an age range of 35-56 years with a median of 45.5 years and those with grade III tumours had an age range of 47-66 years with a median of 56.5 years.

6.3 *IDH* MUTATION AND *MGMT* PROMOTER METHYLATION ANALYSIS

The mutation status of *IDH1* and *IDH2* was determined in 17 biopsy tissues and their paired cell cultures by direct sequencing and the results are summarised in Table 6.1. *IDH1* mutation was detected in seven biopsy tissues comprising 2/9 A (22%), 1/1 OA (100%), 3/5 O (60%) and 1/2 AO (50%) and in all cases, the mutations were heterozygous R132H (CGT to CAT). However, none of these mutations were maintained in the derivative cell cultures. No *IDH2* mutations were detected.

MGMT methylation status was determined by MS-PCR for 12 paired samples (Table 6.1). Methylation was observed in one biopsy tissue (IN2184) and partial methylation was observed in four biopsy tissues (IN99/81, IN2990, IN3020 and UWLV3), all but one of which also carried the *IDH1* R132H mutation. However, no *MGMT* promoter methylation was detected in any of the cell cultures. All four of the tumours with partial methylation were O and the methylated tumour was an AO.

Table 6.1 Tumour samples for *IDH* mutation and *MGMT* promoter methylation analysis

Tumour	Age[a]	Sex[b]	Source[c]	Grade	Histology[d]	*IDH1* Mutation status[e]	*IDH2* Mutation status	*MGMT* methylation status[f]
IN4	56	F	B	II	A	WT	WT	U
			CC			WT	WT	U
IN118/81	47	M	B	II	A	R132H	WT	ND
			CC			WT	WT	ND
IN143	N/A	F	B	II	A	R132H	WT	U
			CC			WT	WT	U
IN1705	47	F	B	II	A	WT	WT	U
			CC			WT	WT	U
IN1853	47	M	B	II	A	WT	WT	U
			CC			WT	WT	U
IN2190	45	M	B	II	A	WT	WT	U
			CC			WT	WT	U
IN2800	32	M	B	II	A	WT	WT	U
			CC			WT	WT	U
IN2985	41	F	B	II	A	WT	WT	ND
			CC			WT	WT	ND
IN3139	74	F	B	II	A	WT	WT	ND
			CC			WT	WT	ND
UWLV7	38	M	B	II	OA	R132H	WT	ND
			CC			WT	WT	ND
IN99/81	N/A	F	B	II	O	R132H	WT	PM
			CC			WT	WT	U
IN2723	55	F	B	II	O	WT	WT	ND
			CC			WT	WT	ND
IN2990	31	F	B	II	O	R132H	WT	PM
			CC			WT	WT	U
IN3020	35	F	B	II	O	WT	WT	PM
			CC			WT	WT	U
UWLV3	43	M	B	II	O	R132H	WT	PM
			CC			WT	WT	U
IN2184	47	F	B	III	AO	R132H	WT	M
			CC			WT	WT	U
IN3045	66	M	B	III	AO	WT	WT	U
			CC			WT	WT	U

[a] Age at diagnosis in years; [b] M, male; F, female; [c] B, biopsy tissue; CC, cell culture; [d] A, astrocytoma; OA, oligoastrocytoma; O, oligodendroglioma; AO, anaplastic oligodendroglioma; [e] R132H, *IDH1* mutant; WT, wild type; [f] M, methylated; PM, partially methylated; U, unmethylated; ND, not done.

6.4 COMPARISON OF COPY NUMBER CHANGES IN PAIRED BIOPSY AND CELL CULTURE SAMPLES

In order to determine whether any other genetic abnormalities are maintained in cell culture, aCGH was performed on a 244K array using high quality DNA from eight paired samples of biopsy tissues and short-term cell cultures, IN118/81 (A), IN1853 (A), IN2190 (A), IN2800 (A), UWLV7 (OA), IN2723 (O), UWLV3 (O) and IN2184 (AO) as detailed in Table 6.2. The *IDH1*-R132H mutation was detected in four biopsy tissues, IN188/81, UWLV3, UWLV7 and IN2184, while no mutation of *IDH2* was present in any of the samples assessed by direct sequencing analysis. Following genomic segmentation to obtain the CNAs, gains/losses on the chromosomes were identified. CNAs were detected in all eight pairs and common aberrations were identified for each pair.

Table 6.2 Tumour samples with paired biopsy tissue and derivative short-term cell cultures used for aCGH analysis

Tumour sample (paired biopsy and culture)	Age[a]	Sex[b]	Grade	Histology[c]	*IDH1* Mutation status[d]	*IDH2* Mutation status
IN118/81	47	M	II	A	R132H	WT
IN1853	47	M	II	A	WT	WT
IN2190	45	M	II	A	WT	WT
IN2800	32	M	II	A	WT	WT
UWLV7	38	M	II	OA	R132H	WT
IN2723	55	F	II	O	WT	WT
UWLV3	43	M	II	O	R132H	WT
IN2184	47	F	III	AO	R132H	WT

[a] Age at diagnosis in years; [b] M, male; F, female; [c] A, astrocytoma; OA, oligoastrocytoma; O, oligodendroglioma; AO, anaplastic oligodendroglioma; [d] R132H, *IDH1* mutant; WT, wild type.

6.4.1 Tumour sample IN118/81

In IN118/81 tumour biopsy, there were 78 CNAs, of which 45 were gains and 33 were losses. In IN18/81 cell culture, there were 45 CNAs with 24 regions of gain and 21 of loss. Only 9% (7/78) of CNAs present in the biopsy tissue were maintained in the cell culture. The genomic summaries for the biopsy and cell culture are shown in Figure 6.1 and the common CNAs are summarised in Table 6.3.

6.4.2 Tumour samples IN1853

In IN1853 biopsy tissue, there were 113 CNAs, of which 78 were regions of gain and 35 were regions of loss. In the IN1853 culture, 103 CNAs were identified with 96 gains and 7 losses. Fifty three percent (61/113) of CNAs were maintained in the cell culture. The genomic summaries for the biopsy and cell culture are shown in Figure 6.2 and the common aberrations are detailed in Table 6.4.

6.4.3 Tumour sample IN2190

In IN2190 biopsy tissue, there were 52 CNAs, of which 40 were regions of gain and 12 were regions of loss. In 2190CC, 84 CNAs were identified with 20 regions of gain and 64 regions of loss. Eleven percent (6/52) of CNAs of the biopsy tissue were maintained in the cell culture. The genomic summaries for the biopsy and cell culture are presented in Figure 6.3 and the common CNAs are listed in Table 6.5.

6.4.4 Tumour sample IN2800

In IN2800 biopsy tissue, 57 CNAs were identified, of which 44 were regions with gain and 13 were regions with loss. In the cell culture, there were 48 CNAs with 33 regions of gain and 15 regions of loss. Eighteen percent (10/57) of the CNAs present in IN2800B were maintained in the cell culture. The genomic summaries for the biopsy and cell culture are shown in Figure 6.4 and the common CNAs are summarised in Table 6.6.

6.4.5 Tumour sample UWLV7

In UWLV7 biopsy tissue, there were 71 CNAs with 58 regions of gain and 13 regions of loss. In the cell culture, there were 26 CNAs, of which 20 were regions with gain and 6 were regions with loss. Only 1% (1/71) of CNA present in the biopsy tissue was maintained in the cell culture. The genomic summaries for the biopsy and cell culture are shown in Figure 6.5. The common CNA was loss on chromosome 14 at 14q11.1 - 14q11.2 with an average copy number of -0.519397 and the overlapping gene was *OR4K1*.

6.4.6 Tumour sample IN2723

In IN2723 biopsy tissue, 45 CNAs were identified, of which 32 were regions of gain and 13 were regions of loss. In the cell culture, there were 93 CNAs with 61 regions of gain and 32 regions of loss. Only 15% (7/45) of CNAs found in IN2723B were maintained in the cell culture. The genomic summaries for the biopsy and cell culture are illustrated in Figure 6.6 and the common CNAs are detailed in Table 6.7.

6.4.7 Tumour sample UWLV3

There were 61 CNAs identified in UWLV3 biopsy tissue, of which 53 were regions of gain and 8 were regions of loss. In the cell culture, there were 33 CNAs with 18 regions of gain and 15 regions of loss. Only 2% (1/61) of CNAs identified in UWLV3B were maintained in the cell culture. The genomic summaries for the biopsy and cell culture are presented in Figure 6.7. The common CNA was gain on chromosome 15 at 15q26.1 with an average copy number of 0.357862 and no gene was present in the region.

6.4.8 Tumour sample IN2184

In IN2184 biopsy tissue, there were 246 CNAs with 112 regions of gain and 134 regions of loss. In the cell culture, there were 209 CNAs, of which 148 were regions of gain and 61 were regions of loss. Less than 1 percent (2/246) of the CNA present in the biopsy tissue was maintained in the cell culture. 1p/19q loss was detected in IN2184B. The genomic summaries for the biopsy and cell culture are shown in Figure 6.8 and the common CNAs are detailed in Table 6.8.

Figure 6.1 Genome summary of CNAs for tumour IN118/81 biopsy and cell culture

IN118/81B

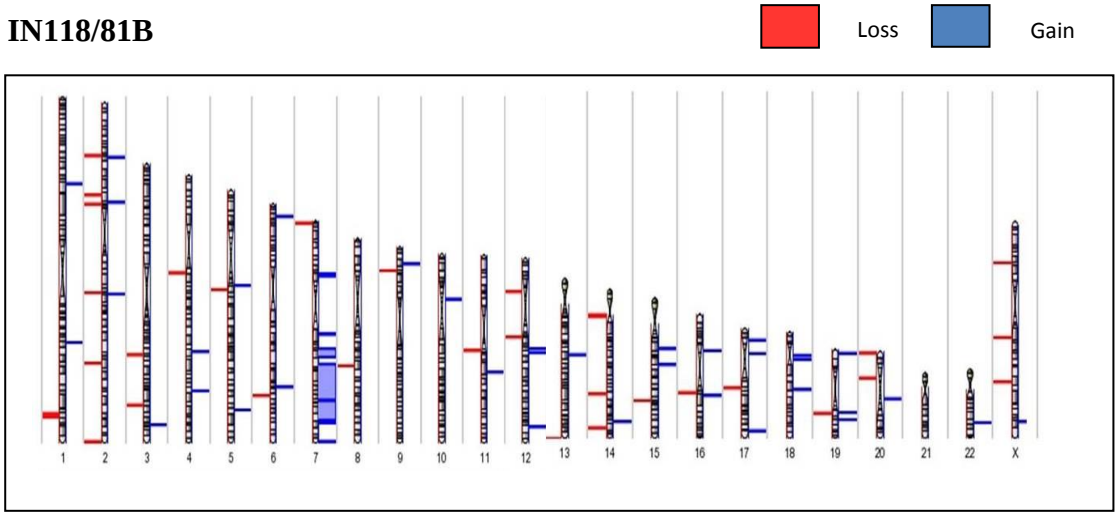

IN118/81CC

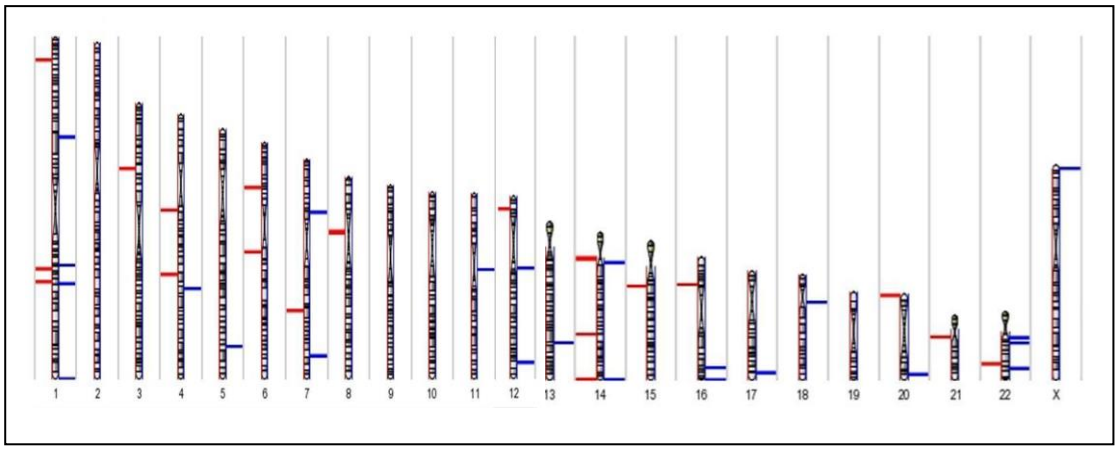

Table 6.3 CNAs maintained in IN118/81 cell culture

Chromosome	Cytoband	CNA	Overlapping genes
4	4q28.1	Gain	*ANKRD50*
5	5q33.3	Gain	*SOX30*
7	7q34	Gain	*LOC100124692, MOXD2P, PRSS58, LOC730441, MTRNR2L6, PRSS1, TRY6*
12	12q24.31	Gain	*CAMKK2, ANAPC5*
14	14q11.1 - 14q11.2	Loss	*POTEM, OR11H2, OR4Q3, OR4M1, OR4N2, OR4K2, OR4K5, OR4K1*
17	17q25.3	Gain	*LOC100507351*
18	18q11.2	Gain	*TTC39C*

Figure 6.2 Genome summary of CNAs for tumour IN1853 biopsy and cell culture

IN1853B

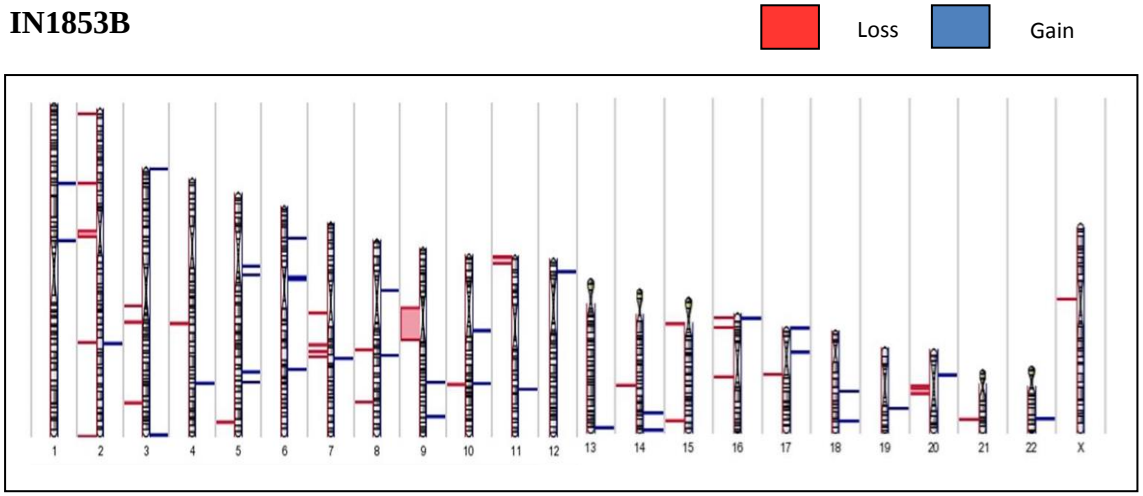

IN1853CC

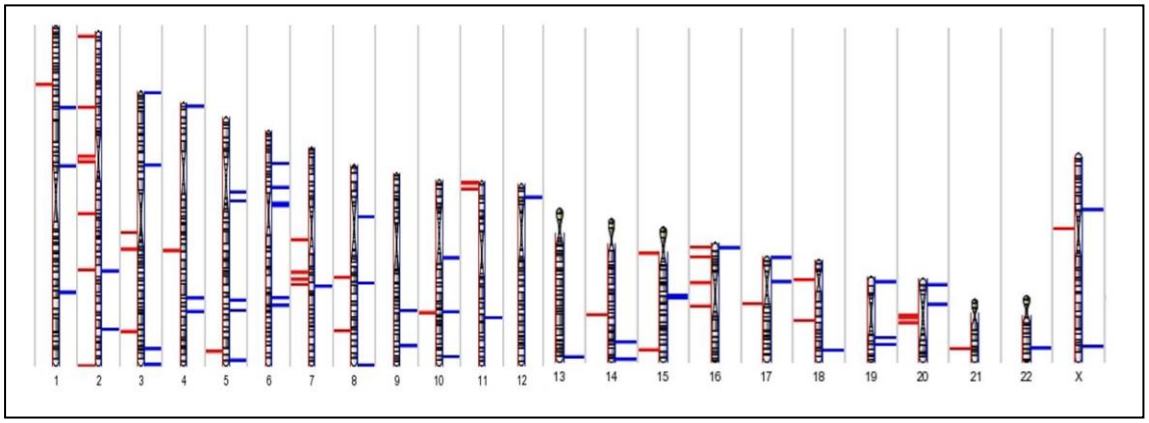

Table 6.4 CNAs maintained in IN1853 cell culture

Chromosome	Cytoband	CNA	Overlapping genes
chr1	1p32.1	Gain	*FGGY*
chr1	1p22.1	Gain	*TGFBR3*
chr2	2q37.3	Deletion	*C2orf85*
chr2	2p16.1	Deletion	*CCDC88A*
chr2	2q31.1	Deletion	*ITGA6*
chr2	2p25.3	Deletion	*LOC100505964*
chr2	2q24.2	Gain	*SLC4A10, DPP4, GCG, FAP, IFIH1, GCA, KCNH7*
chr2	2p23.3	Deletion	*KLHL29*
chr3	3p26.3	Gain	*CNTN6*
chr3	3q29	Gain	*PIGX*
chr3	3q13.2	Deletion	*WDR52*
chr3	3p12.1	Deletion	*ROBO2, ROBO1, GBE1, LOC440970*
chr4	4q21.22	Gain	*TMEM150C, C4orf11*
chr4	4q24	Deletion	*TBCK*
chr5	5q11.2	Gain	*CDC20B*
chr5	5q12.1	Gain	*FLJ37543*
chr5	5q31.1	Gain	*FSTL4*
chr5	5q35.1	Deletion	*KCNMB1*
chr5	5q31.3	Gain	*PCDHA7*
chr6	6p22.2	Gain	*NRSN1*
chr6	6p12.1	Gain	*TINAG*
chr6	6p12.2 - 6p12.1	Gain	*TMEM14A*
chr7	7q21.13	Deletion	*CDK14*
chr7	7q22.1	Deletion	*GJC3*
chr7	7q22.1	Gain	*MOGAT3*
chr7	7q21.3	Deletion	*SLC25A13*
chr7	7q11.22	Deletion	*STAG3L4*
chr8	8q24.12	Deletion	*MAL2*
chr8	8p12	Gain	*RAB11FIP1*
chr8	8q21.2	Gain	*RALYL*
chr8	8q21.13	Deletion	*ZNF704*
chr9	9q22.33	Gain	*HEMGN*
chr9	9q33.2	Gain	*STRBP*
chr10	10q23.33	Deletion	*HELLS*
chr10	10q21.1	Gain	*PCDH15*
chr10	10q23.33	Gain	*TMEM20*
chr11	11q22.1	Gain	*CNTN5*
chr11	11p15.5	Deletion	*LOC338651*
chr11	11p15.4	Deletion	*OR52E4*
chr12	12p13.31	Gain	*CLEC2B*
chr13	13q34	Gain	*COL4A1*
chr14	14q32.33	Gain	*ASPG*
chr14	14q24.2	Deletion	*PCNX*
chr14	14q32.12	Gain	*SMEK1*
chr15	15q11.2	Deletion	*NF1P1*
chr15	15q26.1	Deletion	*ST8SIA2*
chr16	16p13.3	Gain	*CREBBP*
chr16	16p13.13	Deletion	*EMP2*
chr16	16p13.3	Deletion	*NAT15*
chr16	16q12.1	Deletion	*SIAH1*
chr17	17p13.3	Gain	*ABR*
chr17	17q12	Deletion	*ERBB2*
chr17	17p11.2	Gain	*PRPSAP2*
chr18	18q22.2	Gain	*SOCS6*
chr19	19q13.2	Gain	*PSMC4*
chr20	20q11.1 - 20q11.21	Deletion	*FRG1B*
chr20	20p11.23	Gain	*LOC100130264*
chr20	20q11.22	Deletion	*NCOA6*
chr21	21q22.12	Deletion	*SETD4*
chr22	22q13.1	Gain	*GRAP2*
chrX	Xp11.21	Deletion	*RRAGB*

Figure 6.3 Genome summary of CNAs for tumour IN2190 biopsy and cell culture

IN2190B

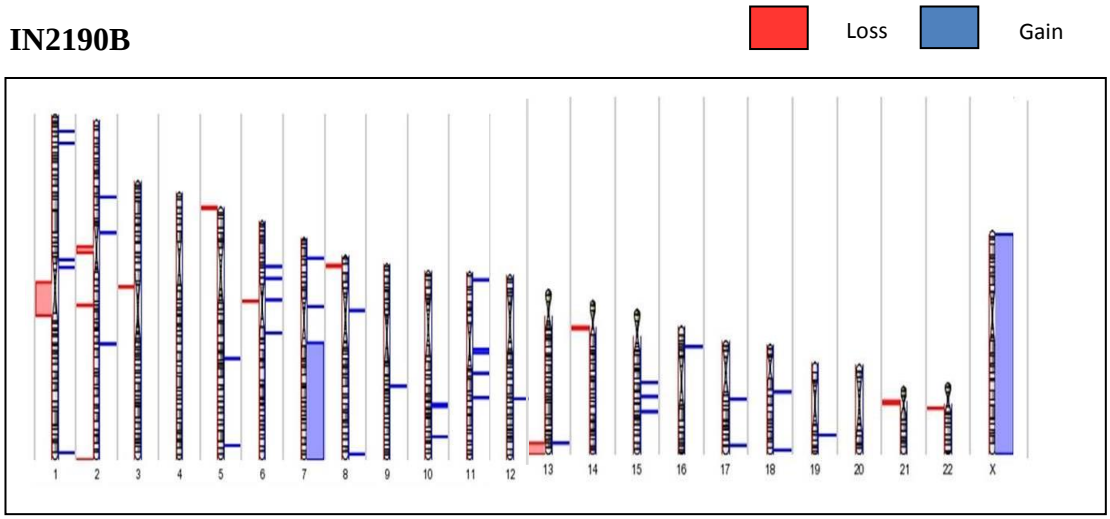

IN2190CC

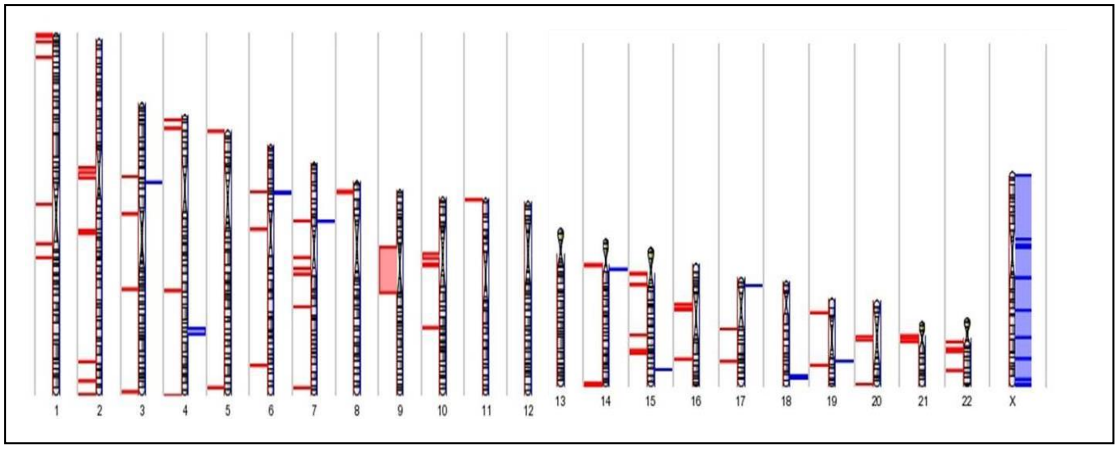

Table 6.5 CNAs maintained in IN2190 cell culture

Chromosome	Cytoband	CNA	Overlapping genes
2	2q37.3	Loss	*C2orf85*
3	3p12.3	Loss	*FAM86DP, FLJ20518, FRG2C, MIR1324*
8	8p23.1	Loss	*FLJ10661*
14	14q11.1 - 14q11.2	Loss	*OR11H2*
21	21p11.2 - 21p11.1	Loss	*BAGE*
X	Xp22.33 - Xp11.23	Gain	*ARAF*

Figure 6.4 Genome summary of CNAs for tumour IN2800 biopsy and cell culture

IN2800B

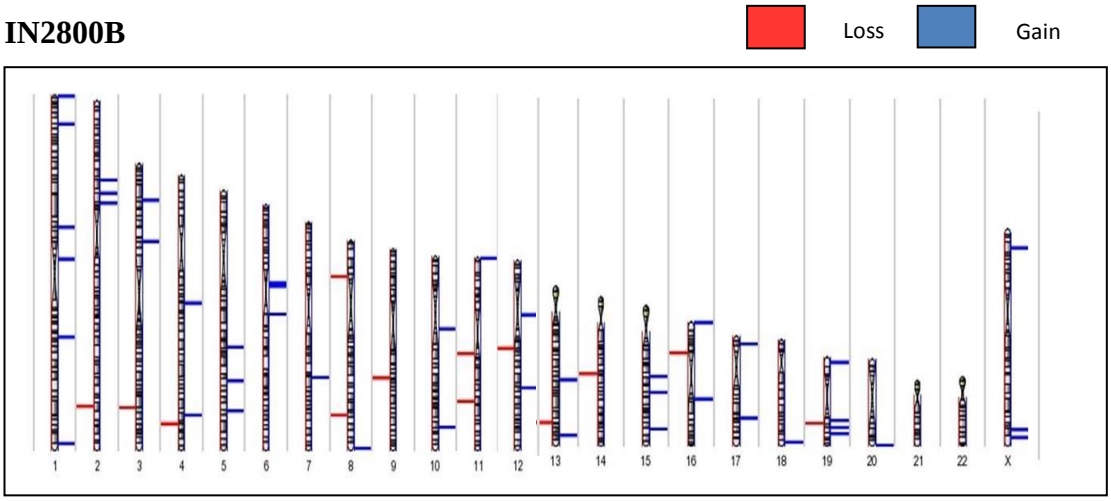

IN2800CC

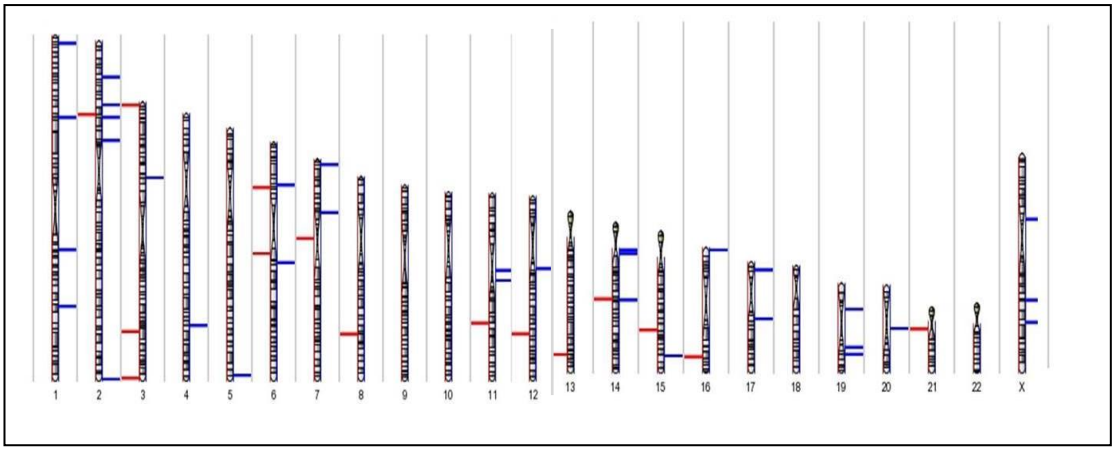

Table 6.6 CNAs maintained in IN2800 cell culture

Chromosome	Cytoband	CNA	Overlapping genes
1	1p32.1	Gain	*JUN*
2	2p16.2	Gain	*SPTBN1*
2	2p13.3	Gain	*ANKRD53*
3	3p21.1	Gain	*CACNA2D3*
11	11q13.1	Loss	*PACS1, KLC2, RAB1B, CNIH2, YIF1A*
15	15q26.1	Gain	*MIR9-3, LOC254559*
16	16p13.3	Gain	*HS3ST6, SEPX1, RPL3L*
17	17p13.2	Gain	*WSCD1*
19	19q13.2	Gain	*PSMC4, ZNF546, ZNF780B*
19	19q13.32	Gain	*APOE, APOC1, APOC1P1, APOC4, APOC2, CLPTM1*

Figure 6.5 Genome summary of CNAs for tumour UWLV7 biopsy and cell culture

UWLV7B

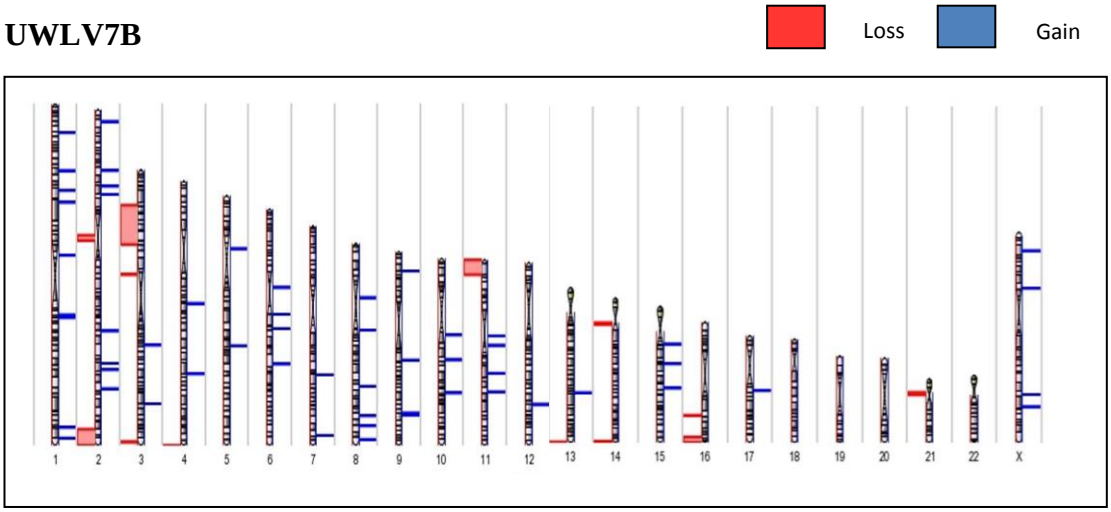

UWLV7CC

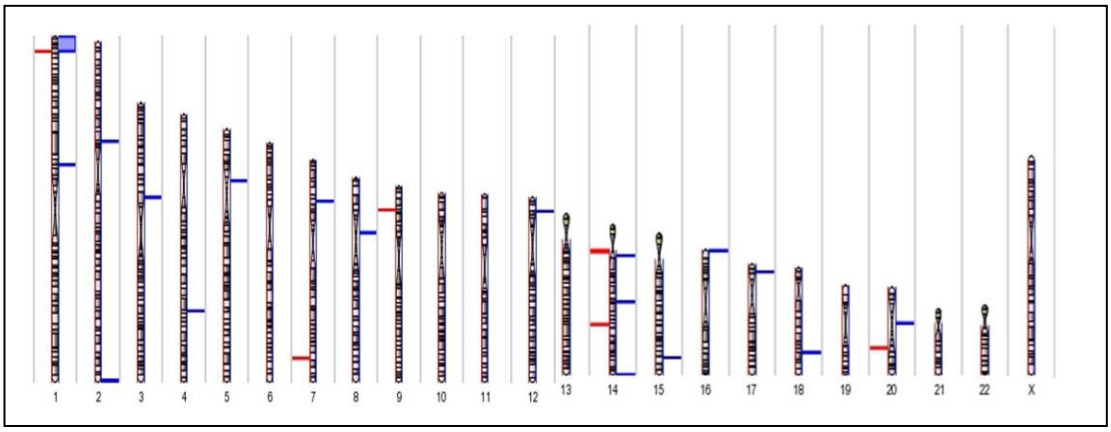

Figure 6.6 Genome summary of CNAs for tumour IN2723 biopsy and cell culture

IN2723B

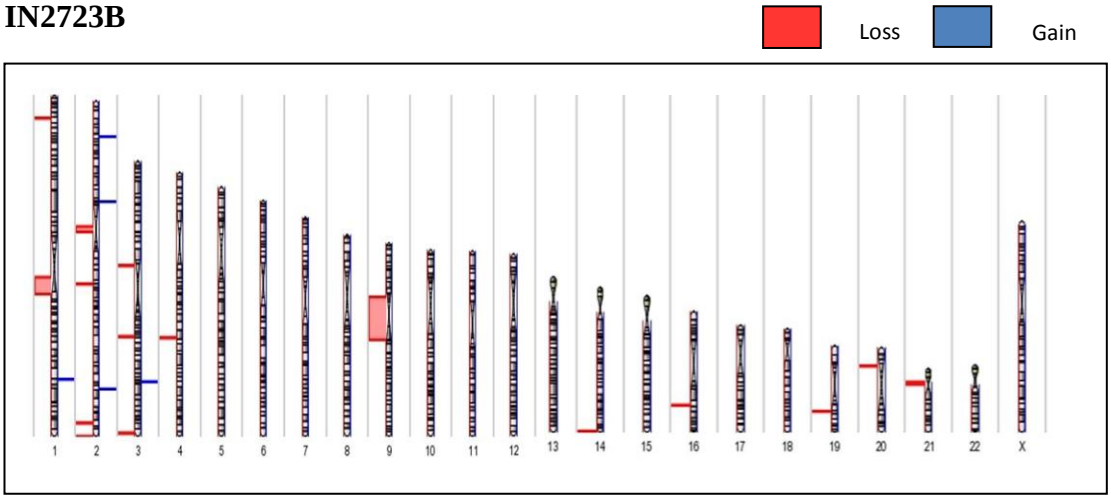

IN2723CC

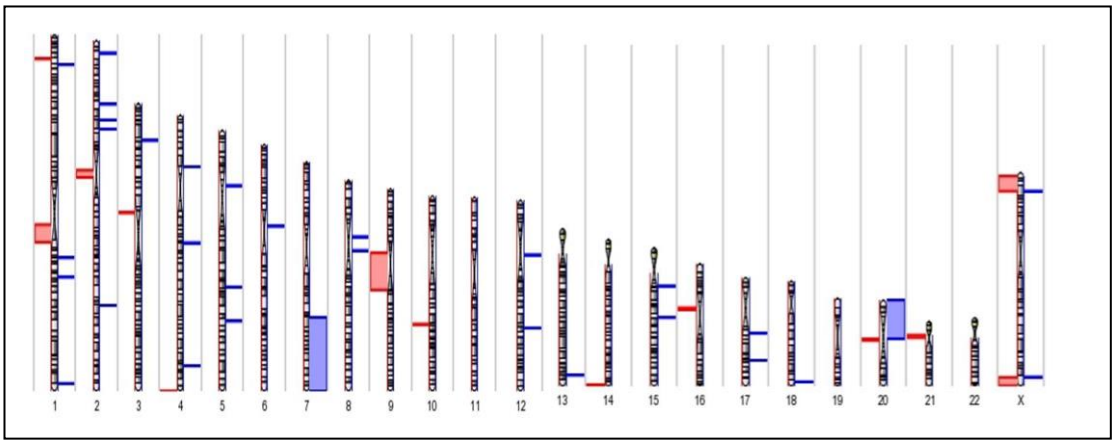

Table 6.7 CNAs maintained in IN2723 cell culture

Chromosome	Cytoband	CNA	Overlapping genes
1	1q12 - 1q21.1	Loss	*NBPF10*
3	3p12.3	Loss	*FAM86DP, FLJ20518, FRG2C, MIR1324, MIR4273, ZNF717, MIR4273*
4	4q35.2	Loss	*TUBB4Q*
10	10q23.2	Loss	*FAM22D*
14	14q32.33	Loss	*TMEM121*
20	20p13 - 20p12.1	Gain	*C20orf7*
21	21p11.2 - 21p11.1	Loss	*BAGE*

Figure 6.7 Genome summary of CNAs for tumour UWLV3 biopsy and cell culture

UWLV3B

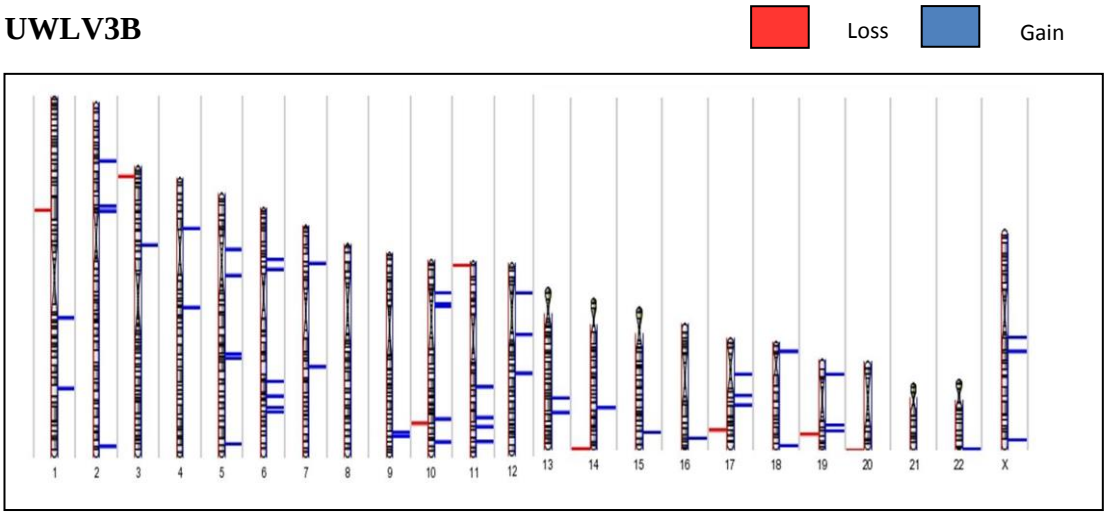

UWLV3CC

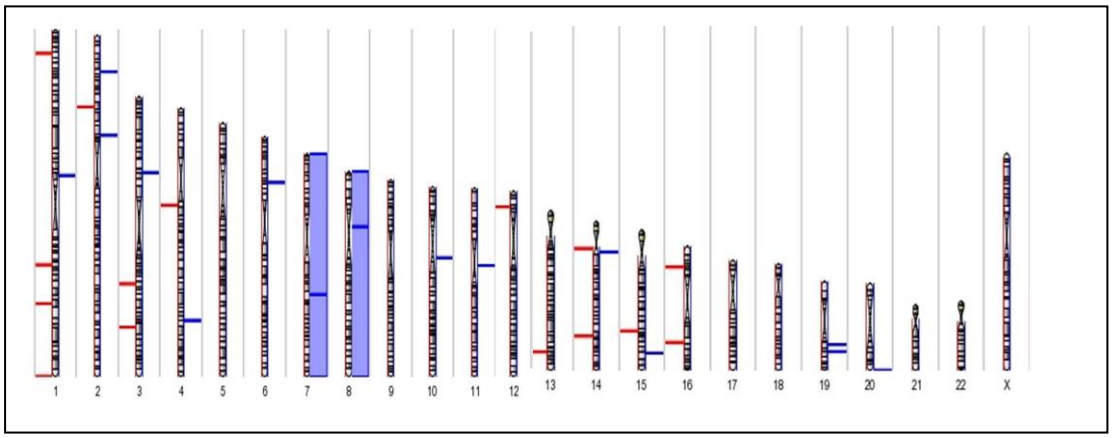

Figure 6.8 Genome summary of CNAs for tumour IN2184 biopsy and cell culture

IN2184B

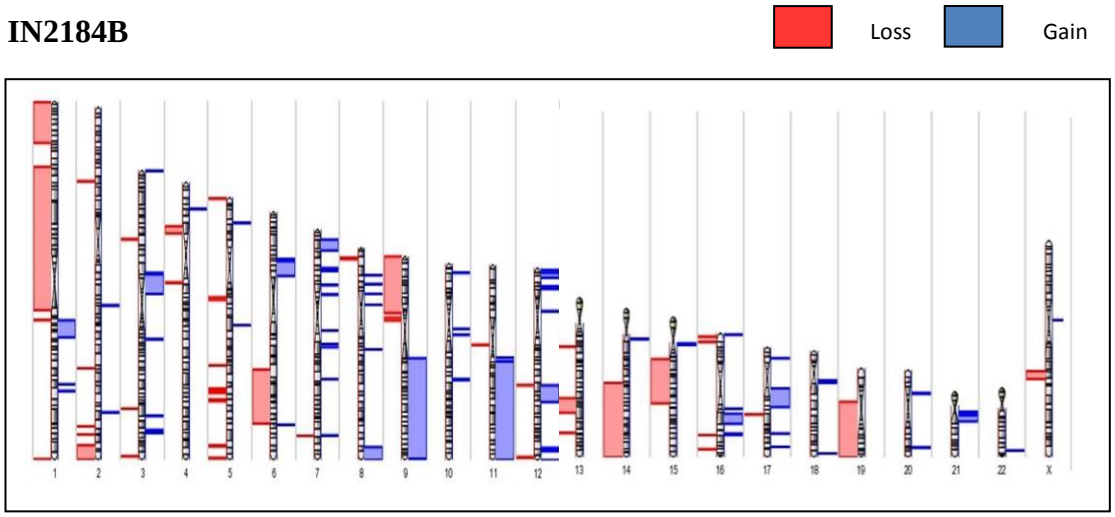

IN2184CC

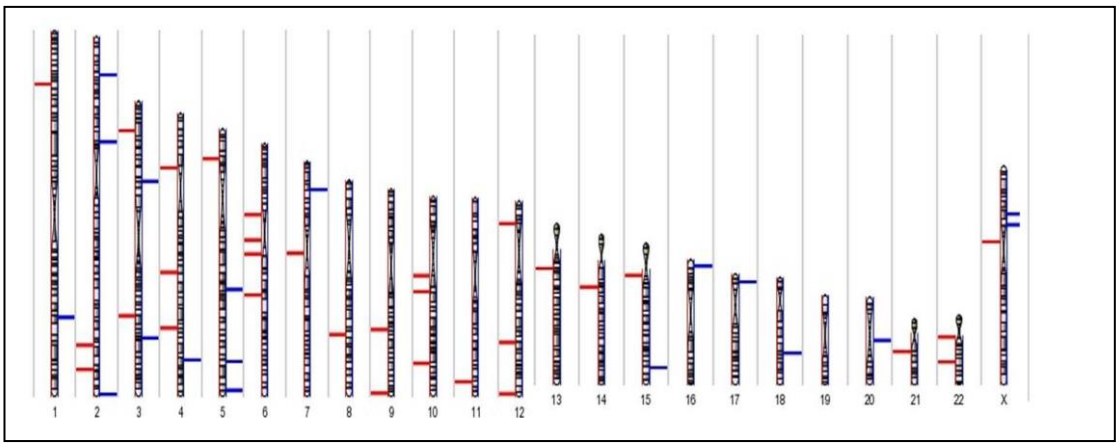

Table 6.8 CNAs maintained in IN2184 cell culture

Chromosome	Cytoband	CNA	Overlapping genes
1	1q21.3 - 1q22	Gain	*ZBTB7B, DCST2, DCST1, ADAM15*
12	12q24.33	Loss	*CDK4, CEP290, CLLU1*

The results from the comparison of biopsy and derived cell cultures in individual tumours are summarised in Table 6.9. In grade II tumours, the number of CNAs present in the biopsy tissue ranged from 45-113 and, with the exception of gain 7q in IN118/81 and IN2190 and loss 3p in UWLV7, gains and losses were restricted to small interstitial regions. In contrast, 246 CNAs were present in the AO tumour IN2184, including whole arm aneuploidies. In addition to deletion (1p,19q), loss of 9p and gain of 9q and 11q were identified. There were also many large interstitial regions of both loss (6q, 13, 14 and 15) and gain (6p, 12q and 17q). Within the grade II group of biopsies, there was no difference in the frequency or spectrum of CNAs between tumours with mutant R132H, *IDH1* and wild type *IDH1* or between histological subtypes.

It is apparent that the majority of CNAs present in tumour biopsy are not maintained in the derivative short-term cell cultures, particularly large regions of loss and gain such as gain of 7q in biopsy samples IN118/18 and IN2190. Conversely, additional gains and losses were observed in the cell cultures compared to their paired biopsies. The cell culture derived from UWLV3 had trisomy 7 and 8, neither of which was present in the tumour tissue. Similarly, cell culture IN2723 had additional gain of the short arm of 20 and a large gain on 7q. All of the CNAs that were maintained in the derivative cell cultures involved small regions, which were often centromeric, telomeric or in other heterochromatic regions where the accuracy of aCGH is sub-optimal.

Table 6.9 Comparison of CNAs in tumour samples with biopsy and derived culture

Tumour sample (paired biopsy and culture)	Grade	Histology[a]	*IDH1* Mutation status[b]	*IDH2* Mutation status	Number of CNAs in biopsy[c]	CNAs maintained in culture[d]
IN118/81	II	A	R132H	WT	78	8%
IN1853	II	A	WT	WT	113	53%
IN2190	II	A	WT	WT	52	10%
IN2800	II	A	WT	WT	57	18%
UWLV7	II	OA	R132H	WT	71	1%
IN2723	II	O	WT	WT	45	9%
UWLV3	II	O	R132H	WT	61	2%
IN2184	III	AO	R132H	WT	246	<1%

[a] A, astrocytoma; OA, oligoastrocytoma; O, oligodendroglioma; AO, anaplastic oligodendroglioma;[b] R132H, *IDH1* mutant; WT, wild type; [c] CNAs, copy number aberrations; [d] Percentage of CNAs maintained in culture.

6.5 COMPARISON OF miRNA EXPRESSION IN PAIRED BIOPSY AND CELL CULTURE SAMPLES

Expression profiling of miRNA was carried out on 5 paired samples of biopsy tissue and derived short-term cell cultures from grade II tumours. The cohort comprised IN2190 (A), IN2800 (A), UWLV7 (OA), IN2723 (O) and UWLV3 (O). *IDH1*-R132H mutation was detected in 2 biopsy tissues, UWLV3 and UWLV7, while no mutation of *IDH2* was present in any of the samples assessed by direct sequencing analysis (Table 6.10).

6.5.1 miRNA array and data analysis

miRNA expression analysis was performed using 3D Gene Human miRNA oligo chips (Toray, Japan) as described previously in Chapters 2 and 4. Data analysis was carried out using Partek Genomics Suite (version 6.6; Partek Inc., USA). Raw data was normalised with $\log_2$ median and one-way ANOVA test was used to determine differentially expressed miRNAs with $\geq$ 2-fold change. Unsupervised clustering analysis was performed with all biopsy and cell culture samples (n = 10). Identification of differentially expressed miRNAs was carried out between each tumour biopsy and its derived cell culture (n= 5) and commonly differentiated miRNAs for each paired analysis were noted. PCA was used to demonstrate differences in miRNA expression profiles amongst the pairs. miRNAs with significantly differential expression (p value < 0.05) were reported in the study.

Table 6.10 Paired samples of biopsy tissues and cell cultures used for miRNA analysis

Sample	Age at diagnosis[a]	Sex[b]	Grade	Histology[c]	*IDH1* mutation[d]	*IDH2* mutation
IN2190	45	M	II	A	WT	WT
IN2800	32	M	II	A	WT	WT
UWLV7	38	M	II	OA	R132H	WT
IN2723	55	F	II	O	WT	WT
UWLV3	43	M	II	O	R132H	WT

[a] Age at diagnosis in years; [b] M, male; F, female; [c] A, astrocytoma; OA, oligoastrocytoma; O, oligodendroglioma; [d] R132H, *IDH1* mutant; WT, wild type.

Unsupervised hierarchical clustering was performed using 1719 miRNAs and is represented by a dendrogram with samples having similar expression profiles clustered together (Figure 6.9). IN2190B and IN2800B clustered independently of any other samples while the remaining samples formed another cluster that further splits into two. Four of the cell cultures (IN2723CC, UWLV3CC, IN2800CC and UWLV7CC) had very similar expression profiles and clustered closely, indicating that culture conditions impart a strong influence on miRNA expression profiles.

The number of differentially expressed miRNAs with ≥ 2-fold change in expression between each tumour biopsy and its derived short-term cell culture are listed in Table 6.11. The greatest number of differentially expressed miRNAs was observed between the biopsy and cell culture in the astrocytoma sample IN2800 (249 miRNAs). In contrast, there were relatively few differences in miRNA expression between biopsy and cell culture in the oligodendroglioma sample UWLV3 (34 differentially expressed miRNAs). This is illustrated using PCA which confirms that the UWLV3 paired sample had the most similar expression profile compared to the IN2190 and IN2800 pairs that had the most different expression profiles (Figure 6.10).

Table 6.11 Differentially expressed miRNAs for each tumour sample (CC vs B) with ≥ 2-fold change in expression

Pairs	Histology at diagnosis[a]	Grade	Differentially expressed miRNAs (CC vs B) (≥ 2-fold change)[b]
IN2190	A	II	86
IN2800	A	II	249
UWLV7	OA	II	82
IN2723	O	II	64
UWLV3	O	II	34

[a] A, astrocytoma; OA, oligoastrocytoma; O, oligodendroglioma; [b] CC, cell culture; B, biopsy tissue.

Figure 6.9 Unsupervised hierarchical clustering for biopsy samples and their derived cell cultures

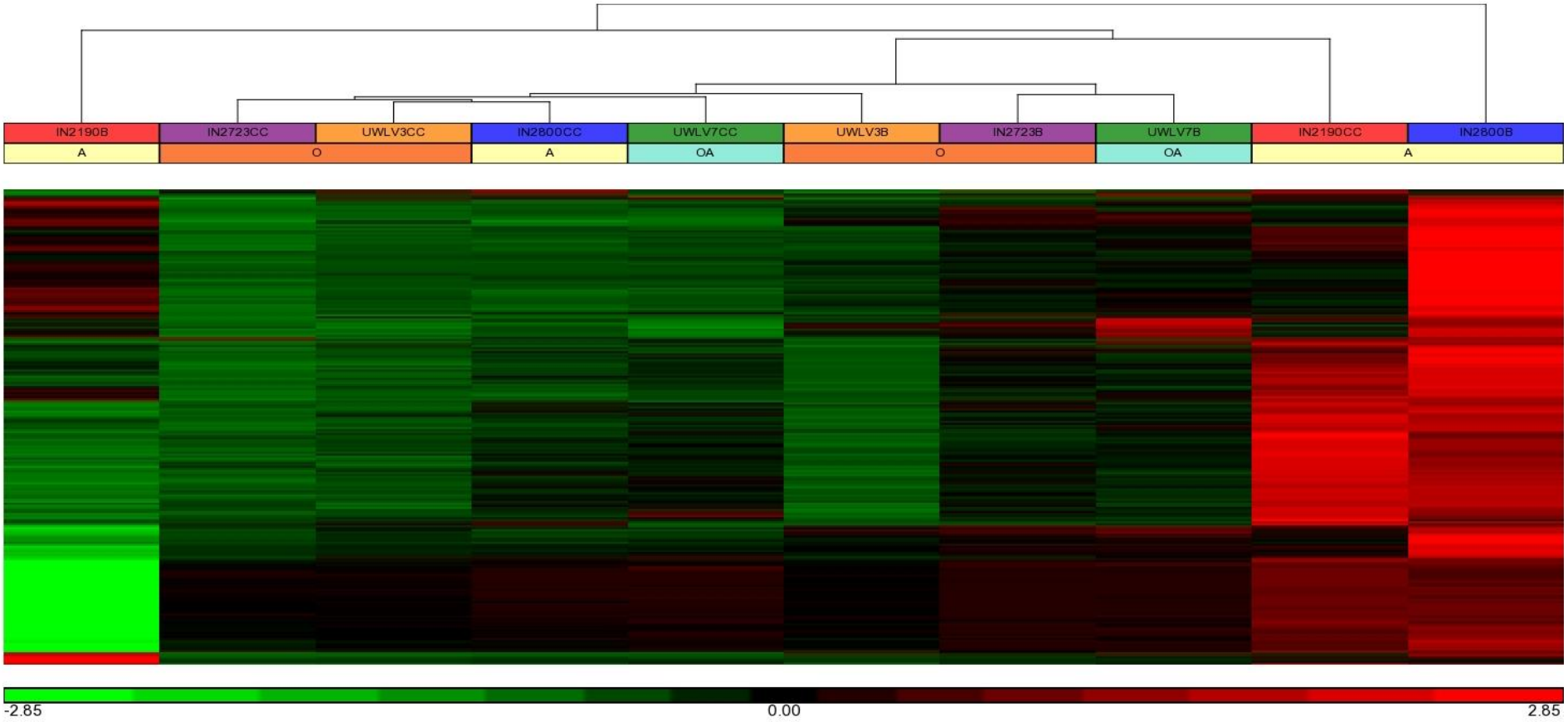

Expression of 1719 miRNAs shown in 5 paired samples using Partek Genomics Suite. Red colour represents high levels of miRNA expression and green colour represents low levels of miRNA expression in the tumour. B – biopsy tissue, CC – cell culture.

Figure 6.10 PCA of biopsy samples and their derived cell cultures

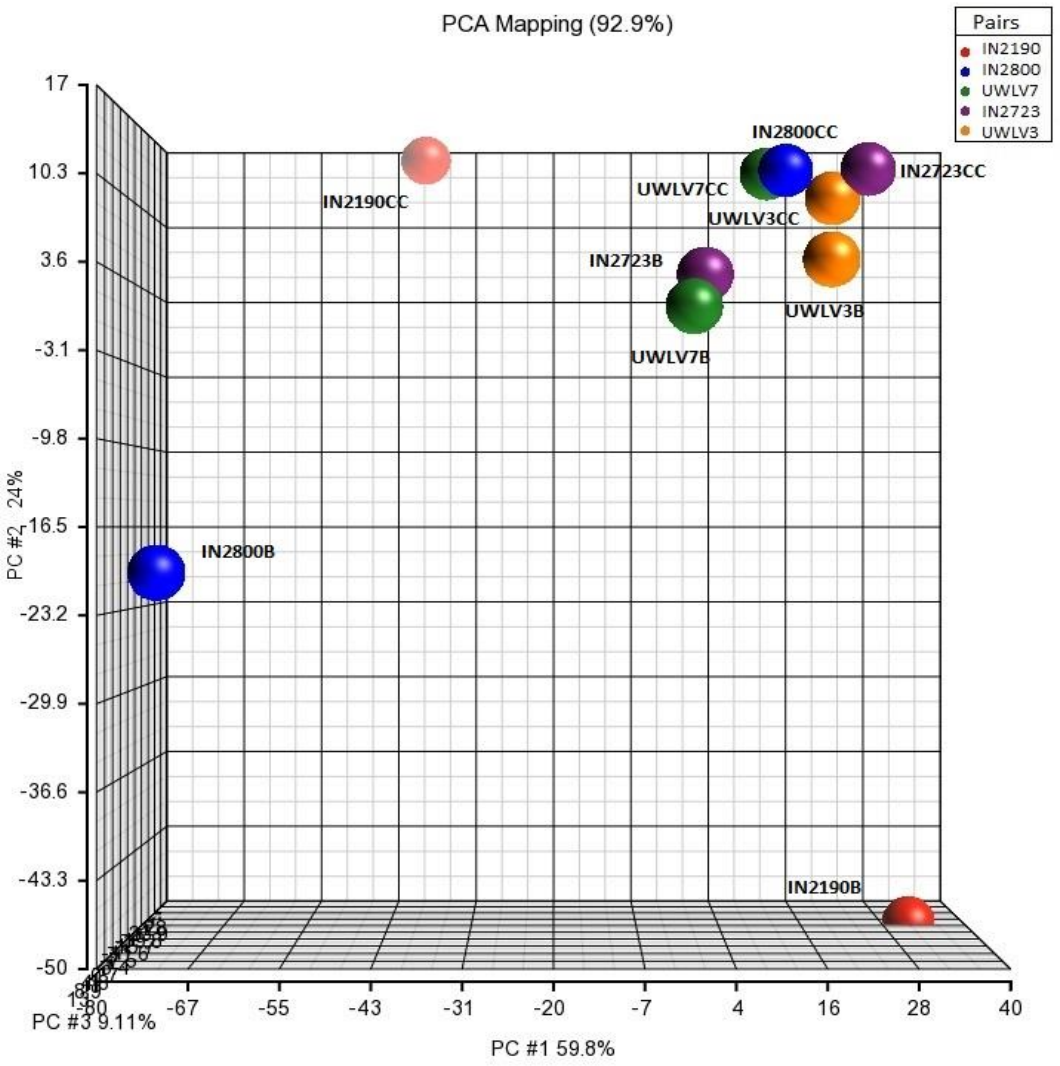

The results are depicted 3-dimensionally with PC1 (59.8%), PC2 (24%) and PC3 (9.11%) as the X, Y and Z axes, respectively. Biopsy and short-term cell culture for the same tumour are shown by the same colour. B, biopsy tissue; CC, cell culture.

6.5.2 Tumour sample IN2190

There were 86 differentially expressed miRNAs (> 2-fold change) between the biopsy and cell culture of which 38 were upregulated and 48 were downregulated in the cell culture compared to its biopsy tissue. The 10 most differentially expressed miRNAs are listed in Table 6.12 with the miRNA targets and deregulated pathways.

6.5.3 Tumour sample IN2800

In tumour sample IN2800, there were 249 differentially expressed miRNAs with > 2-fold change in expression; 4 miRNAs were upregulated and 245 were downregulated in the cell culture compared to its biopsy tissue. The 10 most differentially expressed miRNAs are listed in Table 6.13 with the targets and pathways.

6.5.4 Tumour sample UWLV7

There were 82 differentially expressed miRNAs (> 2-fold change) identified between tumour biopsy UWLV7 and its derivative culture with 3 upregulated miRNAs and 79 downregulated miRNAs in the cell culture compared to its biopsy tissue. The 10 most differentially expressed miRNAs are listed in Table 6.14 with the targets and pathways.

6.5.5 Tumour sample IN2723

A total of 64 miRNAs with differential expression (> 2-fold change) were identified, of which 1 was upregulated and 63 were downregulated in the cell culture compared to its

biopsy tissue. The 10 most differentially expressed miRNAs were listed in Table 6.15 with the targets and pathways.

6.5.6 Tumour sample UWLV3

In tumour sample UWLV3, 34 differentially expressed miRNAs with > 2-fold change in expression were identified, of which 10 were upregulated and 24 were downregulated in the cell culture compared to its biopsy tissue. The 10 most differentially expressed miRNAs were listed in Table 6.16 with the targets and pathways.

Table 6.12 The 10 most differentially expressed miRNAs in IN2190 pair with the predicted targets and pathways.

miRNA	Fold change (CC vs B)[a]	Target	Pathway
miR-4787-3p	17.8897	*GABRA4, SNX22, SLC25A13, IMPAD1, USP29, PCBP2*	Inositol phosphate metabolism, Synaptic vesicle cycle, Phosphatidylinositol signalling system, Sulfur metabolism, SNARE interactions in vesicular transport
miR-4762-5p	15.3156	*ARMC8, EIF2C1, HOOK3, FAT1, NUCKS1, TRAM1, FGF7, NLK, TRA2B, PTBP3*	Spliceosome, mRNA surveillance pathway, Insulin signalling pathway, Neurotrophin signalling pathway, Lysine degradation
miR-21	10.2508	*YOD1, KRIT1, WTH3DI, GPR64, PLEKHA1, SKP2, FBXO11, MALT1, PELI1, PBRM1*	Cytokine-cytokine receptor interaction, TGF-beta signalling pathway, MAPK signalling pathway, Melanoma
miR-636	9.84185	*AP3M1, ONECUT2, ARID4B, PKN2, PHC3, HAPLN1, RUNX2, VSIG10, ABCA13, RPS6KA3*	Adipocytokine signalling pathway, RNA degradation, PI3K-Akt signalling pathway, Vascular smooth muscle contraction, Insulin signalling pathway
miR-4733-3p	9.55126	*CHMP1A, DGAT1, SLC46A2, LARP1, RIMS3, DDX18, FKBP15, CCL8, MIS12, PPP6R2*	ABC transporters, Pathogenic Escherichia coli infection, Gap junction, ECM-receptor interaction, Cyanoamino acid metabolism
miR-4787-5p	-11.2118	*NFIX, TMEM2, SURF4, FGF18, PLK4, RBM41, DNAJB5, SPTSSA, FAM64A, HIPK2*	Propanoate metabolism, Glioma, Melanoma, Prostate cancer, PI3K-Akt signalling pathway
miR-122	-11.7277	*KCNN3, ATF6, HNRNPU, CCNG1, SPOCK2, NICN1, RFXAP, RBM43, ANKRD13C, RBMS2*	Hematopoietic cell lineage, T cell receptor signalling pathway, Neuroactive ligand-receptor interaction
miR-720	-24.7896	*GALR1, TUSC1, DNMT3A, SPTLC3, TMEM200B, NHSL1, NANOG, FBXO24, CYP4F11, FEZ1*	Nicotine addiction, Other types of O-glycan biosynthesis, Synaptic vesicle cycle, Taste transduction, Endocrine and other factor-regulated calcium reabsorption
miR-9	-29.6037	*POU2F1, ONECUT2, PRTG, LYVE1, SH3TC2, MDGA2, TNC, SLC35B3, PRDM6, STARD13*	Cell adhesion molecules (CAMs), Axon guidance, Cytokine-cytokine receptor interaction, Pathways in cancer, Tight junction
miR-4723-5p	-41.1579	*MECP2, PLXNA4, PPP1R9B, SNX29, PACS1, NAT16, SLC28A1, CREB1, MUC3A, FOXE1*	Glycosaminoglycan biosynthesis - chondroitin sulphate, Tight junction, Circadian rhythm, Synaptic vesicle cycle, Cell adhesion molecules (CAMs)

[a] CC, cell culture; B, biopsy tissue. Gene targets and pathways that were common between the miRNAs are highlighted in different coloured text.

Table 6.13 The 10 most differentially expressed miRNAs identified in IN2800 pair with the predicted targets and pathways.

miRNA	Fold change (CC vs B)[a]	Target	Pathway
miR-21	5.87631	*YOD1, KRIT1, WTH3DI, GPR64, PLEKHA1, SKP2, FBXO11, MALT1, PELI1, PBRM1*	Cytokine-cytokine receptor interaction, TGF-beta signalling pathway, MAPK signalling pathway, Melanoma
miR-27a	2.50142	*CUX1, INO80D, FECH, PCDHB4, KCTD20, SAMD12, CD1C, PSMA1, PIGK, EIF1AX*	Vasopressin-regulated water reabsorption, Cell adhesion molecules (CAMs), Leukocyte transendothelial migration, Intestinal immune network for IgA production, Base excision repair
miR-142-3p	2.42483	*WASL, TSEN34, TAB2, BOD1, DCUN1D4, ASH1L, FAM208B, CLTA, CASK, GAB1*	Axon guidance, Dopaminergic synapse, Pancreatic secretion, Pancreatic cancer, NF-kappa B signalling pathway
miR-24	2.14467	*SRSF11, FMR1, HNRNPU, IGIP, SRPK2, ACTR2, CALD1, TM9SF3, TNFAIP8, LAMTOR3*	Glycerophospholipid metabolism, MAPK signalling pathway, Osteoclast differentiation, Pathways in cancer, Colorectal cancer
miR-3658	-26.3272	*AEBP2, DCUN1D5, LPP, MCTS1, GNB4, LRP6, TMED5, UBE2K, SMAD5, UHMK1*	TGF-beta signalling pathway, GABAergic synapse, Wnt signalling pathway, Prostate cancer, Chronic myeloid leukemia
miR-4526	-26.4359	*MIER1, FNBP1L, RIN2, FAM104B, CSF2RB, ATF3, RORA, RAP1A, MGAT4A, ATXN7*	Neurotrophin signalling pathway, Caffeine metabolism, Propanoate metabolism, Glioma, ErbB signalling pathway
miR-4661-5p	-26.9255	*FRS2, LCORL, DNALI1, HDGFRP3, DEPDC1B, JAG1, NFIB, WEE1, CCNB1, PRKAA1*	Synaptic vesicle cycle, Cell cycle, SNARE interactions in vesicular transport, Spliceosome, mRNA surveillance pathway
miR-4481	-27.777	*GNG13, GMEB1, VAPA, EZH1, ARF3, AP1G1, FZD3, APOBEC3H, DHRS3, PHYHIP*	Circadian entrainment, Cholinergic synapse, Arginine and proline metabolism, Taste transduction
miR-323b-5p	-47.1917	*TAF5, STK38, PIK3R3, BTAF1, JAK1, LMAN1, SERF2, GLRA2, TBC1D23, SLC39A9*	Metabolism of xenobiotics by cytochrome P450, D-Glutamine and D-glutamate metabolism, Phenylalanine, tyrosine and tryptophan biosynthesis, Proximal tubule bicarbonate reclamation, Proteasome
miR-122	-51.9519	*KCNN3, ATF6, HNRNPU, CCNG1, SPOCK2, NICN1, RFXAP, RBM43, ANKRD13C, RBMS2*	Hematopoietic cell lineage, T cell receptor signalling pathway, Neuroactive ligand-receptor interaction

[a] CC, cell culture; B, biopsy tissue. Gene targets and pathways that were common between the miRNAs are highlighted in different coloured text.

Table 6.14 The 10 most differentially expressed miRNAs identified in UWLV7 pair with the predicted targets and pathways.

miRNA	Fold change (CC vs B)[a]	Target	Pathway
miR-3978	5.80892	*SV2B, ONECUT2, FCHO2, OSBP2, SNAP25, RDX, GATM, KLF8, FAR1, HGSNAT*	Hematopoietic cell lineage, Glycerophospholipid metabolism, Endocrine and other factor-regulated calcium reabsorption, PI3K-Akt signalling pathway, Acute myeloid leukemia
miR-432*	3.97517	*GSG1L, FAM169B, TLK2, TM9SF3, LYST, PRKCA, ATL2, YPEL2, CDH6, SLC8A1*	Pathogenic Escherichia coli infection, Gap junction, ABC transporters, Regulation of actin cytoskeleton, Arrhythmogenic right ventricular cardiomyopathy (ARVC)
miR-4418	2.43276	*ORAI2, PRR11, N4BP1, VPS53, TNRC6B, FAM168B, OPA3, CLSPN, RAB11A, GNL3L*	Other glycan degradation, mTOR signalling pathway, Biosynthesis of unsaturated fatty acids, Oocyte meiosis, D-Glutamine and D-glutamate metabolism
miR-30c	-5.59553	*TNRC6A, CELSR3, MIER3, EED, LHX8, PPARGC1B, PHTF2, SCN2A, ANKRA2, RTKN2*	Neuroactive ligand-receptor interaction, Phosphatidylinositol signalling system, Dilated cardiomyopathy, Axon guidance, Focal adhesion
miR-4302	-5.83664	*FGD6, KCNK10, RAB31, QTRTD1, NFAT5, DDX46, NR1D2, AP2B1, KCNK3, PREPL*	Pathways in cancer, Acute myeloid leukemia, Chronic myeloid leukemia, B cell receptor signalling pathway, ErbB signalling pathway
miR-9	-8.18236	*POU2F1, ONECUT2, PRTG, LYVE1, SH3TC2, MDGA2, TNC, SLC35B3, PRDM6, STARD13*	Cell adhesion molecules (CAMs), Axon guidance, Cytokine-cytokine receptor interaction, Pathways in cancer, Tight junction
miR-124	-8.31175	*TXNRD1, SNX2, RSU1, FLRT3, DSCR6, COPS2, TMEM56, STRBP, UHRF1, ATPBD4*	Hypertrophic cardiomyopathy (HCM), Neurotrophin signalling pathway, Dilated cardiomyopathy, Arrhythmogenic right ventricular cardiomyopathy (ARVC), Axon guidance
miR-323b-5p	-14.5479	*TAF5, STK38, PIK3R3, BTAF1, JAK1, LMAN1, SERF2, GLRA2, TBC1D23, SLC39A9*	Metabolism of xenobiotics by cytochrome P450, D-Glutamine and D-glutamate metabolism, Phenylalanine, tyrosine and tryptophan biosynthesis, Proximal tubule bicarbonate reclamation, Proteasome
miR-449c	-21.9275	*NUP50, STMN2, CDK19, ODZ1, CREB1, PAPOLA, MAPK1IP1L, ACTL6A, TMEM48, STK38L*	Hepatitis B, Phosphatidylinositol signalling system, ErbB signalling pathway, Salmonella infection, Inositol phosphate metabolism
miR-191	-22.5432	*TMOD2, DDHD1, SLC25A24, TAF5, MAPK9, AMMECR1L, NRCAM, ORC3, SPO11, EHHADH*	Calcium signalling pathway, Glioma, Long-term potentiation, Long-term depression, Melanoma

[a] CC, cell culture; B, biopsy tissue. Common gene targets and pathways between the miRNAs are highlighted in different coloured text.

Table 6.15 The 10 most differentially expressed miRNAs identified in IN2723 pair with the predicted targets and pathways.

miRNA	Fold change (CC vs B)[a]	Target	Pathway
miR-21	4.55833	*YOD1, KRIT1, WTH3DI, GPR64, PLEKHA1, SKP2, FBXO11, MALT1, PELI1, PBRM1*	Cytokine-cytokine receptor interaction, TGF-beta signalling pathway, MAPK signalling pathway, Melanoma
miR-3650	-4.72264	*KCNIP1, CREB3, ECM1, GRIP2, GEMC1, RPP14, ABCB5, TSC1, KPNB1, CSMD2*	Renal cell carcinoma, Nicotinate and nicotinamide metabolism, mTOR signalling pathway
miR-4526	-5.30246	*MIER1, FNBP1L, RIN2, FAM104B, CSF2RB, ATF3, RORA, RAP1A, MGAT4A, ATXN7*	Neurotrophin signalling pathway, Caffeine metabolism, Propanoate metabolism, Glioma, ErbB signalling pathway
miR-4787-3p	-5.33518	*GABRA4, SNX22, SLC25A13, IMPAD1, USP29, PCBP2*	Inositol phosphate metabolism, Synaptic vesicle cycle, Phosphatidylinositol signalling system, Sulfur metabolism, SNARE interactions in vesicular transport
miR-181a*	-5.49688	*ALDH18A1, ATP13A4, ALDH6A1, NIPA2, RIBC1, SLC20A2, CFL2, RHOBTB1, HIF0, AP1S3*	Pathways in cancer, Acute myeloid leukemia, Chronic myeloid leukemia, Colorectal cancer, Prostate cancer
miR-3658	-5.83977	*AEBP2, DCUN1D5, LPP, MCTS1, GNB4, LRP6, TMED5, UBE2K, SMAD5, UHMK1*	TGF-beta signalling pathway, GABAergic synapse, Wnt signalling pathway, Prostate cancer, Chronic myeloid leukemia
miR-9	-6.7221	*POU2F1, ONECUT2, PRTG, LYVE1, SH3TC2, MDGA2, TNC, SLC35B3, PRDM6, STARD13*	Cell adhesion molecules (CAMs), Axon guidance, Cytokine-cytokine receptor interaction, Pathways in cancer, Tight junction
miR-4481	-6.75082	*GNG13, GMEB1, VAPA, EZH1, ARF3, AP1G1, FZD3, APOBEC3H, DHRS3, PHYHIP*	Circadian entrainment, Cholinergic synapse, Arginine and proline metabolism, Taste transduction
miR-191	-10.2189	*TMOD2, DDHD1, SLC25A24, TAF5, MAPK9, AMMECR1L, NRCAM, ORC3, SPO11, PWWP2A*	Calcium signalling pathway, Glioma, Long-term potentiation, Long-term depression, Melanoma
miR-122	-14.2231	*MBTD1, FAM178A, COL11A2, CNO, HAPLN1, FGFR4, UBE2I*	Hematopoietic cell lineage, T cell receptor signalling pathway, Neuroactive ligand-receptor interaction

[a] CC, cell culture; B, biopsy tissue. Common pathways between the miRNAs are highlighted in different coloured text.

Table 6.16 The 10 most differentially expressed miRNAs identified in UWLV3 pair with the predicted targets and pathways.

miRNA	Fold change (CC vs B)[a]	Target	Pathway
miR-21	9.17437	*YOD1, KRIT1, WTH3DI, GPR64, PLEKHA1, SKP2, FBXO11, MALT1, PELI1, PBRM1*	Cytokine-cytokine receptor interaction, TGF-beta signalling pathway, MAPK signalling pathway, Melanoma
miR-4418	4.41772	*ORAI2, PRR11, N4BP1, VPS53, TNRC6B, FAM168B, OPA3, CLSPN, RAB11A, GNL3L*	Other glycan degradation, mTOR signalling pathway, Biosynthesis of unsaturated fatty acids, Oocyte meiosis, D-Glutamine and D-glutamate metabolism
miR-27a	3.06853	*CUX1, INO80D, FECH, PCDHB4, KCTD20, SAMD12, CD1C, PSMA1, PIGK, EIF1AX*	Vasopressin-regulated water reabsorption, Cell adhesion molecules (CAMs), Leukocyte transendothelial migration, Intestinal immune network for IgA production, Base excision repair
miR-142-3p	2.8793	*WASL, TSEN34, TAB2, BOD1, DCUN1D4, ASH1L, FAM208B, CLTA, CASK, GAB1*	Axon guidance, Dopaminergic synapse, Pancreatic secretion, Pancreatic cancer, NF-kappa B signalling pathway
miR-432*	2.62519	*GSG1L, FAM169B, TLK2, TM9SF3, LYST, PRKCA, ATL2, YPEL2, CDH6, SLC8A1*	Pathogenic Escherichia coli infection, Gap junction, ABC transporters, Regulation of actin cytoskeleton, Arrhythmogenic right ventricular cardiomyopathy (ARVC)
miR-26a	-3.67749	*MAN1A2, HS6ST3, ENPP4, SLC30A5, CALCOCO2, TACR1, CDK6, SLC6A14, GJB2, SMARCE1*	GnRH signalling pathway, Neurotrophin signalling pathway
miR-449c	-4.42601	*NUP50, STMN2, CDK19, ODZ1, CREB1, PAPOLA, MAPK1IP1L, ACTL6A, TMEM48, STK38L*	Hepatitis B, Phosphatidylinositol signalling system, ErbB signalling pathway, Salmonella infection, Inositol phosphate metabolism
miR-122	-4.67672	*KCNN3, ATF6, HNRNPU, CCNG1, SPOCK2, NICN1, RFXAP, RBM43, ANKRD13C, RBMS2*	Hematopoietic cell lineage, T cell receptor signalling pathway, Neuroactive ligand-receptor interaction
miR-9	-6.58838	*POU2F1, ONECUT2, PRTG, LYVE1, SH3TC2, MDGA2, TNC, SLC35B3, PRDM6, STARD13*	Cell adhesion molecules (CAMs), Axon guidance, Cytokine-cytokine receptor interaction, Pathways in cancer, Tight junction
miR-191	-10.4976	*TMOD2, DDHD1, SLC25A24, TAF5, MAPK9, AMMECR1L, NRCAM, ORC3, SPO11, EHHADH*	Calcium signalling pathway, Glioma, Long-term potentiation, Long-term depression, Melanoma

[a] CC, cell culture; B, biopsy tissue. Common pathways between the miRNAs are highlighted in different coloured text.

Interestingly, a large proportion of differentially expressed miRNAs in 4/5 pairs (IN2800, UWLV7, IN2723 and UWLV3) were downregulated in the cell culture as compared to the biopsy tissue. This may be due to the cell culture conditions not replicating the tumour environment *in vivo*. IN2190 (A) was the only pair that had a relatively small difference in the number of upregulated and downregulated miRNAs in the cell culture compared to its biopsy tissue. The largest changes in fold expression were identified in the A pairs followed by OA and O pairs respectively.

Results from the hierarchical clustering, PCA analysis and individual comparisons between tumour biopsies and their derived cultures suggest that O and OA cell cultures are more representative of the biopsy tissues than the A cell cultures with regard to miRNA expression profiles.

The most common miRNAs amongst the pairwise comparisons were miR-9, miR-21 and miR-122 present in 80% of the pairs followed by miR-191 present in 60% of the pairs. miR-9 was downregulated in the cell culture of four pairs (IN2190, UWLV7, IN2723 and UWLV3). miR-21 was upregulated in the cell culture of four pairs (IN2190, IN2800, IN2723 and UWLV3). miR-122 was downregulated in the cell culture of four pairs (IN2190, IN2800, IN2723 and UWLV3). miR-191 was downregulated in the cell culture of three pairs (UWLV7, IN2723 and UWLV3). Histology comparison revealed miR-21 and miR-122 as the most common miRNAs in A pairs (IN2190, IN2800) and miR-9, miR-21, miR-122 and miR-191 in O pairs (IN2723, UWLV3). Amongst all the pairs, the most common pathways were melanoma and cytokine-cytokine receptor interactions present in 60% of the pairs, axon guidance, TGF-β signalling pathway, pathways in cancer and CAMs present in 40% of the pairs.

The five paired samples had 11 common miRNAs with differential expression, identified by a Venn diagram (Figure 6.11). Of the 11 miRNAs, 7 miRNAs (mir-4456, miR-4534, miR-29b, miR-2113, miR-3650, miR-9 and miR-191) were downregulated in all the cell cultures, 3 miRNAs (miR-4733-3p, miR-4740-5p and miR-4748) were downregulated in 80% and 1 miRNA (miR-21) was downregulated in 20% of cell cultures compared to the biopsy tissues. The common miRNAs are detailed in Table 6.17 with percentage of differential expression in the pairs.

Figure 6.11 Venn diagram showing unique and common miRNAs in all pairs

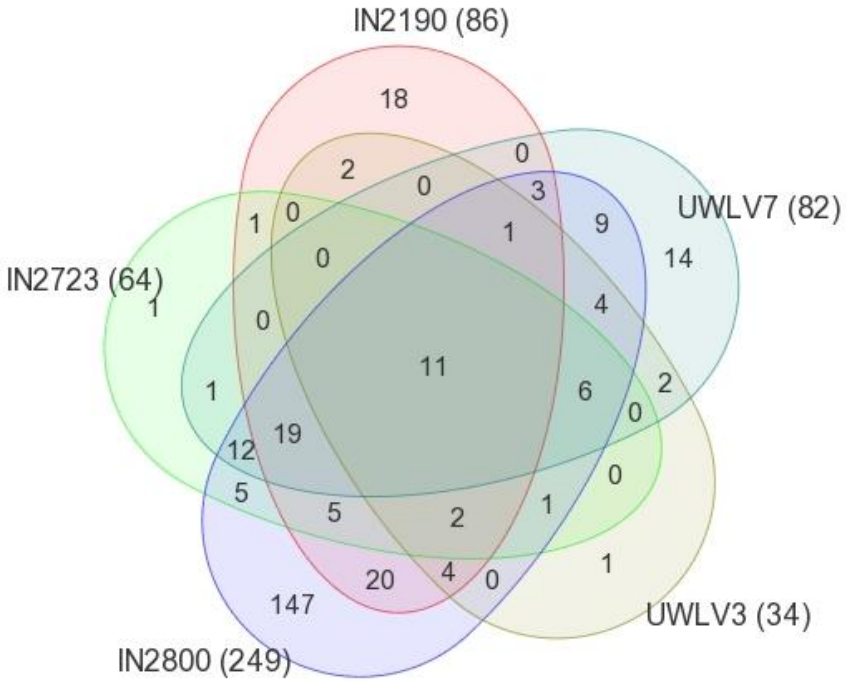

Using Partek Genomics Suite, paired samples were compared and differentially expressed miRNAs were identified with ≥ 2-fold change in expression and significance of $p < 0.05$ by ANOVA. IN2190 pair had 86 differentially expressed miRNAs, UWLV7 had 82 miRNAs, UWLV3 had 34 miRNAs, IN2800 had 249 miRNAs and IN2723 had 64 miRNAs that were differentially expressed. Eleven common differentially expressed miRNAs were identified among the five paired samples.

Table 6.17 Common miRNAs in the biopsy/cell culture pairs with percentage of differential expression.

miRNA	Upregulation (%)[a]		Downregulation (%)		Target	Pathway
	CC	B	CC	B		
miR-4456	0	100	100	0	*ERC1, RND2, FAM101B, NACC1, CNR1, RANBP10, DNAJC6, PACS1, GCC2, MBL2*	Axon guidance, N-Glycan biosynthesis, Histidine metabolism, Glycosylphosphatidylinositol (GPI)-anchor biosynthesis, Cyanoamino acid metabolism
miR-4534	0	100	100	0	*OLA1, GNG13, SPN, LRRTM2, NAB1, KLK10, CHRNB2, PDP2, PLCXD1, RBBP5*	Glutamatergic synapse, Taste transduction, Pathogenic Escherichia coli infection, Oocyte meiosis, Circadian entrainment
miR-4740-5p	20	80	80	20	*PDK3, THSD4, STAM2, ENOPH1, AGAP1, RBMS3, RAG1, MSR1,SPTLC2, ARAP2*	Glycosphingolipid biosynthesis – lacto and neolacto series, Morphine addiction, Circadian entrainment, GABAergic synapse, SNARE interactions in vesicular transport
miR-29b	0	100	100	0	*USP28, NEUROD1, ZDHHC5, LIN9, TNPO3, CLEC2B, WDR26, SNX30, SLC30A7, PROS1*	ECM-receptor interaction, Small cell lung cancer, Focal adhesion, Axon guidance, Pathways in cancer
miR-2113	0	100	100	0	*PIK3C2A, COL4A3BP, CRH, ELL2, NCBP1, CNTLN, MAP4K3, CASK, SNTB2, CCDC6*	Notch signalling pathway, Pathways in cancer, Renal cell carcinoma, Long-term potentiation, Adherens junction
miR-4748	20	80	80	20	*TSFM, PPP2R5A, KALRN, CTSL2, GABRG2, TMEM106B, SNF8, ABCD4, GM2A, FERMT1*	Colorectal cancer, Endometrial cancer, Epstein-Barr virus infection, B cell receptor signalling pathway
miR-3650	0	100	100	0	*RTN41P1, CDK14, ABO, SH3BP2, DCLRE1C, ELN, STEAP2, EIF2C3, BNC2, HDX*	Pathways in cancer, Prostate cancer, Pancreatic cancer, Adherens junction, MAPK signalling pathway
miR-4733-3p	20	80	80	20	*CHMP1, DGAT1, LARP1, RIMS3, FKBP15, DDX18, CCL8, MIS12, PPP6R2, ABHD4*	ABC transporters, Pathogenic Escherichia coli infection, Gap junction, ECM-receptor interaction, Cyanoamino acid metabolism
miR-21	80	20	20	80	*YOD1, KRIT1, WTH3DI, GPR64, PLEKHA1, SKP2, FBXO11, MALT1, PELI1, PBRM1*	Cytokine-cytokine receptor interaction, TGF-beta signalling pathway, MAPK signalling pathway, Melanoma
miR-9	0	100	100	0	*POU2F1, ONECUT2, PRTG, LYVE1, SH3TC2, MDGA2, TNC, SLC35B3, PRDM6, STARD13*	Cell adhesion molecules (CAMs), Axon guidance, Cytokine-cytokine receptor interaction, Pathways in cancer, Tight junction
miR-191	0	100	100	0	*TMOD2, DDHD1, SLC25A24, TAF5, MAPK9, NRCAM, ORC3, EHHADH, SATB, CERS6*	Phosphatidylinositol signalling system, GnRH signalling pathway, Adherens junction, Cytokine-cytokine receptor interaction, Cell adhesion molecules (CAMs)

[a] CC, cell culture; B, biopsy tissue. Common pathways between the miRNAs are highlighted in different coloured text.

6.6 PROTEIN EXPRESSION OF GENETIC MARKERS IN BIOPSY TISSUES AND CELL CULTURES

IHC was performed on four biopsy/cell culture pairs (IN2190 (A), IN2800 (A), UWLV7 (OA) and UWLV3 (O)) and four additional cell cultures for which no further biopsy tissue was available for analysis (IN118/81 (A), IN1853 (A), IN2723 (O), IN2184 (AO)) using antibodies against GFAP, IDH1 R132H mutant protein, Nestin, Ki-67, p53, CD34 and EMA and the results are summarised in Table 6.18. There was no staining for GFAP, IDH1 R132H mutant protein, p53, CD34 and EMA in any sample. Positive cytoplasmic staining was detected for Nestin in all 8 cultures and 2 biopsy samples (UWLV7 and UWLV3). For Ki-67, the astrocytoma cell culture IN118/81CC showed the highest protein expression at 67%, considerably greater than any other sample. This was surprising as this culture had the longest doubling time. The levels of Ki67 staining between the paired biopsy/cell culture samples were very similar for IN2190 (21% and 22% respectively) and UWLV7 (14% and 13%, respectively). In the UWLV3 biopsy, 12% of cells stained positive for Ki67 although no signal was detected in the UWLV3 cell culture. Ki67 expression was detected in less than 1% of cells of the IN2800 biopsy and again, no signal was detected in the IN2800 cell culture or the unpaired IN1853 cell culture. The remaining 2 unpaired cell cultures, IN2723 and IN2184 had very low levels of Ki-67 expression (< 1%). Examples for Nestin and Ki-67 in both cell culture and biopsy tissue are shown in Figure 6.12.

Table 6.18 Expression of nestin and Ki67 in LGG determined by IHC

Sample[a]	Grade	Histology[b]	Nestin[c]	Ki67 (%)[d]
IN2190B	II	A	0	21
IN2190CC			c2	22
IN2800B	II	A	0	<1
IN2800CC			c2	0
UWLV7B	II	OA	c2	14
UWLV7CC			c3	13
UWLV3B	II	O	c1	12
UWLV3CC			c3	0
IN118/81CC	II	A	c3	67
IN1853CC	II	A	c3	0
IN2723CC	II	O	c3	<1
IN2184CC	III	AO	c3	<1

[a] Paired samples of biopsy tissue (B) and cell culture (CC); [b] A, astrocytoma; OA, oligoastrocytoma; O, oligodendroglioma; AO, anaplastic oligodendroglioma; [c] 0: no staining, 1: weak staining, 2: moderate staining, 3: strong staining; c: cytoplasmic; [d] Percentage of cells with staining.

Figure 6.12 Immunohistochemistry staining for cell cultures

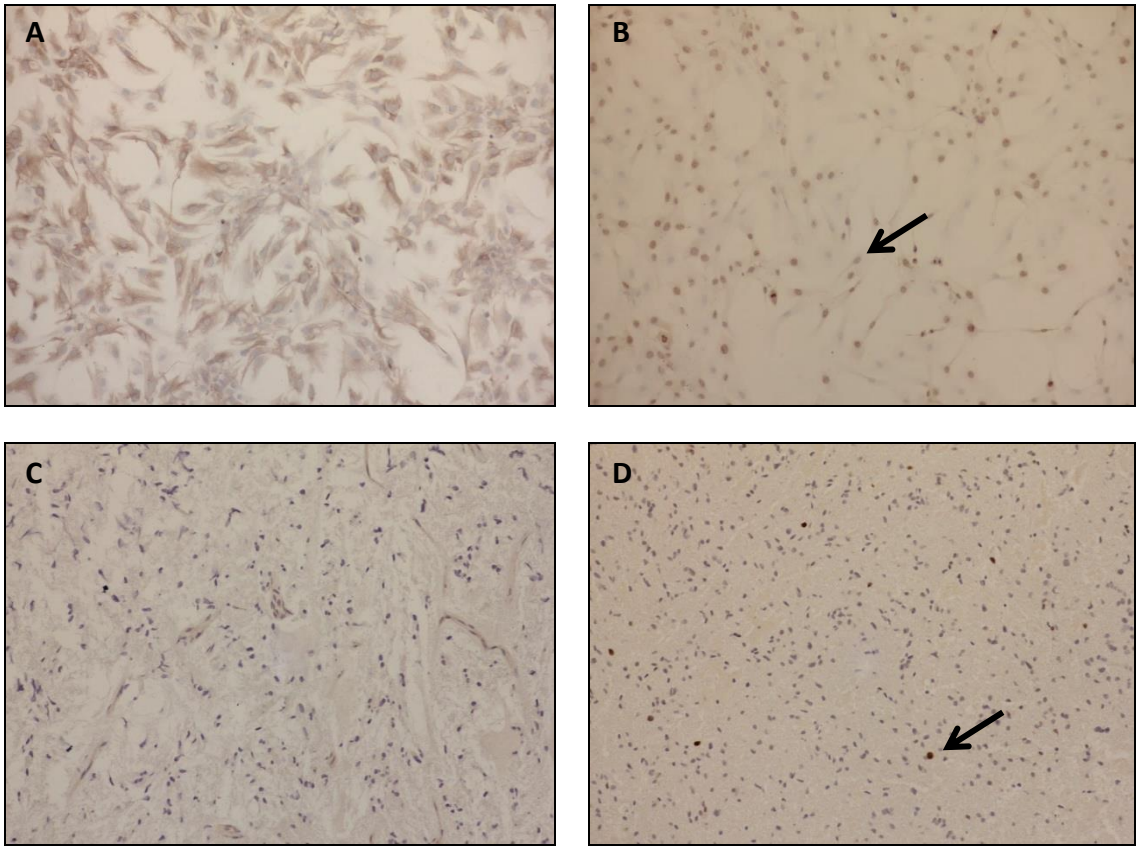

Representative example, photographs were taken at 20x magnification. A: Positive staining for UWLV3CC Nestin (c3), B: IN118/81CC Ki-67 (67%), C: UWLV7B Nestin (c2) and D: UWLV3B Ki-67 (12%). Arrow highlights a positively stained cell.

6.7 CHARACTERISATION OF GROWTH CHARACTERISTICS OF LGG SHORT-TERM CULTURES

Growth curves were generated for six LGG cell cultures, IN118/81 (A), IN1853 (A), IN2190 (A), IN2800 (A), UWLV7 (OA) and UWLV3 (O) in order to calculate doubling times.

Cells were seeded at a plating density of 5000 cells/well for all cell cultures between passages 7-11 as previously described in Chapter 2. The three replicate experiments for each cell culture are shown in the same graph. The passage number at the time of plating increased by 1 for each replicate experiment (Figure 6.13). Cells were grown and counted over a maximum period of 11 days.

Doubling times in hours were calculated for each experiment and the mean ± standard deviation is presented in Table 6.19. The doubling times of the 6 cultures ranged from 27-42 hours with a mean of 33 hours. The slowest and fastest growing cell cultures were IN118/81 and IN2190 respectively. There was no significant difference in the doubling times of the four astrocytoma cultures compared to the two cultures with oligodendroglial differentiation ($p = 0.778$).

Figure 6.13 Growth curves for 6 LGG cell cultures used in this study

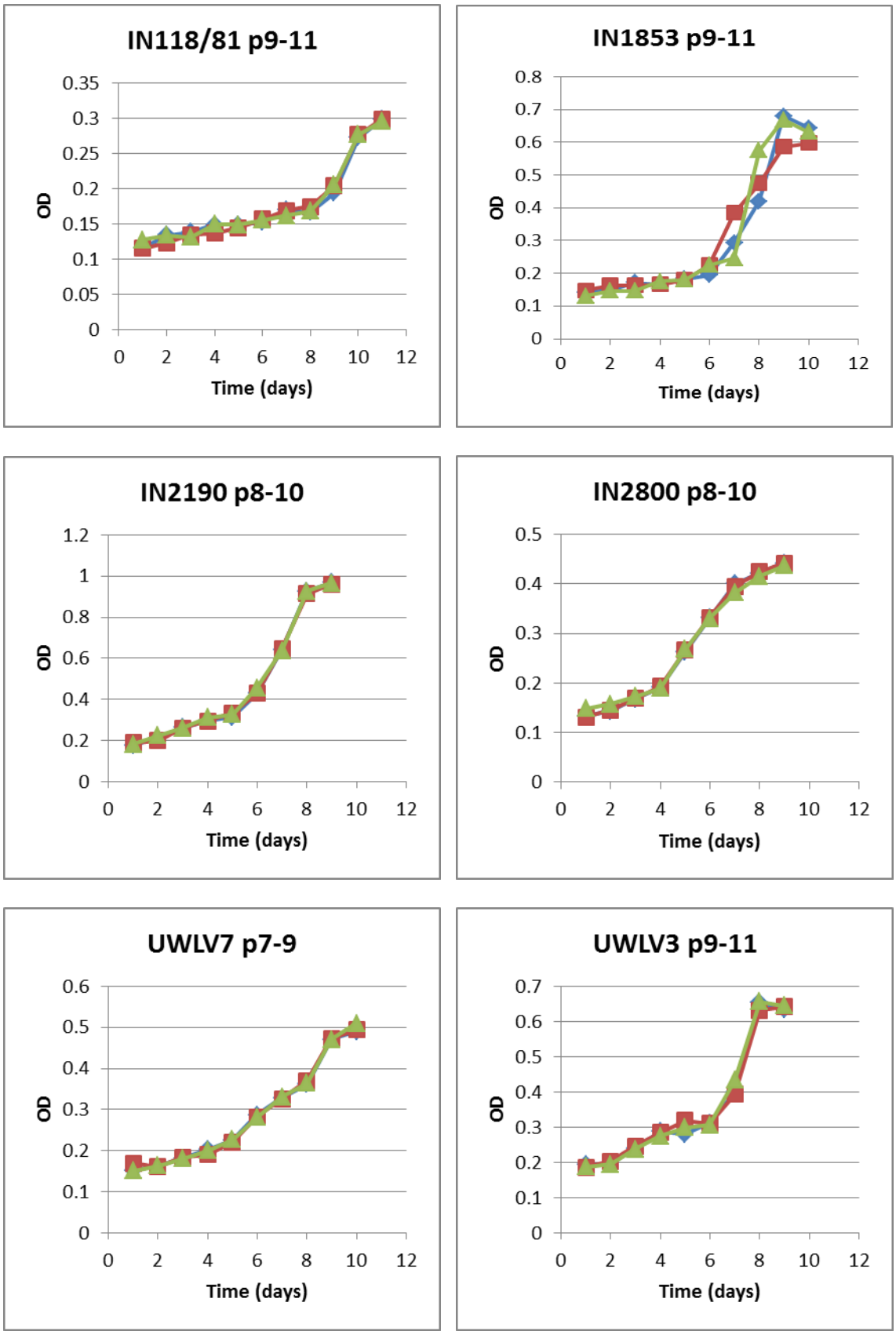

Three replicate experiments for each cell culture have been shown on the same graph. Passages 7-11 used for the six cell cultures.

Table 6.19 Cell cultures used for growth curves

Cell culture	Histology[a]	Mean Doubling time (hrs) ± Standard deviation
IN118/81	A	41.6 ± 0.69
IN1853	A	32.6 ± 0.25
IN2190	A	27.1 ± 0
IN2800	A	31.5 ± 0.17
UWLV7	OA	34.2 ± 0.11
UWLV3	O	29.3 ± 0

[a] A, astrocytoma; OA, oligoastrocytoma; O, oligodendroglioma.

6.8 ABILITY OF LGG CELLS TO GROW ON A FEEDER LAYER

LGG cells were seeded on to a feeder layer of mitomycin-treated 3T3 cells and monitored for growth of colonies. The colony assay was performed for 6 cell cultures, IN118/81 (A), IN1853 (A), IN2190 (A), IN2800 (A), UWLV7 (OA) and UWLV3 (O) and cultures were seeded at passage numbers 4-12. Photographs of each cell culture were taken every 3 days and examples of colonies are shown in Figure 6.14. Colony growth was observed for a maximum period of 24 days, during which time all LGG cultures formed at least one colony. The culture for which least number of colonies was observed was IN118/81, also the culture which had the longest doubling time.

Figure 6.14 Colonies for LGG cells on 3T3 feeder layer

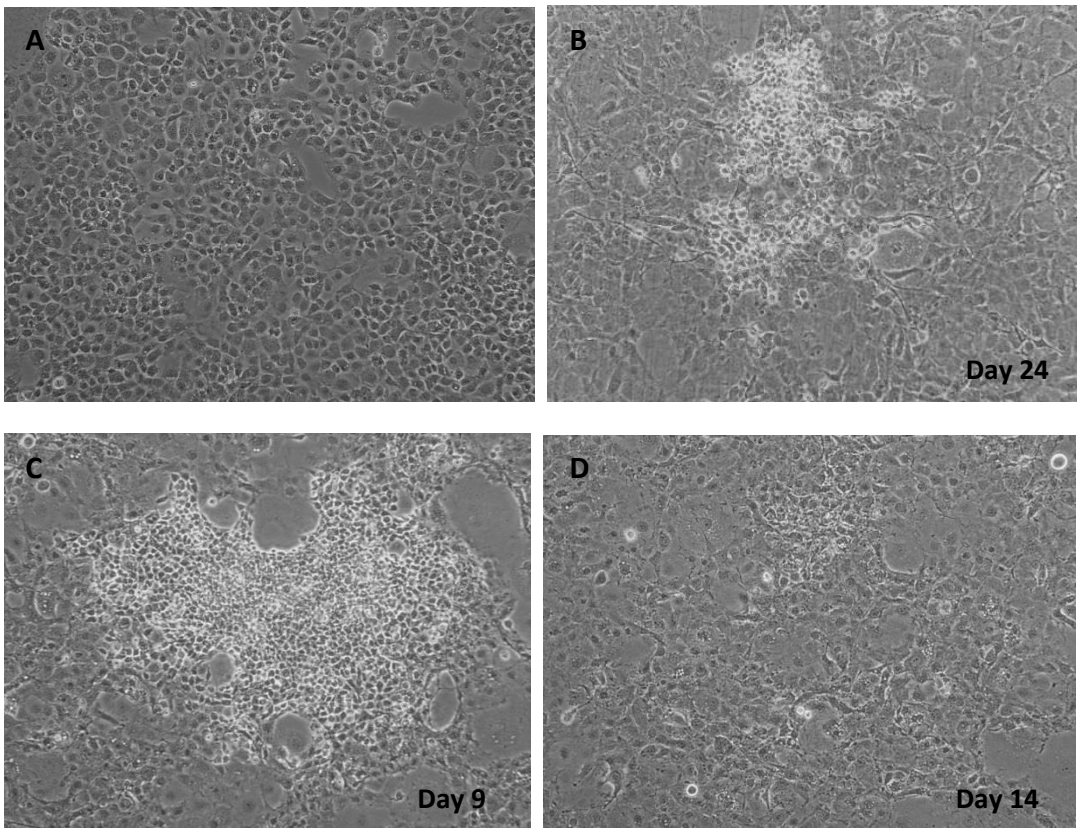

Photographs were taken with 20x magnification. A: 3T3 cells treated with mitomycin; B: IN118/81 p4; C: IN2800 p9 and D: UWLV3 p12.

6.9 DISCUSSION

This chapter describes the characterisation of the short term cell cultures derived from lower grade glioma tumour biopsy tissues. Comparison of paired samples was performed to identify genomic changes and differentially expressed miRNAs within each pair.

6.9.1 *IDH1* mutation *in vitro*

In the first instance, the *IDH* mutation status was established in tumour biopsies and derived cell cultures and *IDH1* mutation was not maintained in any cell culture. The artificial culture conditions select the cell populations that can thrive in the artificial growth environment and hence, the more stable *IDH1* wild type cells grow and the sub-population of cells with *IDH1* mutation are lost. This has been reported by Piaskowski *et al*., (2011) and described previously in Chapter 1. Similarly, *MGMT* methylation (if any) was present in only the biopsy tissues and not in any cell cultures. Serum used in the growth medium was always batch tested and the same batch of serum was used for a year in order to avoid any variability in the cell culture conditions.

Stoczynska-Fidelus *et al*., (2014) established eight glioma 3D cell cultures with *IDH1*-R132H mutation from GBM tumours and analysed *in vitro* senescence. In artificial growth conditions, *IDH1* R132H-positive cells decreased rapidly in number and in GBM, these cells were present up to 4 passages. The remaining *IDH1* R132H-negative cells proliferated efficiently and subsequently, overgrew the *IDH1* R132H-positive cells. 3D culture conditions maintained the *IDH1* R132H mutation for 1-2 months in contrast to monolayer cultures. The lack of proliferation of these *IDH1* R132H-positive

cells was linked with *in vitro* senescence, characterised by SA-β-Gal activity and morphological changes. The observed senescence is induced by the cell culture conditions (both classical and serum-free). *IDH1* R132H-positive cells showed expression of SOX2, a stemness marker.

6.9.2 Copy number analysis

Few studies have reported genomic aberrations in grade II astrocytoma, which were identified using CGH and aCGH analysis. Hirose *et al*., (2003) also used CGH to determine CNAs in 30 grade II astrocytoma tumours. The most frequent aberrations determined were gain on chromosome 7q (12 cases), losses on 19q (7 cases) and 1p (6 cases) and gain on 5p (5 cases). The current study also detected gain on 7q (2 cases) and loss on 19q (2 cases).

Wiltshire *et al*., (2004) used CGH to identify copy number changes in astrocytoma tumours. The authors reported that 10 grade II astrocytoma detected gains and losses on chromosomes 3, 7, 11, 13, 19, 22, X and Y. These results were in line with the present study that showed both gains and losses on chromosomes 3, 7, 13 and 19.

Arslantas *et al*., (2007) identified genomic aberrations using CGH in 18 low-grade astrocytoma and the most frequent were gains on chromosomes 7/7q (5 cases), 8q (4 cases), 20q (3 cases) and loss of 19q (3 cases). Some of these aberrations were also observed in the current study including gains on 7q and 8q. The most frequent aberration in grade II astrocytoma reported in previous studies was gain on 7q which was observed in 50% of the cases in the current study.

It is apparent from this study that the majority of numerical genomic changes present in LGG biopsies are not maintained in short-term cell cultures. The copy number analysis shows difference in the genomic profiles of the paired samples where 75% of the pairs have more aberrations in the biopsy tissues compared to their cell cultures. This indicates that along with *IDH1* mutation and *MGMT* methylation, other genetic features are eliminated due to the cell culture conditions. The total number of aberrations for the AO pair (IN2184) was the highest while OA (UWLV7) and one of the O (UWLV3) had a relatively smaller number. This may contribute to a more aggressive behaviour of the anaplastic tumour although there was only one in the sample cohort. The four astrocytoma pairs were compared to identify common CNAs in biopsy tissues and cell cultures respectively. Similarly, the two oligodendroglioma pairs were compared. The limitation of this comparison was the small number of tumours with same histology.

6.9.3 miRNA expression

In this chapter, comparison of miRNA expression profiles for five paired samples was performed in order to identify changes in each pair. To date, miRNA expression profiles in biopsy and cell culture paired samples have not been investigated. Unsupervised hierarchical clustering shows 4/5 cell cultures forming a cluster and 2/5 biopsy tissues with similar miRNA expression profiles (Figure 6.13). The two remaining biopsy tissues had different profiles from the rest of the samples in the analysis. The expression profiles did not have any significant differences between the *IDH* mutant and *IDH* wild type tumours. This may be due to the small sample size with different histology types. PCA showed UWLV3 pair to have the most similar profile, whereas IN2190 and IN2800 had the most variation in profiles. Following the pairwise comparisons, all

paired samples were combined together resulting in 11 differentially expressed miRNAs that were common among all 5 pairs. None of the miRNAs have been studied in cell cultures and therefore, their role in cell culture and the change in expression levels in both biopsy tissue and cell culture derived from the same tumour needs to be investigated further.

6.9.4 Growth characteristics

The experiments used to assess the growth characteristics show that LGG cells are slow-growing and tumorigenic as they formed colonies on the 3T3 feeder layer. The cell cultures investigated here were grown from the biopsy tissue as described previously in Chapter 2. The profile of the cell cultures studied here represents a cell population of the LGG tumours but the profile may not involve the majority of tumour mass population. This accounts for variation in the biopsy tissues and cell cultures from the same tumour which is illustrated in the array CGH and miRNA expression analysis.

In summary, this study shows that *IDH1* R132H mutation was not maintained in the derived cell cultures established from the *IDH1* R132H mutant biopsy tissues. Also, it was demonstrated that biopsy tissues and short-term cell cultures from the same tumour show variation in genomic and miRNA expression profiles. It was evident from the results in the present study that cells in culture undergo various alterations that influence the genetic profile. Moreover, these findings suggest that a better model needs to be identified in order to study the LGG tumours *in vitro*.

CHAPTER 7

SUMMARY AND FUTURE STUDIES

In this study, mutation status of *IDH1* and *IDH2* and promoter methylation status of *MGMT* was determined in a sample cohort. The key findings were that *IDH1* mutation was an independent favourable prognostic factor for OS and patients with grade II tumours having *IDH1* mutation had a better outcome. *MGMT* promoter methylation was not significantly associated with OS in either of the two grades.

For mutation analysis and clinical correlation, *IDH2* mutant tumours were classed different from *IDH1* mutant tumours. Only one sample carried *IDH2* mutation in the entire cohort used in this study. *IDH1* and *IDH2* mutation do not cause the same effects and little is known about the biological consequences of *IDH2* mutation. *IDH1* mutation was widely studied for correlation with different clinical parameters in this study. For miRNA expression analysis, *IDH1* R132H and *IDH2* mutant tumours were combined and represented as *IDH* mutant tumours. The *IDH2* mutant tumour did not seem to influence the expression profiles of the mutant tumours. A number of studies mentioned in chapters 3 have grouped *IDH1* R132H mutant and *IDH2* mutant tumours for varied analyses including correlation of *IDH* mutation with *MGMT* methylation and association with OS and PFS. The question remains whether *IDH2* mutation is to be grouped with *IDH1* R132H mutation in an analysis. The consequences of *IDH2* mutation need to be investigated further.

MGMT methylation status is heterogeneous in malignant glioma, hence, identifying methylation status of tumours can be challenging. Methodologies such as IHC have limitations that include non-specificity of the antibody, subjective scoring and controls

for positive staining against the antibodies. A study by Quillien *et al*. (2012), compared five methods to analyse *MGMT* comprising of MS-PCR, MethyLight, Pyrosequencing, Methylation-Sensitive High-Resolution Melting and IHC. IHC is used despite its limitations as the technique is inexpensive and widespread with visualisation of tumour cells and significant association of MGMT protein with outcome has been reported for glioma patients. For IHC to be established as a reliable technique, a standard protocol is required which takes into account the staining process including slide pretreatment, antibody type and dilution as well as the method of scoring positively stained cells.

Cell cultures can have further variation growing in a monolayer, as a 2-dimensional culture or as a result of FCS in the growth medium. On the other hand, MS PCR is a more reliable technique and primers for MS PCR can be designed in a way such that all the CpG sites for methylation are covered. In future studies, degree of *MGMT* methylation, protein expression and enzyme activity should all be considered to identify the promoter methylation status of tumours.

There was lack of treatment information across the three centres, from where the samples were collected and the treatment information that was available in some cases did not provide information about the time when treatment was carried out. This needs to be provided in order to correlate treatment regimen, i.e. chemotherapy using TMZ with *MGMT* promoter methylation.

miRNA analysis was carried out to identify a panel of miRNAs that can be used in a clinical trial to predict tumour progression. This can be achieved by comparing miRNAs identified in this study to miRNAs found in previous studies, including any other cancer or disease. Candidate miRNAs could be identified following further pathway analysis that gives common pathways exclusive to each histological group or grade. Correlation

of copy number aberrations and differentially expressed miRNAs should be performed and target genes for these miRNAs should be linked to the array CGH results.

One of the miRNAs, miR-181d has been previously associated with *MGMT* methylation. miR-181d was studied using 82 GBM samples and it was shown that *MGMT* is a downstream target of miR-181d (Zhang *et al*., 2012). The authors transfected a mimic of miR-181d in A1207 GBM cell line that resulted in downregulation of the mRNA and protein expression of MGMT. Expression of miR-181d was found to be inversely correlated with overall survival in a TCGA validation set ($p = 0.001$) analysed by qRT-PCR. miRNAs such as miR-181d that regulate MGMT could be used as a biomarker to predict response of patients to TMZ. In a study by Shi *et al*. (2010), miR-21 was shown to protect U87-MG cells from TMZ induced apoptosis. Conversely, overexpression of miR-21 in U87-MG cells significantly reduced TMZ induced apoptosis ($p < 0.05$). This was induced by decreased ratio of anti-apoptotic proteins, Bax/Bcl-2 and change in caspase-3 activity.

Novel miRNAs were identified when comparing primary tumours of grade II and grade III. These may contribute to a miRNA signature pattern in the two tumour grades. In grade II tumours, OA were more similar to O with regard to expression profiles, while in grade III tumours, AOA were more similar to AA. OA tumours apparently are a mix of cells similar to those present in A and O. The results from this study identified the pattern of miRNA expression for OA and AOA. Also, it was seen that tumour grade greatly influenced the miRNA expression but not *IDH* mutation status.

Tumours of histological types, O and OA are difficult to differentiate between, with the two types having different prognosis and treatment regimes. A new WHO classification system is due to come out next year which will be based on the molecular biology and

not the pathology of glioma. Also, OA histological group will no longer exist as it has been quite controversial. OA is often thought to be a tumour that the pathologists fail to classify under either the A or O histological groups. Biomarkers such as copy number aberrations and differentially expressed miRNAs will be useful for molecular classification of glioma.

This is the first study to compare primary and recurrent paired tumour samples by aCGH and miRNA expression analysis. Copy number analysis showed that all of the recurrent tumours analysed developed additional genomic changes at recurrence. These additional changes may play a role in tumour progression. These included gains on chromosomes 2q, 7q, 10p, 14q, 15q, 16q, whole chromosome 17, 20q and 21q and losses at 1p, 2q, 4q, 6p-q, 9p, 10, 11p, 14q, 15p, 18q, 19 and Xp. As part of the future work, overlapping genes in these genomic regions need to be validated.

It is for the very first time that paired samples of biopsy and derived short-term cell cultures of lower grade diffuse glioma have been investigated. The paired samples were analysed for copy number changes and miRNA expression. 1p/19q loss was detected by aCGH in one AO. Tumour samples were not screened for co-deletion of 1p/19q loss due to limited tissue availability, which was primarily used for *IDH1* and *IDH2* mutation analysis and aCGH analysis. Archival paraffin tissues yielded low quality DNA, suitable only for *IDH* mutation analysis or *MGMT* methylation analysis. Large genomic aberrations present in the tumour biopsy were not maintained in the derived short-term cell culture. The cell cultures contained only small interstitial changes. CNAs maintained in the cell cultures ranged from < 1% to 53%. miRNA expression analysis showed majority of the cell cultures forming a cluster, representing similar expression profiles. Histology may play an important role as the A paired sample had the maximum

number of differentially expressed miRNAs, while O paired sample had the least number of differentially expressed miRNAs. In IHC, it was surprising that two of the *IDH1*-R132H mutant tumours, UWLV3 and UWLV7 did not show any staining for the IDH1 mutant protein. For Ki-67, no protein expression was detected in the three cell cultures, although mitotic figures were distinctly visible when examined under the microscope. The experiments carried out using short-term cell cultures clearly indicate that LGG cell cultures are not a good representative model of the tumour *in vivo*.

In a study by Turcan *et al*. (2012), human astrocytes were transfected with wild type and mutant *IDH1*-R132H using retroviruses. *IDH1* mutant cells were analysed for 50 passages and methylome was collected to identify methylated genes. The present study on the other hand, used monolayer culture to grow cells and *IDH1*-R132H mutation present in the tumour biopsy was not maintained in the corresponding cell culture. Similarly, a previous study by Piaskowski *et al*. (2011) reportedly was unable to maintain *IDH1* mutation in cell cultures as well as in 15 commercially available cell lines. Future work would include developing a 3D cell culture model, retaining the *IDH1*-R132H mutation and using retroviruses and adenoviruses to tranfect cells with *IDH1* mutation to examine the effects of the mutation *in vitro*.

The present study contributes to a better understanding of LGG tumours with regard to the genetic and miRNA profiles as well as developing a good model of LGG tumours for future work. It also imparts information on the tumour progression through primary/recurrent paired tumour samples.

REFERENCES

Alentorn. A., van Thuijl, H.F., Marie, Y., Alshehhi, H., Carpentier, C., Boisselier, B., Laigle-Donadey, F., Mokhtari, K., Scheinin, I., Wesseling, P., Ylstra, B., Capelle, L., Hoang-Xuan, K., Sanson, M., Delattre, J.Y., Reijneveld, J.C., Idbaih, A. (2014) Clinical value of chromosome arms 19q and 11p losses in low-grade glioma. *Neuro-oncology*, **16**(3), 400-408.

Amary, M.F., Bacsi, K., Maggiani, F., Damato, S., Halai, D., Berisha, F., Pollock, R., O'Donnell, P., Grigoriadis, A., Diss, T., Eskandarpour, M., Presneau, N., Hogendoorn, P.C., Futreal, A., Tirabosco, R., Flanagan, A.M. (2011) *IDH1* and *IDH2* mutations are frequent events in central chondrosarcoma and central and periosteal chondromas but not in other mesenchymal tumours. *J Pathol*, **224**(3), 334–343.

Ambros, V. and Lee, R.C. (2004) Identification of microRNAs and other tiny noncoding RNAs by cDNA cloning. *Methods Mol Biol*, **265**, 131–58.

Arslantas, A., Artan, S., Oner, U., Müslümanoglu, M.H., Ozdemir, M., Durmaz, R., Arslantas, D., Vural, M., Cosan, E., Atasoy, M.A. (2007) Genomic alterations in low-grade, anaplastic astrocytomas and glioblastomas. *Pathology oncology research*, **13**(1), 39–46.

Bailey, J.M. and Colman, R.F. (1987) Distances among coenzyme and metal sites of NADP+-dependent isocitrate dehydrogenase using resonance energy transfer. *Biochemistry*, **26**(15), 4893–4900.

Balss, J., Meyer, J., Mueller, W., Korshunov, A., Hartmann, C., von Deimling, A. (2008) Analysis of the *IDH1* codon 132 mutation in brain tumors. *Acta Neuropatho*l, **116**(6), 597–602.

Barbano, R., Palumbo, O., Pasculli, B., Galasso, M., Volinia, S., D'Angelo, V., Icolaro, N., Coco, M., Dimitri, L., Graziano, P., Copetti, M., Valori, VM., Maiello, E., Carella, M., Fazio, VM., Parrella, P. (2014) A MiRNA Signature for Defining Aggressive Phenotype and Prognosis in Glioma. *PLoS One*, **9**(10): e108950.

Barbashina, V., Salazar, P., Holland, E.C., Rosenblum, M.K., Ladanyi, M. (2005) Allelic Losses at 1p36 and 19q13 in Glioma: Correlation with Histologic Classification, Definition of a 150-kb Minimal Deleted Region on 1p36, and Evaluation of CAMTA1 as a Candidate Tumor Suppressor Gene. *Clin Cancer Res*, **11**(3), 1119-28.

Ben-Porath, I. and Benvenisty, N. (1996) Characterization of a tumor associated gene, a member of a novel family of genes encoding membrane glycoproteins. *Gene*, **183**(1-2), 69–75.

van den Bent, M.J., Dubbink, H.J., Marie, Y., Brandes, A.A., Taphoorn, M.J., Wesseling, P., Frenay, M., Tijssen, C.C., Lacombe, D., Idbaih, A., van Marion, R., Kros, J.M., Dinjens, W.N., Gorlia, T., Sanson, M. (2010) *IDH1* and *IDH2* mutations are prognostic but not predictive for outcome in anaplastic oligodendroglial tumors: a report

of the European Organization for Research and Treatment of Cancer Brain Tumor Group. *Clin Cancer Res*, **16**(5), 1597–1604.

van den Bent, M.J., Afra, D., de Witte, O., Ben Hassel, M., Schraub, S., Hoang-Xuan, K., Malmström, P.O., Collette, L., Piérart, M., Mirimanoff, R., Karim, A.B.; EORTC Radiotherapy and Brain Tumor Groups and the UK Medical Research Council. (2005) Long term results of EORTC study 22845: a randomized trial on the efficacy of early versus delayed radiation therapy of lowgrade astrocytoma and oligodendroglioma in the adult. *Lancet*, **366**(9490), 985–90.

van den Bent, M.J., Snijders, T.J. and Bromberg, J.E.C. (2012) Current treatment of low grade glioma. *Memo*, **5**(3), 223–227.

Berenstein, R., Blau, I.W., Kar, A., Cay, R., Sindram, A., Seide, C., Blau, O. (2014) Comparative examination of various PCR-based methods for DNMT3A and IDH1/2 mutations identification in acute myeloid leukemia. *J Exp Clin Cancer Res*, **33**(1), 44.

de Biase, D., Visani, M., Morandi, L., Marucci, G., Taccioli, C., Cerasoli, S., Baruzzi, A., Pession, A.; PERNO Study Group. (2012) miRNAs expression analysis in paired fresh/frozen and dissected formalin fixed and paraffin embedded glioblastoma using real-time pCR. *PloS one*, **7**(4), p.e35596.

Birner, P., Pusch, S., Christov, C., Mihaylova, S., Toumangelova-Uzeir, K., Natchev, S., Schoppmann, S.F., Tchorbanov, A., Streubel, B., Tuettenberg, J., Guentchev, M. (2014) Mutant *IDH1* inhibits PI3K/Akt signaling in human glioma. *Cancer*, **120**(16), 2440–7.

Björner, S., Fitzpatrick, P.A., Li, Y., Allred, C., Howell, A., Ringberg, A., Olsson, H., Miller, C.J., Axelson, H., Landberg, G. (2014) Epithelial and stromal microRNA signatures of columnar cell hyperplasia linking Let-7c to precancerous and cancerous breast cancer cell proliferation. *PLos One*, **9**(8): e105099.

Boots-Sprenger, S.H., Sijben, A., Rijntjes, J., Tops, B.B., Idema, A.J., Rivera, A.L., Bleeker, F.E., Gijtenbeek, A.M., Diefes, K., Heathcock, L., Aldape, K.D., Jeuken, J.W., Wesseling, P. (2013) Significance of complete 1p/19q co-deletion, *IDH1* mutation and *MGMT* promoter methylation in glioma: use with caution. *Modern Pathol*, **26**(7), 922–9.

Brasil Caseiras, G., Ciccarelli, O., Altmann, D.R., Benton, C.E., Tozer, D.J., Tofts, P.S., Yousry, T.A., Rees, J., Waldman, AD., Jäger, H.R. (2009) Low-grade glioma: six-month tumor growth predicts patient outcome better than admission tumor volume, relative cerebral blood volume, and apparent diffusion coefficient. *Radiology*, **253**(2), 505–12.

Brell, M., Tortosa, A., Verger, E., Gil, J.M., Viñolas, N., Villá, S., Acebes, J.J., Caral, L., Pujol, T., Ferrer, I., Ribalta, T., Graus, F. (2005) Prognostic significance of O6-methylguanine-DNA methyltransferase determined by promoter hypermethylation and immunohistochemical expression in anaplastic gliomas. *Clin Cancer Res*, **11**(14), 5167–74.

Brennecke, J., Hipfner, D.R., Stark, A., Russell, R.B., Cohen, S.M. (2003) bantam encodes a developmentally regulated microRNA that controls cell proliferation and regulates the proapoptotic gene hid in Drosophila. *Cell*, **113**(1), 25–36.

Brown, P.D., Buckner, J.C., O'Fallon, J.R., Iturria, N.L., O'Neill, B.P., Brown, C.A., Scheithauer, B.W., Dinapoli, R.P., Arusell, R.M., Curran, W.J., Abrams, R., Shaw, E.G.; North Central Cancer Treatment Group; Mayo Clinic. (2004) Importance of baseline mini-mental state examination as a prognostic factor for patients with low-grade glioma. *Int J Radiation Oncol Biol Phys*, **59**(1), 117-25.

Capper, D., Mittelbronn, M., Meyermann, R., Schittenhelm, J. (2008) Pitfalls in the assessment of MGMT expression and in its correlation with survival in diffuse astrocytomas: proposal of a feasible immunohistochemical approach. *Acta Neuropathol*, **115**(2), 249–59.

Carlier, M. and Pantaloni, D. (1978) Slow association-dissociation equilibrium of NADP-linked isocitrate dehydrogenase from beef liver in relation to catalytic activity. *Eur J Biochem*, **89**(2), 511–16.

Chakrabarti, M., Banik, N.L. and Ray, S.K. (2013) Photofrin based photodynamic therapy and miR-99a transfection inhibited FGFR3 and PI3K/Akt signaling mechanisms to control growth of human glioblastoma In vitro and in vivo. *PloS one*, **8**(2), p.e55652.

Chang, E.F., Smith, J.S., Chang, S.M., Lamborn, K.R., Prados, M.D., Butowski, N., Barbaro, N.M., Parsa, A.T., Berger, M.S., McDermott, M. (2008) Preoperative prognostic classification system for hemispheric low-grade glioma in adults. *J Neurosurg*, **109**(5), 817–24.

Cheng, A.M., Byrom, M.W., Shelton, J., Ford, L.P. (2005) Antisense inhibition of human miRNAs and indications for an involvement of miRNA in cell growth and apoptosis. *Nucleic Acids Res*, **33**, 1290–1297.

Chang, E.F., Potts, M.B., Keles, G.E., Lamborn, K.R., Chang, S.M., Barbaro, N.M., Berger, M.S. (2008) Seizure characteristics and control following resection in 332 patients with low-grade glioma. *J Neurosurg*, **108**(2), 227-35.

Cheng, C., Fan, Q. and Weiss, W. (2009) PI3K Signaling in glioma-animal models and therapeutic challenges. *Brain Pathol*, **19**(1), 112-120.

Chotirat, S., Thongnoppakhun, W., Promsuwicha, O., Boonthimat, C., Auewarakul, C.U. (2012) Molecular alterations of isocitrate dehydrogenase 1 and 2 (IDH1 and IDH2) metabolic genes and additional genetic mutations in newly diagnosed acute myeloid leukemia patients. *J Hematol Onco*l, **7**(5), 5.

Chowdhury, R., Yeoh, K.K., Tian, Y.M., Hillringhaus, L., Bagg, E.A., Rose, N.R., Leung, I.K., Li, X.S., Woon, E.C., Yang, M., McDonough, M.A., King, O.N., Clifton, I.J., Klose, R.J., Claridge, T.D., Ratcliffe, P.J., Schofield, C.J., Kawamura A. (2011) The oncometabolite 2-hydroxyglutarate inhibits histone lysine demethylases. *EMBO Rep*, **12**(5), 463–469.

Colman, R. (1972) Role of metal ions in reactions catalyzed by pig heart triphosphopyridine nucleotide-dependent isocitrate dehydrogenase. II. Effect on catalytic properties and reactivity of amino acid residues. *J Biol Chem*, **247**(1), 215–23.

Correa, D.D., Shi, W., Thaler, H.T., Cheung, A.M., DeAngelis, L.M., Abrey, L.E. (2008) Longitudinal cognitive follow-up in low grade glioma. *J Neurooncol*, **86**(3), 321–7.

Dang, L., White, D.W., Gross, S., Bennett, B.D., Bittinger, M.A., Driggers, E.M., Fantin, V.R., Jang, H.G., Jin, S., Keenan, M.C., Marks, K.M., Prins, R.M., Ward, P.S., Yen, K.E., Liau, L.M., Rabinowitz, J.D., Cantley, L.C., Thompson, C.B., Vander Heiden, M.G., Su, S.M. (2009) Cancer associated IDH1 mutations produce 2-hydroxyglutarate. *Nature*, **462**(7274), 739–744.

Daniels, T.B., Brown, P.D., Felten, S.J., Wu, W., Buckner, J.C., Arusell, R.M., Curran, W.J., Abrams, R.A., Schiff, D., Shaw, E.G. (2011) Validation of EORTC prognostic factors for adults with low-grade glioma: a report using intergroup 86-72–51. *Int J Radiation Oncol Biol Phys*, **81**(1), 218–24.

Debien, E., Hervouet, E., Gautier, F., Juin, P., Vallette, F.M., Cartron, P.F. (2011) ABT-737 and/or folate reverse the PDGF-induced alterations in the mitochondrial apoptotic pathway in low-grade glioma patients. *Clinical epigenetics*, **2**(2), 369–381.

von Deimling, A., Fimmers, R., Schmidt, M.C., Bender, B., Fassbender, F., Nagel, J., Jahnke, R., Kaskel, P., Duerr, E.M., Koopmann, J., Maintz, D., Steinbeck, S., Wick, W., Platten, M., Müller, D.J., Przkora, R. Waha, A., Blümcke, B., Wellenreuther, R., Meyer-Puttlitz, B., Schmidt, O., Mollenhauer, J., Poustka, A., Stangl, A.P., Lenartz, D., von Ammon, K. (2000) Comprehensive allelotype and genetic anaysis of 466 human nervous system tumors. *J Neuropathol Exp Neurol*, **59(6)**, 544–558.

Devlin, T. (2006) *Textbook of Biochemistry with Clinical Correlations.*, Hoboken, N.J: Wiley-Liss.

Dobson, J.R., Taipaleenmäki, H., Hu, Y.J., Hong, D., van Wijnen, A.J., Stein, J.L., Stein, G.S., Lian, J.B., Pratap, J (2014) hsa-mir-30c promotes the invasive phenotype of metastatic breast cancer cells by targeting NOV/CCN3. *Cancer Cell Int*, **14**, 73.

Douw, L., Klein, M., Fagel, S.S., van den Heuvel, J., Taphoorn, M.J., Aaronson, N.K., Postma, T.J., Vandertop, W.P., Mooij, J.J., Boerman, R.H., Beute, G.N., Sluimer, J.D., Slotman, B.J., Reijneveld, J.C., Heimans, J.J. (2009) Cognitive and radiological effects of radiotherapy in patients with low-grade glioma: long-term follow-up. *Lancet Neurol*, **8**(9), 810–8.

Duffau, H., Capelle, L., Lopes, M., Bitar, A., Sichez, J.P., van Effenterre, R. (2002) Medically intractable epilepsy from insular low-grade glioma: improvement after an extended lesionectomy. *Acta Neurochir (Wien)*, **144**(6), 563–72.

Ernst, A., Campos, B., Meier, J., Devens, F., Liesenberg, F., Wolter, M., Reifenberger, G., Herold-Mende, C., Lichter, P., Radlwimmer, B. (2010) De-repression of CTGF via

the miR-17-92 cluster upon differentiation of human glioblastoma spheroid cultures. *Oncogene*, **29**(23), 3411–22.

Esquela-Kerscher, A. and Slack, F. (2006) Oncomirs - microRNAs with a role in cancer. *Nat Rev Cancer*, **6**(4), 259–69.

Esteller, M., Hamilton, SR., Burger, PC., Baylin, SB., and Herman, JG. (1999) Inactivation of the DNA Repair Gene O6-Methylguanine-DNA Methyltransferase by Promoter Hypermethylation is a Common Event in Primary Human Neoplasia. Cancer Res., **59**(4), 793-797.

Esteller, M., Garcia-Foncillas, J., Andion, E., Goodman, S.N., Hidalgo, O.F., Vanaclocha, V., Baylin, S.B., Herman, J.G. (2000) Inactivation of the DNA-repair gene mgmt and the clinical response of glioma to alkylating agents. *N Engl J Med*, **343**(19), 1350–1354.

Figueroa, M.E., Abdel-Wahab, O., Lu, C., Ward, P.S., Patel, J., Shih, A., Li, Y., Bhagwat, N., Vasanthakumar, A., Fernandez, H.F., Tallman, M.S., Sun, Z., Wolniak, K., Peeters, J.K., Liu, W., Choe, S.E., Fantin, V.R., Paietta, E., Löwenberg, B., Licht, J.D., Godley, L.A., Delwel, R., Valk, P.J., Thompson, C.B., Levine, R.L., Melnick, A. (2010) Leukemic *IDH1* and *IDH2* mutations result in a hypermethylation phenotype, disrupt TET2 function, and impair hematopoietic differentiation. *Cancer Cell*, **18**(6), 553–567.

Fisher, B.J., Lui, J., Macdonald, D.R., Lesser, G.J., Coons, S., Brachman, D., Ryu, S., Werner-Wasik, M., Bahary, J.P., Hu, C., Mehta, M.P. A phase II study of atemozolomide-based chemoradiotherapy regimen for high-risk LGG: preliminary results of RTOG 0424. *Proc Am Soc Clin Oncol 2013 (Abstract 2008)*.

Fornari, F., Gramantieri, L., Ferracin, M., Veronese, A., Sabbioni, S., Calin, G.A., Grazi, G.L., Giovannini, C., Croce, C.M., Bolondi. L., Negrini. M. (2008) MiR-221 controls CDKN1C/p57 and CDKN1B/p27 expression in human hepatocellular carcinoma. *Oncogene*, **27**(43), 5651–61.

Forst, D.A., Nahed, B.V., Loeffler, J.S., Batchelor, T.T. (2014) Low-Grade Glioma. *Oncologist*, **19**(4), 403–413.

Gabriely, G., Wurdinger, T., Kesari, S., Esau, C.C., Burchard, J., Linsley, P.S., Krichevsky, A.M. (2008) MicroRNA 21 promotes glioma invasion by targeting matrix metalloproteinase regulators. *Mol Cell Biol*, **28**(17), 5369–80.

Garofalo, M., Di Leva, G., Romano, G., Nuovo, G., Suh, S.S., Ngankeu, A., Taccioli, C., Pichiorri, F., Alder, H., Secchiero, P., Gasparini, P., Gonelli, A., Costinean, S., Acunzo, M., Condorelli, G., Croce, C.M.(2009) miR-221&222 regulate TRAIL resistance and enhance tumorigenicity through PTEN and TIMP3 downregulation. *Cancer Cell.*, **16**(6), 498–509.

Geisbrecht, B. and Gould, S. (1999) The human PICD gene encodes a cytoplasmic and peroxisomal NADP(+)-dependent isocitrate dehydrogenase. *J Biol Chem*, **274**(43), 30527–33.

Gerson, S. (2004) MGMT: its role in cancer etiology and cancer therapeutics. *Nat Rev Cancer*, **4**(4), 296–307.

Grzeschik, K. (1976) Assignment of a gene for human mitochondrial isocitrate dehydrogenase (ICM-M, EC 1.1.1.41) to chromosome 15. *Hum Genet*, **34(1)**, 23–28.

Guha, A., Dashner, K., Black, P.M., Wagner, J.A., Stiles, C.D. (1995) Expression of PDGF and PDGF receptors in human astrocytoma operation specimens supports the existence of an autocrine loop. *Int J Cancer*, **60**(2), 168–173.

Gunnarsson, T., Olafsson, E., Sighvatsson, V., Hannesson, B. (2002) Surgical treatment of patients with low-grade astrocytomas and medically intractable seizures. *Acta Neurol Scand.*, **105**(4), 289–92.

Gupta, R., Flanagan, S., Li, C.C., Lee, M., Shivalingham, B., Maleki, S., Wheeler, H.R., Buckland, M.E. (2013) Expanding the spectrum of IDH1 mutations in gliomas. *Mod pathol*, **26**(5), 619–25.

Hao, J., Zhang, C., Zhang, A., Wang, K., Jia, Z., Wang, G., Han, L., Kang, C., Pu, P. (2012) miR-221/222 is the regulator of Cx43 expression in human glioblastoma cells. *Oncol Rep*, **27**(5), 1504–10.

Hao, M., Zang, M., Wendlandt, E., Xu, Y., An, G., Gong, D., Li, F., Qi, F., Zhang, Y., Yang, Y., Zhan, F., Qiu, L. (2014) Low serum miR-19a expression as a novel poor prognostic indicator in multiple myeloma. *Int J Cancer*, **00**, 1–10.

Hartmann, C., Meyer, J. and Balss, J. (2009) Type and frequency of *IDH1* and *IDH2* mutations are related to astrocytic and oligodendroglial differentiation and age : a study of 1,010 diffuse glioma. *Acta neuropathologica*, **118**(4), 469–474.

Hartmann, C., Hentschel, B., Wick, W., Capper, D., Felsberg, J., Simon, M., Westphal, M., Schackert, G., Meyermann, R., Pietsch, T., Reifenberger, G., Weller, M., Loeffler, M., von Deimling, A. (2010) Patients with IDH1 wild-type anaplastic astrocytomas exhibit worse prognosis than IDH1- mutated glioblastomas, and IDH1 mutation status accounts for the unfavorable prognostic effect of higher age: implications for classification of gliomas. *Acta Neuropathol*, **120**(6), 707–718.

Hartong, D.T., Dange, M., McGee, T.L., Berson, E.L., Dryja, T.P., Colman, R.F. (2008) Insights from retinitis pigmentosa into the roles of isocitrate dehydrogenases in the Krebs cycle. *Nat Genet*, **40** (10), 1230–4.

Hegi, M.E., Diserens, A.C., Godard, S., Dietrich, P.Y., Regli, L., Ostermann, S., Otten, P., Van Melle, G., de Tribolet, N., Stupp, R. (2004) Clinical trial substantiates the predictive value of O-6-methylguanine-DNA methyltransferase promoter methylation in glioblastoma patients treated with temozolomide. *Clin Cancer Res*, **10**(6), 1871–4.

Hegi, ME., Diserens, A.C., Gorlia, T., Hamou, MF., de Tribolet, N., Weller, M., Kros, J.M., Hainfellner, J.A., Mason, W., Mariani, L., Bromberg, J.E., Hau, P., Mirimanoff, R.O., Cairncross, J.G., Janzer, R.C., Stupp, R. (2005) MGMT gene silencing and benefit from temozolomide in glioblastoma. *N Engl J Med*, **352**(10), 997–1003.

Hermanson, M., Funa, K., Koopmann, J., Maintz, D., Waha, A., Westermark, B., Heldin, C.H., Wiestler, O.D., Louis, D.N., von Deimling, A., Nistér, M. (1996) Association of loss of heterozygosity on chromosome 17p with high platelet-derived growth factor alpha receptor expression in human malignant glioma. *Cancer Res*, **56**(1), 164–171.

Hermanson, M., Funa, K., Hartman, M., Claesson-Welsh, L., Heldin, C.H., Westermark B., Nistér, M. (1992) Platelet-derived growth factor and its receptors in human glioma tissue: expression of messenger RNA and protein suggests the presence of autocrine and paracrine loops. *Cancer Res*, **52**(11), 3213–3219.

Herrlinger, U., Rieger, J., Koch, D., Loeser, S., Blaschke, B., Kortmann, RD., Steinbach, J.P., Hundsberger, T., Wick, W., Meyermann, R., Tan, T.C., Sommer, C., Bamberg, M., Reifenberger, G., Weller, M. (2006) Phase II trial of lomustine plus temozolomide chemotherapy in addition to radiotherapy in newly diagnosed glioblastoma: Ukt-03. *J Clin Oncol*, **24**(27), 4412–4417.

Hirose, Y., Aldape, K.D., Chang, S., Lamborn, K., Berger, M.S., Feuerstein, B.G. (2003) Grade II astrocytomas are subgrouped by chromosome aberrations. *Cancer genetics and cytogenetics*, **142**(1), 1–7.

Holland, H., Koschny, T., Ahnert, P., Meixensberger, J., Koschny, R. (2010) WHO grade-specific comparative genomic hybridization pattern of astrocytoma - a meta-analysis. *Pathology, research and practice*, **206**(10), 663–8.

Horbinski, C. (2013) What do we know about IDH1/2 mutations so far, and how do we use it? *Acta neuropathologica*, **125**(5), 621–36.

Huang, Y.H., Lin, K.H., Chen, H.C., Chang, M.L., Hsu, C.W., Lai, M.W., Chen, T.C., Lee, W.C., Tseng, Y.H., Yeh, C.T. (2012) Identification of postoperative prognostic microRNA predictors in hepatocellular carcinoma. *PloS one*, **7**(5), p.e37188.

Ichimura, K., Bolin, M.B., Goike, H.M., Schmidt, E.E., Moshref, A., Collins, V.P. (2000) Deregulation of the p14ARF/Mdm2/p53 pathway is a prerequisite for human astrocytic glioma with G1-S transition control gene abnormalities. *Cancer Res*, **60**(2), 417–424.

Ichimura, K., Bolin, M.B., Goike, H.M., Schmidt, E.E., Moshref, A., Collins, V.P. (2009) *IDH1* mutations are present in the majority of common adult glioma but rare in primary glioblastomas. *Neuro-oncology*, **11**(4), 341–7.

Idbaih, A., Omuro, A., Ducray, F., Hoang-Xuan, K. (2007) Molecular genetic markers as predictors of response to chemotherapy in gliomas. *Curr Opin Oncol*, **19**, 606–11.

Jaeckle, K.A., Eyre, H.J., Townsend, J.J., Schulman, S., Knudson, H.M., Belanich, M., Yarosh, D.B., Bearman, S.I., Giroux, D.J., Schold, S.C. (1998) Correlation of tumour O6 methylguanine- DNA methyltransferase levels with survival of malignant astrocytoma patients treated with bis-chloroethylnitrosourea: a Southwest Oncology Group study. *J Clin Oncol*, **16**(10), 3310–15.

Jeuken, J., von Deimling, A. and Wesseling, P. (2004) Molecular pathogenesis of oligodendroglial tumors. *J Neurooncol*, **70**(2), 161–181.

John, B., Enright, A.J., Aravin, A., Tuschl, T., Sander, C., Marks, D.S. (2004) Human MicroRNA targets. *PLoS Biol*, **2**(11), p.e363.

Johnson, C.D., Esquela-Kerscher, A., Stefani, G., Byrom, M., Kelnar, K., Ovcharenko, D., Wilson, M., Wang, X., Shelton, J., Shingara, J., Chin, L., Brown, D., Slack, F.J. (2007) The let-7 microRNA represses cell proliferation pathways in human cells. *Cancer research*, **67**(16), 7713–22.

Johnson, B.E., Mazor, T., Hong, C., Barnes, M., Aihara, K., McLean, C.Y., Fouse, S.D., Yamamoto, S., Ueda, H., Tatsuno, K., Asthana, S., Jalbert, L.E., Nelson, S.J., Bollen, A.W., Gustafson, W.C., Charron, E., Weiss, W.A., Smirnov, I.V., Song, J.S., Olshen, A.B., Cha, S., Zhao, Y., Moore, R.A., Mungall, A.J., Jones, S.J., Hirst, M., Marra, M.A., Saito, N., Aburatani, H., Mukasa, A., Berger, M.S., Chang, S.M., Taylor, B.S., Costello, J.F. (2014) Mutational Analysis Reveals the Origin and Therapy-driven Evolution of Recurrent Glioma. *Science*, **343**(6167), 189–193.

Juratli, T.A., Kirsch, M., Geiger, K., Klink, B., Leipnitz, E., Pinzer, T., Soucek, S., Schrock, E., Schackert, G., Krex, D. (2012) The prognostic value of *IDH* mutations and *MGMT* promoter status in secondary high-grade gliomas. *J Neurooncol*, **110**(3), 325–333.

Kaloshi, G., Benouaich-Amiel, A., Diakite, F., Taillibert, S., Lejeune, J., Laigle-Donadey, F., Renard, M.A., Iraqi, W., Idbaih, A., Paris, S., Capelle, L., Duffau, H., Cornu, P., Simon, J.M., Mokhtari, K., Polivka, M., Omuro, A., Carpentier, A., Sanson, M., Delattre, J.Y., Hoang-Xuan, K. (2007) Temozolomide for low-grade glioma: predictive impact of 1p/19q loss on response and outcome. *Neurology*, **68**(21), 1831–6.

Kanehisa, M., Goto, S., Sato, Y., Furumichi, M., Tanabe, M. (2012) KEGG for integration and interpretation of large-scale molecular data sets. *Nucleic acids research*, **40**(Database issue), D109–14.

Karim, A.B., Maat, B., Hatlevoll, R., Menten, J., Rutten, E.H., Thomas, D.G., Mascarenhas, F., Horiot, J.C., Parvinen, L.M., van Reijn, M., Jager, J.J., Fabrini, M.G., van Alphen, A.M., Hamers, H.P., Gaspar, L., Noordman, E., Pierart, M., van Glabbeke, M. (1996) A randomized trial on dose-response in radiation therapy of low-grade cerebral glioma: European Organization for Research and Treatment of Cancer (EORTC) Study 22844. *Int J Radiation Oncol Biol Phys*, **36**(3), 549–556.

Karsy, M., Arslan, E. and Moy, F. (2012) Current Progress on Understanding MicroRNAs in Glioblastoma Multiforme. *Genes & cancer*, **3**(1), 3–15.

Kelly, J. and Plaut, G. (1981)a. Kinetic evidence for the dimerization of the triphosphopyridine nucleotide-dependent isocitrate dehydrogenase from pig heart. *J Biol Chem*, **256**(1), 335–42.

Kelly, J. and Plaut, G. (1981)b. Physical evidence for the dimerization of the triphosphopyridine-specific isocitrate dehydrogenase from pig heart. *J Biol Chem*, **256**(1), 330–34.

Kesari, S., Schiff, D., Drappatz, J., LaFrankie, D., Doherty, L., Macklin, E.A., Muzikansky, A., Santagata, S., Ligon, K.L., Norden, A.D., Ciampa, A., Bradshaw, J., Levy, B., Radakovic, G., Ramakrishna, N., Black, P.M., Wen, P.Y. (2009) Phase II study of protracted daily temozolomide for low-grade glioma in adults. *Clin Cancer Res.*, **15**(1), 330–337.

Kim, Y.H., Nobusawa, S., Mittelbronn, M., Paulus, W., Brokinkel, B., Keyvani, K., Sure, U., Wrede, K., Nakazato, Y., Tanaka, Y., Vital, A., Mariani, L., Stawski, R., Watanabe, T., De Girolami, U., Kleihues, P., Ohgaki, H.(2010) Molecular classification of low-grade diffuse glioma. *The American Journal of Pathology*, **177**(6), 2708–14.

Kleihues, P. et al. (2000) Diffuse astrocytoma. In: Kleihues P, Cavenee WK (eds) Pathology and genetics of tumors of the nervous system. World Health Organization classification of tumors. *IARC, Lyon*, 22–26.

Kloosterhof, N.K., Bralten, L.B., Dubbink, H.J., French, P.J., van den Bent, M.J. (2011) Isocitrate dehydrogenase-1 mutations: a fundamentally new understanding of diffuse glioma? *Lancet oncology*, **12**(1), 83–91.

Knoll, S., Emmrich, S. and Pützer, B. (2013) The E2F1-miRNA cancer progression network. *Adv Exp Med Biol*, **774**, 135–47.

Kölker, S., Pawlak, V., Ahlemeyer, B., Okun, J.G., Hörster, F., Mayatepek, E., Krieglstein, J., Hoffmann, G.F., Köhr, G. (2002) NMDA receptor activation and respiratory chain complex V inhibition contribute to neurodegeneration in d-2-hydroxyglutaric aciduria. *Eur J Neurosci*, **16**(1), 21–8.

Koul, D. (2008) *PTEN* signaling pathways in glioblastoma. *Cancer Biol Ther*, **7**(9), 1321–1325.

Kozomara, A. and Griffiths-Jones, S. (2011) miRBase: integrating microRNA annotation and deep-sequencing data. *Nucleic acids research*, **39**(Database issue), D152–7.

Kraus, J.A., Koopmann, J., Kaskel, P., Maintz, D., Brandner, S., Schramm, J., Louis, D.N., Wiestler, O.D., von Deimling, A. (1995) Shared allelic losses on chromosomes 1p and 19q suggest a common origin of oligodendroglioma and oligoastrocytoma. *J Neuropathol Exp Neurol*, **54**(1), 91–95.

Kujas, M., Lejeune, J., Benouaich-Amiel, A., Crinière, E., Laigle-Donadey, F., Marie, Y., Mokhtari, K., Polivka, M., Bernier, M., Chretien, F., Couvelard, A., Capelle, L., Duffau, H., Cornu, P., Broët, P., Thillet, J., Carpentier, A.F., Sanson, M., Hoang-Xuan, K., Delattre, J.Y. (2005) Chromosome 1p loss: a favorable prognostic factor in low-grade glioma. *Annals of neurology*, **58**(2), 322–6.

Kunz, M., Thon, N., Eigenbrod, S., Hartmann, C., Egensperger, R., Herms, J., Geisler, J., la Fougere, C., Lutz, J., Linn, J., Kreth, S., von Deimling, A., Tonn, J.C., Kretzschmar, H.A., Pöpperl, G., Kreth, F.W. (2011) Hot spots in dynamic (18)FET-PET delineate malignant tumor parts within suspected WHO grade II glioma. *Neuro Oncol*, **13**(3), 307–16.

Kuo, L.T., Tsai, S.Y., Chang, C.C., Kuo, K.T., Huang, A.P., Tsai, J.C., Tseng, H.M., Kuo, M.F., Tu, Y.K. (2013) Genetic and epigenetic alterations in primary-progressive paired oligodendroglial tumors. *PloS one*, **8**(6), p.e67139.

Latini, A., Scussiato, K., Rosa, R.B., Llesuy, S., Belló-Klein, A., Dutra-Filho, CS., Wajner, M. (2003) D-2-hydroxyglutaric acid induces oxidative stress in cerebral cortex of young rats. *Eur J Neurosci*, **17**, 2017–22.

Lee, R., Feinbaum, R. and Ambros, V. (1993) The C. elegans heterochronic gene lin-4 encodes small RNAs with antisense complementarity to lin-14. *Cell*, **75**(5), 843–54.

Lee, Y. and Dutta, A. (2009) MicroRNAs in cancer. *Annu Rev Pathol.*, **4**, 199–227.

Leu, S., von Felten, S., Frank, S., Vassella, E., Vajtai, I., Taylor, E., Schulz, M., Hutter, G., Hench, J., Schucht, P., Boulay, J.L., Mariani, L. (2013) IDH/MGMT-driven molecular classification of low-grade glioma is a strong predictor for long-term survival. *Neuro-Oncology*, **15**(4), 469–79.

Lewis, B., Burge, C. and Bartel, D. (2005) Conserved seed pairing, often flanked by adenosines, indicates that thousands of human genes are microRNA targets. *Cell*, **120**(1), 15–20.

Li, M., Li, J., Liu, L., Li, W., Yang, Y., Yuan, J. (2013) MicroRNA in Human Glioma. *Cancers*, **5**(4), 1306–31.

Li, Y., Guessous, F., Zhang, Y., Dipierro, C., Kefas, B., Johnson, E., Marcinkiewicz, L., Jiang, J., Yang, Y., Schmittgen, T.D., Lopes, B., Schiff, D., Purow, B., Abounader, R. (2009) microRNA-34a inhibits glioblastoma growth by targeting multiple oncogenes. *Cancer Res*, **69**(19), 7569–7576.

van Lith, S.A., Navis, A.C., Verrijp, K., Niclou, S.P., Bjerkvig, R., Wesseling, P., Tops, B., Molenaar, R., van Noorden, C.J., Leenders, W.P. (2014) Glutamate as chemotactic fuel for diffuse glioma cells: Are they glutamate suckers? *Biochimica et biophysica acta*, **1846**(1), 66–74.

Louis, D.N., Ohgaki, H., Wiestler, O.D., Cavenee, W.K., Burger, P.C., Jouvet, A., Scheithauer, B.W., Kleihues, P. (2007) The 2007 WHO classification of tumours of the central nervous system. *Acta neuropathologica*, **114**(2), 97–109.

Luchman, H.A., Stechishin, O.D., Dang, N.H., Blough, M.D., Chesnelong, C., Kelly, J.J., Nguyen, S.A., Chan, J.A., Weljie, A.M., Cairncross, J.G., Weiss, S. (2012) An in vivo patient-derived model of endogenous IDH1-mutant glioma. *Neuro Oncol*, **14**(2), 184-91.

Maintz, D., Fiedler, K., Koopmann, J., Rollbrocker, B., Nechev, S., Lenartz, D., Stangl, A.P., Louis, D.N., Schramm, J., Wiestler, O.D., von Deimling, A. (1997) Molecular genetic evidence for subtypes of oligoastrocytomas. *J Neuropathol Exp Neurol*, **56**(10), 1098–1104.

Malmström, A., Grønberg, B.H., Marosi, C., Stupp, R., Frappaz, D., Schultz, H., Abacioglu, U., Tavelin, B., Lhermitte, B., Hegi, M.E., Rosell, J., Henriksson, R.; Nordic Clinical Brain Tumour Study Group (NCBTSG). (2012) Temozolomide versus standard 6-week radiotherapy versus hypofractionated radiotherapy in patients older than 60 years with glioblastoma: the Nordic randomised, phase 3 trial. *Lancet Oncol*, **13**, 916–926.

Malzkorn, B., Wolter, M., Liesenberg, F., Grzendowski, M., Stühler, K., Meyer, H.E., Reifenberger, G. (2010) Identification and functional characterization of microRNAs involved in the malignant progression of glioma. *Brain pathology (Zurich, Switzerland)*, **20**(3), 539–50.

Marko, N. and Weil, R. (2013) The molecular biology of WHO Grade II glioma. *Neurosurg Focus*, **34**(2), E1.

Masliah-Planchon, J., Pasmant, E., Luscan, A., Laurendeau, I., Ortonne, N., Hivelin, M., Varin, J., Valeyrie-Allanore, L., Dumaine, V., Lantieri, L., Leroy, K., Parfait, B., Wolkenstein, P., Vidaud, M., Vidaud, D., Bièche, I. (2013) MicroRNAome profiling in benign and malignant neurofibromatosis type 1-associated nerve sheath tumors: evidences of PTEN pathway alterations in early NF1 tumorigenesis. *BMC genomics*, **14**, 473.

Masui, K., Cloughesy, T.F. and Mischel, P.S. (2012) Review: molecular pathology in adult high-grade glioma: from molecular diagnostics to target therapies. *Neuropathology and applied neurobiology*, **38**(3), 271–91.

McBride, S.M., Perez, D.A., Polley, M.Y., Vandenberg, S.R., Smith, J.S., Zheng, S., Lamborn, K.R., Wiencke, J.K., Chang, S.M., Prados, M.D., Berger, M.S., Stokoe. D., Haas-Kogan, D.A. (2010) Activation of PI3K/mTOR pathway occurs in most adult low-grade gliomas and predicts patient survival. *Journal of neuro-oncology*, **97**(1), 33–40.

Megova, M., Drabek, J., Koudelakova, V., Trojanec, R., Kalita, O., Hajduch, M. (2014) Isocitrate dehydrogenase 1 and 2 mutations in glioma. *Journal of neuroscience research*, **92**(12), 1611–20.

Megova, M., Drabek, J., Koudelakova, V., Trojanec, R., Kalita, O., Hajduch, M. (2011) IDH1 and IDH2 mutations, immunohistochemistry and associations in a series of brain tumours. *J Neurooncol*, **105**(2), 345–357.

Mellai, M., Piazzi, A., Caldera, V., Monzeglio, O., Cassoni, P., Valente, G., Schiffer, D. (2011) *IDH1* and *IDH2* mutations, immunohistochemistry and associations in a series of brain tumours. *J Neurooncol*, **105**(2), 345–357.

Mellai, M., Piazzi, A., Caldera, V., Annovazzi, L., Monzeglio, O., Senetta, R., Cassoni, P., Schiffer, D. (2013) Promoter hypermethylation of the EMP3 gene in a series of 229 human glioma. *BioMed research international*.

Metellus, P., Coulibaly, B., Colin, C., de Paula, A.M., Vasiljevic, A., Taieb, D., Barlier, A., Boisselier, B., Mokhtari, K., Wang, X.W., Loundou, A., Chapon, F., Pineau, S., Ouafik, L., Chinot, O., Figarella-Branger, D. (2010) Absence of IDH mutation identifies a novel radiologic and molecular subtype of WHO grade II glioma with dismal prognosis. *Acta Neuropathol*, **120**(6), 719–729.

Miao, L.J., Huang, S.F., Sun, Z.T., Gao, Z.Y., Zhang, R.X., Liu, Y., Wang, J. (2013) MiR-449c targets c-Myc and inhibits NSCLC cell progression. *FEBS letters*, **587**(9), 1359–65.

Molenaar, R.J., Radivoyevitch, T., Maciejewski, J.P., van Noorden C.J., Bleeker, F.E. (2014) The driver and passenger effects of isocitrate dehydrogenase 1 and 2 mutations in oncogenesis and survival prolongation. *Biochimica et biophysica acta*, **1846**(2), 326–341.

Monzo, M., Navarro, A., Bandres, E., Artells, R., Moreno, I., Gel, B., Ibeas, R., Moreno, J., Martinez, F., Diaz, T., Martinez, A., Balagué, O., Garcia-Foncillas, J. (2008) Overlapping expression of microRNAs in human embryonic colon and colorectal cancer. *Cell Res*, **18**(8), 823–33.

Motomura, K., Mittelbronn, M. Paulus, W., Brokinkel, B., Keyvani, K., Sure, U., Wrede, K., Nakazato, Y., Tanaka, Y., Nonoguchi, N., Pierscianek, D., Kim, Y.H., Mariani, L., Vital, A., Perry, A., Ohgaki, H. (2013) PDGFRA Gain in Low-Grade Diffuse Glioma. *J Neuropathol Exp Neurol*, **72**(1), 61–66.

Mueller, W., Hartmann, C., Hoffmann, A., Lanksch, W., Kiwit, J., Tonn, J., Veelken, J., Schramm, J., Weller, M., Wiestler, O.D., Louis, D.N., von Deimling, A. (2002) Genetic signature of oligoastrocytomas correlates with tumor location and denotes distinct molecular subsets. *Am J Pathol*, **161**(1), 313–319.

Myung, J.K., Cho, H.J., Park, C.K., Kim, S.K., Phi, J.H., Park, S.H. (2012) *IDH1* mutation of glioma with long-term survival analysis. *Oncology reports*, **28**(5), 1639–44.

Nakasu, S., Fukami, T., Baba, K., Matsuda, M. (2004) Immunohistochemical study for O6-methylguanine-DNA methyltransferase in the non-neoplastic and neoplastic components of gliomas. *J Neurooncol*, **70**(3), 333–40.

Narahara, K., Kimura, S., Kikkawa, K., Takahashi, Y., Wakita, Y., Kasai, R., Nagai, S., Nishibayashi, Y., Kimoto, H (1985) Probable assignment of soluble isocitrate dehydrogenase (IDH1) to 2q33.3. *Hum Genet*, **71**, 37–40.

Nishizaki, T., Ozaki, S., Harada, K., Ito, H., Arai, H., Beppu, T., Sasaki, K. (1998) Investigation of genetic alterations associated with the grade of astrocytic tumor by comparative genomic hybridization. *Genes, chromosomes & cancer*, **21**(4), 340–6.

Nobusawa, S., Watanabe, T., Kleihues, P., Ohgaki, H. (2009) *IDH1* mutations as molecular signature and predictive factor of secondary glioblastomas. *Clinical Cancer Res*, **15**(19), 6002–7.

Northrop, D. and Cleland, W. (1974) The kinetics of pig heart triphosphopyridine nucleotide-isocitrate dehydrogenase. II. Dead-end and multiple inhibition studies. *J Biol Chem*, **249**(9), 2928–31.

Noushmehr, H., Weisenberger, D.J., Diefes, K., Phillips, H.S., Pujara, K., Berman, B.P., Pan, F., Pelloski, C.E., Sulman, E.P., Bhat, K.P., Verhaak, R.G., Hoadley, K.A., Hayes, D.N., Perou, C.M., Schmidt, H.K., Ding, L., Wilson, R.K., Van Den Berg, D., Shen, H., Bengtsson, H., Neuvial, P., Cope, L.M., Buckley, J., Herman, J.G., Baylin, S.B., Laird, P.W., Aldape, K.; Cancer Genome Atlas Research Network. (2010) Identification of a CpG Island Methylator Phenotype that Defines a Distinct Subgroup of Glioma. *Cancer Cell.*, **17**(5), 510–522.

Ohgaki H and Kleihues P. (2005) Population-based studies on incidence, survival rates and genetic alterations in astrocytic and oligodendroglial glioma. *J Neuropathol Exp Neurol*, **64**(6), 479–89.

Ohgaki, H. and Kleihues, P. (2009) Genetic alterations and signalling pathways in the evolution of glioma. *Cancer Sci*, **100**(12), 2235–41.

Ohgaki, H. and Kleihues, P. (2007) Genetic pathways to primary and secondary glioblastoma. *The American journal of pathology*, **170**(5), 1445–53.

Okamoto, Y, Di Patre, P.L., Burkhard, C., Horstmann, S., Jourde, B., Fahey, M., Schüler, D., Probst-Hensch, N.M., Yasargil, M.G., Yonekawa, Y., Lütolf, U.M., Kleihues, P., Ohgaki, H. (2004) Population-based study on incidence, survival rates and genetic alterations of low-grade astrocytomas and oligodendroglioma. *Acta Neuropathol*, **108**(1), 49–56.

Olson, J., Riedel, E. and DeAngelis, L. (2000) Long-term outcome of low-grade oligodendroglioma and mixed glioma. *Neurology*, **54**(7), 1442–8.

Osada, H. and Takahashi, T. (2011) let-7 and miR-17-92: small-sized major players in lung cancer development. *Cancer Sci*, **102**(1), 9–17.

Ostrom, Q.T., Bauchet, L., Davis, F.G., Deltour, I., Fisher, J.L., Langer, CE., Pekmezci M., Schwartzbaum, J.A., Turner, M.C., Walsh, K.M., Wrensch, M.R., Barnholtz-Sloan, J.S. (2014) The epidemiology of glioma in adults: a "state of the science" review. *Neuro-oncology*, **16**(7), 896–913.

Pamir, M.N., Özduman, K., Yıldız, E., Sav, A., Dinçer, A. (2013) Intraoperative magnetic resonance spectroscopy for identification of residual tumor during low-grade glioma surgery: Clinical article. *J Neurosurg*, **118**(6), 1191–8.

Pamir, M. and K, Ö. (2009) 3-T ultrahigh-field intraoperative MRI for low-grade glioma resection. *Expert Rev Anticancer Ther*, **9**(11), 1537–1539.

Papagiannakopoulos, T., Shapiro, A. and Kosik, K. (2008) MicroRNA-21 targets a network of key tumor-suppressive pathways in glioblastoma cells. *Cancer Res.*, **68**(19), 8164–72.

Parsons, D.W., Jones, S., Zhang, X., Lin, J.C., Leary, R.J., Angenendt, P., Mankoo, P., Carter, H., Siu, I.M., Gallia, G.L., Olivi, A., McLendon, R., Rasheed, B.A., Keir, S., Nikolskaya, T., Nikolsky, Y., Busam, D.A., Tekleab, H., Diaz, L.A. Jr., Hartigan, J., Smith, D.R., Strausberg, R.L., Marie, S.K., Shinjo, S.M., Yan, H., Riggins, G.J., Bigner, D.D., Karchin, R., Papadopoulos, N., Parmigiani, G., Vogelstein, B., Velculescu, V.E., Kinzler, K.W. (2008) An integrated genomic analysis of human glioblastoma multiforme. *Science*, **321**(5897), 1807–1812.

Paschka, P., Schlenk, R.F., Gaidzik, V.I., Habdank, M., Krönke, J., Bullinger, L., Späth, D., Kayser, S., Zucknick, M., Götze, K., Horst, H.A., Germing, U., Döhner, H., Döhner, K. (2010) *IDH1* and *IDH2* mutations are frequent genetic alterations in acute myeloid leukemia and confer adverse prognosis in cytogenetically normal acute myeloid leukemia with NPM1 mutation without FLT3 internal tandem duplication. *J Clin Oncol*, **28**(22), 3636–3643.

Pastor, W., Aravind, L. and Rao, A. (2013) TETonic shift: biological roles of TET proteins in DNA demethylation and transcription. *Nat. Rev. Mol. Cell Bio*, **14**(6), 341–356.

Patel, K.P., Barkoh, B.A., Chen, Z., Ma, D., Reddy, N., Medeiros, L.J., Luthra, R. (2011) Diagnostic testing for IDH1 and IDH2 variants in acute myeloid leukemia an algorithmic approach using high-resolution melting curve analysis. *J Mol Diagn*, **13**(6), 678–686.

Paz, M.F., Yaya-Tur, R., Rojas-Marcos, I., Reynes, G., Pollan, M., Aguirre-Cruz, L., García-Lopez, J.L., Piquer, J., Safont, M.J., Balaña, C., Sanchez-Cespedes, M., García-Villanueva, M., Arribas, L., Esteller, M. (2004) CpG island hypermethylation of the DNA repair enzyme methyltransferase predicts response to temozolomide in primary gliomas. *Clin Cancer Res*, **10**(15), 4933–8.

Piaskowski, S., Bienkowski, M., Stoczynska-Fidelus, E., Stawski, R., Sieruta, M., Szybka, M., Papierz, W., Wolanczyk, M., Jaskolski, D.J., Liberski, P.P., Rieske, P. (2011) Glioma cells showing IDH1 mutation cannot be propagated in standard cell culture conditions. *British journal of cancer*, **104**(6), 968–70.

Piccirilli, M., Bistazzoni, S., Gagliardi, F.M., Landi, A., Santoro, A., Giangaspero, F., Salvati, M. (2006) Treatment of glioblastoma multiforme in elderly patients. Clinico-therapeutic remarks in 22 patients older than 80 years. *Tumouri*, **92**, 98–103.

Pickering, M., Stadler, B. and Kowalik, T. (2009) miR-17 and miR-20a temper an E2F1-induced G1 checkpoint to regulate cell cycle progression. *Oncogene*, **28**(1), 140–5.

Pignatti, F., van den Bent, M., Curran, D., Debruyne, C., Sylvester, R., Therasse, P., Afra, D., Cornu, P., Bolla, M., Vecht, C., Karim, A.B.; European Organization for Research and Treatment of Cancer Brain Tumor Cooperative Group; European

Organization for Research and Treatment of Cancer Radiotherapy Cooperative Group. (2002) Prognostic factors for survival in adult patients with cerebral low-grade glioma. *J Clin Oncol.*, **20**(8), 2076–84.

Pollack, I.F., Hamilton, R.L., Sobol, R.W., Burnham, J., Yates, A.J., Holmes, E.J., Zhou, T., Finlay, J.L. (2006) O6-methylguanine-DNA methyltransferase expression strongly correlates with outcome in childhood malignant gliomas: results from the CCG-945 Cohort. *J Clin Oncol*, **24**, 3431–7.

Pouratian, N., Asthagiri, A., Jagannathan, J., Shaffrey, M.E., Schiff, D. (2007) Surgery insight: The role of surgery in the management of low-grade glioma. *Nat Clin Pract Neurol*, **3**(11), 628–639.

Quillien, V., Lavenu, A., Karayan-Tapon, L., Carpentier, C., Labussière, M., Lesimple, T., Chinot, O., Wager, M., Honnorat, J., Saikali, S., Fina, F., Sanson, M., Figarella-Branger, D. (2012) Comparative assessment of 5 methods (methylation-specific polymerase chain reaction, MethyLight, pyrosequencing, methylation-sensitive high-resolution melting, and immunohistochemistry) to analyze O6-methylguanine-DNA-methyltranferase in a series of 100 gliomablastoma patients. *Cancer*, **118**(17), 4201–11.

Quinn, J.A., Reardon, D.A., Friedman, A.H., Rich, J.N., Sampson, J.H., Provenzale, J.M., McLendon, R.E., Gururangan, S., Bigner, D.D., Herndon, J.E. 2nd, Avgeropoulos, N., Finlay, J., Tourt-Uhlig, S., Affronti, M.L., Evans, B., Stafford-Fox, V., Zaknoen, S., Friedman, H.S. (2003) Phase II trial of temozolomide in patients with progressive low-grade glioma. *J Clin Oncol*, **21**(4), 646–651.

Reifenberger, G. and Louis, D. (2003) Oligodendroglioma: toward molecular definitions in diagnostic neuro-oncology. *J Neuropathol Exp Neurol*, **62**(2), 111–126.

Reifenberger, G. and Collins, V.P. (2004) Pathology and molecular genetics of astrocytic glioma. *Journal of molecular medicine (Berlin, Germany)*, **82**(10), 656–70.

Reifenberger, G., Hentschel, B., Felsberg, J., Schackert, G., Simon, M., Schnell, O., Westphal, M., Wick, W., Pietsch, T., Loeffler, M., Weller, M.; German Glioma Network (2012) Predictive impact of *MGMT* promoter methylation in glioblastoma of the elderly. *Int J Cancer*, **131**, 1342–1350.

Reifenberger, J., Reifenberger, G., Liu, L., James, C.D., Wechsler, W., Collins, V.P. (1994) Molecular genetic analysis of oligodendroglial tumors shows preferential allelic deletions on 19q and 1p. *Am J Pathol*, **145**(5), 1175–1190.

Reijneveld, J.C., Sitskoorn, M.M., Klein, M., Nuyen, J., Taphoorn, M.J. (2001) Cognitive status and quality of life in suspected versus proven low-grade glioma. *Neurology*, **56**(5), 618–23.

Reitman, Z.J. and Yan, H. (2010) Isocitrate dehydrogenase 1 and 2 mutations in cancer: alterations at a crossroads of cellular metabolism. *Journal of the National Cancer* Institute, **102**(13), 932–41.

Riehmer, V., Gietzelt, J., Beyer, U., Hentschel, B., Westphal, M., Schackert, G., Sabel, M.C., Radlwimmer, B., Pietsch, T., Reifenberger, G., Weller, M., Weber, R.G., Loeffler, M.; German Glioma Network. (2014) Genomic Profiling Reveals Distinctive Molecular Relapse Patterns in IDH1 / 2 Wild-Type Glioblastoma. *Genes, chromosomes & cancer*, **605**, 589–605.

Sabha, N., Knobbe, C.B., Maganti, M., Al Omar, S., Bernstein, M., Cairns, R., Çako, B., von Deimling, A., Capper, D., Mak, T.W., Kiehl, T.R., Carvalho, P., Garrett, E., Perry, A., Zadeh, G., Guha, A., Sidney, Croul. (2014) Analysis of IDH mutation, 1p/19q deletion, and PTEN loss delineates prognosis in clinical low-grade diffuse glioma. *Neuro-oncology*, **16**(7), 914–23.

Sanai, N., Chang, S. and Berger, M. (2011) Low-grade gliomas in adults. *J Neurosurg.*, **115**, 948–65.

Sanger, F., Nicklen, S., & Coulson, AR. (1977) DNA sequencing with chain-terminating inhibitors. Proc Natl Acad Sci U S A, **74**(12), 5463–5467.

Sanson, M., Marie, Y., Paris, S., Idbaih, A., Laffaire, J., Ducray, F., El Hallani, S., Boisselier, B., Mokhtari, K., Hoang-Xuan, K., Delattre, J.Y. (2009) Isocitrate dehydrogenase 1 codon 132 mutation is an important prognostic biomarker in gliomas. Journal of clinical oncology : official journal of the American Society of Clinical Oncology, **27**(25), 4150–4.

Sasayama, T., Nishihara, M., Kondoh, T., Hosoda, K., Kohmura, E. (2009) MicroRNA-10b is overexpressed in malignant glioma and associated with tumor invasive factors, uPAR and RhoC. *International journal of cancer*, **125**(6), 1407–13.

Schiff, D., Brown, P. and Giannini, C. (2007) Outcome in adult low-grade glioma: the impact of prognostic factors and treatment. *Neurology*, **69**(13), 1366–1373.

Schröck, E., Blume, C., Meffert, M.C., du Manoir, S., Bersch, W., Kiessling, M., Lozanowa, T., Thiel, G., Witkowski, R., Ried, T., Cremer, T. (1996) Recurrent gain of chromosome arm 7q in low-grade astrocytic tumors studied by comparative genomic hybridization. *Genes Chromosomes Cancer*, **15**(4), 199–205.

Schröck, E., Blume, C., Meffert, M.C., du Manoir, S., Bersch, W., Kiessling, M., Lozanowa, T., Thiel, G., Witkowski, R., Ried, T., Cremer, T. (1996) Recurrent gain of chromosome arm 7q in low-grade astrocytic tumors studied by comparative genomic hybridization. *Genes, chromosomes & cancer*, **15**(4), 199–205.

Sempere, L.F., Freemantle, S., Pitha-Rowe, I., Moss, E., Dmitrovsky, E., Ambros, V. (2004) Expression profiling of mammalian microRNAs uncovers a subset of brain-expressed microRNAs with possible roles in murine and human neuronal differentiation. *Genome Biol*, **5**(3), 13.

Shapiro, J.R. (2002) Genetic alterations associated with adult diffuse astrocytic tumors. *American journal of medical genetics*, **115**(3), 194–201.

Shaw, E., Arusell, R., Scheithauer, B., O'Fallon, J., O'Neill, B., Dinapoli, R., Nelson, D., Earle, J., Jones, C., Cascino, T., Nichols, D., Ivnik, R., Hellman, R., Curran, W., Abrams, R. (2002) A prospective randomized trial of low versus high dose radiation in adults with a supratentorial low grade glioma: initial report of a NCCTG-RTOG-ECOG study. *J Clin Oncol*, **20**(9), 2267–76.

Shaw, E., Arusell, R., Scheithauer, B., O'Fallon, J., O'Neill, B., Dinapoli, R., Nelson, D., Earle, J., Jones, C., Cascino, T., Nichols, D., Ivnik, R., Hellman, R., Curran, W., Abrams, R. (2012) Randomized trial of radiation therapy plus procarbazine, lomustine, and vincristine chemotherapy for supratentorial adult low-grade glioma: Initial results of RTOG 9802. *J Clin Oncol*, **30**(25), 3065–3070.

Shi, L., Chen, J., Yang, J., Pan, T., Zhang, S., Wang, Z. (2010) MiR-21 protected human glioblastoma U87MG cells from chemotherapeutic drug temozolomide induced apoptosis by decreasing Bax/Bcl-2 ratio and caspase-3 activity. *Brain Res*. **1352**, 255-64.

Shibahara, I., Sonoda, Y., Kanamori, M., Saito, R., Yamashita, Y., Kumabe, T., Watanabe, M., Suzuki, H., Kato, S., Ishioka, C., Tominaga, T. (2012) IDH1/2 gene status defines the prognosis and molecular profiles in patients with grade III gliomas. *Int J Clin Oncol*, **17**, 551–561.

Soffietti, R. et al. (2005) Efficacy of radiation therapy on seizures in low-grade astrocytomas. *Neuro-Oncology*, **7**, 389.

Song, L., Lin, C., Gong, H., Wang, C., Liu, L., Wu, J., Tao, S., Hu, B., Cheng, S.Y., Li, M., Li, J. (2013) miR-486 sustains NF-κB activity by disrupting multiple NF-κB-negative feedback loops. *Cell Res*, **23**(2), 274–89.

Sonoda, Y., Kumabe, T., Nakamura, T., Saito, R., Kanamori, M., Yamashita, Y., Suzuki, H., Tominaga, T. (2009) Analysis of *IDH1* and *IDH2* mutations in Japanese glioma patients. *Cancer Sci*, **100**(10), 1996–1998.

Stupp, R., Mason, W.P., van den Bent, M.J., Weller, M., Fisher, B., Taphoorn, M.J., Belanger, K., Brandes, A.A., Marosi, C., Bogdahn, U., Curschmann, J., Janzer, R.C., Ludwin, S.K., Gorlia, T., Allgeier, A., Lacombe, D., Cairncross, J.G., Eisenhauer, E., Mirimanoff, R.O.; European Organisation for Research and Treatment of Cancer Brain Tumor and Radiotherapy Groups; National Cancer Institute of Canada Clinical Trials Group. 2005. Radiotherapy plus concomitant and adjuvant temozolomide for glioblastoma. *N Engl J Med*, **352**(10), 987–96.

Surma-aho, O., Niemelä, M., Vilkki, J., Kouri, M., Brander, A., Salonen, O., Paetau, A., Kallio, M., Pyykkönen, J., Jääskeläinen, J. (2001) Adverse long-term effects of brain radiotherapy in adult low-grade glioma patients. *Neurology*, **56**(10), 1285–90.

Sylvestre, Y., De Guire, V., Querido, E., Mukhopadhyay, U.K., Bourdeau, V., Major, F., Ferbeyre, G., Chartrand, P. (2007) An E2F/miR-20a autoregulatory feedback loop. *J Biol Chem*, **282**(4), 2135–43.

Takahashi, Y., Nakamura, H., Makino, K., Hide, T., Muta, D., Kamada, H., Kuratsu, J. (2013) Prognostic value of isocitrate dehydrogenase 1, O6-methylguanine-DNA methyltransferase promoter methylation, and 1p19q co-deletion in Japanese malignant glioma patients. *World journal of surgical oncology*, **11**(1), 284.

Tan, X., Wang, S., Zhu, L., Wu, C., Yin, B., Zhao, J., Yuan, J., Qiang, B., Peng, X. (2012) cAMP response element-binding protein promotes gliomagenesis by modulating the expression of oncogenic microRNA-23a. *Proc Natl Acad Sci U S A*, **109**(39), 15805–10.

Taphoorn, M.J., Schiphorst, A.K., Snoek, F.J., Lindeboom, J., Wolbers, J.G., Karim, A.B., Huijgens, P.C., Heimans, J.J. (1994) Cognitive functions and quality of life in patients with low-grade glioma: the impact of radiotherapy. *Ann Neurol*, **36**(1), 48–54.

Taylor, V., Welcher, A.A., Program, A.E., Suter, U. (1995) Epithelial membrane protein-1, peripheral myelin protein 22, and lens membrane protein 20 define a novel gene family. *The Journal of Biological Chemistry*, **270**(48), 28824–28833.

Taylor, V. and Suter, U. (1996) Epithelial membrane protein-2 and epithelial membrane protein-3: two novel members of the peripheralmyelin protein 22 gene family. *Gene*, **175**(1-2), 115–120.

Tejero, R., Navarro, A., Campayo, M., Viñolas, N., Marrades, R.M., Cordeiro, A., Ruíz-Martínez, M., Santasusagna, S., Molins, L., Ramirez, J., Monzó, M. (2014) miR-141 and miR-200c as markers of overall survival in early stage non-small cell lung cancer adenocarcinoma. *PloS one*, **9**(7), p.e101899.

Thon, N., Eigenbrod, S., Kreth, S., Lutz, J., Tonn, J.C., Kretzschmar, H., Peraud, A., Kreth, F.W. (2012) *IDH1* mutations in grade II astrocytomas are associated with unfavorable progression-free survival and prolonged postrecurrence survival. *Cancer*, **118**(2), 452–60.

Ueki, K., Nishikawa, R., Nakazato, Y., Hirose, T., Hirato, J., Funada, N., Fujimaki, T., Hojo, S., Kubo, O., Ide, T., Usui, M., Ochiai, C., Ito, S., Takahashi, H., Mukasa, A., Asai, A., Kirino. T. (2002) Correlation of histology and molecular genetic analysis of 1p, 19q, 10q, TP53, EGFR, CDK4, and CDKN2A in 91 astrocytic and oligodendroglial tumors. *Clin Cancer Res*, **8**(1), 196–201.

Villafranca, J. and Colman, R. (1972) Role of metal ions in reactions catalyzed by pig heart triphosphopyridine nucleotide-dependent isocitrate dehydrogenase. I. Magnetic resonance and binding studies of the complexes of enzyme, manganous ion, and substrates. *J Biol Chem*, **247**(1), 209–14.

Vlachos, I.S., Kostoulas, N., Vergoulis, T., Georgakilas, G., Reczko, M., Maragkakis, M., Paraskevopoulou, M.D., Prionidis, K., Dalamagas, T., Hatzigeorgiou, A.G. (2012) DIANA miRPath v.2.0: investigating the combinatorial effect of microRNAs in pathways. *Nucleic acids research*, **40**(Web Server issue), pp.W498–504.

Wang, X. (2008) miRDB : A microRNA target prediction and functional annotation database with a wiki interface. *RNA*, **14**(6), 1012–1017.

Wang, X. and El Naqa, I.M. (2008) Prediction of both conserved and nonconserved microRNA targets in animals. *Bioinformatics (Oxford, England)*, **24**(3), 325–32.

Wang, X.W., Ciccarino, P., Rossetto, M., Boisselier, B., Marie, Y., Desestret, V., Gleize, V., Mokhtari, K., Sanson, M., Labussière, M. (2014) *IDH* Mutations: Genotype-Phenotype Correlation and Prognostic Impact. *BioMed Research International*, Epub.

Watanabe, T., Nobusawa, S., Kleihues, P., Ohgaki, H. (2009) *IDH1* mutations are early events in the development of astrocytomas and oligodendroglioma. *Am J Pathol*, **174**(4), 1149–1153.

Watanabe, T., Nobusawa, S., Kleihues, P., Ohgaki, H. (2010) *MGMT* promoter methylation in malignant glioma: ready for personalized medicine? *Nat Rev Neurol.*, **6**(1), 39–51.

Wen, P. and Kesari, S. (2008) Malignant glioma in adults. *N Engl J Med*, **359**(5), 492–507.

Wessels, P.H., Twijnstra, A., Kessels, A.G., Krijne-Kubat, B., Theunissen, P.H., Ummelen, M.I., Ramaekers, F.C., Hopman, A.H. (2002) Gain of chromosome 7, as detected by in situ hybridization, strongly correlates with shorter survival in astrocytoma grade 2. *Genes Chromosomes Cancer*, **33**(3), 279–284.

Westphal, M. & Lamszus, K. (2011) The neurobiology of gliomas: from cell biology to the development of therapeutic approaches. *Nat Rev Neurosci.*, **12**, 495–508.

Wick, W., Hartmann, C., Engel, C., Stoffels, M., Felsberg, J., Stockhammer, F., Sabel, M.C., Koeppen, S., Ketter, R., Meyermann, R., Rapp, M., Meisner, C., Kortmann, R.D., Pietsch, T., Wiestler, O.D., Ernemann, U., Bamberg, M., Reifenberger, G., von Deimling, A., Weller, M. (2009) Noa-04 randomized phase III trial of sequential radiochemotherapy of anaplastic glioma with procarbazine, lomustine, and vincristine or temozolomide. *J Clin Oncol*, **27**(35), 5874–5880.

Wick, W., Platten, M., Meisner, C., Felsberg, J., Tabatabai, G., Simon, M., Nikkhah, G., Papsdorf, K., Steinbach, J.P., Sabel, M., Combs, S.E., Vesper, J., Braun, C., Meixensberger, J., Ketter, R., Mayer-Steinacker, R., Reifenberger, G., Weller, M.; NOA-08 Study Group of Neuro-oncology Working Group (NOA) of German Cancer Society. (2012) Temozolomide chemotherapy alone versus radiotherapy alone for malignant astrocytoma in the elderly: the NOA-08 randomised, phase 3 trial. *Lancet Oncol.*, **13**, 707–715.

Wightman, B., Ha, I. and Ruvkun, G. (1993) Posttranscriptional regulation of the heterochronic gene lin-14 by lin-4 mediates temporal pattern formation in C. elegans. *Cell*, **75**(5), 855–62.

Wiltshire, R.N., Herndon, J.E., Lloyd, A., Friedman, H.S., Bigner, D.D., Bigner, S.H., McLendon, R.E. (2004) Comparative genomic hybridization analysis of astrocytomas: prognostic and diagnostic implications. *J Mol Diagn.*, **6**(3), 166-79.

Woods, K., Thomson, J. & Hammond, S., 2007. Direct regulation of an oncogenic micro-RNA cluster by E2F transcription factors. *J Biol Chem.*, **282**(4), 2130–4.

Wu, P.Y., Zhang, X.D., Zhu, J., Guo, X.Y., Wang, J.F. (2014) Low expression of microRNA-146b-5p and microRNA-320d predicts poor outcome of large B-cell lymphoma treated with cyclophosphamide, doxorubicin, vincristine, and prednisone. *Human pathology*, **45**(8), 1664–73.

Xu, W., Yang, H., Liu, Y., Yang, Y., Wang, P., Kim, S.H., Ito, S., Yang, C., Wang, P., Xiao, M.T., Liu, L.X., Jiang, W.Q., Liu, J., Zhang, J.Y., Wang, B., Frye, S., Zhang, Y., Xu, Y.H., Lei, Q.Y., Guan, K.L., Zhao, S.M., Xiong, Y. (2011) Oncometabolite 2-Hydroxyglutarate Is a Competitive Inhibitor of a-Ketoglutarate-Dependent Dioxygenases. *Cancer Cell*, **19**(1), 17–30.

Xu, P., Vernooy, S.Y., Guo, M., Hay, B.A. (2003) The Drosophila microRNA Mir-14 suppresses cell death and is required for normal fat metabolism. *Curr Biol*, **13**, 790–795.

Yan, H., Parsons, D.W., Jin, G., McLendon, R., Rasheed, B.A., Yuan, W., Kos, I., Batinic-Haberle, I., Jones, S., Riggins, G.J., Friedman, H., Friedman, A., Reardon, D., Herndon, J., Kinzler, K.W., Velculescu, V.E., Vogelstein, B., Bigner, D.D. (2009) *IDH1* and *IDH2* mutations in Glioma. *N Engl J Med*, **360**(8), 765–773.

Yan, H., Bigner, D.D., Velculescu, V., Parsons, D.W. (2009) Mutant metabolic enzymes are at the origin of glioma. *Cancer research*, **69**(24), 9157–9.

Yang, B., Jing, C., Wang, J., Guo, X., Chen, Y., Xu, R., Peng, L., Liu, J., Li, L. (2014) Identification of microRNAs associated with lymphangiogenesis in human gastric cancer. *Clin Transl Oncol.*, **16**(4), 374-9.

Yao, Y., Chan, A.K., Qin, Z.Y., Chen, L.C., Zhang, X., Pang, J.C., Li, H.M., Wang, Y., Mao, Y., Ng, H.K., Zhou, L.F. (2013) Mutation analysis of IDH1 in paired gliomas revealed IDH1 mutation was not associated with malignant progression but predicted longer survival. *PloS one*, **8**(6), p.e67421.

Yin, A.A., Zhang, L.H., Cheng, J.X., Dong, Y., Liu, B.L., Han, N., Zhang, X. (2014) The predictive but not prognostic value of MGMT promoter methylation status in elderly glioblastoma patients: a meta-analysis. *PloS one*, **9**(1), p.e85102.

Yong, F. L., Wang, C. W., Roslani, A. C., & Law, C. W. (2014). The involvement of miR-23a/APAF1 regulation axis in colorectal cancer. *International Journal of Molecular Sciences*, **15**(7), 11713–29.

Zavadil, J., Narasimhan, M., Blumenberg, M., Schneider, RJ. (2007) Transforming growth factor-beta and microRNA:mRNA regulatory networks in epithelial plasticity. *Cells Tissues Organs*, **185**(1-3), 157–61.

Zhang, C.Z., Zhang, J.X., Zhang, A.L., Shi, Z.D., Han, L., Jia, Z.F., Yang, W.D., Wang, G.X., Jiang, T., You, Y.P., Pu, P.Y., Cheng, J.Q., Kang, C.S. (2010) MiR-221 and miR-222 target PUMA to induce cell survival in glioblastoma. *Mol Cancer*, **9**, 229.

Zhang, W., Zhang, J., Hoadley, K., Kushwaha, D., Ramakrishnan, V., Li, S., Kang, C., You, Y., Jiang, C., Song, S.W., Jiang, T., Chen, C.C. (2012) miR-181d: a predictive glioblastoma biomarker that downregulates MGMT expression. *Neuro Oncol.*, **14**(6), 712-9.

Zhang, Y., Dutta, A. and Abounader, R. (2012) The role of microRNAs in glioma initiation and progression. *Front Biosci (Landmark Ed)*, **17**, 700–712.

Zhang, L., Qian, J., Qiang, Y., Huang, H., Wang, C., Li, D, Xu, B. (2014) Down-Regulation of miR-4500 Promoted Non-Small Cell Lung Cancer Growth. *Cellular Physiol Biochem*, **34**(4), 1166–74.

Zhao, S., Lin, Y., Xu, W., Jiang, W., Zha, Z., Wang, P., Yu, W., Li, Z., Gong, L., Peng, Y., Ding, J., Lei, Q., Guan, K.L., Xiong, Y. (2009) Glioma-derived mutations in IDH1 dominantly inhibit IDH1 catalytic activity and induce HIF-1alpha. *Science*, **324**(5924), 261–265.

Zou, P., Xu, H., Chen, P., Yan, Q., Zhao, L., Zhao, P., Gu, A. (2013) *IDH1*/*IDH2* mutations define the prognosis and molecular profiles of patients with glioma: a meta-analysis. *PloS one*, **8**(7), p.e68782.

APPENDIX

Appendix I

Supplier information

Product	Supplier
HEPES Ham's F10 nutrient mix	Life Technologies Ltd, 3 Fountain Drive, Inchinnan Business Park, Paisley, PA4 9RF. UK www.lifetechnologies.com
Penicillin	Sigma-Aldrich Company Ltd, The Old Brickyard, New Road, Gillingham, Dorset, SP8 4XT. UK www.sigmaaldrich.com
Streptomycin	Sigma-Aldrich Company Ltd, The Old Brickyard, New Road, Gillingham, Dorset, SP8 4XT. UK www.sigmaaldrich.com
Kanamycin	Sigma-Aldrich Company Ltd, The Old Brickyard, New Road, Gillingham, Dorset, SP8 4XT. UK www.sigmaaldrich.com
Foetal calf serum	Life Technologies Ltd, 3 Fountain Drive, Inchinnan Business Park, Paisley, PA4 9RF. UK www.lifetechnologies.com
Collagenase	Sigma-Aldrich Company Ltd, The Old Brickyard, New Road, Gillingham, Dorset, SP8 4XT. UK www.sigmaaldrich.com
Hank's buffered salt solution	Sigma-Aldrich Company Ltd, The Old Brickyard, New Road, Gillingham, Dorset, SP8 4XT. UK www.sigmaaldrich.com
Trypsin EDTA	Life Technologies Ltd, 3 Fountain Drive, Inchinnan Business Park, Paisley, PA4 9RF. UK www.lifetechnologies.com
Dimethyl sulfoxide	Sigma-Aldrich Company Ltd, The Old Brickyard, New Road, Gillingham, Dorset, SP8 4XT. UK www.sigmaaldrich.com
TCA	Sigma-Aldrich Company Ltd, The Old Brickyard, New Road, Gillingham, Dorset, SP8 4XT. UK www.sigmaaldrich.com
SRB	Sigma-Aldrich Company Ltd, The Old Brickyard, New Road, Gillingham, Dorset, SP8 4XT. UK

	www.sigmaaldrich.com
Acetic acid	Sigma-Aldrich Company Ltd, The Old Brickyard, New Road, Gillingham, Dorset, SP8 4XT. UK www.sigmaaldrich.com
Mitomycin C	Sigma-Aldrich Company Ltd, The Old Brickyard, New Road, Gillingham, Dorset, SP8 4XT. UK www.sigmaaldrich.com
GFAP antibody	Dako UK Ltd, Cambridge House, St Thomas Place, Ely, Cambridgeshire, CB7 4EX, UK www.dako.com
IDH1-R132H antibody	GmbH / Warburgstr. 45/20354 Hamburg, Germany www.dianova.com
Nestin antibody	Millipore (U.K.) Limited, Suite 3 & 5, Building 6, Croxley Green Business Park Watford, Hertfordshire WD18 8YH, UK www.merckmillipore.com
Ki-67 antibody	Dako UK Ltd, Cambridge House, St Thomas Place, Ely, Cambridgeshire, CB7 4EX, UK www.dako.com
p53 antibody	Dako UK Ltd, Cambridge House, St Thomas Place, Ely, Cambridgeshire, CB7 4EX, UK www.dako.com
CD34 antibody	Leica Biosystems Newcastle Ltd, Balliol Business Park West, Newcastle Upon Tyne, NE12 8EW, UK www.leicabiosystems.com
EMA antibody	Leica Biosystems Newcastle Ltd, Balliol Business Park West, Newcastle Upon Tyne, NE12 8EW, UK www.leicabiosystems.com
MGMT antibody	Abcam, 330 Cambridge Science Park, Cambridge CB4 0FL, UK www.abcam.com
Vectastain Universal Elite ABC Kit	Vector Laboratories Ltd, 3, Accent Park, Bakewell Road Orton Southgate, Peterborough, PE2 6XS, UK

	www.vectorlabs.com
Vectastain Elite ABC Reagent	Vector Laboratories Ltd, 3, Accent Park, Bakewell Road, Orton Southgate, Peterborough, PE2 6XS, UK www.vectorlabs.com
DAB solution	Dako UK Ltd, Cambridge House, St Thomas Place, Ely, Cambridgeshire, CB7 4EX, UK www.dako.com
QIAamp DNA Mini and Blood kit	Qiagen Ltd, Skelton House, Lloyd Street North, Manchester M15 6SH. UK www.qiagen.com
Phosphate buffered saline	Sigma-Aldrich Company Ltd, The Old Brickyard, New Road, Gillingham, Dorset, SP8 4XT. UK www.sigmaaldrich.com
Sodium thiocyanate	Sigma-Aldrich Company Ltd, The Old Brickyard, New Road, Gillingham, Dorset, SP8 4XT. UK www.sigmaaldrich.com
100bp ladder	Thermo Fisher Scientific Inc., 81 Wyman Street, Waltham, MA 02454. UK www.thermofisher.com
mirVana miRNA isolation kit	Life Technologies Ltd, 3 Fountain Drive, Inchinnan Business Park, Paisley, PA4 9RF. UK www.lifetechnologies.com
Acid-Phenol:Chloroform	Sigma-Aldrich Company Ltd, The Old Brickyard, New Road, Gillingham, Dorset, SP8 4XT. UK www.sigmaaldrich.com
HotStarTaq polymerase	Qiagen Ltd, Skelton House, Lloyd Street North, Manchester M15 6SH. UK www.qiagen.com
Deoxynucleotide set	Sigma-Aldrich Company Ltd, The Old Brickyard, New Road, Gillingham, Dorset, SP8 4XT. UK www.sigmaaldrich.com
Primers	Sigma-Aldrich Company Ltd, The Old Brickyard, New Road, Gillingham, Dorset, SP8 4XT. UK www.sigmaaldrich.com

Magnesium chloride	Qiagen Ltd, Skelton House, Lloyd Street North, Manchester M15 6SH. UK www.qiagen.com
Agarose	Sigma-Aldrich Company Ltd, The Old Brickyard, New Road, Gillingham, Dorset, SP8 4XT. UK www.sigmaaldrich.com
GenElute PCR Clean-Up Kit	Sigma-Aldrich Company Ltd, The Old Brickyard, New Road, Gillingham, Dorset, SP8 4XT. UK www.sigmaaldrich.com
BigDye® Terminator v3.1 cycle Sequencing kit	Life Technologies Ltd, 3 Fountain Drive, Inchinnan Business Park, Paisley, PA4 9RF, UK www.lifetechnologies.com
EZ DNA Methylation-Gold Kit	Zymo Research Europe GmbH, Güterhallenstrasse 3, 79106 Freiburg, Deutschland. www.zymoresearch.eu
50bp ladder	Thermo Fisher Scientific Inc., 81 Wyman Street, Waltham, MA 02454. UK www.thermofisher.com
HighRanger 1kb DNA ladder	Geneflow Ltd, Paul Fisher House, 1 The Sycamore Tree, Elmhurst Business Park, Elmhurst, Lichfield, Staffordshire, WS13 8EX www.geneflow.co.uk
ULS-Cy3 and ULS-Cy5	Agilent Technologies UK Ltd., 610 Wharfedale Road, IQ Winnersh, Wokingham, Berkshire, RG41 5TP. UK www.agilent.com
Reference DNA (male and female)	Promega, Delta House, Southampton Science Park, Southampton SO16 7NS. UK www.promega.com
ULS Labelling Kit	Agilent Technologies UK Ltd., 610 Wharfedale Road, IQ Winnersh, Wokingham, Berkshire, RG41 5TP. UK www.agilent.com
100x blocking agent	Agilent Technologies UK Ltd., 610 Wharfedale Road, IQ Winnersh, Wokingham, Berkshire, RG41 5TP. UK www.agilent.com

Cot-1 DNA	Invitrogen, Life Technologies Ltd, 3 Fountain Drive, Inchinnan Business Park, Paisley, PA4 9RF. UK www.lifetechnologies.com
HI-RIPM hybridisation buffer	Agilent Technologies UK Ltd., 610 Wharfedale Road, IQ Winnersh, Wokingham, Berkshire, RG41 5TP. UK www.agilent.com
Agilent CGH block	Agilent Technologies UK Ltd., 610 Wharfedale Road, IQ Winnersh, Wokingham, Berkshire, RG41 5TP. UK www.agilent.com
Human Genome CGH Microarray Kit 244K	Agilent Technologies UK Ltd., 610 Wharfedale Road, IQ Winnersh, Wokingham, Berkshire, RG41 5TP. UK www.agilent.com
miRCURY LNA Array miR labelling kit	Exiqon A/S, Skelstedet 16, 2950 Vedbaek, Denmark www.exiqon.com
3D Gene Human miRNA oligo chips	Toray Industries Inc., Nihonbashi Mitsui Tower, 1-1, Nihonbashi-Muromachi 2-chome, Chuo-ku, Tokyo 103-8666, Japan www.toray.com
1kb ladder	Life Technologies Ltd, 3 Fountain Drive, Inchinnan Business Park, Paisley, PA4 9RF. UK www.lifetechnologies.com

APPENDIX II

Gel image showing aCGH samples after heat fragmentation

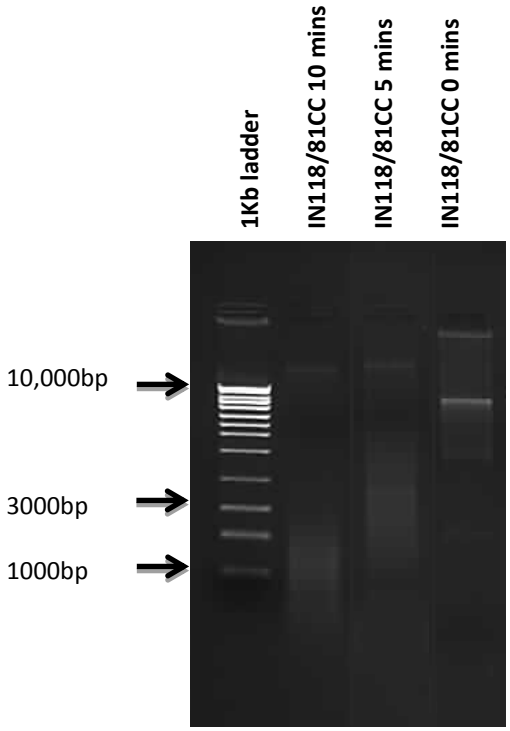

APPENDIX III

Treatment information available for patients in this study

Tumour	Age[a]	Sex[b]	Grade	Histology[c]	Treatment[d]	Overall survival[e]
BTNW17	69	F	II	A	Radiotherapy	4.5 (D)
BTNW20	26	M	II	A	Radiotherapy	83.5 (A)
BTNW124	29	M	II	A	Radiotherapy, Chemotherapy (TMZ)	65.5 (D)
BTNW160	35	M	II	A	Radiotherapy	67.5 (A)
BTNW203	42	F	II	A	Chemotherapy (TMZ)	64.5 (A)
BTNW210	53	F	II	A	Radiotherapy	64 (A)
BTNW212	50	M	II	A	Radiotherapy	45.5 (D)
BTNW365	42	F	II	A	Radiotherapy	37.5 (D)
BTNW367	56	M	II	A	Radiotherapy	51.5 (A)
BTNW870	17	M	II	A	Chemotherapy (TMZ)	22.5 (A)
Liv002	34	F	II	A	Radiotherapy	25 (A)
Liv007	40	M	II	A	Radiotherapy	8 (D)
BTNW726	45	M	II	OA	Chemotherapy (TMZ)	33 (A)
BTNW929	43	F	II	OA	Chemotherapy (TMZ)	18 (A)
BTNW326	56	F	II	O	Radiotherapy	37.5 (D)
Liv026	58	M	II	O	Radiotherapy	13.5 (A)
BTNW14	43	M	III	AOA	Chemotherapy (PCV)	85 (A)

[a] Age at diagnosis in years; [b] M, male; F, female; [c] A, astrocytoma; OA, oligoastrocytoma; O, oligodendroglioma; AOA, anaplastic oligoastrocytoma; [d] TMZ, temozolomide; PCV, procarbazine, lomustine (CCNU), and vincristine; [e] OS in months; A, alive; D, dead.

MGMT methylation status of primary tumours by IHC and MS PCR

Tumour	Grade	Histology[a]	Proportion				Proportion score	Intensity score	Combined score	MS PCR[b]
			Count 1	Count 2	Count 3	Total (%)				
BTNW20	II	A	0/100	0/100	2/100	< 1	1	3	4	U
BTNW61	II	A	77/100	64/104	70/100	69	5	3	8	U
BTNW160	II	A	19/100	22/100	21/100	21	3	1	4	PM
BTNW203	II	A	71/121	47/100	51/119	50	4	2	6	U
BTNW210	II	A	1/100	0/100	0/100	< 1	1	2	3	U
BTNW212	II	A	26/108	21/110	16/101	20	3	2	5	M
BTNW365	II	A	37/103	26/103	24/102	28	3	2	5	ND
BTNW367	II	A	100/100	100/100	100/100	100	5	3	8	PM
BTNW380	II	A	88/100	97/100	94/100	93	5	2	7	U
BTNW381	II	A	6/100	5/100	8/100	6	2	2	4	U
BTNW680	II	A	72/100	78/101	85/104	77	5	2	7	U
BTNW736	II	A	0/100	0/100	1/100	< 1	1	2	3	U
BTNW761	II	A	0	0	0	0	0	0	0	U
BTNW818	II	A	87/100	78/100	92/100	86	5	3	8	U

BTNW823	II	A	22/100	25/100	18/100	22	3	3	6	U
BTNW830	II	A	50/101	59/116	54/105	51	4	2	6	U
BTNW870	II	A	43/100	40/100	30/100	38	4	2	6	U
BTNW868	II	A	42/100	31/100	34/100	36	4	3	7	U
BTNW931	II	A	40/100	41/106	34/111	36	4	2	6	ND
BTNW13	II	OA	67/100	62/104	59/101	62	4	2	6	U
BTNW503	II	OA	30/100	26/100	27/106	27	3	1	4	U
BTNW613	II	OA	97/100	100/100	94/100	97	5	3	8	PM
BTNW726	II	OA	80/100	84/100	89/100	84	5	3	8	U
BTNW929	II	OA	15/100	22/100	20/100	19	3	2	5	ND
BTNW188	II	O	54/100	60/100	54/108	54	4	2	6	M
BTNW326	II	O	49/100	72/100	54/100	58	4	3	7	M
BTNW531	II	O	21/114	19/104	23/109	19	3	2	5	M
BTNW882	II	O	33/100	41/100	28/100	34	4	2	6	U
BTNW38	III	AA	12/101	16/114	17/121	13	3	2	5	PM
BTNW126	III	AA	55/100	52/100	51/100	53	4	2	6	U
BTNW173	III	AA	5/100	3/100	4/100	4	2	1	3	U

BTNW196	III	AA	13/101	12/110	9/100	11	3	1	4	U
BTNW211	III	AA	51/100	42/124	39/109	40	4	2	6	U
BTNW421	III	AA	74/103	69/101	81/100	74	5	3	8	U
BTNW458	III	AA	36/100	23/100	15/100	25	3	2	5	M
BTNW925	III	AA	0	2/100	0	< 1	1	1	2	U
BTNW9	III	AOA	1/100	2/119	0/100	< 1	1	2	3	U
BTNW14	III	AOA	1/100	0/100	0/100	< 1	1	2	3	M
BTNW120	III	AOA	5/100	1/100	4/100	3	2	2	4	PM
BTNW174	III	AOA	30/100	30/100	16/103	25	3	1	4	M
BTNW183	III	AOA	38/100	35/100	32/100	35	4	2	6	PM
BTNW325	III	AOA	32/105	30/107	31/103	29	3	2	5	ND
BTNW495	III	AOA	34/102	26/100	24/100	28	3	2	5	U
BTNW515	III	AOA	62/100	56/100	52/100	57	4	2	6	ND
BTNW527	III	AOA	0	0	0	0	0	0	0	U
BTNW614	III	AOA	78/100	85/100	90/101	84	5	3	8	U
BTNW703	III	AOA	69/100	55/100	62/100	62	4	3	7	U
BTNW749	III	AOA	0	0	0	0	0	0	0	ND

BTNW778	III	AOA	0	0	1/100	< 1	1	1	2	ND
BTNW825	III	AOA	4/100	1/100	1/100	2	2	1	3	U
BTNW864	III	AOA	17/100	25/120	25/100	21	3	3	6	U
BTNW15	III	AO	27/101	17/103	21/105	21	3	2	5	M
BTNW460	III	AO	29/100	25/100	16/100	23	3	3	6	U
BTNW738	III	AO	3/108	5/100	7/100	5	2	2	4	U
BTNW757	III	AO	41/100	41/100	30/100	37	4	2	6	U
BTNW804	III	AO	48/100	31/100	34/100	38	4	2	6	PM

[a] A, astrocytoma; OA, oligoastrocytoma; O, oligodendroglioma; AA, anaplastic astrocytoma; AOA, anaplastic oligoastrocytoma; AO, anaplastic oligodendroglioma; [b] M, methylated; PM, partially methylated; U, unmethylated; ND, not done.

MGMT methylation status of primary/recurrent pairs by IHC and MS PCR

Tumour	Grade	Histology[a]	Proportion				Proportion score	Intensity score	Combined score	MS PCR[b]
			Count 1	Count 2	Count 3	Total (%)				
BTNW365	II	A	37/103	26/103	24/102	28	3	2	5	ND
BTNW861	III	AA	23/108	17/102	15/121	17	3	2	5	ND
BTNW946	IV	GBM	0	0	0	0	0	0	0	PM
BTNW974	IV	GBM	74/125	66/102	59/102	60	4	2	6	PM
BTNW367	II	A	100/100	100/100	100/100	100	5	3	8	PM
BTNW380	II	A	88/100	97/100	94/100	93	5	2	7	U
BTNW126	III	AA	55/100	52/100	51/100	53	4	2	6	U
BTNW196	III	AA	13/101	12/110	9/100	11	3	1	4	U
BTNW325	III	AOA	32/100	30/100	31/100	31	3	2	5	ND
BTNW515	III	AOA	62/100	56/100	52/100	57	4	2	6	ND
BTNW778	III	AOA	0/100	0/100	1/100	<1	1	1	2	ND
BTNW614	III	AOA	78/100	85/100	90/101	84	5	3	8	U
BTNW848	IV	GBM	20/104	27/103	16/101	20	3	2	5	PM

[a] A, astrocytoma; OA, oligoastrocytoma; AA, anaplastic astrocytoma; AOA, anaplastic oligoastrocytoma; GBM, glioblastoma multiforme; [b] M, methylated; PM, partially methylated; U, unmethylated; ND, not done.